UNIVERSITY OF SOUTHAMPTON

FACULTY OF ENGINEERING AND THE ENVIRONMENT

Computational Engineering and Design Group

Structural Fidelity Variation for Aircraft Wing Configurations: Design Exploration and Optimisation in Conceptual and Preliminary Design Stages.

by

Isherdeep Singh

Thesis for the degree of Doctor of Philosophy

May 2018

UNIVERSITY OF SOUTHAMPTON

ABSTRACT

FACULTY OF ENGINEERING AND THE ENVIRONMENT
Computational Engineering and Design Group

Doctor of Philosophy

STRUCTURAL FIDELITY VARIATION FOR AIRCRAFT WING CONFIGURATIONS: DESIGN EXPLORATION AND OPTIMISATION IN CONCEPTUAL AND PRELIMINARY DESIGN STAGES.

by Isherdeep Singh

In an aircraft design process, as the design progresses through various design stages, concerted effort to introduce optimization capabilities, explore alternate designs, and introduce novel ideas becomes limited by the process chains, and reliance on higher fidelity analysis. Therefore introduction of global search and optimisation capability is limited to the conceptual design stage, where lower fidelity tools are utilised. These tools, although verified and validated for known trends, limit the exploration of novel design spaces, as they are reliant on empirical data sets. In this work a multidisciplinary program, which is designed to utilise physics based tools to achieve design exploration capabilities, is presented. In addition to this, the code presented aids in the assessment of the impact of structural analysis on the observed design space, for top level geometric parameters. The importance of fidelity variation on the design exploration of the wing configuration for mass, drag and cost is also explored.

Presented in this work are trends for wing performance characteristics derived from models for varying structural fidelity, for variations in Aspect Ratio (AR) , Sweep ($SWPI$), Area (SG), and thickness to chord at the root (t/c_{r}). The models include; a simple beam model, a three dimensional wing box model (with spars, covers, and ribs), and the three dimensional wing box model with the addition of stingers. The trend variance resulting from the inclusion of incremental physics, and certification based analysis in the coupled structural and aerodynamic analysis, provides a guide to the fidelity required to successfully optimise the aircraft wing configuration. Following the assessment of trends, sensitivity studies are conducted for multiple variables, at different levels of structural fidelity. These sensitivity studies allow the visualisation of the wing performance characteristics in two and three dimensions, and facilitate the understanding of design variable sensitivity.

Finally Response Surface Models (RSMs) and design space visualisation studies (using parallel and hierarchical axes techniques, and Pareto fronts) were conducted in order to fulfil the overall aims of the thesis; appropriate structural fidelity selection, reduction of the data overhead between design levels, and design space exploration.

Contents

List of Figures

List of Tables

Nomenclature

$2D$	= two dimensional
$3D$	= three dimensional
A	= area
AoA	= angle of attack
AR	= wing aspect ratio
$alt.$	= altitude
B	= flange width
BM	= bending moment
b	= width
C	= coefficient or chord
CoM	= Centre of Mass
D	= drag
d	= section depth
E	= energy
g	= gravitational acceleration
h	= trailing edge kink position
I	= second moment of area
J	= torsional constant
k	= fraction of tip washout at kink
L	= lift
LE	= leading edge
m	= mass
MoS	= margin of safety
$MTOW$	= maximum take-off weight
n	= load factor
P	= pressure
p	= Kriging hyperparameter
q	= dynamic pressure
Re	= Reynold's number
S	= spanwise section length
SG	= gross wing area
$SWPI$	= wing sweep

T = temperature
TE = trailing edge
TT = torsional thickness
t = thickness
t/c = thickness to chord ratio
V = volume
w = washout at tip
X = design variables
x = x-axis
Y = stringer design variables
y = y-axis
z = z-axis

Greek Symbol

δ = displacement
θ = rotation, deg, or Kriging hyperparameter
λ = wing taper ratio
ρ = density
σ = stress

Abbrevviations

$AirCONICS$= Aircraft Configuration through Integrated Cross-disciplinary Scripting
$ANOVA$ = Analysis of Varaince
BC = Boundary Condition
CAD = Computer Aided Design
CFD = Computational Fluid Dynamics
CO = Collaborative Optimisation
$COBYLA$ = Constrained Optimisation By Linear Approximation.
$COTS$ = Commercial off the shelf
CSM = Computational Structural Mechanics
CT = Cost Tool
DLR = Deutschen Zentrums fur Luft und Raumfahrt
DoE = Design of Experiments
DOC = Direct Operating Cost
$FAME$ = Fast and Advanced Mass Estimation of Wings
FE = Finite Element
FEA = Finite Element Analysis
FEM = Finite Element Method
FFD = Free Form Deformation

$FIDO$	= Framework for Interdisciplinary Design Optimisation
$FLOPS$	= FLight OPtimisation System
FP	= Full Potential
GA	= Genetic Algorithm
$GFEM$	= Global Finite Element Model
HPC	= High Performance Computer
HWB	= Hybrid Wing Body
KBE	= Knowledge Based Engineering
LCC	= Life Cost Cycle
LHS	= Latin Hypercube Sampling
MAM	= Multipoint Approximation Method
MD	= Multidisciplinary
$MDAACE$	= Multidisciplinary Aircraft Architecture Convergence and Evaluation
MDA	= Multidisciplinary Analysis
$MDAO$	= Multidisciplinary Analysis and Optimisation
MDF	= Multidisciplinary Framework
MDO	= Multidisciplinary Optimisation
MMI	= Mass Mode 1
$MMII$	= Mass Mode 2
MoE	= Mixtures of Experts
MSE	= Mean Squared Error
MSD	= Mean Standard Deviation
NN	= Neural Network
OA	= Orthogonal Arrays
OML	= Outer Mould Line
$PrADO$	= Preliminary Aircraft Design and Optimisation
PSO	= Particle Swarm Optimisation
RBF	= Radial Basis Functions
$RANS$	= Reynolds Averaged Navier Stokes
RSM	= Response Surface Model
SQP	= Sequential Quadratic Programming
$T.A.C.E$	= Transport Aircraft Configuration Evaluation
UD	= Uniform Design
$WISE$	= Weight and Sizing Evaluation
VLM	= Vortex Lattice Method

Subscript

0	= sea level
$1, 2, 3, 4$	= rear spar, upper cover, front spar, and lower cover

bar	= centroid location
d	= drag
f	= flight
i	= initial
in	= inboard
k	= kink
l	= lift
n	= new
opt	= optimum
out	= outboard
p	= pressure
r	= root
ri	= rib
s	= stringers
sec	= section
sa	= shear allowable
t	= tip
w	= wing
y	= yield

Declaration of Authorship

I, Isherdeep Singh , declare that the thesis entitled *Structural Fidelity Variation for Aircraft Wing Configurations: Design Exploration and Optimisation in Conceptual and Preliminary Design Stages.* and the work presented in the thesis are both my own, and have been generated by me as the result of my own original research. I confirm that:

- this work was done wholly or mainly while in candidature for a research degree at this University;
- where any part of this thesis has previously been submitted for a degree or any other qualification at this University or any other institution, this has been clearly stated;
- where I have consulted the published work of others, this is always clearly attributed;
- where I have quoted from the work of others, the source is always given. With the exception of such quotations, this thesis is entirely my own work;
- I have acknowledged all main sources of help;
- where the thesis is based on work done by myself jointly with others, I have made clear exactly what was done by others and what I have contributed myself;
- parts of this work have been published as: Singh, Isherdeep., Keane, Andy J., Holden, Carren M.E. ''Structural Fidelity Variation for Aircraft Wing Configuration, Design and Optimisation in Preliminary Design.'' 5th Aircraft Structural Deisgn Conference Proceedings, Manchester, UK, 2016.

Signed:.....

Date:.....

Acknowledgements

I would like to start by thanking my supervisors Professor Andy Keane, and Dr. Carren Holden for giving me the opportunity to undertake this research. It was through their guidance, encouragement, and enthusiasm that I was able to successfully complete this work. Throughout the duration of my PhD, both Andy and Carren always took the time to help, guide and nurture my work and for this I am thankful.

I would like to also thank the three most important people in my life; my mother Gursharan, my brother Richard, and partner Emma-Louise. They endured countless hours of neglect as a result of this PhD, but always found ways to keep me happy, motivated, and excited about my work, and the future. If it wasnt for their love and care this thesis would not have been attempted, yet alone completed. So to them I'd like to apologise for the hours that I was not there, and thank them for the hours they were there for me. Love you all, forever.

Next I would like to take the opportunity to thank all the people I have had the pleasure to work with as part of my industrial placement. The foremost of these is Edward Kay, who was not only my colleague but someone from whom I learnt much. In addition to his mentoring, Ed took the time to listen to my ideas, observations, and ramblings and for that I thank him. I also had the pleasure of working with the MDAACE team at Airbus, this team consists of many individuals some of whom I would like to quickly note; Steve McKenna, Doug Smith, Steve Dean, Pete Denner, Stephane Grihon, Bob Heath, Thomas Englebrecht, Roland Kelm and many others, with whom I worked. This team made me feel welcome and provided a great environment for me to work, helping me take responsibility for important tasks, and providing much needed support. There are many other people I would like to thank, but simply put it would fill this entire page, but to anyone who helped me in my time at Airbus and to all who welcomed me as part of their team, my deepest thanks for your help, and your time.

My stay in industry would not have been possible if not for the many friends with whom I would drink coffee, visit the pub, and play football. Many of these shall remain unnamed but special thanks to Jeff Fox, Clive Staines, Jose Candau, Nick Rogers, and Wes Tilbury. In addition I would like to thank the wonderful PhD community at Airbus and in particular my friends; Hamza, Gabriele, Jean, and Simone.

Finally I would like to thank my colleagues at Southampton University for making me feel welcome, and offering much needed companionship, making each lunch time, coffee break, and pub visit memorable and fun. I'd like to thank you all for your jokes, your insults, and your friendship. In particular I'd like to thank Nick who took the time to listen and offered help and advice on some key issues within my research. Thanks Nick and I know you'll be a Dr. in no time.

A final thank you to all those unnamed above, to anyone whom I worked with at Airbus and Southampton, and to the many friends I made along the way. Thank you!

Chapter 1

Introduction

In order to explore the nature of high fidelity analysis in design it is first important to define what it means in context of aircraft design. The process of aircraft design can be divided into three broad stages, the first of which is the conceptual design stage; here mission profiles, and market conditions are used to formulate a design configuration which offers improved performance, and lowered costs for the operator. The required performance is assessed using low fidelity analysis models based in spreadsheets, empirical tools, and simple physics based tools which provide sufficient information to market the new design.

Having identified a potentially marketable design the process moves to the preliminary stage where aspects or components of the design are considered by specialised (aerodynamics, structures, mass, etc.) teams using higher fidelity tools. However as we move into this stage each team has localised expert knowledge and designers whose experience is important in the overall design, Keane and Nair (2005). At this stage of design more accurate performance estimates are provided and the design is evolved to a point where the product can be subject to formal offers and key performance characteristics can be guaranteed, Jameson and Caughey (1977).

The overall expenditure at this stage still remains minimal, as the manufacturer has not committed to any detailed design, and manufacturing. The preliminary stage is crucial to the aircraft design process, here sufficient understanding of the design is required but many trade-offs must be considered in order to ensure that the product is competitive and achieves/exceeds customer requirements. These two requirements often conflict and existing knowledge of detailed designs is used to supplement the preliminary design analysis, over investment in extensive trade studies.

This is due to two major reasons: firstly the lack of tools which have the required fidelity to provide detail design characteristics for new configurations, and secondly constrained time limits. In an effort to overcome these constraints, greater emphasis is placed on

the use higher fidelity tools, and improved interaction between disciplines which can facilitate a multidisciplinary analysis (MDA).

For each discipline at the preliminary design stage the detail of the analysis and design representation is increased. Computer aided design (CAD) technology has improved the definition of geometry during this design stage for use in complex physics based computational fluid dynamics (CFD) and finite element analysis (FEA) analysis engines, which can be used in conjunction with high performance computers (HPCs). Augmented with this increased fidelity, discipline specific methodologies are employed to improve the analysis quality. However conflicts arise between competing designs goals for different disciplines.

The current trend in research is to strive towards a multidisciplinary (MD) environment at this design stage in order to replace discipline specific design objectives with holistic design objectives. This approach is designed to avoid local and small scale improvements to aircraft design and facilitate global design improvement in order to surpass performance targets. However in reality the coupling of high fidelity tools increases the complexity of the design process, which can be difficult to manage on a technical and a non-technical level.

Multidisciplinary refers to the combination of disciplines such that the overall methodologies and assumption remain similar without significant impact from other disciplines. In an engineering environment this is usually implemented through an organised framework. Interdisciplinary on the other hand refers to the integration of disciplines in such a way that the disciplinary methodologies and assumption evolve and become interdependent, often changing the disciplines themselves, McGowan et al. (2014).

There are significant challenges in realising a multidisciplinary environment in industry relating not just to technical barriers such as complexity, but also non-technical obstacles such as the culture of the company, and the lack of confidence in such methodologies, Belie (2002). Such challenges are yet to be fully overcome but significant improvements have been made in the technical front through the exploration of frameworks, which can be used to implement multidisciplinary optimisation (MDO) at the preliminary design stage, using high fidelity analysis. The improvements in non-technical issues remain subjective and vary from organisation to organisation.

In any multidisciplinary system there is an inherent focus on coupling of two or more disciplines which enhance the quality of trade-offs between said disciplines and offers the user greater knowledge and understanding of the key drivers. Many programs or codes offer coupling between two or more key disciplines. As there are a larger quantity of disciplines in the preliminary design stage, the key disciplines often play an important role in the makeup of the program. These disciplines become the focal point and the best coupling between them is an area of active research. Often each discipline may have its own sub process for analysis which is connected to a global analysis process.

At the preliminary design many multidisciplinary processes tend to have a greater focus on one or more disciplines with some simplified considerations for others deemed to be less critical. It is because of this that the interests of research can sometimes diverge, as demonstrated in the literature in chapter 2. The application of these developed technologies in industry is always limited by the organisational paradigm, capability, and the certification culture. The multidisciplinary framework for organising the design process must offer a route to evaluate the design such that certification can be achieved. Therefore any research into higher fidelity multidisciplinary systems, must account for certification.

Many programs create an analysis chain which can demonstrate the development of a new methodology. However minimal attention is given towards understanding how the analysis process may vary within industry and where key contributions could be made. Through observation of the Multidisciplinary Aircraft Architecture Convergence & Evaluation (MDAACE) analysis process for airframe and understanding of the limitations in industry, it was decided that in order to successfully develop high fidelity methodologies, an analysis program that reflects industrial design practise was required.

From building the analysis program in chapter 3 and through partaking in industrial trade studies, areas of research interest were identified. It was noted that the primary challenge in industry with regards to multidisciplinary systems was to utilise them to improve design exploration. Often the design process can be choked in the preliminary design stage where the reliance on high fidelity methods and data overhead between conceptual and preliminary design can limit design exploration, to a single point of interest. The industrial solution has been to create an analysis process which can be situated between these levels of design and compensate for the data overhead with rapid analysis. However the challenge remains, that due to the nature for the design process, high fidelity inputs are required and often the analysis can become limited and data intensive.

Here our research goal is to utilise the analysis program created to conduct variable fidelity modelling, to account for sub-design problems. Through global analysis and simulation the goal is to demonstrate multipoint analysis, design exploration, and optimisation, without loss of trust in the multidisciplinary analysis methodology. In order to ensure design quality is preserved, it was also identified that design sensitivity and visualisation of the design space at this stage would be key in ensuring trust in a lower fidelity analysis methodology, which although physics based can still be conservative or optimistic. This has helped to formulate the aims and objectives of this thesis.

1.1 Aims

To create an experimental analysis program which reflects industrial capability, using commercial-off-the-shelf (COTS) tools, to analyse aircraft wing configurations between the conceptual and preliminary design stage. The code created will form the basis of research in area of wing structural fidelity variation, design sensitivity analysis, and global wing optimisation using response surfaces. In addition to this the metamodeling and design visualisation and search capability should provide a route to answer specific industrial problems regarding data overhead, trust in multidisciplinary optimisation technology, and fidelity selection.

1.2 Objectives

1. To create a multidisciplinary analysis code, and to validate this code at varying degrees of structural fidelity, by calibrating against industrially validated analysis tools.
2. Use the created code to identify wing performance trends at different fidelity levels within the conventional design space of transport aircraft, for validation purposes.
3. To investigate the sensitivity of key top level geometric variables on wing performance outputs at different levels of structural analysis fidelity, in order to introduce confidence in the response surface creation methodology.
4. Create response surfaces using Kriging for top level wing design variable at multiple fidelity levels, in order to demonstrate optimisation potential using surrogate models and data visualisation.
5. To identify and highlight the resolution of fidelity and visualisation methodology, which can allow successful design exploration in an industrial context.

1.3 Thesis Layout

This thesis consists of a further six chapters, which demonstrate the progress of the research aims and the investigations conducted to fulfil the aims and objectives highlighted above.

Chapter 2: Provides an introduction to the field of multidisciplinary analysis and optimisation, alongside some key examples. An overview of several disciplines in the design process is presented. In addition details of an industrial multidisciplinary system known as MDAACE are provided.

Chapter 3: In this chapter the Transport Aircraft Configuration Evaluation (T.A.C.E) code is presented. This has been created to facilitate the research aims of this thesis. The breakdown of this framework; the process, methodology, and implementation are described.

Chapter 4: A short study demonstrating the calibration of the T.A.C.E code is presented. This chapters also seeks to validate the T.A.C.E analysis process for existing aircraft wing designs and to establish performance trends. These trends form an effective means by which to establish confidence in the sensitivity studies, response surface model creation, and design space visualisation in subsequent chapters. In addition this program is compared with other academic programs in order to assess its strengths and weaknesses.

Chapter 5: Having established trends within the known design which are representative of high fidelity models, the next step was to vary the level of structural fidelity. Design variables were coupled as pairs, and design of experiments were generated for multi-point analysis using T.A.C.E. This data was then used to create response surface models using kriging.

Chapter 6: Having assessed the sensitivity of the performance variables, the viability of response surface based design search and optimisation was investigated. The methodology established in chapter 5 for response surface creation was further expanded for a larger number of design variables. The data generated was used for three types of design visualisation; parallel axis plots, Hierarchical Axis (HAT) plots, and Pareto fronts.

Chapter 7: In this chapter an overall discussion is presented on the degree of success to which this thesis fulfils the aims and objectives. This is followed by a conclusion on the achievements of the thesis and some recommendations for future work.

Chapter 2

Multidisciplinary Design and Analysis Fidelity

2.1 Introduction to Aircraft Design

The aircraft design process can be categorised into three stages, in the following order; preliminary, conceptual, and detailed. In conceptual design top level requirements for an aircraft are established based on sales, performance and cost. This is followed by low-fidelity trade studies for various configurations. These studies are empirical and feature some low fidelity analysis and optimisation. The aim of these studies is to establish a competitive product, and gauge the sensitivity of aircraft performance to top level changes in design variables.

The design and data from conceptual studies is transferred to the preliminary design stage, where higher fidelity analysis is used to conduct realistic design studies which take certification in to account. Here the goal is to establish a design configuration which can meet customer requirements. The analysis at this stage can cause re-evaluation or adjustment of performance targets at the conceptual design stage. However the problem arises with the overhead or missing data from conceptual tools. A further barrier to analysis at this level is the conversion of geometry from geometric variables to two or three dimensional representations. Factors such as the link between the geometry and disciplinary analysis, the computational time, and the cost (both labour and computational) limit the exploration of designs at the preliminary design stage. Following preliminary analysis, the design can be frozen and progressed to the detailed stage.

The detailed design stage is where the investment in the aircraft ramps to a critical level. A design which successfully reaches this stage requires a significant investment of resources to be developed further. The data from preliminary analysis is cascaded to individual departments and design teams where the focus is on the analysis, and

development of specific components and features. The scope of this stage can be years, with the final outcome of the process being a certified, manufactured, and market ready product. During this design phase information is often traversed to and from the preliminary design stage where the targets set previously are evolved, reassessed, and edited. For this reason it is important for the design to be on course to meet or exceed performance requirement at the preliminary and conceptual design stages. To achieve this optimisation is required. However the reliance on high fidelity inputs and analysis can hinder the successful implementation of optimisation at the preliminary design stage.

The design process in large manufactures becomes a single point analysis chain from the end of the conceptual design stage, in order to lower the overall cost associated with the analysis of multiple design configurations. There are advantages to this; where expert knowledge can be used to streamline analysis, detailed models and analysis can be instigated readily, and complex tool chains can be utilised for accurate performance estimations. This process has been developed and refined over decades for many products and reduces the overall expense in design variation, innovation, or integration of new technologies. However it also serves to constrain the design space exploration, as higher fidelity detail is needed to complete the analysis process. This leads to less time to expand the scope of trade and optimisation studies, and it a key limitation of the process as it stands. In conjunction with the exploration constraints, strict deadline, and reliance on high fidelity data inputs, leads to a lack of global design exploration.

This has led to the consideration of multi-point analysis, which can increase the frequency of optimisation and trade studies in early design. It has been theorised that a move towards cohesive multidisciplinary design can be a means by which this can be achieved. The space between conceptual and preliminary design offers the least risk, most opportunity, and lowest cost in the implementation of optimisation methodologies. This is because required performance targets are available, and rapid and somewhat accurate tools are present. In addition smaller teams with dedicated specialists can be utilised, and greater flexibility on absolute design values and design exploration boundaries is possible. This can be done at a lower cost, whilst the analysis fidelity is lower than that at the preliminary design stage. However challenges (technical and non-technical) remain in implementing this analysis, from a non-procedural view these can be broadly categorised as; the reliance on high fidelity data, data overhead between design stages, project timelines, and lack of optimisation expertise.

The limitations in optimisation capability in the preliminary design stage are the part of the problem we are trying to solve within this thesis, with the aim of tailoring the solution to the existing industrial design process. The issue of high fidelity data, leading to overhead can be alleviated through variable fidelity structural models. In addition these models can aid design exploration, with surrogate modelling techniques to build optimisation capability. The following literature review seeks to provide a detailed overview of the aircraft design process. Following this the disciplines which features in analysis

of an aircraft or wing are explored, with focus on the selection of appropriate structural fidelity. The nature of multidisciplinary analysis systems, frameworks, and optimisation is explored, featuring examples of all three and the industrial system known as MDAACE. Finally response surface modelling in engineering analysis explored to provide background on the work in this thesis.

2.2 Multidisciplinary Analysis and Optimisation Frameworks

2.2.1 Introduction

Programs created for engineering systems for multidisciplinary analysis capture and manage detailed inputs and outputs from the tools which are used to populate it. At any level of analysis fidelity the system must however have certain characteristics to ensure success. Padula and Gillian (2006) show that from of survey of just a handful of such systems, certain key attributes can be found. These include the need for modularity, data handling, parallel processing, and user interfaces. The following sections aim to provide an overview of multidisciplinary systems and codes in literature and how they satisfy such characteristics, and if they fulfil industrial requirements.

Frameworks can be categorised based on discipline or type. Martins and Lambe (2013) provide detailed information on the myriad of successful architectures found in aerospace literature. This paper provides a good overview and can be used a starting point in understanding the commonalities and differences between successful multidisciplinary frameworks, which according to Rocca and van Tooren (2009) should have the following features:

1. Adaptability to multiple design cases.
2. Integration of design tools and methodology.
3. Compatibility with commercial-off-the-shelf tools and in-house codes.
4. High and low fidelity analysis integration.
5. Coherence and synchronisation of data/models between disciplines and optimisation.
6. Automation of repetitive tasks.

The adaptability and compatibility can be related to the ability to manipulate geometry and variation geometric fidelity. Work by La Rocca et al. (2012) is an example of these

requirements for multidisciplinary optimisation can be met. The research presented in this work is based on knowledge based engineering and computationally aided design models for aircraft analysis and optimisation. The author(s) demonstrate this capability and highlight how the structuring and coding of such knowledge based systems are beneficial to the flexibility and overall structuring of an analysis process with detailed inputs.

Multidisciplinary optimisation problems can be decomposed in to multiple levels as suggested by Vanderplaats and Kim (1988). The connection between disciplines in multidisciplinary optimisation can be formulated in two distinct ways: with, and without gradient information, March and Willcox (2012). Cavagna et al. (2011) is an example of a successful decomposed multidisciplinary problem which uses physics based computational tools for analysis, to reduce cost and weight in the conceptual design stage. Additional industrial based research on this topic from Piperni et al. (2013) suggests a multi-level approach can also be incorporated in industrial analysis programs. These decomposed problems methodologies presented use aircraft field and flight performance to formulate optimisation constraints at global and system level. The optimisation conducted in individual disciplines links fidelity levels and disciplines to improve optimisation quality at lower fidelity. An overview of optimisation techniques is offered by Keane and Scanlan (2007), and these can be further explored in Keane (2003).

Mastroddi et al. (2012) demonstrates that the performance characteristics utilised need not be broad and conventional, and considerations such as, weight estimation, loads, aeroelasticity, and buckling can be incorporated in the optimisation problem. This can facilitate optimisation for numerous goals; weight, range, endurance, and aerodynamic efficiency, with based on the governing equations of each discipline. Coupled with this, efficient formulation of the global optimisation problem can be achieved using geometrical variables. Which reiterates that geometry representation in multidisciplinary problems is crucial to success of the analysis and optimisation.

There are many ways to organise and structure multidisciplinary programs and optimisation problems. However the author would like to draw attention to the conclusion of March and Willcox (2012), where it is implied that in the early stages of the design gradient information is not of paramount importance to achieving successful optimisation, but some gradient capability can be beneficial. This is the converse to the formulation of some high fidelity optimisation problems in literature. In addition Mastroddi et al. (2012) highlights that simplification of geometry detail can have a similar effect.

This geometrical detail is important to preliminary and even conceptual analysis and often no direct gradient information can be calculated. This leaves the designer operating within a multidisciplinary environment with two distinct options by which to achieve optimisation; adopt detailed high fidelity tools earlier in the design process and calculate

gradient information. Secondly the designer can decrease the fidelity through decomposition and seek to achieve greater design exploration prior to more detailed design. This second approach can be beneficial for integration of multidisciplinary optimisation and is of interest for the work in this thesis.

2.2.2 Review of Multidisciplinary Optimisation systems

A good introduction to multidisciplinary optimisation can be found in the collected works of Kroo et al. (2010), which represent the efforts of the Massachusetts Institute of Technology and Stanford University on the topic of multi-fidelity analysis and optimisation. This research presents tools, and methodologies for optimisation and analysis of supersonic aircraft configurations, with the modelling of uncertainty, and optimisation. This work provides an overview of important optimisation methodologies from leading researchers and is recommended for an overview of key architectures. Additionally the work of Sobieszczanski-Sobieski and Haftka (1997) though dated, provides an excellent entry point on the understanding of optimisation architectures and methodologies. This thesis is not concerned about relative applicability of a certain optimisation architectures, but rather the integration of optimisation in existing industrial multidisciplinary analysis processes.

In literature multidisciplinary systems can be the focus of the improvement of design through optimisation, where improvements are assessed with regards to aircraft performance. Coroneos and Pai (2012) present a program for structural analysis and optimisation known as Multidisciplinary Analysis and Optimisation (MDAO) or openMDAO, so called due to its open source accessibility. This code allows for the testing of common structural benchmark problems with respect to design variable upper and lower bounds, and constraints on the stress, displacement, and natural frequency of the structure. Further detail on this code can be found on the website (http://openmdao.org/). The openMDAO program shows promise for the testing methodologies and techniques in multidisciplinary optimisation, however its employment of lower fidelity analysis tools reduces the process viability within a complex design enviroment.

Multifidelity fidelity multidisciplinary analysis capability is demonstrated in Mastroddi et al. (2012), where aeroelastic objective formulation is used for optimisation. Simplified structural beam bending and torsional models, aeroelastic stability analysis are shown as a means to achieve optimisation. This work demonstrates coupling of a high fidelity code with a numerical optimisation algorithm and presents a unique objective formulation for multidisciplinary objectives to achieve design improvements in preliminary design.

The work of Kenway and Martins (2014) is an example of high fidelity aerostructural optimisation within preliminary design. This work is considered state of art in the field of aerostructural coupling and builds on, Martins et al. (2005). The authors demonstrate

the adjoint capability using RANS aerodynamics analysis, with additional structural analysis and sizing, for two optimisation problems; for gross take-off weight, and fuel burn. The overall objective is formulated as the range of the aircraft, where the lift to drag coefficient ratio or weight ratio is fixed, depending on the optimisation for fuel burn or weight. This work demonstrates the importance of capturing multidisciplinary interaction at high fidelity. This work is skewed towards higher fidelity aerodynamics over structural analysis, and requires development of the structural methodology in order to validate the supposed efficiency of the areostructural coupling.

Ronzheimer et al. (2010) is an example of research in aero-structural coupling for multidisciplinary optimisation. This work follows Heinrich et al. (2008), which presents the aerostructural methodology established at DLR. The implementations of the DLR aerostructural methodology can be seen in Keye et al. (2014). This body of work cumulates with the work of Brezillon et al. (2012) and is aligned with the industrial drive towards high fidelity aerostructural coupling in the MDOrmec program. The multidisciplinary presented is designed to conduct high fidelity optimisation post preliminary design, prior to detailed design. This work focuses on ensuring matched high fidelity in both the aerodynamic and structural disciplines.

Lee et al. (2012) present a preliminary design stage based code to facilitate fully integrated structural analysis, optimisation and manufacturing cost assessment using parametric models. The system established is used to create surrogates of weight and manufacturing cost, which are coupled with a multi-objective gradient based optimisation to find non-dominated solutions, aiding trade-off studies between weights and manufacturing cost. This code is highlighted due to the choice of tools, the focus on structural analysis, the use of industrially viable commercial tools, and many similarities with MDAACE presented in section 2.2.3.

Ghoman et al. (2012) present the multifidelity program; M3DOE. This is a collection of aerodynamic, aeroelastic, and structural codes combined at various levels of fidelity, to facilitate shape, topology, and sizing optimisation, individually or in combination. It is implemented for a business jet test case to minimise the aircraft dry weight, subject to constraints for range, take-off distance, static margin, and wing tip location. The organisation of the program and optimisation problem, to include these constraints is of note and demonstrates a novel way in which multidisciplinary systems can be structured to provide varying levels of fidelity. Allowing optimisation, and trades where the user can dictate the change in the level of performance improvement.

The impact on the performance outputs with design changes is not always assessed in terms of market impact in. Davendralingam and Crossley (2014) seeks to address this issue through statistical methods. The methodology presented assesses the impact of the design changes with regards to integrated aircraft design, airline operations, and passenger demand, to compute relative risk and profit. This methodology is in line with

considerations of design in the preliminary design stage, where a competitive and viable design is the focus.

Shirley et al. (2014) features high fidelity trade studies in lift-to-drag, and weight sensitivity for three different wing configurations of a mid-range transport aircraft. This work uses an established high fidelity framework for optimisation, to assess the impact of cantilever, strut braced, and truss braced, wings on the aerodynamic and weight performance. This provides greater understanding of the various trade-offs associated with each change.

The work of Skillen and Crossley (2008) shows how high fidelity analysis can be used to create a framework for analysing novel wing configurations, such as the morphing wing. Where coupling of higher fidelity analysis tools, simplification of the novel configurations, and known optimisation tools can be used for analysis and optimisation. Such work demonstrates that through inclusion of higher fidelity methods with appropriate assumptions, the design space can be expanded to give greater knowledge of designs in conceptual and preliminary phases. However assumptions for novel design configurations must be validated and in line with certification requirements. This can be achieved using lower fidelity empirical tools to validate such assumptions.

Dorbath (2014) is an example of a code based on wing mass estimation using a computational model, and higher fidelity tools. This code uses the established work at DLR and is unique due to its consideration for physics based mass estimation. Laughlin et al. (2013), presents another weight estimation which analyses Hybrid Wing Body (HWB) design configurations. The program created demonstrates the coupling of higher fidelity structural analysis tools to provide structural mass breakdowns. The trades conducted using such physics based methods provide detailed sensitivity information and enhance knowledge of novel design configurations. Gern et al. (2000) couples detailed high fidelity analysis tools to demonstrate enhanced preliminary analysis capability for a HWB. From literature it is clear that there are two clear schools of thought regarding the utilisation of fidelity in multidisciplinary analysis methodology; the high fidelity detailed optimisation, or the lower fidelity design exploration.

Hürlimann et al. (2011) present an analysis process structured around CATIA. The CAD methodology employed is based on the use of templates and knowledge based engineering. This use of CATIA is similar to the framework in Dean (2008), however here higher fidelity is used for the estimation of loads. The MDCAD program is based in industry, whereas the work presented by Hürlimann et al. (2011) is based on industrial tools, and methodologies. These methods demonstrate that a possible means of introducing optimisation capability in industry through high fidelity analysis models.

Kaufmann et al. (2011) utilise cost and structures coupling in optimisation. The direct operating cost (DOC) links aerodynamic, structural, and mass inputs and is an ideal objective function. This work highlights that multidisciplinary optimisation need not

be driven by an optimisation or search algorithm, but can be driven by rule bases. The work of Price et al. (2011) is a novel example on how analysis systems can be managed using rules which capture design knowledge and performance criteria, ensuring convergence towards an optimum solution. Such work is novel and lacks drive in an industrial environment currently, however it does show that once coupling is achieved, and novel ways of driving the design process can be implemented to the benefit of the optimisation.

From the survey of literature it would appear that the prominent approach for introducing optimisation is through increasing the analysis fidelity earlier in design. However certain examples have highlighted that a balance between fidelity can help to capture the detail required between conceptual and preliminary design, whilst allowing design exploration and optimisation. There are clearly two route by which to achieve optimisation for multiple disciplines in early design stages; high, and low fidelity. If the high fidelity optimisation route is taken, greater accuracy and precision can be achieved, however this is at the cost of design space exploration capability. If a lower fidelity route is taken, there is a penalty in accuracy and precision, but design space exploration capability and data overhead issues can be tackled. The aim of this thesis is to explore if though fidelity variation, and surrogate modelling it is possible to achieve all three objectives, of accurate and precise analysis, reduction of data overhead, and greater design exploration capability.

Section 2.5 explores how it is possible to vary fidelity within multidisciplinary systems and what discipline specific methodologies facilitate this. However it is important that we establish how the programs highlighted here compare to an industrially based program known as MDAACE, which forms the focal point for comparison in this thesis.

2.2.3 Multidisciplinary Design Aircraft Architecture Convergence & Evaluation (MDAACE)

2.2.3.1 Introduction

In the preliminary design stage there is clear segregation of work, which results in a significant turnover in time for trade studies. A method of reducing this cost is to lower the fidelity of the analysis. Much of the research in this field lies between the conceptual and preliminary stages and advocates the use of high fidelity analysis methods to facilitate detailed design studies and design optimisation. This is often a process of balancing the desired number of evaluations with the level of accuracy, where lowering the overall fidelity increases design space knowledge, whilst reducing overall accuracy. However if the correct performance can be identified from the additional evaluations, the quality of the higher fidelity analysis can be enhanced; due to greater knowledge of the design,

its sensitivities, and the design space. Having surveyed some key successful multidisciplinary analysis programs, it is now important to cover the basis of the multidisciplinary system which led to the inception of this thesis.

2.2.3.2 Framework, Methodology, and Tools

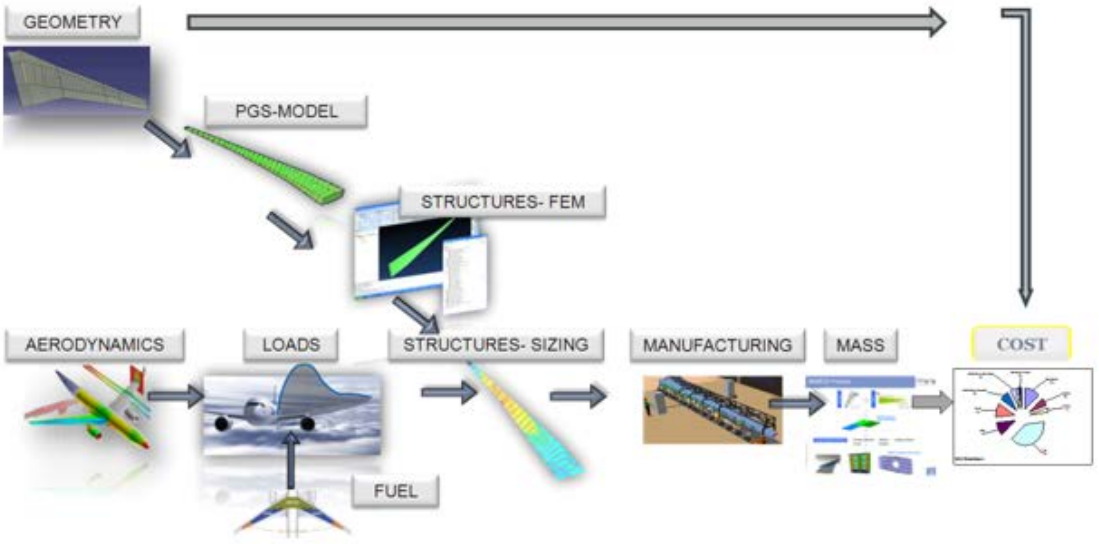

Figure 2.1: MDAACE design process and disciplinary analysis chain, Di Pasquale et al. (2014).

The Multidisciplinary Aircraft Architecture Convergence and Evaluation (MDAACE) analysis system based in industry has been designed to provide a quick turn over of trade studies based on geometrical variations of the wing, fuselage, and or theoretically any other aircraft structures. It utilises conceptual data and expert knowledge at each disciplinary level to conduct multidisciplinary analysis. The analysis codes are integrated to connect data models for simulation tools and provide a workbench for an architect (project manager/expert user) to drive, define, configure, and steer the trade-off study. The methods and tools which drive this workflow lie between conceptual analysis and department specific analysis, and are used to balance the correct level of fidelity bridging the knowledge gap between design stages. The overall process employed in MDAACE can be seen in figure 2.1.

The substitution of tools and variation of fidelity within MDAACE is an attractive feature for any optimisation system and allows direct control over the computational, resource, and data expenditure. However limitations in data management create a data overhead and limit the use of direct global optimisation. In order to achieve the aims and objectives highlighted in sections 1.1 and 1.2, MDAACE has been replicated as a program to explore its limitations, and to explore methods which can achieve variable fidelity analysis and optimisation. This new program is discussed further in

chapter 3. The following sections provide a brief description of the software components and disciplines specific analysis methods implemented within MDAACE.

Geometry The geometry module provides a baseline CAD model for global FEM (GFEM) creation. The geometry creation methodology used is on the use of parametric templates, which are assembled to provide a wing model. The templates are variable in detail and type for generic feature(s), and can be rapidly grouped, and parameterised using design tables. The geometry creation process requires high fidelity information; the stringers, ribs and manhole distribution and placement as inputs. In addition optimal aerofoil sections are required for the creation of lofts, and profiles.

Iterative analysis is required to provide the inputs, and outputs to and from the geometry module. This is a restriction in the early design stage and is detrimental to the speed of the overall analysis. Note the structural inputs are crucial within this system, which is designed to provide a weight variance data for the given design configuration.

Global Finite Element Model The finite element model creation code requires the CAD model as an input, as the design table data is used to instantiate features. Additional requirements for the creation process are the loads, and material data. The model is created specifically to suit the purposes of sizing. It is important to note that the creation process is a conversion process, with key geometrical decisions having been made during the CAD modelling. The process can vary in terms of input and validation depending on the chosen material: metal or composite.

Aerodynamics The aerodynamic calculations provide performance data for the geometry, and the loads department respectively. When working with variants of existing aircraft this process easily navigated. However there is a significant overhead for novel configurations, requiring some assumptions, and iterations with lower fidelity aerodynamics tools. The primary outputs of this process include wing shape, aerofoil placements, and aerofoil profiles. Di Pasquale et al. (2014) presents how the aerodynamics process can be automated through the use of commercially available software, and reduced fidelity aerodynamics. This work demonstrates the MDAACE code development, towards improved disciplinary coupling, and automation, to facilitate optimisation.

Loads The loads process is important to the overall success of the analysis process, as the critical sizing load cases (for wing certification) are identified, calculated, and output. The full loads process employed within the preliminary design stage can be complex and time consuming, with numerous iterative loops, complicated analysis, and large quantities of data. For MDAACE a simplified loads process was created at a lower

fidelity which still requiring expert navigation of various stages, including the selection of critical load cases.

Structural Sizing Using the aforementioned finite element model, loads, and failure modes, the structural sizing process can be conducted. This process is designed to find the stress, and weight optimal solution of the given airframe for stiffened panels under the loading conditions provided. This is achieved using a coupling of failure analysis tools and finite element analysis software. The solution procedure is an aggregate of material, failure mode, stringer, cover, and other critical information. This can be over a large or small design space, depending on the pre-preparation time given, and the nature of the study. The tools utilised within the sizing process and their methodology is highlighted in section 2.2.3.3.

Manufacturing This manufacturing process model applies appropriate manufacturing rules (material ramp rates, minimum manufacturing thicknesses, etc.) to convert the weight optimal solution from the sizing process into a manufacturing optimal solution. This includes the addition or removal of material in key areas across the airframe, where the sizing solution cannot be manufactured using current capabilities.

Mass Estimation Following the application of manufacturing rules to the structural sizing, the collective geometrical, aerodynamic, loads, and structural outputs are used to initiate the mass estimation process. This is an automated process using data storage, and workflow definitions to provide absolute values (subject to assumptions), and mass sensitivities for the design in question. The weight accounting methodology implemented reflects the method presented by Cheesman and Smith (2001). During the calculation process all additional airframe and sized wing components are considered, in addition to the wing box. The absolute output values can vary and are subject to the assumption implemented however the variance from the known baseline, is a useful measure of the design performance, and quality.

Costing The costing tool known as CADCO aggregates all known data of the design configuration to provide an estimate for recurring and non-recurring cost(s). These are categorised into three separate domains; maintenance, manufacturing, and flying, all associated with the overall design and the airframe structure in question. The outputs are compared to a baseline configuration and once again absolute values and variance are given. Note this tool is calibrated to the specific manufacturing processes and methods.

2.2.3.3 Structural Sizing Tools

The sizing process a focal point within MDAACE and understanding the analysis process can help to determine how data overheads, technical barriers and issues can be avoid within structural analysis. Prior to sizing the finite element model, a failure mode analysis is conducted separately and used to facilitate the creation of a database of structural solutions for given loading conditions, structural technologies, geometrical parameters, and materials.

Industrial Analytical Stress Methods To facilitate rapid stress data generation an analysis program has been created to encompass the analytical stress analysis of the entire aircraft structure without expensive FEA. This framework features failure mode analysis interactively or in batch, allowing the user to select a method for structural, buckling or strength analysis, developed from open source knowledge and in-house knowledge. For stiffened panel analysis, open source methods are coupled with specific additions from the handbook of structural stability Semonian and Peterson (1955), and Gerard and Becker (1957). The analysis is cheap, and ideal for creation of databases and design curves, which can be coupled with a rapid sizing tool.

Rapid Sizing Tool: PRESTO The rapid sizing tool PRESTO is used to map loads and database information to a finite element model. The tool is designed to avoid the use of sensitivities for calculation, providing a rapid solution, but not necessarily an optimal one. It was designed to lighten the fidelity of the preliminary design tools by reducing the number of design variables, and simplifying stress analysis methodology to providing reliable weight estimations. The combinations of discrete dimensions of panels, and material properties in the database limit the mapping of options on the analysis model. Panel geometrical values are mapped to database values and the finite element model is designed to reflect the database, and sizing regions. Once the mapped, finite element analysis is conducted, and internal loads information is extracted and used for enumeration for the lightest weight stringer which satisfies the target reserve factor allowable.

The internal loads founds are used to search the failure mode database and locate all stringers which withstand that load for the given region. Once all possibilities are identified, a minimum weight constraint is used to locate the lowest weight structure. The enumeration is completed for the desired region or the entire model. The tool features a material re-distribution capability in order to achieve manufacturing solutions and minimise excess mass in the structure. This capability known as target sizing or smoothing is implemented through the declaration for a target thicknesses or areas for given panels or stringers. Each target thickness and/or area can be determined through quick calculations, expert judgement, or iterative refinement.

2.3 Design Search and Optimisation and Response Surface Modelling

An alternative to gradient based optimisation is response surface based optimisation, which offers a cheap, quick, and accurate optimal solution. An additional advantage of these models is the ability to utilise visualisation as part of the optimisation and design studies, and create databases of information. In this chapter we briefly explore some literature regarding metamodeling, discuss prominent methods which can be used to create these models, and the limitations of these methods.

Surrogate, response surface modelling, or metamodels are a way of referring to mathematical methods of data fitting. This can be in multiple dimensions, with visualisation limited to three. These methods provide a way of determining mathematical relationships between outputs and inputs of engineering systems. The most basic method of achieving data fitting is through polynomial equations, other prominent methods including Kriging and Radial Basis Functions (RBF). A good overview of surrogate modelling using these methods is found in Queipo et al. (2005). Other notable methods include Neural Networks (NN), Freeman and Skapura (1991). Some key literature in the field of surrogates includes Santner et al. (2013) and response models in optimisation by Sacks et al. (1989). Jones (2001) also offers a taxonomy of methodologies used currently, where details of the underlying mathematics, advantages, disadvantages, and examples are provided.

When using surrogate methodologies it is important to have a method of data selection, this is known in surrogate modelling terms as a Design of Experiment (DoE). This can be done randomly, or using mathematical formulation, to minimise the number of data points, whilst sampling the entire design space, to improve data fitting accuracy. In general more points leads to an increase in accuracy, but increases the time required to create the surrogate model. Therefore a full factorial sampling of the design space with a large number of points is not ideal, if speed is paramount to the analysis. Some notable literature in this field can be found in Morris and Mitchell (1995), where establishing DoE for computational experiments is investigated. McKay et al. (2000) presents the underlying theory and advantages of three methods for data selection, these include random sampling, stratified sampling, and Latin Hypercube Sampling (LHS).

Fang et al. (2000) highlights the application of Uniform Design (UD) in design of experiments, where design points are spaced in a uniform manner in a given design space. The advantage of this method is that it is orthogonal and minimises the non-uniformity over the designs, whilst using a minimum number of experiments. Queipo et al. (2005) compare several DoE methodologies, including: LHS, orthogonal arrays (OA), optimal LHS, OA-based LHS, and optimal OA-based LHS. It is important to note that the DoE methodology employed can affect the accuracy of the surrogate model created, however

it is important to note that the raw data gathered from the analysis using the DoE points can be beneficial for the purposes of design exploration.

Surrogate models have become prominent in multidisciplinary optimisation literature and their use in analysis programs continues to increase. This because they offer a convenient method of modelling complex analysis data, and identifying the relationships between variables. Kriging is an example of one such modelling method and is favoured in this thesis.

Kriging originates in the work of thesis of Krige (1951) and was later adapted for application by Matheron (1973). A concise derivation for this method is found in Jones (2001). Kriging works by predicting the value of a function at any given point as a weighted average of the known values of the function, for points in close proximity to the evaluation point. A condensed explanation of the mathematics is provided by Parr et al. (2010).

2.4 Structural Fidelity in Multidisciplinary Design and Analysis Frameworks

Having discussed possible frameworks, and techniques through which MDO can be instigated. The next step is to understand how the structural fidelity impacts the various disciplines which are incorporated as part of the MDA process.

2.4.1 Structural Analysis Fidelity

2.4.1.1 Geometry

As the aim of this thesis is to improve implementation of optimisation methodology using existing industrially based systems for multidisciplinary analysis. Computational models of the geometry have a direct impact on the fidelity options available within the analysis, as aerodynamics and structural analysis are reliant on geometrical information.

Since the introduction of computational aided design (CAD) modelling tools in engineering analysis, it has stipulated that to realise the potential of individual analyses, full integration was required, Jameson and Caughey (1977). Its use has led to developments in the methodology, and quality of software, and leading software tools to feature parametric modelling, scripting, and data transfer between analysis software. The integration of scripting in particular has allowed the integration of CAD tools with commercial tools and in-house codes, helping to realise the full potential of such codes. However with the increased complexity of geometric models, and the specific nature of the tools, the process of geometry development requires specialist direction, and high

fidelity inputs. Works such as Townsend et al. (1998) show how integration with multidisciplinary systems is possible.

To achieve success in multidisciplinary optimisation, geometric parameterisation must be possible. The advantages of using a CAD based and CAD free methods of parameterisation are discussed by Fudge et al. (2005). The work of Matthews et al. (2006) shows that the use of parametric variables in geometry can enhance the exploration of the design space, reducing the reliance on single point evaluations. Features of the parametric models can be used in evolutionary optimisation as suitability criteria, aiding the optimisation process.

It is important to note that authors such as Holden and Wright (2000) have shown that parameterisation of geometry outside of a CAD model can be successfully achieved using splines and Bezier curves. These methodologies are easily linked with a gradient based or complex genetic optimisation methods. This allows optimisation to be introduced at a disciplinary and global level Holden et al. (2002).The interaction between the optimisation algorithm, and the parametric variables and features, directly influences the use of such models in a given analysis method. The chosen methodology for geometry manipulation, instantiation, and representation can drastically skew the nature of the analysis and the optimisation capability.

Amadori et al. (2012) implements commercial tools in conceptual design for design process automation. This body of work focuses on the creation of model templates, to build flexible and robust geometry models, which can be incorporated in a high-fidelity multidisciplinary analyses. Knowledge based engineering (KBE) linked with parametric geometry, is presented as a means of automation and intuitive parameterisation. This methodology was initially proposed by Chapman and Pinfold (2001) for the automation of automotive structure design processes. CAD modelling based on capturing design knowledge, rules and relations, using topographical transformations and topological instantiation, is shown to provide successful fidelity selection. This work is closely linked with industry and represents the current trends in geometry modelling methodology.

This body of work is built on research by Ledermann et al. (2005) where a methodology for organising and creating effective, and detailed parametric models is presented. The method specifies a hierarchical component organisation structure with various levels of model fidelity, creating an organisational matrix of geometrical models, which can be accessed in a multidisciplinary analysis framework. The importance of identifying appropriate design variables for such parameterisation is highlighted in Amadori et al. (2008). Parametric models and knowledge based integration can also be used to automate discipline specific analyses, and optimisation, as demonstrated in Ledermann et al. (2006), La Rocca et al. (2012) and Nawjin et al. (2006).

Introducing parametric geometry models without using KBE and templates can be achieved using free form deformation (FFD), Sederberg and Parry (1986). Nurdin

et al. (2012) implement this deformation methodology with direct manipulation for optimisation of the shape of the wing connection to the fuselage. The direct manipulation modification (found in Menzel et al. (2006)) is useful for coupling CAD with aerodynamic analysis, and shape optimisation. Free form deformation can be coupled with other mathematical methodology to improve the parameterisation as noted by Lassila and Rozza (2010). However such methods are yet to be developed to tackle more complex geometric problems.

Sobester (2014) suggests that parameterised conceptual geometries are suited to hierarchical aircraft structural modelling and lead to automated design engines. These flexible and robust models can be used with search engine methodologies to achieve greater design capabilities in multidisciplinary optimisation frameworks, Sóbester et al. (2005). Using design knowledge and computational geometric modelling capabilities it is possible to create refined parametric geometries, which can be used as part of multidisciplinary analysis or individually with appropriate design tools.

Specific tools for aircraft geometry handling in multidisciplinary optimisation (MDO) exist, an example of which is the Geometry Centric MDO of Aircraft Configurations with High Fidelity (GeoMACH), Hwang and Martins (2012). This program uses an outer mould line (OML) approach using B-Splines with parameterisation using free form deformation to create a geometrical configuration with inputs from various disciplines. This code provides structural and aerodynamic models, which can be readily analysed using high fidelity tools.

A developed example of a script based computation aided design engine for geometry can be seen in the work of Sóbester (2015) and Sóbester and Forrester (2014) on self-designing geometries. This work has cumulated in the creation of the Aircraft Configuration through Integrated Cross-disciplinary Scripting (AirCONICS) tool (https://aircraftgeometrycodes.wordpress.com/airconics/). This work clearly presents state of the art research in the field of geometry handling in aircraft design. However this method does not offer direct access to certification tools. The most important aspect of this work is the focus on exposing a limited number of top level geometric design variables, which can in turn help simplify global optimisation.

For the purposes of the research in this thesis, the goal was to achieve design space exploration using the existing geometry representations in industry. Keane and Scanlan (2007) demonstrate that parametric models using CAD can be integrated in an analysis process, to provide a high degree of freedom during design space exploration. This work focuses on the link between the geometry model and the aerodynamic domain. However such parametric capability can also be used to explore design exploration in the structural domain. In order to determine how this is feasible, we must understand the nature of the structural domain, and the domains upon which it is dependent. In addition the coupling of structures with aerodynamics and its influence on the geometric

representation and fidelity must be investigated. Finally the coupling effect of each domain to the performance outputs such as weight and cost is of interest to this research.

2.4.1.2 Structures

For multidisciplinary analysis the structural discipline often forms the focal point of the analysis. Here information from the aerodynamics, and loads disciplines is consolidated and utilised to provide critical aircraft performance parameters such as stress, mass, displacements, and additional information used to determine cost, and fuel burn. The coupling of aerodynamics and structures can also form the basis for understanding aero-elastic performance early in the design stage. This can help to improve the design and reduce the impact of phenomena such as flutter in the detailed design stage.

Understanding the nature of the structural performance, the stress distribution, the material allocation, can help to fix mass parameters, and determine mass targets. The structural analysis can explore new materials, structural member, and features of the aircraft, such as landing gear, engines, and wing tips. The structural analysis is preceded by aerodynamics, and loads, but it can be critical to the design feasibility, and overall analysis. Before the literature for this discipline is presented, note that the focus of this research is on metallic airftact wings, and references for the analysis of composite wings are omitted.

Conceptual structural design can be facilitated using literature such as Torenbeek (1992), Megson (2012) and Raymer (1989). In addition sources such as Niu (1988), Shanley (1960), and Bruhn (1965) are excellent sources for an introduction to structural design and analysis and fundamental analysis techniques. However so as not to cover exiting grounds these sources are not dissected here. The methodologies highlighted in these sources, when coupled with simplified analysis approaches such as Giles (1986) and Giles (1989), using plate models initial estimates of the wing box performance can be found.

Such structural representations can be enhanced using three dimensional parametric geometry models which can be converted into a finite element models. Some of the benefits of this are highlighted by Komarov and Weisshaar (2002) which shows that by linking such finite element models to structural optimisation, in the early stages of design it is possible to achieve a lower aircraft structural weight. At a conceptual design stage formal structural optimisation is limited to empirical or semi-empirical methods unless higher fidelity representations of aerodynamics and structures can be introduced.

Two important resources in the understanding of structural analysis are the analysis and design studies conducted by NASA, and the collection of specific technical sheets gathered by ESDU. The collection of works by Ardema and co. (Ardema (1972), Ardema (1988), Ardema et al. (1996a), Chambers et al. (1996),and Ardema et al. (1996b)), and studies such as Neill et al. (1990), James and Dovit (1985), and Schmit and

Farshi (1974), provide important markers in developing structural design and analysis methodology. The works highlighted focus on global process development for structural analysis and weight estimation, and offer detailed and well developed methodologies to achieve this. ESDU provides a collection of technical sheets and tools, which are accessible for the implementation of specific analyses, for select components, or for a given performance metric, such as buckling or fatigue. These large institutional resources are often fundamental for the development of complex multidisciplinary analysis techniques, which feature structural analysis.

An important aspect of the structural design process is the structural sizing of panels, stringers, and spars of the wing box. This is so an accurate weight estimates can be found. Many authors have automated the sizing procedure to include optimisation, Giles et al. (1972), improving the accuracy of mass estimation. A higher-fidelity approach to this problem requires the use of commercial tools as demonstrated by Ainsworth et al. (2010). This work is idealistic as formal optimisation cannot always be undertaken during the structural design and sizing process. This trade-off is best captured in the Honda jet structural design process, detailed in Fujino (2005).

A finite element model of thee structural evolved from CAD model can form the basis of a sizing process as demonstrated by Schut and van Tooren (2007). This work highlights the possibility to automate structural sizing during conceptual design in order to reduce manual workload. Schuhmacher et al. (2002) detail the use of structural sizing in the conceptual design stage at Fairchild Dornier for regional aircraft, using optimisation methodology. The approach suggested shows promise and is reflective of the constraints. Structural sizing forms a key aspect of the overall structural analysis and design process, thus the next section investigates the structural sizing of panels in the wing as a topic of interest, and how it has an impact on the optimisation of structures. Thus for this research it was important to understand this impact and how sizing should be utilised, to achieve the aims and objectives of this research.

2.4.1.3 Structural sizing

The sizing of structural members is an important aspect of structural analysis, this involves the determination of dimensions, and thicknesses, of key structural features, for a given airframe. For a wing this includes, the covers, spars, and ribs. At the early stages of design these members are isolated and represented using simplified models or methods. As the design stages progress emphasis is placed on the use of physics based methods and detailed analysis. The sizing is subject to many inputs including loads, materials, and overall geometrical constraints. These inputs are used to determine what size the members need to be to withstand loads, without failure. The structural members are assessed with regards to their buckling, fatigue and damage tolerance, acoustic, and dynamic performance.

At the early stage of design this is done using fundamental literature such as Niu (1988). However as the design progresses the structural members must be resized using physics based methodologies, which coincide with the increase in fidelity of the design process. For the purposes of this thesis we are interested in understanding how optimisation can feature in the sizing process, and how the variation of fidelity, and optimisation methodology impacts the sizing process.

Structural sizing is an area where there is an opportunity for optimisation, Grihon et al. (2010), and the opportunity to couple optimisers with specific sizing analysis tools is an area of interest for research. From a survey of literature, it can be concluded that there are three approaches to the panel optimisation problem, including but not limited to:

1. Coupling with response surface models.
2. Direct coupling with optimisation algorithms.
3. Multidisciplinary instantiation or coupling.

The approaches can be further discretised into low or high fidelity, and global or local optimisation. The work of Schmit and Rarnanathznil (1978) highlights the importance of capturing buckling behaviour in any structural weight minimisation problem. Vitali et al. (2002) demonstrate a response surface based approach to stiffened panel optimisation, using a finite element model of a stiffened panel as a basis for the surface creation. These surrogate models are created for the panel and stringer design variables, and the buckling load factor.

Merval et al. (2006) is an example of a response surface methodology applied in an industrial setting and focuses on capturing non-linear relationships between sizing inputs and outputs. The method utilises Neural Networks (NN), with a combination of the Mixtures of Experts (MoE) to fuse local surrogates of different panel behaviour. These highlighted case are computationally expensive, but offer distinct advantages over direct coupling.

When coupling analysis tools or functions which govern sizing, direct methods can often be the most inexpensive, as demonstrated by Chintapalli et al. (2010). This paper shows the formulation of a panel analysis tool box using underlying theory from Niu (1999), Giles (1986), and Young and Budynas (2002) to establish a direct optimisation, for an equivalent use case. More recently the work of Zhao et al. (2014) shows that a simpler approach can be used quickly and cheaply. Here the focus is the co-dependency of stiffened panel optimisation problems on other disciplines such as manufacturing and cost. It is demonstrated that various objective functions related to cost and weight with different optimisation algorithms can influence the optimal structural solution.

Most structural sizing is based on fulfilment of buckling, manufacturing, and certification criteria. Much of the buckling criteria is based on buckling of plates and can be traced to fundamental literature such as Timoshenko and Gere (2012), Niu (1999), and Bulson (1969). Direct coupling of such methods with optimisers offers the easiest route for application in large scare programs. Bisagni and Vescovini (2009) provide an example of a rapid failure mode analysis code, coupled with optimisation algorithms and high fidelity finite element analysis. This work uses analytical equations as a basis for the preliminary structural sizing, with high fidelity analysis for validation and verification of optimal results.

There are more condensed buckling methods for conceptual design, the most prominent of which is seen in Riks (2000). Here a finite strip method is used for calculation of buckling and post-buckling characteristics, of a stiffened panel. The application of the finite strip method in industry is limited and classical methods are preferred in conceptual design phase, with finite element analysis based sizing for preliminary/detailed design.

The work of Schutte et al. (2004), decomposes sizing and structural design into a multilevel problem, to reflect standard practise. The decomposition of the sizing problem allows the coupling of sizing methods directly with optimisation tools using surrogates, as shown in Liu et al. (2004).In Cavagna et al. (2011) a structural sizing methodology using beam modelling coupled with aeroelastic and aerodynamic analysis is presented. Here a simplified structural sizing methodology facilitates greater design flexibility and direct coupling of disciplines without compromising the overall accuracy greatly. This work highlights how structural sizing is both important and can be implemented non-intrusively in a multidisciplinary chain. The key to achieving this is to reducing the fidelity at which the structural members are represented (as lumped masses, or smeared panels), whilst implementing aerostructural coupling at a matching level of fidelity.

The work of Chedrik (2013) demonstrates the use of higher fidelity multidisciplinary analysis for stiffened panel design. The program presented couples various disciplines for structural analysis of stiffened panels using finite element analysis, for a business jet wing test case. The work of Barkanov et al. (2014) is an example of high fidelity structural analysis. Here the sizing problem is instantiated entirely within the finite element analysis environment, providing improved performance for weight optimisation, with respect to linear buckling constraints. Where the optimisation uses response surfaces, built using the high fidelity analysis code. Colson et al. (2010) is also a structural analysis and optimisation based study which compares four different optimisation methods. This work recommends the use of derivate based optimisation and suggests the use of surrogates as an alternative.

Note that structural analysis, sizing, and design is subject to inputs from aerodynamics and loads, in addition to the geometry. Loads generation, is a complex and detailed

procedure, and recent research trends favour the use of aerostructural coupling to simulate loads and to understand the quasi-static, and dynamic behaviour of the structure. It important to understand aerodynamic capabilities and to explore the nature of aerostructural coupling and its potential benefit to this research.

2.4.1.4 Aerodynamics

The design processes links the geometry output to aerodynamics, as this is frequently the primary discipline for which a new design is optimised. This is due to the overarching link of aerodynamic performance on geometry, structural design, cost, certification loads, and weight. As the aircraft moves through the design process the complexity of the aerodynamics increases, to match the fidelity of geometry. This improves the accuracy of aerodynamic performance assessment, allowing overall performance targets to be achieved through optimisation.

In conceptual design empirical methods are used for the rapid estimation of aerodynamic performance. These methods scale the lift or drag characteristics based on existing aircraft of similar size. These scaling methods vary between conceptual frameworks and between institutions. The datasets change and are matched to the product being designed or the academic study being conducted. This can see great variation but the dataset is often based on existing or rival products.

A step up in analysis fidelity from empirical methods are linear potential ones, such as the panel method, examples of which can be found in Bristow (1980), Youngren et al. (1983), Maskew (1987), and Ashby et al. (1991). Panel methods can also be used for aerofoil analysis and optimisation at the conceptual or preliminary design stage, as demonstrated by Drela (1989). Robinson and Keane (2001) and the works Keane and Petruzzelli (2000b) and Petruzzelli and Keane (2001).The work of Keane (2003) discusses the limitations of design trade-offs made using empirical code and how these can be overcome by fusing data from empirical and computational fluid dynamics based drag routines using design of experiments and Kriging. More recently Keane and Petruzzelli (2007) also tested various fidelity aerodynamic codes in the conceptual design stage.

In more detailed conceptual design multidisciplinary systems or in low fidelity preliminary design, full potential methods can also be implemented. This method was initially developed by Boeing in the works of Murman and Cole (1970). Following on from this three dimensional full potential methods were presented by Jameson and Caughey (1977), and Freestone (2003) where the latter method was adapted by Toal (2009), and is used in the research presented in section 3.2.2.3.

As the need for detailed performance analysis increases the Euler and Reynolds averaged Navier-Stokes (RANS) methods are preferred for aerodynamic analysis. These discretisation methods allow for the inclusion of shocks, and contact surfaces. In RANS

methods turbulence can be analysed, through the use of specific mathematical models which increase the accuracy, but are computationally expensive. Here a description of RANS and Euler methods, and their coupling with various turbulence models, is not provided. Instead it should be noted that these methods are considered as high fidelity aerodynamics.

In industry often in-house high fidelity codes are preferred, and can be coupled with other disciplines in multidisciplinary systems as shown in Martins et al. (2005), Tomac and Eller (2011), and Gebbie et al. (2007). As aerodynamic optimisation is not the focus of this research, no further exploration of the relevant aerodynamics literature is presented. The determination of the loads is often the next step in the design of aircraft. This discipline is often closely coupled with the aerodynamics and structural analysis. A coupling can be achieved at various levels of fidelity using techniques categorised as aerostructures in literature.

2.4.1.5 Aerostructural coupling

The coupling of aerodynamic and structural analysis has been a topic of research for many decades, and has been covered thoroughly in literature such as Bisplinghoff et al. (2013), Dowell et al. (2004), Hodges and Pierce (2011), and Wright and Cooper (2008). The consideration of aeroelasticity improves the understanding of complex physical interaction (dynamic, static, linear, and non-linear) between a body and the loads (aerodynamic, inertial, and elastic) acting on it in flight. Considering the behaviour of these two disciplines in connection captures realistic behaviour, and helps to identify phenomenon such as flutter, which cannot be captured by either disciplinary analyses independently. This improves the quality, realism, and understanding of wing design.

The most basic aeroelastic phenomenon are divergence and control reversal, the former is related to wing twist, and the latter to control surfaces on the wing. The reason to cover these phenomena is due to their importance on structural deformation, where twist produces a large discrepancy between aerodynamic calculations and experimental data, Keye et al. (2014). It is also stated in CS-25 certification document that such deformations, should not lead to instability in flight, and divergence or control reversal should be evaluated. The aforementioned phenomena can be considered early in the design process and are often referred to as static aeroelastics. The simplest way to implement this is through empirical aeroelastic tailoring equations. The theory, methodology, and application of this is covered in Shirk et al. (1986), and industrial application in conceptual design can be found in Kelm et al. (1999).

Livne (2003) identifies that aeroelastic analysis in aircraft design offers greater understanding of global and local behaviour, new technologies, novel concept, and aircraft

control and stability. In addition it is highlighted that aeroelastics can improve realisation of multidisciplinary optimisation, and the analysis of novel wing configurations. This work offers a comprehensive collection of aeroelastic works up to its publication and is a recommended starting point in aeroelastic research. For this research we seek to evaluate and assess the argument that aeroelastics can be used to facilitate multidisciplinary optimisation. Works such as Kenway and Martins (2014) and Piperni et al. (2007), and Piperni et al. (2013) demonstrate that this is possible, and improves performance assessment.

In order to couple structural and aerodynamic analysis the mapping of structural deformation to aerodynamic analysis is important, as it allows the determination of the flight or jig shape of the wing. The flight shape is the shape of the wing in flight, at a specific optimal cruise point, and the jig shape is the baseline state at which the wing starts, and in which the wing is manufactured. The standard practise is to determine a suitable flight shape which can meet performance requirements, and to reverse engineer a jig shape, Wright and Cooper (2008), based on this known flight shape.

The work of Stanford et al. (2015) explores the use of three dimensional structural models, coupled with low fidelity aerodynamics for the transfer of aerodynamic loads and static aeroelastics. This work highlights the ability to couple higher fidelity structural models with lower fidelity aerodynamics, and achieve structural, rib, and spar topology optimisation, Stanford and Dunning (2014). This work demonstrates how academic research can be condensed to reduce the reliance on a specific loads module in multidisciplinary analysis. As such this concept features prominently in this thesis, where we seek to couple varying fidelity structural models to a fixed low fidelity aerodynamics tool.

The work of Cavagna et al. (2011) is an example of low fidelity aerostructural coupling. Where low fidelity aerodynamic analysis is connected to a condensed structural beam representation. The representation and transfer of aerodynamic loads and structural deformations is achieved through matrix manipulation, and leads to rapid assessment of coupled aerostructural performance. Such models have been demonstrated in optimisation, sizing, and trade study uses cases throughout the project. Vepa (2008) is an example of how governing equations of each domain can be manipulated to facilitate the transfer of data between structural and aerodynamic domains. This work shows that aerostructural coupling can be achieved through manipulation of fundamental governing equations, and low fidelity models.

High fidelity Euler and RANS codes can also be easily coupled with structural analysis as shown in Martins (2002), where sensitivities found from lagged-coupled adjoint solvers facilitate aerostructural optimisation. The work of Kenway and Martins (2014) is an example of high fidelity aerostructural optimisation within preliminary design. This work is considered state of art in the field of aerostructural coupling and builds on

previous work by the authors in Martins et al. (2005). The work of Piperni et al. (2013) based on earlier work by, Piperni et al. (2007) shows that aerostructural coupling and analysis can be achieved at multiple fidelity levels for both the aerodynamics and structural analysis, based on load transfer from the former to the latter and the transfer of deflection vice versa. This coupling method is demonstrated successfully at various levels of fidelity, and used as a basis for aerostructural optimisation. Proving that between the conceptual and preliminary design stages, it is possible to use coupling to simulate aerodynamic loads and account for certification, in wing optimisation.

The review paper of Kroll et al. (2016) offer an overview and reference to the work on high fidelity methods for aeroelastic analysis. The method presented is based on the coupling of high fidelity aerodynamic and structural models, for accurate transfer of data between models. This facilitates static aeroelastic, dynamic, and flutter analyses. The work of Stodieck et al. (2015) is an example of aeroelastic modelling in preliminary design to aid exploration of novel design concepts and composite technology in wing optimisation. This work demonstrates aeroelastic modelling in early design can help explore, evaluate and optimise the aircraft wing structural, and aerodynamic performance.

Flutter is a dynamic non-linear aeroelastic phenomena, of concern within aerodynamic design. It refers to an unstable excitation of the structure, which induces vibration in the structure leading to catastrophic failure, Wright and Cooper (2008). This is a dynamic phenomenon and can occur at a speed which is lower than the divergence speed. It can be hard to design for in the early stages, as the detail analysis of flutter is often required. However the addition of stiffness to the structure can help to ensure that flutter risk is reduced later in the design process. The understanding of aircraft performance in the flight envelope and the implementation of efficient control during the potentially critical flight points, can be key to sizing the structure for optimal flight performance. Literature shows how aeroelastic modelling can help determine loads at critical flight points, and investigate dynamic performance, Raveh and Karpel (1999) & Raveh (2007).

Having explored the literature in the field of structural analysis and sizing during, the aerodynamics, and aerostructural coupling, we can investigate the primary performance outputs of the structural discipline; the weight and the cost. Weight estimation is a key discipline in the assessment of aircraft performance, and is closely linked to cost. This makes it paramount that we understand the impact of the structural analysis and fidelity, on the performance outputs. This allows us to gauge the level of detail required for the weight and cost analysis, when conducting multidisciplinary optimisation.

2.4.1.6 Weight

The estimation of aircraft weight, features throughout the design process, from conceptual weight figures used to gauge customer interest, through to detailed component weight assessment, so overall mass targets of the design can be met. The methods used, vary based on the stage and the nature of the design. These can broadly be categorised into three separate types: reference based estimation, statistical based estimation, and physics based estimation. This section describes briefly the underlying methodology of these various types, and highlights key examples which fit into each category. In addition the advantages and disadvantages of the types of estimations are highlighted.

A mass estimation method is judged on its accuracy and its precision. A method that can provide a weight estimate within a small percentage of the actual weight, can be gauged as accurate, however if it shows a large variation between estimates for similar aircraft, it lacks precision, Cheeseman (2014). Many methods account for only part of the structural weight, and use factors or corrections to compensate for neglected sections. When a factor is used to account for a particular quantity, it removes the causality from the estimation. Where causality refers to the ability to correctly identify all factors, which drive the estimation. Works such as Ballhaus (1947)are early examples of design driver identification for aircraft weight.

Referencing methods are used to gauge preliminary weight targets at the conceptual design stage, using performance data. These methods use specific factors to scale global performance variables, such as maximum take-off weight ($MTOW$), based on compiled statistical data. This allows the design to be placed within a design space and provides figures which can be used as selling points for a new aircraft, concepts, or derivatives. Note these methods give a single performance value, and not a detailed component breakdown. In order to increase accuracy in mass estimation, a statistical mass estimation method can be adopted. These use initial values for geometry and performance data found using reference methods, as a starting point.

These methods are common, have long standing use, and are often the basis of weight estimation at the conceptual design stages. They use known aircraft data for the formulation of equations with coded numerical values or scaling factors, for known top level design variables. The advantage of such methods is that a rapid and reasonably accurate estimate for the mass of an aircraft configuration can be established. Note an advantage of statistical methods over referencing ones is that they allow a component break down of the structure. The most well-known of these types of methods is that of Torenbeek (2013). Which offers a comprehensive and detailed methodology for calculating a global wing weight estimate, with limited information. Other similar methods are presented by Shanley (1960), Shevell (1983), Roskam (1986), and Masseanalyse (2008) amongst others. A comparison of some of these classical methods is offered in the thesis of Elham (2013).

The work of Shanley (1960) uses statistical methods augmented with loading parameters for weight estimation. This body of works recognises that overall loading, the type of loading, and the transfer of load between components has a direct influence in the design and mass of structures. An alternate method based around the loading of components can be found in Udin and Anderson (1992).These methods offer greater sensitivity and allow further transparency regarding the design drivers. However it the nature for the dataset in these methods greatly influences the derivation of the equations and hence is the primary weakness of such methods. As a result of this limitation no novel configurations can be assessed with confidence, and the understanding of design drivers is limited.

Updating traditional methods to facilitate their use in preliminary design can be achieved by coupling them with analytical tools for sizing, load estimation, and volumetric weight estimation. An example of such a semi-analytical method can be found in Macci (1996). Other authors have also proposed enhancements to existing methodologies such as Torenbeek (1992). The work of Liu and Anemaat (2013) seeks to improve the accuracy of the Torenbeek method by taking the centre of gravity of all structural components into account, in order to correct the mass estimation of each component. Many such minor improvements exist for almost all the accepted works, mentioned above. However even the most advanced corrections will not offer greater knowledge of the design at a more detailed design stage, unless higher fidelity analysis tools are used to account for physical performance.

The work of Gersch (1979) on the Weight and Sizing Evaluation (WISE) tool for preliminary design shows the move from traditional methods, to include sizing in the weight estimation process. A further example of a semi-analytical approach can be found in Ajal et al. (2013). There a bottom up sizing and analytical process is used to size primary features such as stringers, skins, spars, and ribs using simple elliptical loading assumptions. In addition this method uses Torenbeek (1992) equations, to account for non-optimum weights, torsional relief, and other non-generic features (mounting, fittings, cut-outs, etc.).

Elham (2013) offers a detailed aero-sectional optimisation methodology which can be coupled with feature sizing, similar to Ajal et al. (2013). This methods overlaps between empirical and physics based mass estimation methods, whilst keeping the analysis fidelity low. These methods can be introduced within an optimisation tool, as shown in Elham et al. (2014). The body of work encompassed by Ardema (1972), Ardema (1988), Ardema et al. (1996a) and the additional work from Chambers et al. (1996), Ardema et al. (1996b) presents a simplified physics based mass estimation methodology for a hypersonic aircraft fuselage and wings. This methodology uses simplified structural beam models and analysis, coupled with rudimentary sizing methodology to determine a more accurate mass estimate for the aircraft.

The work of Bindolino et al. (2010) utilises varying levels of fidelity to capture aerostructural information, and improve mass estimation. An older academic example of a physics based mass estimation methodology can be found in the work of Sensmeier et al. (2006). This shows how finite element modelling can be used within an analysis code to provide data for mass estimation of a wing box. A novel hybrid of a semi-analytical method can be found in Böhnke et al. (2012), which uses physics based estimation for a fully stressed beam model, to determine the volumetric mass estimation for bending, torsion, and shear loading, and provide a wing box weight estimate. This method compensates for a limited data set by updating the design space, and creating a tailor made empirical maximum-take-off-weight function for each update.

The Fast and Advanced Mass Estimation of Wings or FAME-W by Kelm et al. (1995) shows the synthesis of a physics based aerostructural method for weight estimation, using a wire frame structural model. This type of analysis at a conceptual level, shows that through the use of physics based analysis and detailed accounting of components, an accurate mass estimation can be rapidly provided. Another example of a conceptual physics based mass estimation tool can be found in Schweiger et al. (2012), where the work of the Cassidian conceptual design team is presented.

As the design process progresses many variables become fixed and it becomes easier to spot design drivers. However certification is a priority, and the aggregation of weight is deemed the best method which to achieve mass performance targets and meet certification requirements. Certain tools use a bottom up mass estimation approach, which uses the small scale and often fixed details of the component design to trace the design drivers. The method of predictive weight accounting highlighted by Cheesman and Smith (2001), shows the basis of such a mass estimation tool, which can be used at the preliminary design stage. The predictive accounting concept seeks to be applicable to as many parts of the product design as possible reflecting company design philosophy. It does this by removing the reliance on statistical methods and focusing on improved understanding of the causality, as well as controlling it. This methodology is designed to couple with computational geometry models, and other disciplinary data in order to provide a comprehensive method of mass estimation.

An example of the development of feature based mass estimation can be seen in Baker and Smith (2003) and Koeppen (2007), both of which show how features which are normally accounted for as factors within low fidelity estimation methods, can be incorporated into physics based and predictive accounting methods. Further to this a more recent study in Bes-Torres et al. (2012) shows how predictive accounting can be connected to high fidelity analysis tools within the preliminary design stage. The work of Doty (2011) shows the coupling of surrogate modelling methodology with conceptual weight estimation tools. The paper compares the accuracy of evaluation of a light aircraft wing mass in the conceptual design stage. The conceptual mass estimation equation is based

on the methodology presented by Raymer (1989). The work presents studies at various levels of DoE fidelity, and variable screening using Analysis of Variance (ANOVA) methodology, Deep (2006). The variable screen demonstrates that with the use of only design variables to create surrogates, improves the evaluation and optimisation of the design for weight.

Having noted the various methods by which mass estimation is possible, and that predictive accounting methods are preferable. It was decided for use in this research semi-empirical methods offer a more flexible, but less accurate methodology, which can be easily connect to a multidisciplinary analysis code. We must now identify how cost can be evaluated at a similar fidelity level, and what drivers are important for design exploration and evaluation.

2.4.1.7 Cost

Similar to mass estimation, reference based, factor based, and simplified performance models for costing methods can be implemented in any design stage, can give a cost figure for an aircraft. Some simplified methods are presented in works such as Greer Jr and Nussbaum (1990). The costing can be linked with the structural analysis as shown by Alvey and Emero (1967), which suggests the use of design criterion to select an optimum cost/weight design. This criterion is based on material cost, geometrical and manufacturing consideration, and can provide assessment of the overall design. However as the detail of the analysis and knowledge of the design increases, such simplified accounting of cost does not suffice to give a good performance indication. Therefore a more detailed breakdown of the production process, manufacturing, and lifecycle costs is required.

The work of Bao and Freeman (2002) is an example of costing methodology based on the accounting of cost at design phases: conceptual, development, production. This work demonstrates the development of scoring models, hierarchical process, power law cost models, and even regression models, to provide a detailed breakdown of costs at the stages identified. This capability is demonstrated in an multidisciplinary optimisation by Bao and Samareh (2000). This method works well at a conceptual level, however as fidelity increases the costing methods require more detailed information. The work of Rais-Rohani (1998) is an example of a structures based approach to cost formulation. This work demonstrates the use of manufacturing information for the design of structural components, and their subsequent costing.

Using CAD for geometry object orientated cost models is of interest in higher fidelity preliminary design systems. Costing tools can be based on many metrics but tend to use weight traditionally. Recent object oriented costing studies in the DATUM project, Scanlan et al. (2006) present object orientated cost modelling merged with

cost analysis software. A subsequent study in Thokala et al. (2012), presents a program for cost analysis and optimisation, using a hierarchical approach of aircraft components break down. Further sub categories include manufacturing technique, material, and labour. This paper highlights the use of parametric geometry in multidisciplinary optimisation studies, integrated with a life cycle cost (LCC) program, which includes a performance model analysis of the aircraft configuration. This works demonstrates the use of geometric variables in an activity based costing approach.

The work of Reeves et al. (2010) shows how the concept of affordability can be used to create tools capable of identifying cost drivers. This work shows how the breakdown of work processes by cost, and the integration of cost estimates, with accounting of risk and uncertainty leads to a better understanding of the cost. Although such a code may not provide as detailed a break down as the costing processes must also integrate uncertainty management in the design. Gantois and Morris (2004) present a methodology for integrating cost optimisation with multidisciplinary constraints. The costing methodology presented by the authors is based on the hierarchical breakdown of the structural components into their base components, and the calculation of the assembly, manufacturing, and material cost of creating the base component. This method is used to traverse backwards through the component hierarchy, and aggregating the cost at each level, until a cost estimate can be found for the structural component. This is similar to the predictive accounting methodology used in weight estimation tools.

The DATUM model has been extended to aircraft design and is shown to be effective for academic studies, Thokala et al. (2012). It is therefore utilised in the academic research in this thesis, as it has similar methodology to the CADCO cost tool for industrial cost estimation in MDAACE.

2.5 Justifications for the use of Structural Fidelity and Problems with Industrial MDO

Having looked various multidisciplinary systems, optimisation methods, and disciplines interconnected in aircraft design. It is now important to focus on how structural models are represented in some state of the art multidisciplinary programs, and what justifications are prominent, with regards to choice of analysis fidelity to instigate optimisation. The aim is to identify how limitations can be avoided in the program developed for research in this thesis. The aim of this thesis is to have real physics based, design exploration, and optimisation based reasons, to justify the choice analysis fidelity. However first we must identify what justifications are given in literature.

The work of Piperni et al. (2013), is an example of utilisation of high fidelity analysis in multidisciplinary optimisation without express justification, barring a set standard.

In this work there are issues regarding the suitability of the fidelity level choices for this application, and the justification for these choices. The overall goals of the system established, is the optimisation of the aircraft for global performance, and the models are designed to achieve this goal. The lowest fidelity model however only seeks to provide structural properties and stiffness information thought static and dynamic aeroelastics, in addition the sizing of this stick model is done to meet the stiffness requirements. As there is no direct global optimisation featuring this level, it becomes apparent that the variable fidelity provided here seeks to deal with the issue of data overhead rather than optimisation directly.

This is contrast somewhat to the work of Kenway and Martins (2014), where the focus is on having a structural model of a sufficient fidelity, to allow high fidelity aerodynamic optimisation. The goal to provide stiffness data, for the purposes of aerostructural analysis. However the comparable model fidelities from aerodynamics to structures are not similar, and there is a shell element structural model adopted for this research. This is not reflective of complex company specific finite element models. The only justification for the level of fidelity is to emphasize, and enhance the aerostructural methodology proposed. Therefore there is a distinct separation between the fidelity in this research and the equivalent models in an industrial tool. The authors acknowledge this, and propose to remedy this by including greater fidelity in the structural models. However in this work the appropriate structural model fidelity for multidisciplinary optimisation is not investigated, and instead set specifications are matched.

The work of Bindolino et al. (2010) is a more refined example of fidelity decomposition. The work present two distinct levels of fidelity, with a focus on global performance optimisation for weight. The first is a global behaviour model in one dimension, followed by a second higher fidelity wing box, with structural elements for sizing. The third and final level is a verification fidelity level designed to facilitate aeroelastics, and design of specific components. Note for these levels there is coupling introduced through the use of mathematical functions relating to the design variables, and performance outputs. The aim of the studies conducted using this system is to explore the mass optimisation capability for various structural levels. However the lack of aeroelastics at each fidelity levels is a limitation of this work, where the decomposition approach adopted, whilst interesting is not reflective of more complex models which utilised more often. The authors justify this by highlighting the importance of structural fidelity variation in the mass studies, however no concerted effort is given to the justification of these fidelity choices.

The work of Brezillon et al. (2012), is research in the area of multidisciplinary optimisation. With this in mind the program and the structural model established are reflective of a three dimensional model of higher fidelity. This reflects detailed global finite element model of a wing, similar to those at the preliminary design stages. The level of detail entailed in the aerostructural coupling, and the primary and secondary

aircraft structural sizing, is presented as a means by which to incorporate global multidisciplinary optimisation. The overall aim of this work is to gain marginal performance improvements on a design, which has already progressed to have fixed global design variables and performance ranges for certain characteristics. This work correctly justifies the need for complex and high fidelity models featuring physics based structural sizing, and domain coupling, as the means to demonstrate the developed capability.

Aerostructural research conducted by Cavagna et al. (2011) is based in the conceptual design stage, where beam models are given structural elements, and mass properties determined through sizing. The analysis of these beam models is primarily used to support stiffness calculations, required for the coupling. In addition to the beam models, some equivalent plate models are generated to be more representative of complex models, but the focus is on generating stiffness information for aerostructural analysis. Therefore the disparity in the nature of the models when compared to equivalent fidelity models in different codes, is large. The justification for these chosen levels is not expressly given, but it is clear that the authors aim to minimise the level of structural fidelity to conserve computational cost and have successful aerostructural analysis.

Mastroddi et al. (2012) is an example of a global optimisation study which prioritises the creation of Pareto fronts for design exploration, at the preliminary design stage. The aim is to achieve a global performance improvement for a large structural model of the full aircraft, using high fidelity. As the focus is on global aircraft performance, many of the design variables are top level, and relate to the aircraft configuration directly. However as the model is high fidelity, the number of design variables, and the complexity of the optimisation problem, is also high. The justification of this high fidelity is the need to precisely understand the design space, however this is counterproductive, as the level of detail required to instantiate the Pareto front, forces the design space to be constricted to a local region. The system does not acknowledge the benefit of lowering the fidelity in the given model, to achieve greater design space exploration, but remarks at the need for accuracy. This work like many other either cites, accuracy, standard practise, or its own new methodology as the reason for the higher fidelity models.

The work of Zhang et al. (2008) introduces a single fidelity finite element model as a double sandwich beam, including feature details such as spars, skins, and webs. The authors use various kriging methods and the structural model, to analyse a wing at a given flight point, allowing top level design variables such as span, taper, sweep to impact the structural model geometry. The authors create a performance based optimisation problem, featuring wing mass and drag performance as objectives, and proceed to evaluate a set of uniform design variables, which are used for response surface creation using three different methods (polynomials, radial basis functions and kriging). The authors deem that for the given data set and flight point, and any given structural model and aerodynamic/aeroelastic analysis, that kriging and radial basis functions show the most

promise for surrogate creation, which can facilitate optimisation and design space exploration. This work does not tackle the problem of data over head, for sizing, structural analysis, and fixed information for high fidelity models.

Finally we must briefly discuss the fidelity justifications in MDAACE, where the focus of system is the structural sizing. Here the creation of a sizing process, where empirical buckling modes are imprinted on the three dimensional shell element finite element model, forms a limiting factor in the analysis fidelity choice. Therefore MDAACE, is forced towards a fidelity level which is removed from the previous conceptual studies. This enforces the data overhead between design stages. In addition this focus on rapid sizing limits the design exploration capability in MDAACE, and the optimisation potential. By creating a complex non-linear relations which cannot be reasonably validated by previous conceptual tools, a disparity is created between design stages. This issue stems from the inability of the finite element model to be to interface with conceptual or detailed design tools. If varying fidelity models built incrementally from conceptual to physics based sizing were used, there would greater scope for design exploration and multidisciplinary optimisation, whilst tackling the data overhead problem.

From the case studies it is clear that there are three predominant reasons for structural fidelity justification in multidisciplinary analysis programs and codes; the need to meet some set standard requirements, the need to satisfy information required for a given methodology, and the need to achieve accuracy at the given design stage. Whilst all three reasons are valid and understandable, they lack any substance for the purposes of multidisciplinary optimisation, which many codes linked to these models aim to achieve. In addition by trying to achieve one or a multitude of these three justifications, the research often fails to explore if there is a need for such detail or computational investment in structural fidelity. This leads to models which either do not align to use in complex structural codes, or which align to these complex codes but do not offer significant optimisation and design exploration capability, and often solve a smaller tailor made problem. The work in this thesis differs as it identifies the nature of multidisciplinary systems, and seeks to locate a structural fidelity level which can provide a balance of computation speed and accuracy. In addition understandable, relatable and quantifiable, performance outputs are provided which can help achieve design exploration and multidisciplinary optimisation, within existing constraints.

Chapter 3

Framework for Evaluation of Transport Aircraft Wing

3.1 Introduction

This chapter presents the Transport Aircraft Configuration Evaluation program (T.A.C.E), developed to explore the variation of structural analysis fidelity, for aircraft wing. Features of this program include the robust, reliable and accurate assessment of the aircraft wing, with modularity, speed, and focus on physics based structural analysis and aerostructural coupling. The overall system layout and process can be seen in figure 3.1. The details of key disciplines and performance assessment within T.A.C.E are discussed in sections 3.2.2 and 3.2.3.

The focal point of the T.A.C.E process is the structural fidelity and analysis. Most disciplinary tools in this program are fixed (in terms of fidelity and type) for the purposes of the research conducted. T.A.C.E provides access to three distinct levels of FEM fidelity around which further physics based assumption(s), and analyses are implemented. These include a beam wingbox model (level I), a simplified three dimensional wingbox model (level II), and a detailed three dimensional wingbox model (level III), all of which are created within Abaqus, Dassult (2015).

3.2 Transport Aircraft Configuration Evaluation Framework for Wings

3.2.1 Architecture

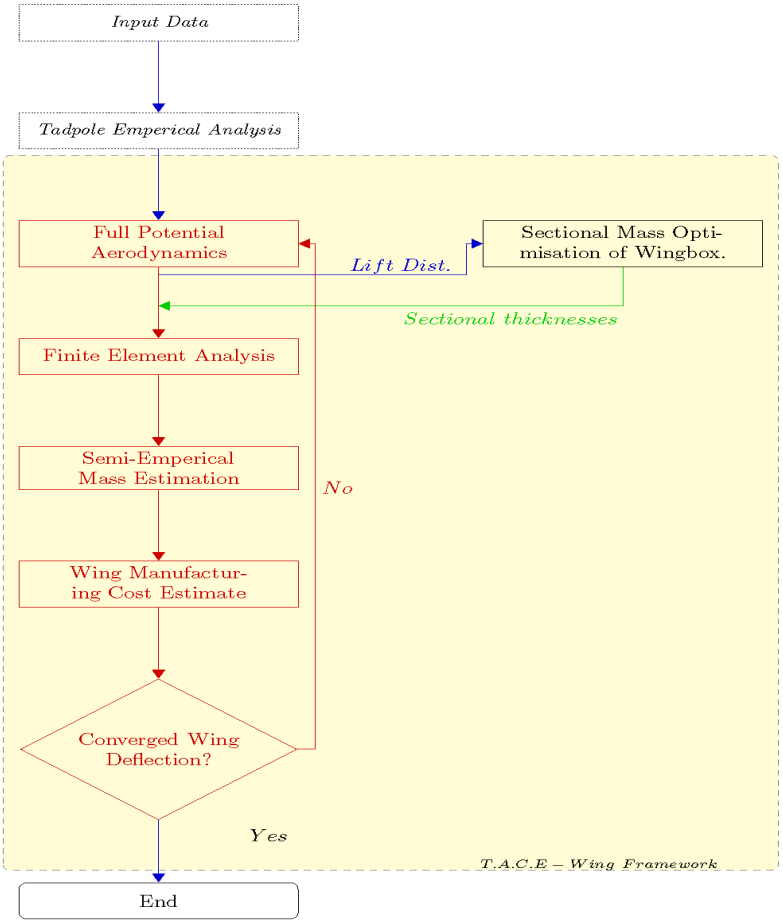

Figure 3.1: T.A.C.E wing analysis process.

Figure 3.1 represents the T.A.C.E program layout. Here the analysis process chain illustrated by the blue arrows is representative of a single analysis chain, and the red arrows indicate an iterative analysis chain, whereas the green arrows represent an external input into the process. The geometric definitions of the wing and the flight conditions form the basis of the initial inputs into this system. This information is processed by the conceptual design tool, Tadpole, which provides relevant, empirical, and validated data for the performance of a given aircraft wing. This data is taken through an analysis chain initially, following which information is sent back to the full potential aerodynamic analysis, which is coupled with the FEA solver for successive iterative re-evaluation of the wing, until convergence.

At each level of structural fidelity within T.A.C.E the aerostructural coupling can be varied fidelity to increase or decrease analysis complexity and computational time. Mass optimisation and estimation modules are included to provide information for structural analysis, updated wingbox geometry, and maximum take-off weight for aerodynamics and finite element analysis. The aerostructural loop utilises the analysis tools within

the single point analysis chain, without Tadpole, to achieve a static aerostructural convergence, where the deflection of the structure is used for analysis convergence. Within the loop the structural deformation is used to twist and deflect the wing within the aerodynamic analysis, updating the wing flight shape.

3.2.2 Fixed Fidelity Domains

3.2.2.1 Tadpole: Methodology and Utilisation

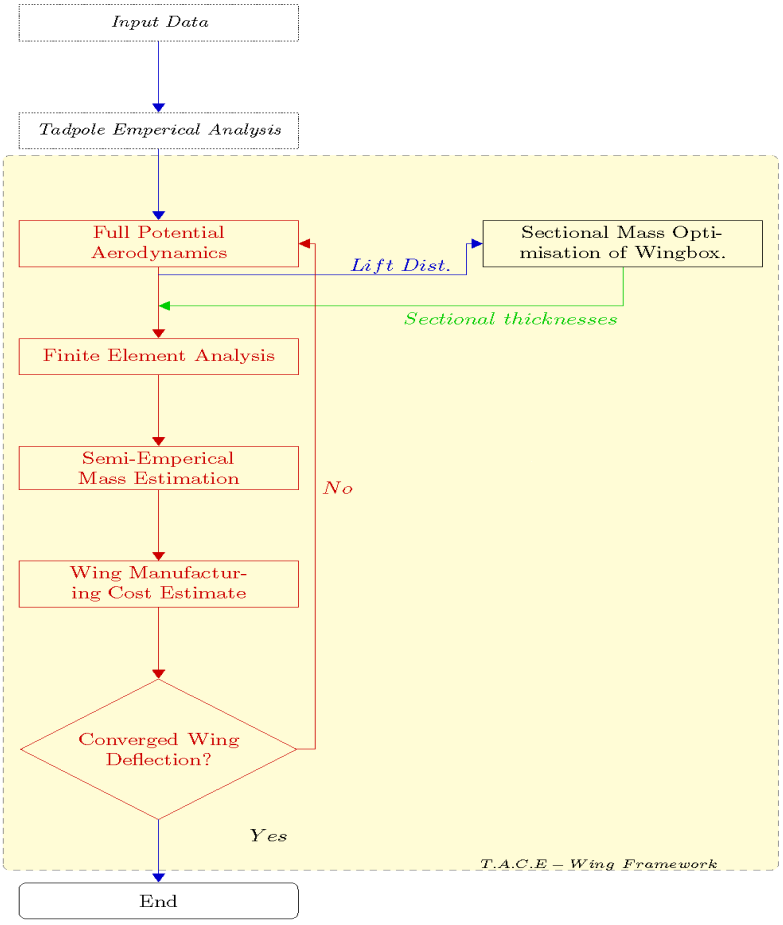

Tadpole is a conceptual design program created and calibrated in an industrial setting, which is part of a conceptual wing design tool, presented in Cousin and Metcalfe (1990). Its features include the choice of various aerodynamic analyses, two semi-empirical wing weight estimation methods based on Torenbeek (1992) and standard practice respectively. As part of T.A.C.E, it is used to assess the performance of the conventional aircraft wings, using top level geometrical information seen in table 3.1. Here Tadpole is configured to evaluate the wing design using empirical CFD and calibrated weight estimation. The output performance characteristics of note are, wing weight (W_{wing}) , $\frac{D}{q}$ (a non-dimensional drag performance criterion), wing volume (V_{wing}), and undercarriage bay length (UC_{bay}), Keane and Nair (2005).

There are several advantages to using Tadpole within T.A.C.E, the foremost of which is the nature of the tool. The underlying physics and design principles integrated within, reflects best practise in conceptual design at the time, and data for higher fidelity analysis is output. This facilitates fast, and reliable (within a conventional design space) trade off and optimisation studies. A further advantage of this tool is that it offers multidisciplinary evaluation of a given design. These advantages do not however completely overcome the fundamental limitation of this tool: the data set.

The performance trends from the empirical data within Tadpole are limited to a conventional transport aircraft and are not reliable when investigating novel designs and modern aircraft families; which feature design and technology improvements. A linked limitation is the calibration of numerical factors and assumptions within the tool, which are fixed to reflect design limitations, when the tool was created. However the relatively low fidelity, high speed, and multidisciplinary nature of the tool, make it ideal for initial performance estimation and analysis within T.A.C.E.

Table 3.1: Wing design variables

Wing design variables	
Variable Symbol	Definition
SG	Wing area
AR	Aspect ratio
$SWPI$	Leading edge sweep
λ_1	Inboard taper ratio
λ_2	Outboard taper ratio
h_{k}	Trailing edge kink position
t/c_{r}	Root thickness/chord
t/c_{k}	Kink thickness/chord
t/c_{t}	Tip thickness/chord
w	Washout at tip
k	Fraction of tip washout at kink

3.2.2.2 Geometry

Following conceptual design evaluation, the T.A.C.E program creates CAD models of the wing. For the beam model fidelity level I, the three dimensional geometry is created within the Abaqus software Dassult (2015). The visual representation of three dimensional geometry in levels II and III is achieved via the Solidworks tool, Systemes (2015), using the equation driven parametrisation capability, applied to the wing box model seen in figure 3.3. The process for this geometry creation is shown in figure 3.2.

Methodology and Assumptions The parametric wingbox model is automated via macros, and driven through a design table functionality. The macro is accessed directly for model instantiation, parametrisation, and finite element model creation. The model

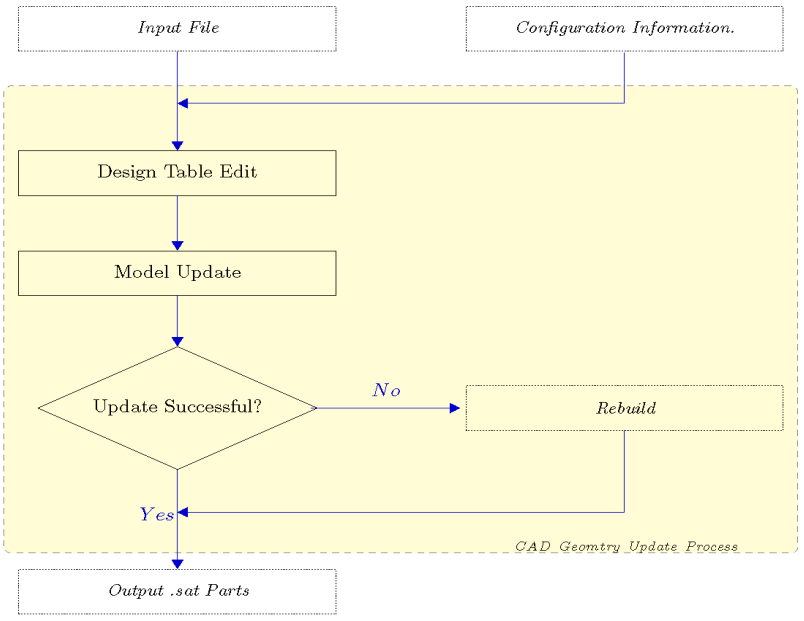

Figure 3.2: Wing-box three dimensional CAD model geometry instantiation process.

separated into three distinct parts, which are automatically stored in an accessible format (.sat), for automated creation within Abaqus. For the design table, simple design rules were captured as equations and used to derive new configurations for the wing box.

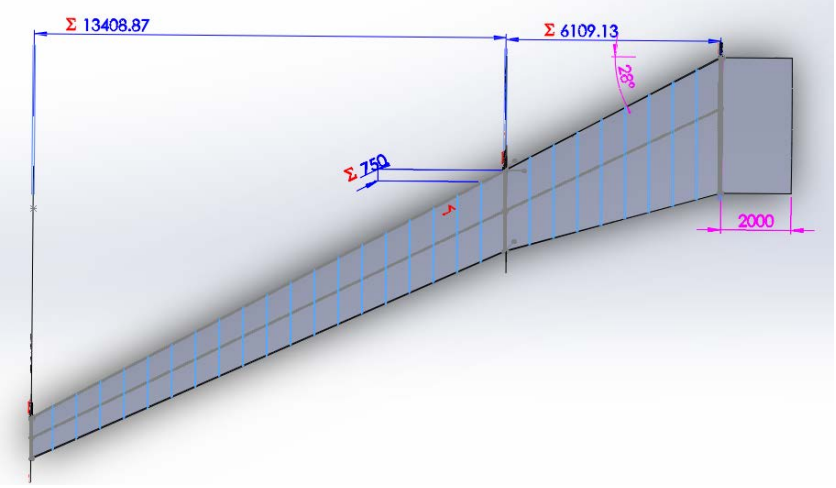

Figure 3.3: Wingbox parametric CAD model within Solidworks, with some annotated dimensions (rib spacing, outboard and inboard wing span, and wing sweep.

The model was designed to be generic, and robust, including only essential structural features of the wing box (covers, spars, ribs), so that additional detail can be integrated within the finite element model. It was constructed using loft features and linear patterns from root to kink, and kink to tip, where the linear patterns are intersected with

the loft features, to create enclosed ribs within the wing box volume. Abaqus scripting capabilities allow the customisation of each model for specific analyses, reducing computational and memory cost associated with detailed CAD models.

3.2.2.3 Full Potential Aerodynamics

Process In order to capture aerodynamic loads the full potential method implemented in Matlab by Toal (2009) was used. It requires the creation of a wetted surface without the need for CAD geometry, as an input. Turbulence modelling is not utilized, but good correlation with existing test cases has been shown as part of optimisation studies by Keane and Petruzzelli (2000a) and Thokala et al. (2012). The overall analysis process for the method in T.A.C.E can be seen in figure 3.4.

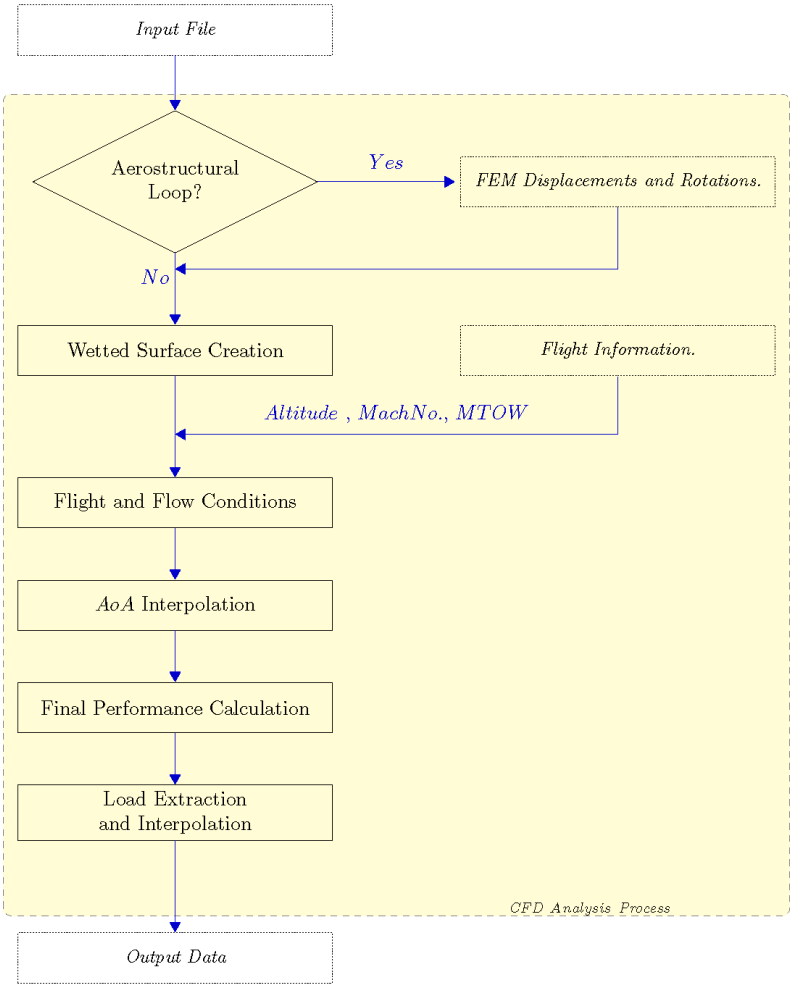

Figure 3.4: Computational Fluid Dynamics analysis process

Aerodynamic Analysis Settings The method implements section specific aerofoils at given spanwise locations, with twist, and crank, providing that leading and trailing edge (LE and TE) coordinates and twist are given. The wing is generated in sections,

the number of which is a user input, however a minimum of three sections at the root, crank, and tip are required. These sections are used for spanwise interpolation to create a wetted surface in three dimensions, for which the flow field can be solved and aerodynamic forces calculated. The surface is meshed using conformal mapping, using a grid generator module. Other modules include the flow solver, and postprocessor (to calculate aerodynamic coefficients, for each aerodynamic wing section).

The method requires flight condition information (altitude, Mach number, temperature (T), density (ρ), and pressure (P)), in order to calculate the lift and drag coefficients (C_l and C_d) for the wing. To determine these coefficients assumptions are made regarding the flight envelope. It is assumed that the cruise case is of paramount importance, which is not reflective of certification methodology. The calculation of flight atmospheric properties can be achieved using the international standard atmospheric relationships. However it is not possible to introduce complex aerodynamic phenomenon within the full potential method to simulate complicated load cases such as manoeuvre(s), taxi, take off, and gust(s).

To take certification into account a factor of 3.75 (representing the 2.5g maneuverer case and a 1.5 margin of safety) is applied to loads extracted for FEA application. To determine the required lift target and angle of attack (AoA), the maximum take-off weight value extracted from Tadpole is used, with each wing expected to generate lift equivalent to $\frac{1}{2}$ of the maximum-take-off-weight. To determine the angle of attack it was assumed that for the angles of attack of between zero and five for the chosen aerofoil, the lift curve slope is linear, with an expected positive gradient. This assumption is used to conduct an interpolation, to determine the required angle of attack for a given lift target.

All wing configurations are initially analysed at an angle of attack of zero and five degrees, and the lift was determined for each. From this, interpolation using the lift target is conducted and an interpolated AoA providing the appropriate lift is found, for which the wing is re-analysed. This is applied to the pre-twisted (Jig) shape of the wing fixed at -4.5 degrees at the wing tip. Within the aerostructural loop for the three dimensional model, the AoA upper bound is changed to be the previous AoA minus an increment of 0.25, helping to prevent divergence from changing wing twist and displacement. This removes some inaccuracies in the AoA interpolation. From the flight conditions and geometry, lift and drag calculations can be run. The output(s) include the coefficients of lift (C_l), drag (C_d), and pressure (C_p).

3.2.2.4 Weight Estimation

Process The mass estimation process is a semi-analytical, and uses the volumetric weight of the wing box from the aerostructural loop, prior to which optimisation has

been conducted, and structural mass inputs have been fixed. The use of loading from static aerostructural convergence, and the sizing of spar, ribs, and panels is accounted for in the primary volumetric weight figure. The method presented here differs from Tadpole program for the basic weight calculation, which is a by-product of the structural analysis in T.A.C.E.

Weight Estimation Methodology and Assumptions The foremost input for the weight estimation module, is the volumetric data of each structural component in the finite element model, excluding the extension. This information can be extracted directly from the model output database. The extracted volume and material density from table 3.3, gives the basic wing mass (W_{basic})

$$W_{\text{basic}} = 2(\rho_{\text{material}} V_{\text{wingbox}}) \tag{3.1}$$

Which is used to find the primary wing mass (W_{primary})

$$W_{\text{primary}} = W_{\text{basic}} + W_{\text{non-opt}} \tag{3.2}$$

This differs from the basic weight estimation within Tadpole, however the calculation of the non-optimal weights remains identical to ensure consistency, as the fidelity of the structural model increases. The non-optimal weight ($W_{\text{non-opt}}$) includes features such as engines, and landing gear amongst others (equation 3.2) to give a primary wing mass (W_{primary}). The overall mass of the wings is then subject to addition of leading (W_{le}) and trailing edge (W_{te}) structure masses.

Tadpole can use calibrated mass estimation which is automated and based on the discretization of the wing into sections and features, with in-built correction factors for wing features. This method is proven in previous research and as shown by Keane and Nair (2005), captures sensible weight trends. In order to compare directly between mass estimation methods in Tadpole and T.A.C.E, a further assumption was added to capture additional components. These additional components are assumed to account for an additional10%, added to the overall mass of the wings. This assumption is directly from the work of Keane and Nair (2005).

The estimation of maximum take-off weight is not fixed based on the output of the Tadpole estimation, which provides and initial estimate. As a new mass of the wings W_{wings} is determined, the maximum take-off weight is recalculated by removing the Tadpole wing mass W_{wtad} and adding the W_{wings} from T.A.C.E, and the change in maximum take-off weight is iteratively minimised, till convergence. This mass estimation module is calibrated using Tadpole and Torenbeek for a baseline configuration in section 4.2.

3.2.2.5 Cost of Wing Production

Process The cost model is the acquisition model developed by Thokala et al. (2010) and used for optimisation in Thokala et al. (2012). The model is part of the Life Cost Cycle (LCC) program, and implements a hierarchical component layout to categorise costs associated with detailed structural components of the wing, as simplified in figure 3.5. The cost is accumulated through aggregation of raw materials, manufacturing, and resources for each major sub-structure of the wing (skin, spar, ribs, and stringers), using geometrical and mass information. The inbuilt knowledge base in the tool is used to populate a dataset, from which costs are accumulated and aggregated, to give a wing manufacturing cost in US Dollars ($). For assessment of accuracy and precision the results from this academic cost suite are compared for equivalent aircraft configurations, with results from the MDAACE cost tool, CADCO. The result of these comparisons are found in chapter 4.

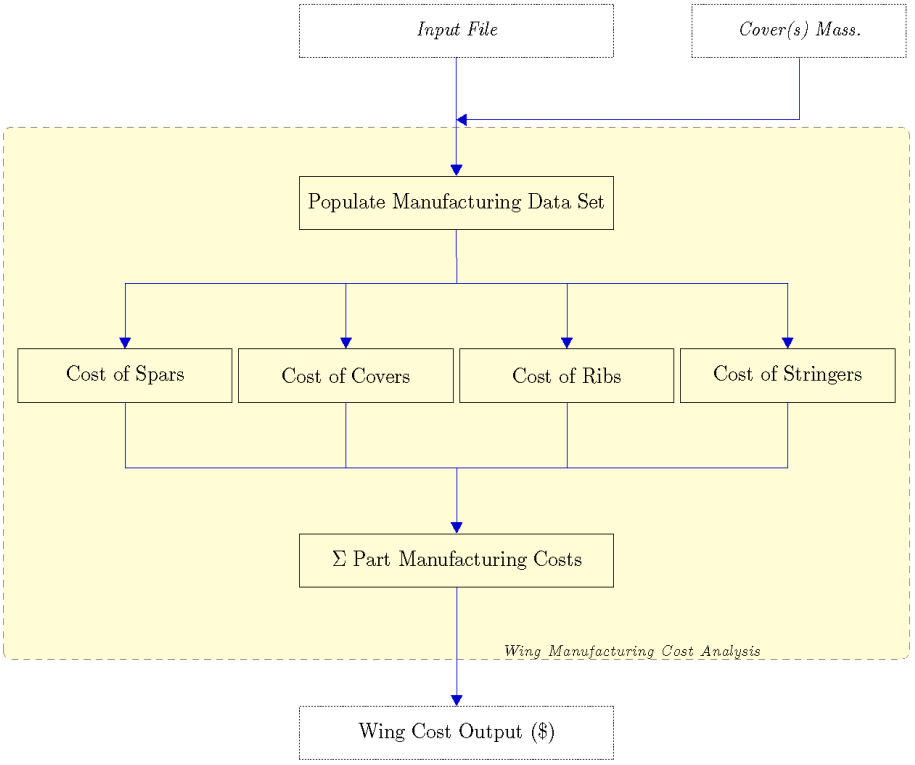

Figure 3.5: Wing manufacturing cost analysis process.

Cost Estimation Methodology and Assumptions The primary inputs to the cost model are the top level geometrical variables and the mass of each wing cover. The model hierarchy is based on the wing structural layout, and instantiated in an object orientated environment, allowing tracing of wing components. Detailed cost information is calculated based on libraries of design rules, material, and costing information (such as buy-to-fly ratios), all of which are stored within the knowledge base of the tool.

This knowledge is used to create data sets of information for each subcomponent, where the raw material, manufacturing and resource costs are noted along with geometrical information.

3.2.3 Varying Fidelity Domains

3.2.3.1 Structural Models

The analytical representations of the wingbox structure within Tadpole and the mass optimisation module, offer an estimate of wing mass for aerodynamic target lift generation, and fix the mass for stress analysis. Details of these analytical models can be found in their respective sections 3.2.2.1 and 3.2.3.3. The analytical representations form the basis of initial structural performance estimates, and reduce the data overhead in the assessment of structural performance at a higher level of fidelity within T.A.C.E. The next highest level of fidelity for the structural models is the beam model (Level I).

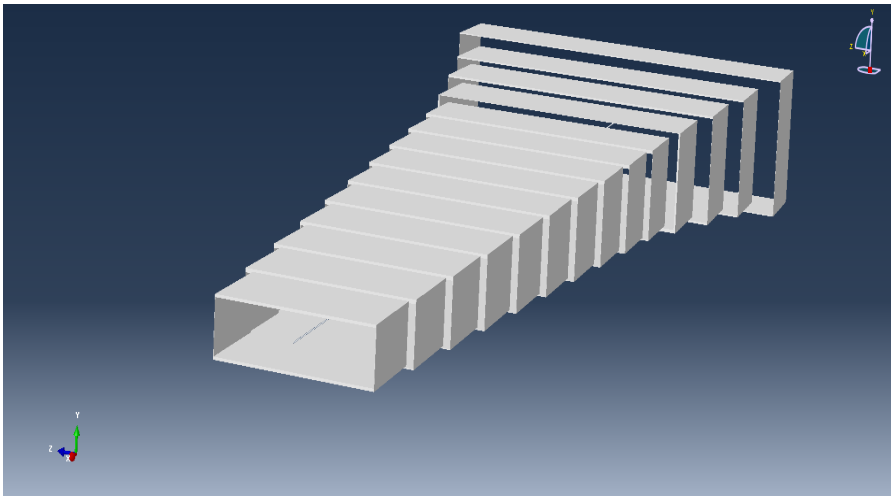

Figure 3.6: Wingbox beam structural FEM with rendered sectional profiles as viewed in Abaqus GUI.

Beam Structural Model The beam structural model allows the fastest aerostructural evaluation. The data transfer for aerostructural analysis at this level is limited to structural deflection. Fundamental bending behaviour and aerostructural analysis, facilitates rapid exploration of known and novel design spaces using this level. The beam model can however limit the exploration of performance characteristics, which are a result of perturbations in wing sweep. Physical phenomena such as torsion, which influence structural behaviour cannot be accurately captured at this level. To counteract this further modifications to the beam structural model are required. Once such modification for the torsion, can be introduced within the analysis, to improve the analytical consideration for torsion. The details of this can be seen in the mass optimisation module in section 3.2.3.3.

3D Structural Model The three dimensional wingbox model (fidelity level II) offers an improved aerostructural convergence; as rotational information can be extracted in addition to the displacements. The three dimensional CAD model is utilised within the Abaqus environment to produce a model which includes covers, spars, and ribs, but no stiffeners. Due to a lack of stiffeners at this level of fidelity the sections are optimised for bending with additional consideration for torsion and shear. This is achieved via improved load transfer through the coupled wing box features. The overall volumetric data extracted (for covers and ribs) from this model improves the accuracy of the basic wingbox mass estimation, increasing the fidelity of mass estimation and accuracy of the wing mass trends in section 4.3. At this level a larger choice of loading methods is available as pressure loads can be appied in uniform, spanwise, or sectional distributions. An example of a three dimensional model at level II can be seen in figure 3.7.

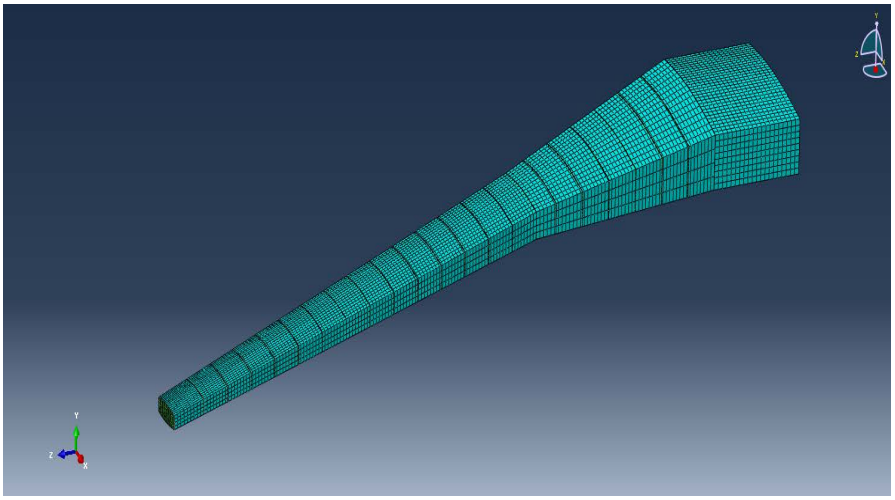

Figure 3.7: Wingbox 3D structural model with visible mesh.

3D Structural Model with Stringers Fidelity level III offers the addition of stringers to the three dimensional finite element model and mass optimisation using finite element analysis based stress constraint evaluation. The stringers alleviate cover and spar stress, improving the structural behaviour and mass optimisation. These stringers can be fixed inputs from known data or sized (using analytical certification failure modes) within the T.A.C.E mass optimisation loop. The improved physics based analysis, methodology, certification, and greater accuracy in structural performance (linear and nonlinear) makes this level computationally expensive but theoretically offers the best opportunity for design optimisation prior to detailed preliminary analysis, improving the design space exploration. At this level in the structural analysis the stress is being driven using physics based analysis. Therefore non-linear behaviour is likely to be expected due to the interaction and competition between these aeroelastic and structural disciplinary optimisation.

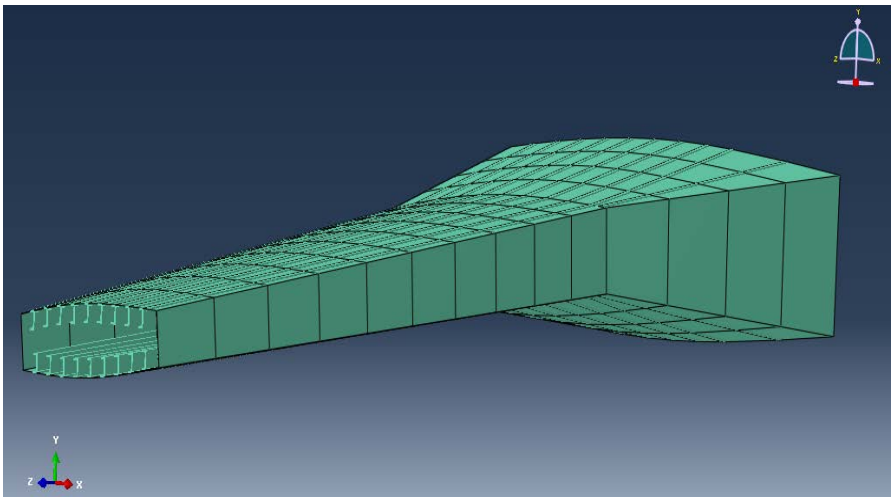

Figure 3.8: Wingbox three dimensional model with stringers, with rendered stringer profiles.

3.2.3.2 Structural Anlaysis with Finite Element Modeling

Structural Analysis Process The structural model is the focal point for fidelity trade studies and provides performance outputs which propagates through the T.A.C.E analysis process. There are three distinct levels (I, II, and III), and each can be modified and altered in terms of assumptions and analysis parameters. The customisation of these baseline models, and their inputs is discussed further in chapter 4, here the underlying assumptions and construction methodology are presented. For finite element analysis, a static general step was chosen, such that a static stress analysis could be conducted and the output stresses, displacements, and rotations extracted. The Abaqus input and output units can be seen in table 3.2.

Table 3.2: Abaqus SI units of measurement

Quantity	Units
Length	mm
Force	N
Mass	Tonne
Stress	N/mm^2
Energy	mJ
Density	$Tonne/mm^3$

Structural Analysis Methodology and Assumptions The fidelity level I process in figure 3.9 creates a truss beam structure without ribs within Abaqus, where the geometry is based on top level geometrical parameters, spanwise increments from aerodynamic analysis, and mass optimisation output thicknesses. The overall turnover time of this level following the finite element analysis process is seconds. All fidelity models feature an extension which connects the wing through the fuselage, and as the model is only for one wing, only half of the extention is modelled from the fuselage centreline.

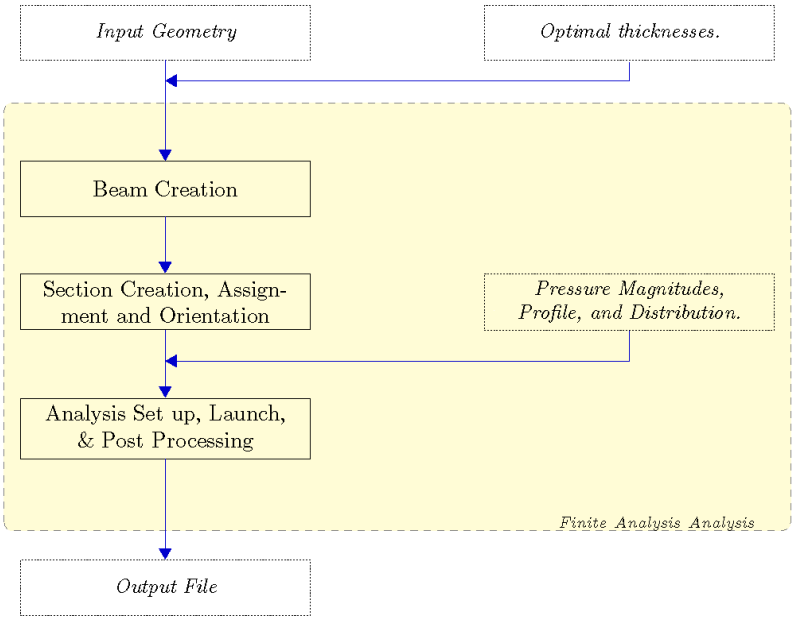

Figure 3.9: Beam structural model analysis process

Table 3.3: Material properties of Aluminium alloy 7050-T7451

Mechanical Properties (Units)	Value
Density ρ_0 ($\frac{\text{kg}}{\text{m}^3}$)	2900
Ultimate tensile strength MPa	524
Tensile yield strength MPa	469
Modulus of elasticity GPa	71.7
Poisson's ratio	0.33
Shear modulus GPa	26.9
Shear strength MPa	303

For level II and III finite element model, appropriate parts from CAD are uploaded within Abaqus. To ensure the quality of model for multifeature parts such as ribs, each rib is loaded individually and meshed independently, all meshed ribs were merged to create a singular part. The material used for all features (covers, spars, ribs) can be seen in table 3.3. The cover is partitioned in the spanwise direction at wetted surface section locations, of the aerodynamic model. This aids displacement and rotation extraction for use in aerostructural convergence, as exact nodal displacements and rotations can be extracted. The thickness assignment for the extension, and ribs varies for each model. The entire, instantiation, pre-processing, analysis, and post processing is shown in figure 3.10, where 3.11, is an example of a partitioned level II finite element model.

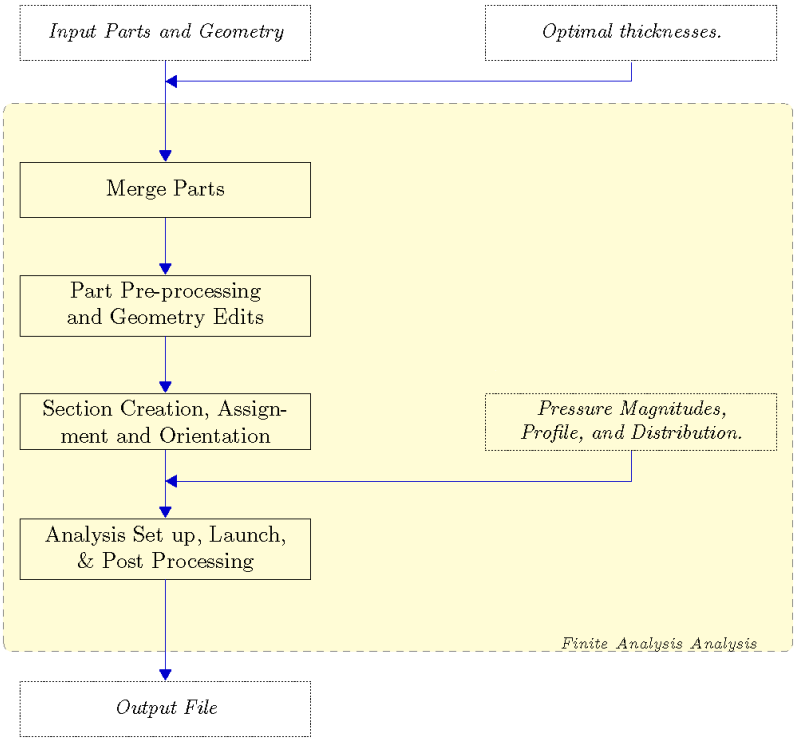

Figure 3.10: Three dimensional structural model analysis process.

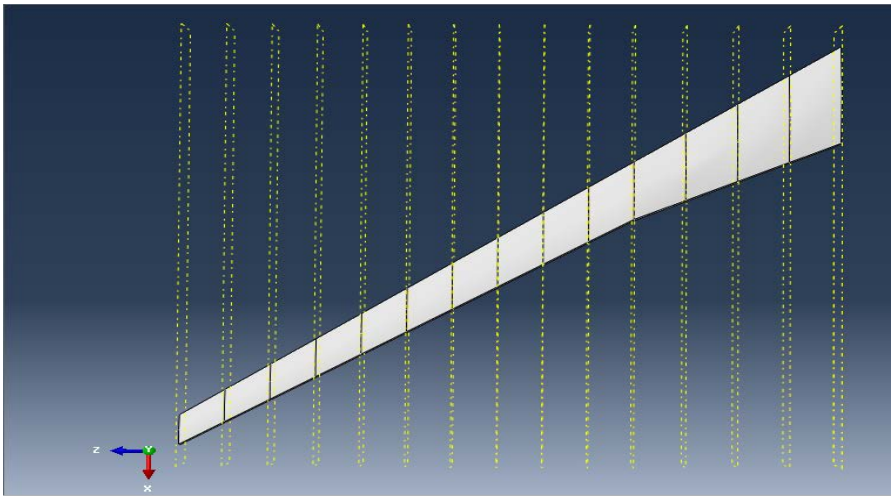

Figure 3.11: Three dimensional finite element model cover partitioning for loading, section assigment, and output extraction.

At level III the stringers are modelled for the covers. These are created via definition of partitioned edges and have distinct sizing inputs and profiles, which are created as sections, and are orientated and meshed prior to analysis. The section profiles can be created arbitrarily, through coordinate data, or pre selectable profiles (I or J for example) within Abaqus. The instantiation of the stringers requires the calculation of geometrical locations, quantities, sizing, and placement, all of which increase the overall computational time of the analysis (3.12).

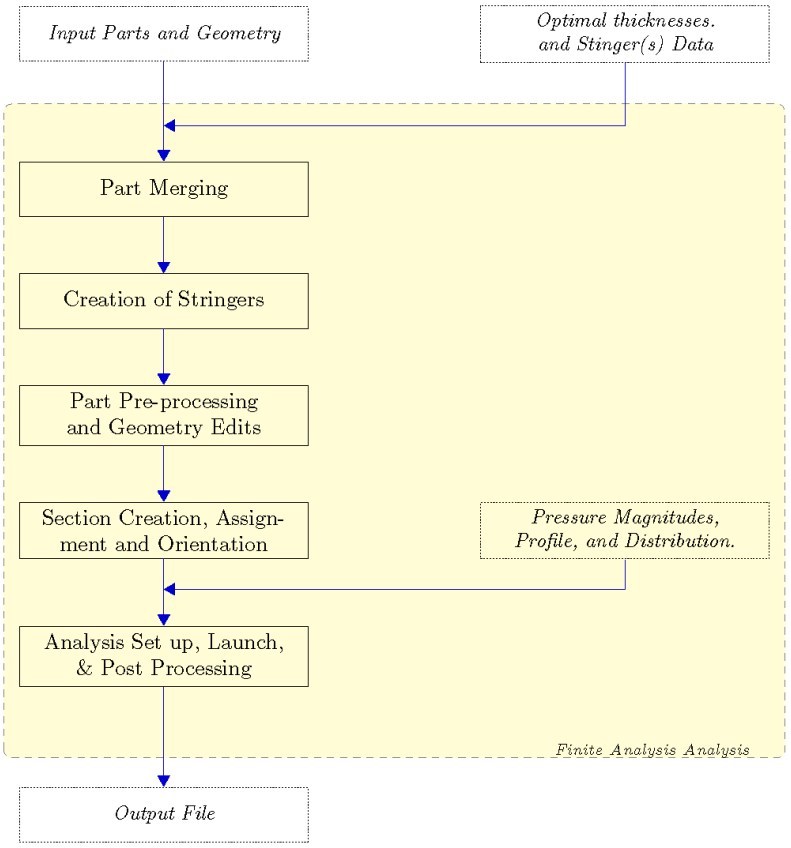

Figure 3.12: Three dimensional finite element model with stingers, analysis process

One direct boundary condition (BC) is applied at all fidelity levels to simulate restrictions on the wingbox. The extension is fixed with no lateral or rotational motion at the fuselage centreline. This ensure that the maximum stresses observed in the models are not localised at the wing root. A constraint at the wing root would introduce local deformation and higher stresses, which are physically inaccurate as some load is transferred to the carry through structure. In order to avoid further localisation of stress in the extension from this BC, the local region of the shell elements in the extension are reinforced by a factor of three, when compared to neighbouring faces on the wing box. This reinforcement creates a damping effect between the loads transferred from the wingbox to the carry through, and offers a more realistic structural boundary condition.

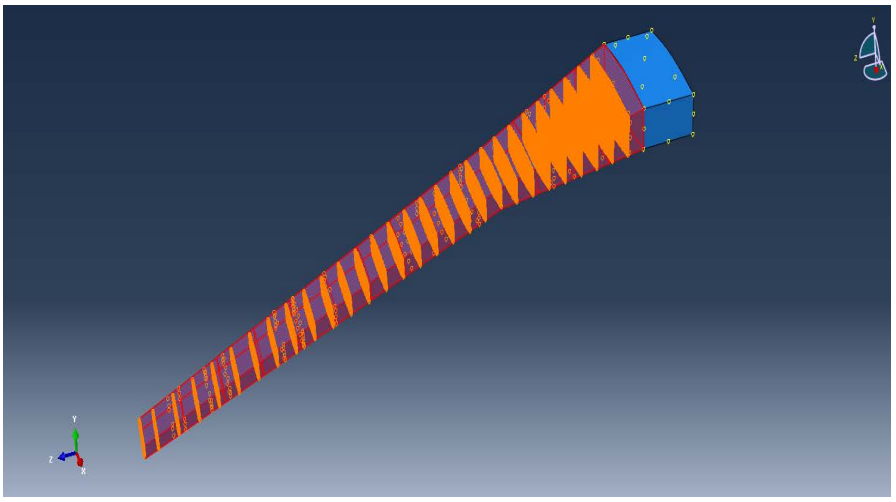

Figure 3.13: Example 3D wingbox FEM wing cover to ribs tie constraint, where the orange and red highlighted areas represent the ribs and cover respectively.

In order to ensure correct load transfer between the ribs, covers, spars, and between the wing box and the extension, tie constraints were used in levels II and III. This type of constraint allows connection of two surfaces; a master surface which dictates the behaviour, and a slave surface which reacts to loading or constraints on the master surface. A tie is placed between the wing box cover and the ribs, where the former is the master and the latter is the slave. Another similar constraint is placed between the extension and the outer surface of the cover, including the spars. The extension is the master in this constraint, as the cover is already constrained to the ribs. The application of the rib to cover constraint can be seen in figure 3.13.

The beam model has no ribs to size and the mass optimisation thicknesses are applied directly to the box section. For the 3D models this is somewhat more complicated, as in addition to the optimisation thickness outputs, sectional properties are required for the ribs. To size the ribs, it is assumed that no critical ribs are present, and a light rib is present at all rib stations. Therefore a minimal thickness approach to rib sizing is adopted, to ensure uniformity in rib sizing and the subsequent weight estimation. The penalties for critical ribs are taken into account during weight estimation. The ribs are sized for minimal thickness (t_{r})

$$t_{\mathrm{r}} = \frac{t_{\mathrm{ro}} B}{s} + \left(\frac{\eta_{\mathrm{f}} W_g B C}{2 d_{\mathrm{ri}} S G \sigma_{\mathrm{sa}}} \right) \tag{3.3}$$

Here s is the rib spacing or pitch,
d is the depth, t_{ro} is the minimum thickness value of 2.5 mm,
W_{g} is the gross aircraft weight,
SG is the wing gross area,
B is the wingbox chord,

C is the wing local chord,
η_f is the flight loading factor applied as 3.75,
σ_{sa} is the allowable shear stress.

The minimal rib thickness equation is utilised at root and tip locations, and linear interpolation is used to size ribs in between these stations, Shanley (1960). In reality the relationship between the sizing of the rib and the area/aspect ratio of the wing is fairly linear as highlighted by Baker and Smith (2003), and this assumption is not detrimental to the weight estimation.

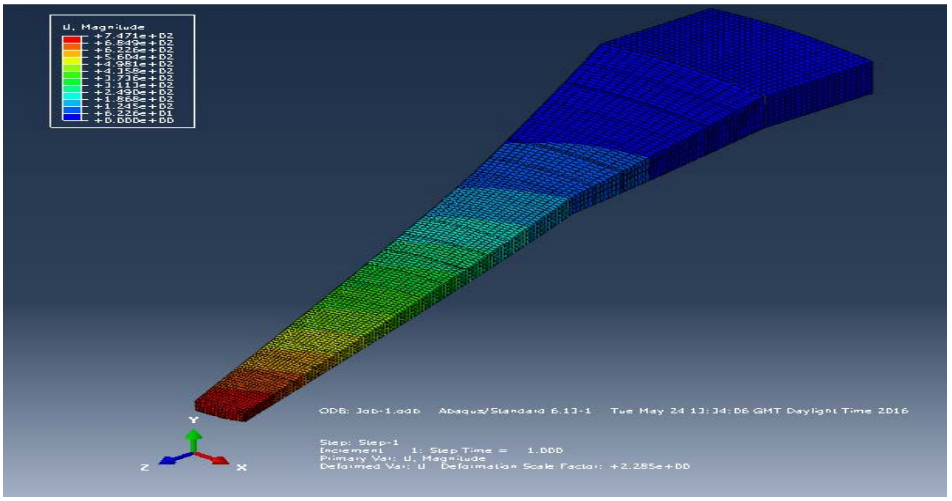

Figure 3.14: Example three dimensional wingbox model displacements.

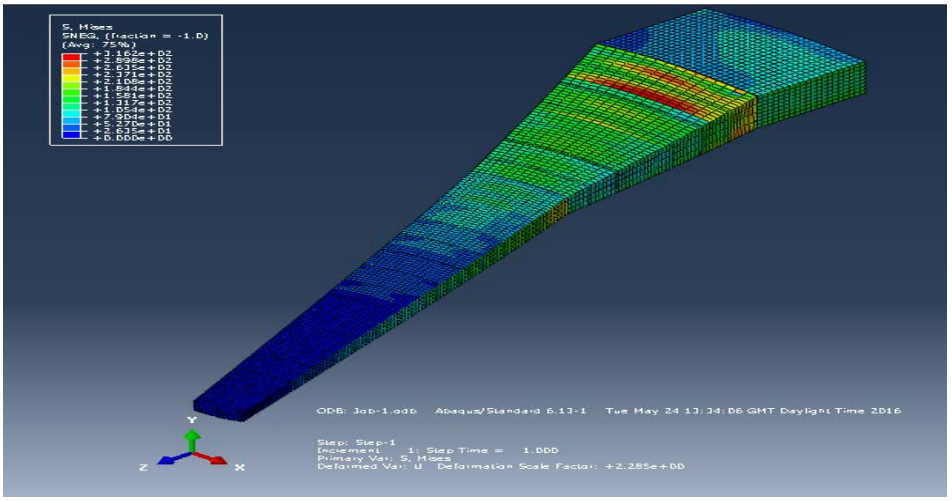

Figure 3.15: Example three dimensional wingbox model stress distribution.

Prior to analysis the models are meshed in a structured manner using an appropriate fixed quad element type, and verified seeding. Post analysis the appropriate maximum stress, displacements, and overall volume are extracted. From this data appropriate rotations, and displacements are transferred to the aerodynamic analysis, for application on the wetted surface. Figures 3.14 and 3.15 are examples of the displacement and stress

responses respectively, for a level II structural model.

3.2.3.3 Mass Modelling and Optimisation

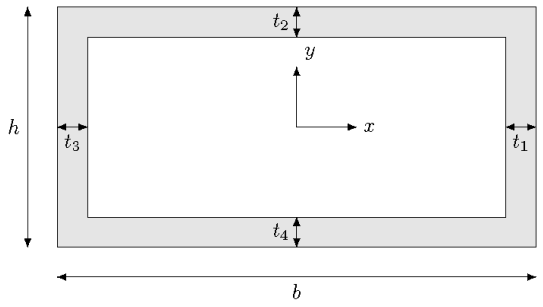

Figure 3.16: Wingbox mass optimisation section representation.

Process The mass optimization algorithm minimises the wing box structural mass, based on the load distribution (aerodynamic and inertial), fixing the internal structure so finite element analysis can be conducted. This mass minimisation is subject to stress constraints, the magnitude of which is evaluated using beam theory

$$\sigma = \frac{My}{I} \tag{3.4}$$

Or finite element analysis. Where two distinct options can be selected in the optimisation module. The first is an analytical optimisation for bending, with post optimisation consideration for torsional performance, and the second is a finite element analysis stress based optimisation. In both modes (I, and II) the representation of the structure remains similar, as the analytical method output is the starting point for the FEA based optimisation. The process seen in figure 3.17 varies marginally between the modes of optimisation in this section, where for the mass optimisation using the finite element analysis optimisation of sections is conducted globally, as opposed to sequentially.

Mass Optimisation Methodology and Assumptions The geometry representation for each section is shown in figure 3.16. For the analytical optimisation flight loads are applied via a spanwise lift distribution, and inertial relief is determined. When a finite element model is utilised for stress evaluation, the aerodynamic pressure loading is applied directly to the model. The spanwise and chordwise balance between wing lift and inertial forces allows for bending and shear relief. Torque is sensitive to the chordwise balance of inertial forces, as well as thrust and control surface inertia. Here to implement only spanwise inertial relief three separate contributors are considered; the fuel, the engine, and the landing gear.

Within this module the force balance is conducted prior to structural optimisation, in the spanwise direction. The fuel tank boundaries are fixed such that there are two tanks,

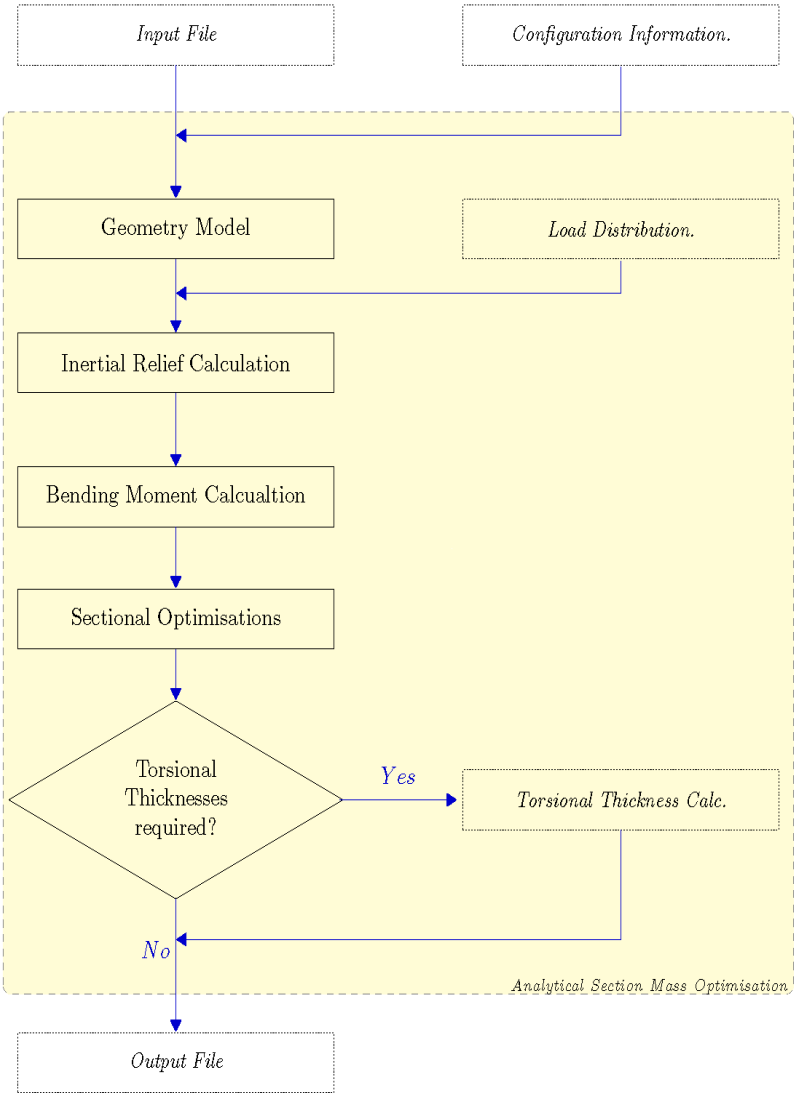

Figure 3.17: Analytical wingbox mass optimisation process.

inboard and outboard of the wing crank. Tadpole provides a gross fuel mass, which is the basis for inertial relief calculations. The fuel is assumed to distributed at a 2:1 ration between the inner and outer tanks. This is because there is a greater volume inboard to store the fuel, and as there are larger aerodynamic loads inboard, more fuel provides greater inertial relief. The inertial force from the fuel per section are balanced with the sectional lift, reducing the bending moment of the section, reducing the mass, during optimisation.

The optimisation problem can be summarized as shown

$$
\begin{array}{lccccc}
\text{minimize} & & m_{\text{sec.}}(t_1, t_2, t_3, t_4) & & \\
\text{subject to} & & & & \\
0 & \leq & \sigma_{\text{sec.}} & \leq & \sigma_{\text{y}} \\
0 & \leq & y_{\text{bar}} & \leq & \frac{h}{2} \\
0 & \leq & x_{\text{bar}} & \leq & \frac{b}{2} \\
0 & \leq & \sigma_1, \sigma_2, \sigma_3, \sigma_4 & \leq & \frac{\sigma_{\text{y}}}{MoS} \\
0 & \leq & t_1 & \leq & 25 \\
0 & \leq & t_2 & \leq & 35 \\
0 & \leq & t_3 & \leq & 25 \\
0 & \leq & t_4 & \leq & 35
\end{array}
\tag{3.5}
$$

where $m_{\text{sec.}}$ is the mass of a given section,
$\sigma_{\text{sec.}}$ is the stress in that section,
σ_{y} is the yield stress,
x_{bar} and y_{bar} are the locations of the centroid of the section in the x and y plane respectively,
σ 1,2,3,and 4 are the stresses in each individual member of the rectangular section,
And the t 1,2,3, and 4 are the sectional thicknesses corresponding to figure 3.16.

The mass and area (for stress calculation) of each section, based on the sectional representation,

$$m_{\text{sec.}} = \rho_{\text{mat.}} S_{\text{sec.}} A_{\text{sec.}} \tag{3.6}$$

Where $A_{\text{sec.}}$ is the section area,
$S_{\text{sec.}}$ is the length of the section,
$\rho_{\text{mat.}}$ is the material density.

$$A_{\text{sec.}} = A_1 + A_2 + A_3 + A_4 \tag{3.7}$$

$$A_{\text{sec.}} = t_1(h - t_2 - t_4) + bt_2 + t_3(h - t_2 - t_4) + bt_4 \tag{3.8}$$

where b is the depth of the section,
h is the height of the section.

The optimisation problem was solved using the Scipy optimisation module in Python. For the analytical stress evaluation, the optimisation problem is solved using a gradient based Sequential Quadratic Programming (SQP), Kraft (1988), for which objective

function derivatives are calculated. For finite element analysis based optimisation the COBYLA, Powell (2003) method was preferred, as it can function without the need for gradient information, which cannot be readily extracted from Abaqus. A limitation of gradient based methods is the starting point of the optimization. To reduce uncertainty, analytical optimization was conducted using a thousand starting points for each section, which were randomly selected between geometrical bounds. From the acquired solutions, the minimum mass solution for each section was adopted. The optimal solutions were stored and used as starting points for the aerostructural loop mass optimization and FEA based mass optimisation.

As torsion is not considered in the analytical mass optimisation and fidelity level I, additional post processing was introduced. The torsional thickness for a given section ($t_{\mathrm{t}}(i)$) was calculated based on the work by by Ajal et al. (2013)

$$t_{\mathrm{t}}(i) = \frac{Q_{\mathrm{v}}(i) + Q_{\mathrm{t}}(i)}{\sigma_{\mathrm{sa}}} \tag{3.9}$$

where σ_{sa} is the allowable shear stress,
Q_{t} is the shear flow in the web section due to torsional loads,
Q_{v} is the shear flow in the web due to vertical shear loads and is a function of the limit shear force $F_{\mathrm{ylim}}(i)$ in the web

$$Q_{\mathrm{v}}(i) = \frac{FSF_{\mathrm{vlim}}(i)}{h_{\mathrm{tot}}} \tag{3.10}$$

where FS is the factor of safety,
$h_{\mathrm{tot}}(i)$ is the effective height of the given section.

Q_{t} is the shear flow in the web section due to torsional loads is a function of the limit Torque (T(i)) in the web

$$Q_{\mathrm{t}}(i) = \frac{FST_{\mathrm{vlim}}}{2A_{\mathrm{ec}}} \tag{3.11}$$

where A_{ec} is the enclosed area of the given section. In addition the effective height of the spar can be found

$$h_{\mathrm{tot}} = h_{\mathrm{fs}} + h_{\mathrm{rs}} \tag{3.12}$$

where $h_{\mathrm{fs}}(i)$ is the front spar height of the given section,
$h_{\mathrm{rs}}(i)$ is the rear spar height of the given section.

Stringer Sizing and Analysis The initial sizing of the stiffened panels is integrated with the mass optimisation process as shown in figure 3.18. This process shows that

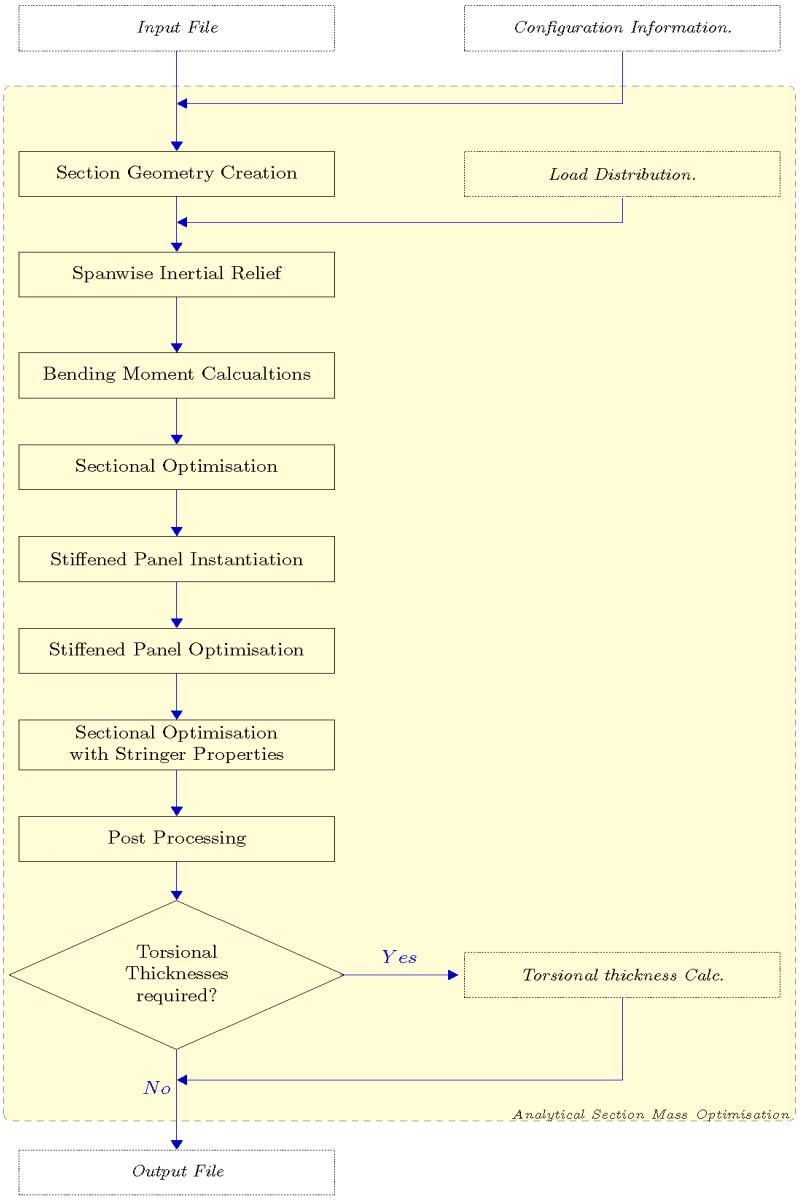

Figure 3.18: Stiffened panel analysis and optimisation process.

initially optimal bending cover thicknesses are found. Following the upper cover is sized for buckling in compression and the number of super stringers ($Num_{\text{stringers}}$), which span the entire span of the wing are calculated.

$$Num_{\text{stringers}} = \frac{c_{\text{s}}}{b_{\text{s}}} \tag{3.13}$$

where c_{s} is the average width of the wingbox,
b_{s} is the width of the stringer.

The chosen section profile is optimised for each section based on the bending moment and cover sizing. For the upper cover the optimal thickness is included in the buckling optimisation. The bending optimisation is re-run to include the new upper cover thicknesses, as a starting point. Here the stringer sectional properties are included to improve accuracy of stress constraint calculation.

The resized cover is taken forward as an optimal solution. For the super stringers; in the upper cover, the highest values of each design variables seen in figures 3.19 an 3.20, are chosen to create uniformly sized stringers. For the lower cover, the lowest values for the stringer variables are chosen instead. There are two stinger profiles currently available in this module: I or J, where both are flanged and share design variables.

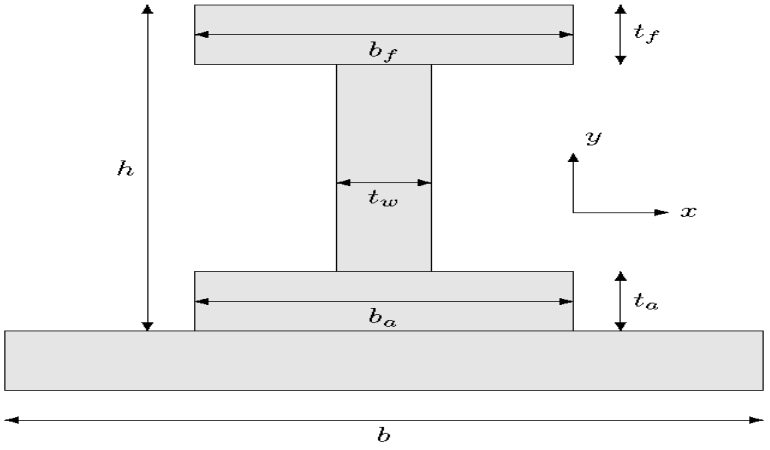

Figure 3.19: I profile stringer with associated design variables.

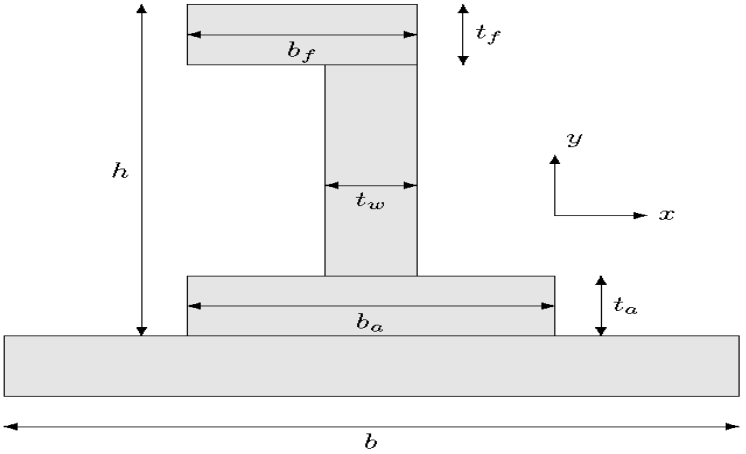

Figure 3.20: J profile stringer with associated design variables.

The optimisation to minimise stringer mass (m_{stringer}) based the geometric, and buckling mode constraints can be represented mathematically as

$$
\begin{array}{lccccc}
\text{minimize} & & m_{stringer}(h, b_\mathrm{a}, b_\mathrm{f}, t_\mathrm{a}, t_\mathrm{w}, t_\mathrm{f}) & & \\
\text{subject to} & & & & \\
1 & \leq & \frac{\sigma_\mathrm{y}}{\min(\sigma_\mathrm{fcb}, \sigma_\mathrm{ir}, \sigma_\mathrm{cc}, \sigma_\mathrm{cb}, \sigma_\mathrm{l.web})} & & \\
2.5 & \leq & h & \leq & 100 \\
2.5 & \leq & b_\mathrm{a} & \leq & 75 \\
2.5 & \leq & b_\mathrm{f} & \leq & 50 \\
2.5 & \leq & t_\mathrm{a} & \leq & 5 \\
2.5 & \leq & t_\mathrm{w} & \leq & 15 \\
2.5 & \leq & t_\mathrm{f} & \leq & 15
\end{array}
\tag{3.14}
$$

Where the stringer mass is subject to stringer and material properties

$$m_\mathrm{stringer} = \rho_\mathrm{mat.} L_\mathrm{panel.} A_\mathrm{stringer} \tag{3.15}$$

where $\rho_\mathrm{mat.}$ is the material density,
$L_\mathrm{panel.}$ is the length of the panel,
A_stringer is the stringer area.
For the panel optimisation problem in equation 3.14, the following buckling modes available:

Initial: Calculated for an unstiffened flat plate, to ensure that the plate without stiffening does not buckle. This is conservative, but the mass added is reduced during a second sectional optimisation. The method highlighted in ESDU (1972) is used to calculate the initial buckling mode

$$\sigma_\mathrm{fcb} = \frac{\sigma_\mathrm{fxe}}{\sigma_\mathrm{fo}} \tag{3.16}$$

where interpolation is used to extrapolate values of $\frac{\sigma_\mathrm{fxe}}{\sigma_\mathrm{fo}}$ from the graph in figure 2 of this document; based on the aspect ratio $(\frac{a}{b})$ of the panel and the edge constraint coefficient (u_r). Note this method can be simplified in the equation below and was validated against the theoretical buckling equation

$$\sigma_\mathrm{fcb} = \left[\frac{\pi^2 E}{12(1-\nu^2)(\frac{b}{t})^2} \right] \tag{3.17}$$

where K is 4.

Inter-rivet: This failure mode assumes that the stingers require rivets to be attached to the panel. This mode from ESDU (1962) is calculated,

$$\sigma_{\text{ir}} = \frac{KE_{\text{t}}\pi^2 t^2}{12s^2} \tag{3.18}$$

The rivet spacing (s) it is assumed that at a minimum 10 rivets will be required, on each side. Secondly the rivet type is assumed to be the most basic form available; flathead rivets (for which K is equal to 4). The critical factor in the calculation of this model is the tangent modulus (E_{t}) of the panel material, assumed to be approximately 70% of the E.

Crippling of webs/flanges: The Crippling mode is calculated using the method of Chintapalli et al. (2010) is used to sum the crippling stress of each segment in the stinger profile.

$$\sigma_{\text{cc}} = \frac{\Sigma b_{\text{n}} t_{\text{n}} \sigma_{\text{ccn}}}{\Sigma b_{\text{n}} t_{\text{n}}} \tag{3.19}$$

Depending on the element and if the section has free edges the following equation is used

$$\sigma_{\text{ccn}} = 0.6121\sigma_{\text{yn}} \left[\frac{b_{\text{n}}}{t} \sqrt{\frac{\sigma_{\text{yn}}}{E_{\text{n}}}} \right]^{-0.7735} \tag{3.20}$$

If there are no free edges then,

$$\sigma_{\text{ccn}} = 1.1819\sigma_{\text{yn}} \left[\frac{b_{\text{n}}}{t} \sqrt{\frac{\sigma_{\text{yn}}}{E_{\text{n}}}} \right]^{-0.7882} \tag{3.21}$$

Where σ_{yn} is the yield stress of the section,
E_{n} is its Youngs modulus,
b and t refer to that sections height/width and thickness.

In flanged stringers such as I and J there is only one segment with a free edge. These relationships are empirical, but provide a good basis for estimation of crippling stress.

Column: The column buckling mode is also calculated using the method of Chintapalli et al. (2010)

$$\sigma_{\text{CB}} = \sigma_{\text{cc}} - \frac{(\sigma_{\text{cc}})^2 [\frac{L}{\rho}]^2}{4\pi^2 E} \tag{3.22}$$

This mode uses the crippling stress calculated (σ_{cc}), the material properties of the panel(3.3), the effective length (L, and the end fixity coefficient, to calculate the column

buckling stress. In essence by ensuring a fixed aspect ratio $\frac{a}{b}$ during panel instantiation, this mode is effectively accounted for as it tends to be prominent only for slender panels. This calculation is effectively a sanity check and rarely influences the reserve factor (RF) constraints used for panel optimisation.

Local Web buckling: This mode is calculated to assess the possibility of buckling of in the stringer web

$$\sigma_{\text{loc.w}} = \left[\frac{0.4\eta\pi^2 E_{\text{str}}}{12(1-\nu^2)(\frac{t_{\text{w}}}{h})^2} \right] \tag{3.23}$$

Where t_{w} is the stringer web thickness,
and h is the height,
E_{str} is Youngs modulus of the stringer material.

All buckling modes are calculated and assessed with respect to the material yield stress (σ_{y}).

The optimisation is designed to optimise the design variables such that mass is minimised and a reserve factor is met

$$RF_{\text{min}} = \frac{\sigma_{\text{y}}}{min(\sigma_{\text{fcb}}, \sigma_{\text{ir}}, \sigma_{\text{cc}}, \sigma_{\text{cb}}, \sigma_{\text{l.web}})} \tag{3.24}$$

Theoretically ensuring that, no buckling occurs prior to stress reaching material yield stress.

Chapter 4

Calibration and Performance Trends for Varying Structural Fidelity

4.1 Introduction

The T.A.C.E program was designed to facilitate trade studies and design space exploration between the conceptual and preliminary design stage. However in order to ensure the results from this multidisciplinary analysis are accurate, two calibration studies were conducted. These include a fidelity level calibration, and a design variable perturbation study. These studies are designed to establish trust in results from the analysis. As the Tadpole tool was utilised for conceptual analysis, it was decide that the work of Keane and Nair (2005), could be used as a basis for calibration, and validation. For calibration, a wing configuration was chosen for which the accuracy and precision of each fidelity level and design modification could be assessed. Section 4.2 provides details of this calibration study and its results.

In section 4.3 experiments assessing the variance in wing performance trends from established trends, at various fidelity levels were conducted. The trend variances from the inclusion of physics based coupled structural and aerodynamic analysis, provide a guide to the fidelity required to successfully optimize the aircraft wing configuration. Highlighted within sections 4.3.1 and 4.3.2 are the results of discussions of experiments which were designed to capture the performance trends. Section 4.4 provides conclusions based on the results of both studies, and the program.

4.2 Calibration

4.2.1 Calibration Methodology

Having constructed the T.A.C.E program, the next step was to conduct experiments in order to determine the validity of results at each level of fidelity, and explore the impact of modification to these levels. To conduct such a study an existing configuration with sufficient background data was required, for comparison and validation. The aim of this study was to compare and understand the variance between established results and each structural fidelity level. This was achieved through comparison of performance outputs at different structural fidelity levels, for various analysis modifications, and several analysis constraints.

Figure 4.1: Visualisation of the calibration wing configuration.

The calibration was conducted with consideration for three criteria; accuracy, precision, and reliability. The accuracy and precision of results was gauged with respect to the Tadpole calibration configuration results. Finally in order to assess the reliability and repeatability of the experiments, a comparison of known outputs of parameters with expected physical behaviour was conducted.

The calibration was conducted using the baseline configuration (visualised in figure 4.1) established in Keane and Nair (2005), and presented in table 4.1. This configuration was analysed using the T.A.C.E analysis process shown in figure 3.1. This was to achieve the goals of the calibration and validation and gauge accuracy, precision, and improve reliability. Secondly it was important to determine which fidelity levels and analysis modification were worthy of progression in subsequent validation studies. The baseline configuration was initially analysed using Tadpole, in order to determine the performance outputs against which Δ (the difference between the Tadpole/baseline and the T.A.C.E analysis outputs) values could be calculated. Following this the fidelity levels and the number of modifications were incrementally increased. The list of modifications, include

Table 4.1: Calibration Wing Design Variables

Design Variable	Value
SG (m^2)	168.5
AR	9.07
$SWPI$ (degrees)	27.1
λ_1	0.598
λ_2	0.506
h_k	0.313
t/c_r	0.15
t/c_k	0.122
t/c_t	0.122
w (degrees)	4.5
k	0.75

changes in the mass optimisation mode for the wing box sections, the loading of finite element models, and the introduction of torsion in the sectional optimisation. These were applied to each fidelity levels I, II, and III, available for the structural analysis within T.A.C.E, can be seen below:

1. Beam structural model (Beam) + Analytical wingbox mass optimisation (MMI).
2. Beam structural model (Beam) + Analytical wingbox mass optimisation (MMI) + Torsional thickness calculation (TT)
3. Three dimensional structural model with spanwise pressure loading (3D Span) + Analytical wingbox mass optimisation (MMI).
4. Three dimensional structural model with spanwise pressure loading (3D Span) + Analytical wingbox mass optimisation (MMI) + Torsional thickness calculation (TT).
5. Three dimensional structural model with sectional pressure loading (3D Sec.) + Analytical wingbox mass optimisation (MMI).
6. Three dimensional structural model with sectional pressure loading (3D Sec.) + Analytical wingbox mass optimisation (MMI) + Torsional thickness calculation (TT).
7. Three dimensional structural model with stringers (3D Str.) + Analytical wingbox mass optimisation (MMI).
8. Three dimensional structural model with stringers (3D Str.) + Analytical wingbox mass optimisation (MMI) + Torsional thickness calculation (TT).
9. Three dimensional structural model with stringers (3D Str.) + Finite element analysis based wingbox mass optimisation (MMII).

4.2.2 Calibration Results

Table 4.2: Performance Outputs from T.A.C.E Calibration Studies Including Δ Variance at fidelity level I

	Fidelity level + Modification		
Output	Tadpole	Beam + MMI	Beam + MMI + TT
Wing Weight (Ton.)	13.0552	16.8417	22.0512
Δ Wing Weight (Ton.)		+3.7865	+8.996
Wing manufacturing Cost ($/1000)	418.321	336.612	406.496
Δ Cost		-81.709	-11.825
D/q (m^2)	3.1447	2.7234	2.794
Δ D/q (m^2)		-0.4213	-0.3507

Table 4.3: Performance Outputs from T.A.C.E Calibration Studies Including Δ Variance at fidelity level II

	Fidelity level + Modification				
Output	Tadpole	3D Span + MM I	3D Span + MM I + TT	3D Sec + MM I	3D Sec. + MM I + TT
Wing Weight (Ton.)	13.0552	13.1326	14.8371	13.1329	14.8373
Δ Wing Weight (Ton.)		+0.0774	+1.7819	+0.0777	+1.7821
Wing manufacturing Cost ($/1000)	418.321	324.767	375.275	309.535	357.171
Δ Cost ($/1000)		-93.554	-43.046	-108.786	-61.15
D/q (m^2)	3.1447	2.1462	2.2572	2.4188	2.466
Δ D/q (m^2)		-0.9985	–0.8875	-0.7259	-0.6787

Table 4.4: Performance Outputs from T.A.C.E Calibration Studies Including Δ Variance at fidelity level III

	Fidelity level + Modification			
Output	Tadpole	3D Str + MM I	3D Str. + MM I + TT	3D Str. + MM II
Wing Weight (Ton)	13.0552	15.1111	13.5619	13.3139
Δ Wing Weight (Ton)		+2.0559	+0.5067	+0.2587
Wing manufacturing Cost ($/1000)	418.321	282.440	282.733	242.134
Δ Cost ($/1000)		-135.881	-135.558	-176.187
D/q (m^2)	3.1447	2.3044	2.217	2.2406
Δ D/q (m^2)		-0.8403	-0.9277	-0.9681

Following the T.A.C.E analysis at the selected levels of fidelity and with the relevant modifications, the delta (Δ) between each T.A.C.E and Tadpole output values was calculated, the results can be seen in tables 4.2 to 4.4. These tables breaks down important Tadpole performance outputs, including Weight (Tonnes) and D/q (m^2). For Cost ($), the results were compared against the industrial tool CADCO, section 2.2.3.

4.2.3 Discussion

From the results in tables 4.2 to 4.4 an obvious trend is present; as the fidelity increases, the additional thickness for torsion has a smaller influence on the wing mass. Following the introduction of stringers this influence is negligible or adverse to that observed at lower fidelity. This is visible in the Δ weight values at each level when compared to Tadpole. For fidelity level I the Δ difference is large and significantly conservative, as expected when using simplified structural approximations and low fidelity aerodynamics. However when sweep is introduced as variable parameter, this modification improves the accounting of sweep based phenomena on the structure (see section 4.3).

At level II where three dimensional finite element models are introduced, there is a clear reduction in the magnitude of the Δ weight values (in table 4.3). At this level for calibration purposes, the different model loading methodologies were assessed. Note at this level ribs are introduced, and as the type of loading varies from spanwise and sectional in the model, the wing deflections and rotations are altered. This impacts the aerostructural analysis and subsequently the mass optimisation, which takes loading inputs from the aerodynamic analysis. In these results there is a plateau in the Δ and there is no clear differentiation. This is due to the agreement of the geometric variables for the calibration configuration wing, which are within the mid-range of design possibilities. However for extreme configurations, the loading methods would have a greater impact. In further studies the sectional loading method is prioritised.

Moving to level III (table 4.4) where stringers and stringer optimisation is introduced, there is a slight shift in the absolute and Δ weight. Note that without torsional thickness the mass of the wing is higher than with torsional thickness, and the Δ is larger than the previous level. This implies that where stringers are present the addition of torsional thickness has an adverse effect, when compared to models without thickness reinforcement. This is likely due change in the bending behaviour of the section and the stringer optimisation with the torsional thickness modification.

This suggests that for all levels of fidelity the addition of torsional thickness is significant, but higher fidelity structural models are less prone to the inaccuracies of empirical modifications. So where it is desirable to introduce torsional thickness at level I and II to match higher fidelity physical phenomena, at higher fidelity (level III) it serves to temper the mass increase from the addition of stiffeners. This conclusion was evaluated for design variable perturbations and performance trends experiments, at different levels of fidelity, in section 4.3.

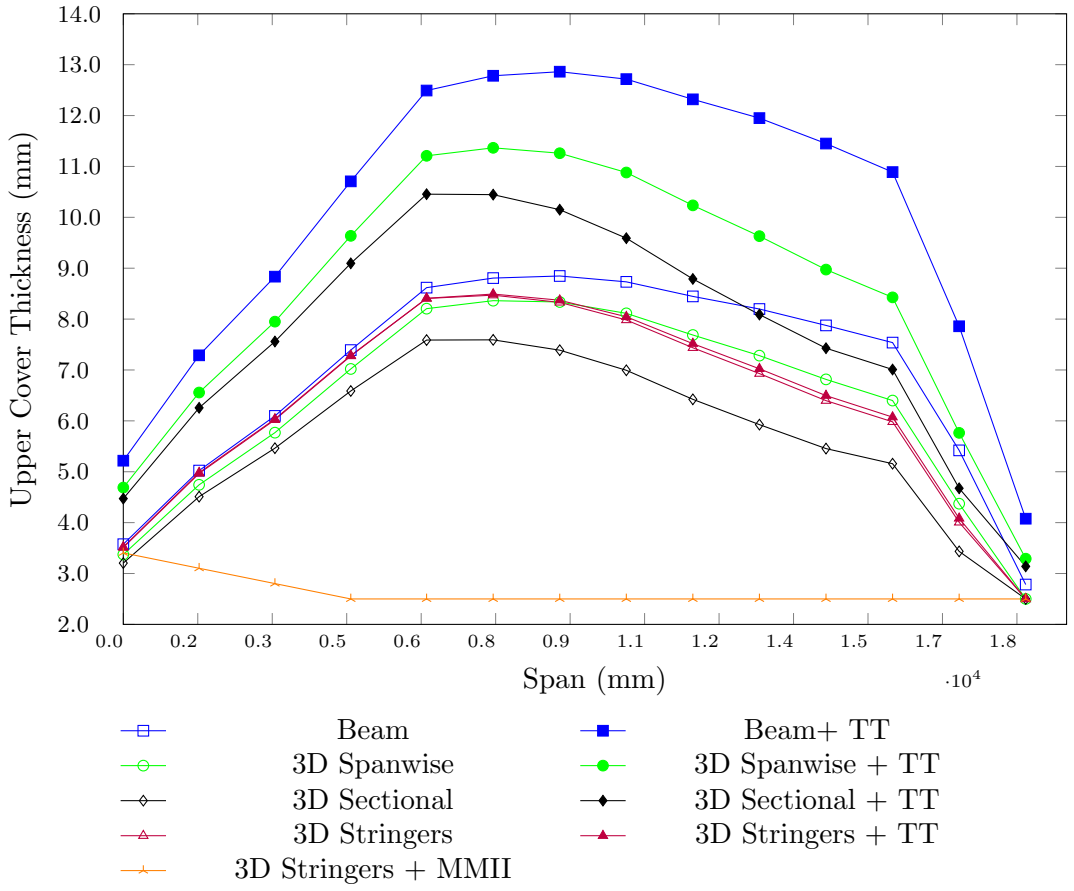

Figure 4.2: Wing upper cover thicknesses per section along span, for the calibration wing test case, at varying levels of fidelity.

The thickness distributions for the upper cover (figure 4.2), show that the spanwise distribution of optimisation thicknesses without and with additional thickness for torsion, form upper and lower thicknesses boundaries, which shift with changing fidelity, and move closer together as the fidelity increases. This narrowing effect coupled with the shift of the bands demonstrates that the increase in fidelity causes a narrowing of the bands, and the overall downward shift of each matching band with or without the torsional thickness is only changed significantly when the stringers are introduced. Where instead of moving further downwards as expected, the bands move up.

This supports the trend observed in the change of Δ weight for increasing fidelity. A further observation from these results is that the distribution profile changes, post kink. At lower fidelity the models have a larger spanwise region post kink where there is little change in thickness, until a drop off point. As the fidelity increases, although the drop off point remains in a similar location, the relative change in values over the same spanwise sections, is greater.

For D/q there is a simple explanation for the observed trend of increasing negative Δ. This trend shows that that the values of D/q are smaller than the empirical Tadpole value

and decrease further, as fidelity increases. This is due to the improved aerostructural coupling, which is more accurate and precise with each increased fidelity level.

When observing the cost Δs, it should be noted that the industrial tool, to which the output cost from the T.A.C.E analysis is compared is highly calibrated. The T.A.C.E costing tool is linear and only accounts for recurring costs, and this linearity manifests in the output. When there is conservatism and greater mass in the wing box structure, the overall Δ is lower. However as the fidelity increases this excess weight is not present and the opposing trend is observed, cost shifts further away from the industrial equivalent value. This highlights that the T.A.C.E costing suite is not as refined, calibrated, or developed as its industrial equivalent. Therefore in these estimations there is a clear trade off in precision, and accuracy, however there is potential to justify the use of this method in if further experiments demonstrate matching performance trends.

As a final note, it is clear that certain levels and modifications show more promise than others at matching Tadpole; the three dimensional with various loading methods, and the models with stringers are of particular note. In contrast the beam level models, show little promise and are incredibly conservative, however they are relatively cheap and offer some understanding of the design, and could be useful. Therefore they are still considered in subsequent experiments in this chapter. Note that for spanwise loading the introduction of additional thickness due to torsion significantly effects the output mass and shows poor correlation with D/q, we know that for sectional loading this is unlikely to be the case. Therefore spanwise loading level can be considered for further experiments, but without the introduction of additional thickness to compensate for torsion. All other levels are also kept for consideration in further validation experiments.

4.3 T.A.C.E-Wing Trends

4.3.1 Methodology

To further validate the results from T.A.C.E, a series of experiments were conducted in order to determine the performance trends for key design variables (SG, AR, $SWPI$, and t/c), and validate these using trends from Tadpole. For the range of design variable values shown in table 4.5, the structural fidelity was increased gradually in order to populate trends for the Weight (tonnes), Cost (\$), and D/q (m^2).Conventionally $\frac{L}{D}$ is the preferred standard aerodynamic criteria, however the results here are directly compared to those of Keane and Nair (2005), and D/q is utilised as the variable for comparison.

Table 4.5: Wing design variables ranges

Variable	Variable Range
SG (m^2)	$100 \leq 250$
AR	$6 \leq 12$
$SWPI$ (degrees)	$25 \leq 40$
t/c_r	$0.1 \leq 0.18$
t/c_k	$0.06 \leq 0.14$
t/c_t	$0.06 \leq 0.14$

The fidelity was increased in increments similar to the calibration study, and each level was designed to gauge how variation in structural model fidelity effects the wing performance. The limitations of the results from these experiments are discussed in section 4.3.2. At each fidelity level, each design variable was perturbed within the given design range, and the performance outputs were collected. The list of levels which were investigated are as follows:

1. Tadpole analysis
2. Beam structural model (Beam) + Analytical wingbox mass optimisation (MMI).
3. Beam structural model (Beam) + Analytical wingbox mass optimisation (MMI) + Torsional thickness calculation (TT)
4. Three dimensional structural model with spanwise pressure loading (3D Span) + Analytical wingbox mass optimisation (MMI).
5. Three dimensional structural model with sectional pressure loading (3D Sec.) + Analytical wingbox mass optimisation (MMI).
6. Three dimensional structural model with sectional pressure loading (3D Sec.) + Analytical wingbox mass optimisation (MMI) + Torsional thickness calculation (TT).
7. Three dimensional structural model with stringers (3D Str.) + Analytical wingbox mass optimisation (MMI).
8. Three dimensional structural model with stringers (3D Str.) + Analytical wingbox mass optimisation (MMI) + Torsional thickness calculation (TT).
9. Three dimensional structural model with stringers (3D Str.) + Finite element analysis based wingbox mass optimisation (MMII).

The aim of these experiments was similar to assess the accuracy, precision, and reliability of the performance trends and the impact of variable structural fidelity on such trends. By noting how the simplification or absence of the sub design problems (ribs,

TT, sizing) effects the fidelity models, the importance of these features/analyses could be determined. This allows assessment of the accuracy and precision of the T.A.C.E program outputs. Helping to improve confidence in the underlying methodologies incorporated in the analysis, allowing investigation of design space exploration capabilities.

4.3.2 Results and Discussion

The resulting trends for the fidelity experiments highlighted in section 4.3 can be found in figures 4.3, 4.4, and 4.5 for the wing weight, manufacturing cost, and D/q respectively. Note in these figures any incomplete trends are primary due to the failure of the aerodynamic analysis.

4.3.2.1 Wing weight

As the wing weight is the primary performance quantity of interest, the trends for which are seen in figure 4.3. At fidelity level I in the finite element model weight trends, for SG, AR, and $SWPI$ are reasonably matched and display some level of accuracy, but overestimate for singular points, implying a lack of precision. However for t/c_{r} the wing weight trend is not as captured accurately. The beam model results suggest it is not possible to extract performance trends using low fidelity finite element models, as the absolute values are conservative.

At structural fidelity level II the three dimensional model loading methodologies offer interesting comparisons. The spanwise pressure loading offers greater realism than the beam models, as shown in the trends for SG and AR which are quite accurate. However this loading methodology fails to capture physical phenomenon from variations in the $SWPI$ and t/c_{r}. This is a limitation of the T.A.C.E analytical mass optimisation (which implements a spanwise load distribution), but highlights the need for an accurate loading methodology. The sectional loading models show greater compatibility with the aerostructural convergence methodology, where the accuracy of loading ensures a full set of weight results can be determined. There is still a level of divergence in the precision of the weight values in the SG and AR trends. However the trends are more accurate than the lower fidelity models and are reflective of the Tadpole baseline.

The addition of stingers and buckling optimisation to the three dimensional structural model has two repercussions on the weight trend. Firstly there is a net increase in the mass with the addition of the stringers, and secondly there are nonlinear effects impacting the trends. The nonlinearities can be categorised into three effects: variable based buckling mode effects, physics based buckling effects, and analysis assumption effects. Prior to the experimentation it was hypothesised that the addition of stringer and buckling optimisation would results in a shift in weight close to the Tadpole observed values, but nonlinearities could be observed.

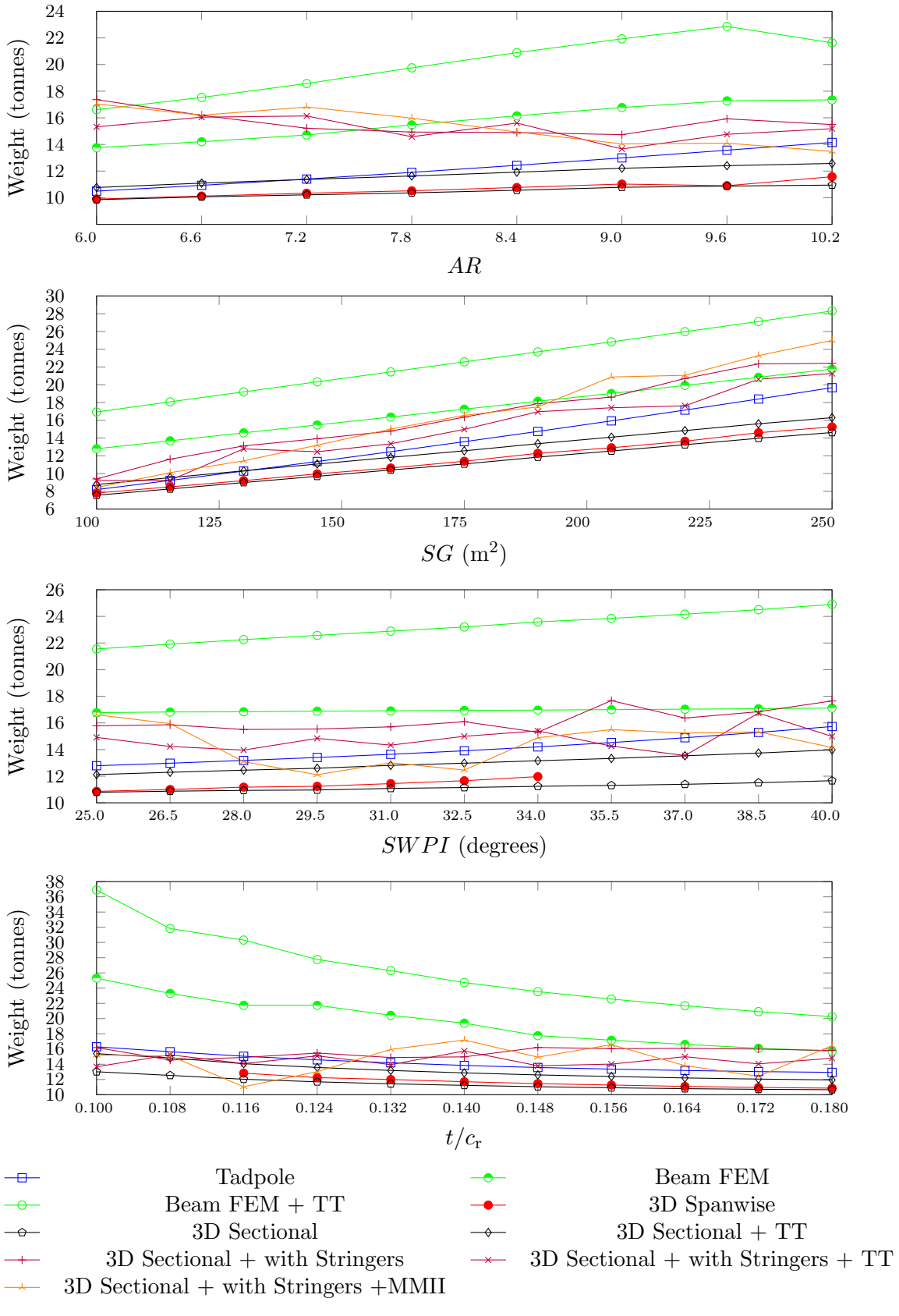

Figure 4.3: Wing weight trends for design variables at various fidelity levels in T.A.C.E.

There are two clear weight trends for which there is a reversal due to the stringer addition. For AR this is due to the change in minimum buckling mode. It has been established that with a change in AR (for fixed SG) there is an increase in the slenderness of the wing. This increasing slenderness results in two distinct phenomena; firstly the column buckling mode becomes more critical, however as panel AR is always equal to 3, there is a contradictory effect to the buckling mode, the reduction of the number of super stringers. The panel optimisation problem avoids the criticality of the column buckling problem, through the panel aspect ratio constraint, and the results observed are a results of the decrease in number of super stringers, for increasing wing AR.

For the t/c_{r} weight trend the introduction of ramps or steps in the trend is due the transition of the covers from a skin dominated, to stringer dominated design. Its clear that at lower t/c_{r} values the introduction of stringers has a minor effect, however this changes as the stringers have a greater influence on the cover thickness. As the number of stringers does not change, the change in loading behaviour has an impact on the design of the stringers. As the load and wingbox depth increase, the stringers are optimised to increase web and flange thicknesses or length, to avoid crippling, or local web buckling. The ramps or steps identify values of wingbox depth, at which there is a significant change in the loading, and a drastic change in stringer properties to meet buckling optimisation criteria.

In the case of $SWPI$ a subtle nonlinearity and limitation influences the weight trend. The increase in $SWPI$ results in increased torsion, whilst the number of stringers remain similar. The shift in load will results in a change in the dimensions of the super stringers and the mass of the covers, but the nature of the buckling modes remains similar. This can be captured with the introduction of a torsional buckling mode, and improved aerodynamic capabilities. The addition of both would result in increased fidelity and limit the overall design exploration. The weight trend observed shows only a marginal change in mass across the range of sweep and inflection/transitional points in the loading profile, resulting in oddities in the overall trend.

The final fidelity level III features FEA based mass optimisation (MMII), in addition to stringer based analytical sizing. We see some minor deviation for AR and SG compared to stringer based optimisation without MMII, where the variation in the trend is dependent on improved stress performance and exploitation of the minimum cover stress constraint. However this not the case for $SWPI$ and t/c_{r}, where there is extensive variation and nonlinear trends. As the loading distribution and structural deformation changes and varies non-linearly, the optimiser can often fail to locate a design which fully exploits the design constraints. In addition it is clear that there is a divergence in the level of physics in the analyses at this level when compared to Tadpole, so we must assess the results of this level independent to Tadpole trends.

In MMII optimisation as only cover thicknesses can be varied, the fluctuations of structural performance metrics such as stress, deflection, and rotation, can cause local minima in the gradient based design problem, forcing the optimiser to settle for a non-optimal solutions for stress, in some cases. Both stress and deflection are being driven at a local and global level respectively, the competition between these variables, and the lack of high fidelity aerostructural coupling leads to limitations in the gradient based optimisation. In order to reduce computation time, each aerostructural iteration is limited to 1000 function evaluations for stress, and the number of aerostructural iterations are halved. It is possible that the numerical noise we observe here is a direct consequence of the underlying physics, the aerostructural coupling, the gradient based optimisation method, and the limitations in computational time.

However these are real challenges in the field of structural engineering and optimisation, and what is important is that we start to observe that there is a fidelity gap when stress is driven in addition to the aerodynamics in multidisciplinary analysis. It can be reasonable at this stage to assume that there may be a resolution point in structural fidelity prior to the introduction of stress based optimisation. However in order to explore this further we must investigate this fidelity level further, and determine the sensitivities between design variables and performance outputs. By compiling these sensitivities at each fidelity level, we can begin to visualise the design space and determine if there is significant numerical noise when stress based optimisation is implemented.

4.3.2.2 Wing manufacturing cost

From the manufacturing cost trends (in figure 4.4), it is apparent that for some variables the costing tool is not compatible with a more detail instry based tool, in terms of precision or accuracy. Although for SG and $SWPI$ the trends are accurate, the remaining variable trends are not. This is due to two primary reasons: the greater design knowledge, detail, and calibration of the design tool, and the limitations of the T.A.C.E costing suite. There is a clear trend in industry program results however, and these trends are specific and are heavily dependent on fixed inputs. To achieve accuracy for AR, and t/c, and precision for SG and $SWPI$, the T.A.C.E cost tool must be calibrated using numerical factors and design knowledge capture. However this is an entirely separate research topic, and outside of the scope of this thesis. For subsequent studies, scepticism should be applied to the absolute values of cost from T.A.C.E.

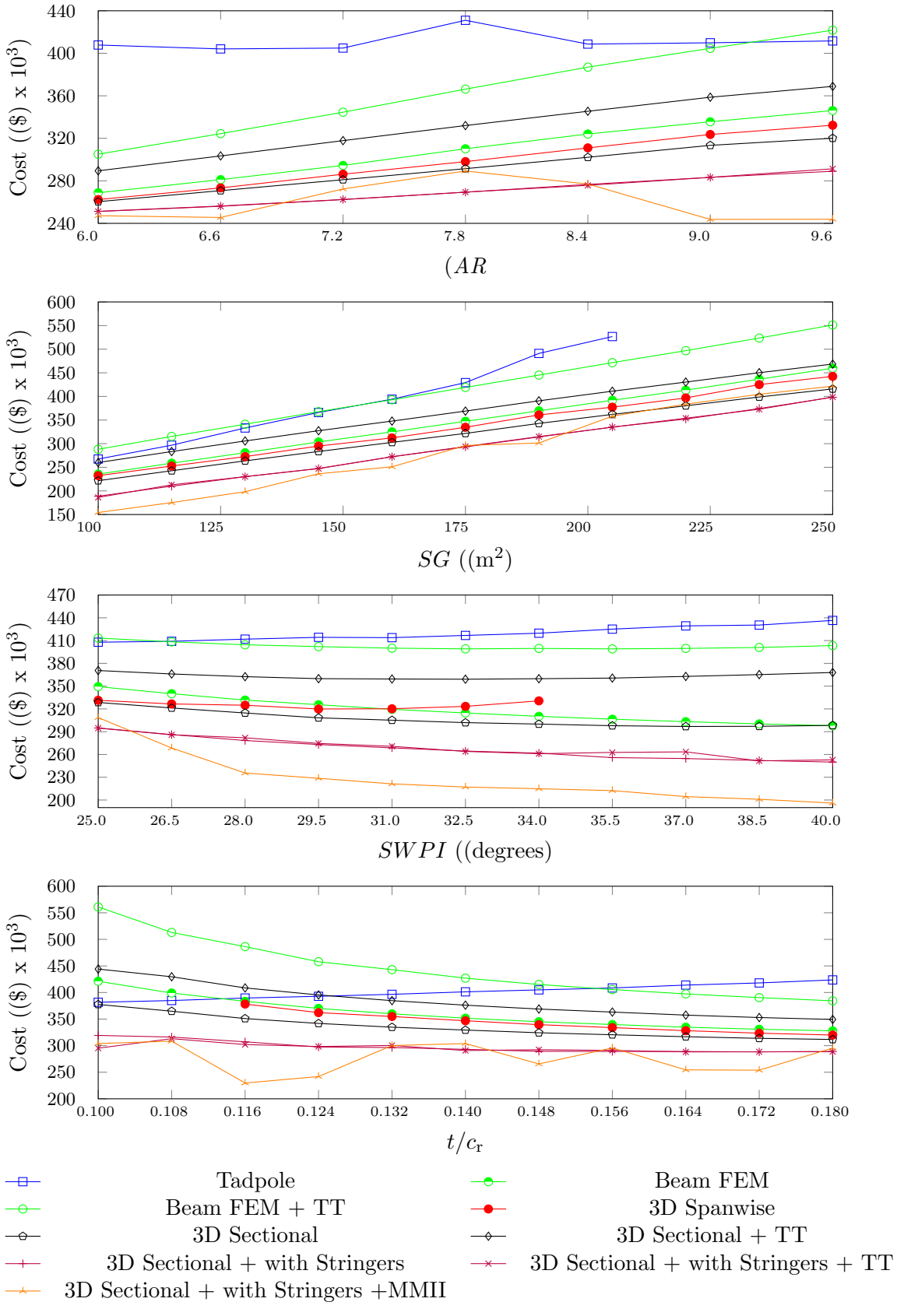

Figure 4.4: Wing manufacturing cost trends for design variables at various fidelity levels in T.A.C.E.

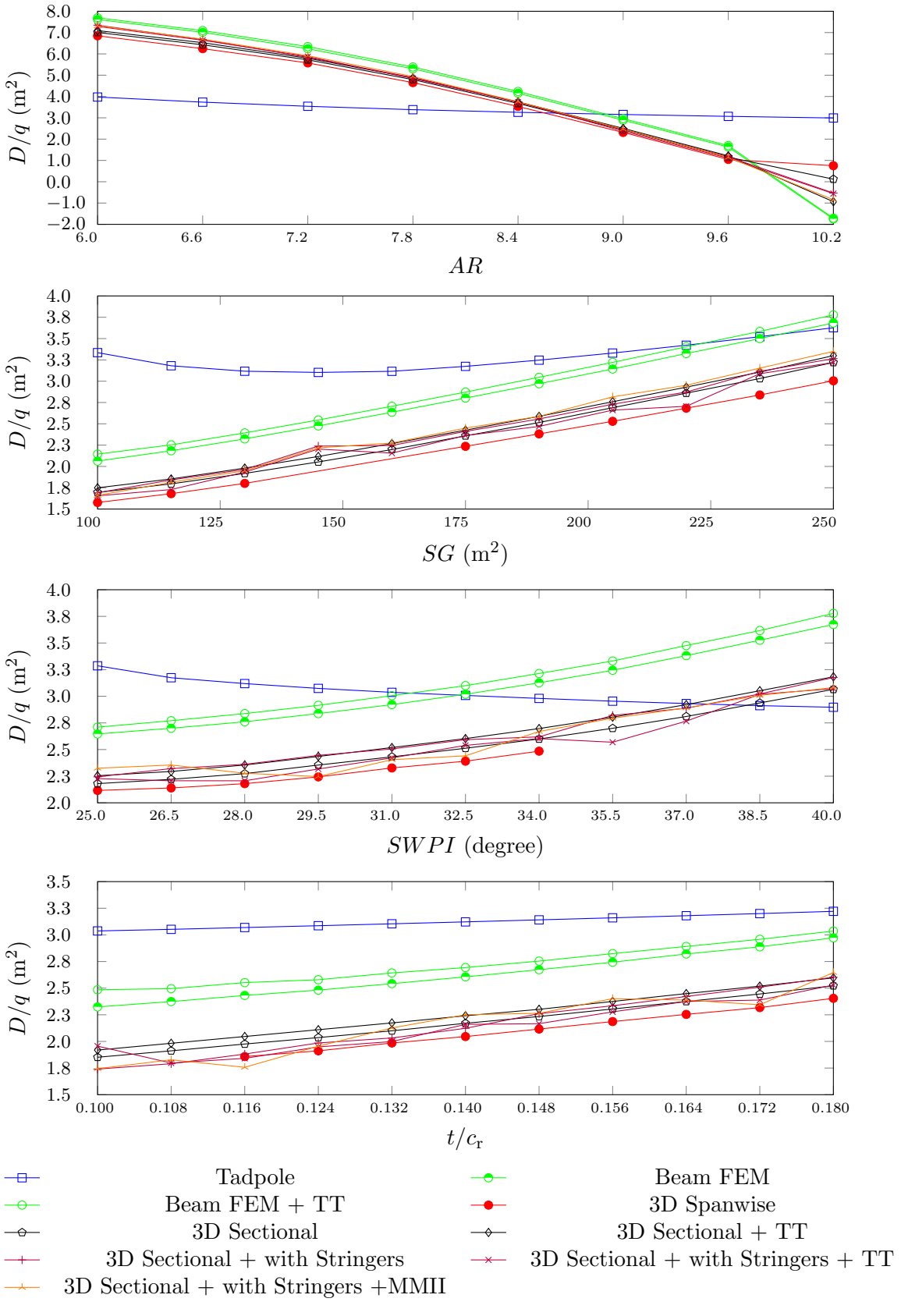

Figure 4.5: Wing aerodynamic performance trends for design variables at various fidelity levels in T.A.C.E.

4.3.2.3 Wing D/q

The D/q trends from Tadpole are empirically derived and is limited to the dataset within the tool. It is clear from trends in figure 4.5, that the aerostructural coupling introduces divergence from the Tadpole trends. This is not the case for the SG and t/c_{r}, where there is difference in absolute values, but the overall trends show some correlation. However for $SWPI$ and AR, the empirically derived values differ significantly from the experimental outputs. For the case of AR the empirical model suggests that the change in aspect ratio with the same area, will not drastically impact the drag. This is not correct and increasing the aspect ratio will lead to a longer and slender wing, which will decrease the induced drag (as less lift is generated outboard). The reason for the lack of data above the AR of 10.2 .is the inability of the solver to converge for such a slender wing.

For $SWPI$ the T.A.C.E analysis results suggests an opposing trend, which implies that drag will increase, as the sweep is increased. In this case the error in the aerodynamic trend is likely due to the limitations of the full potential aerodynamic method. This method was designed to analyse wings in shock-free attached flow, therefore for transonic design cases the shock drag is likely to be incorrect. Where geometrical changes such as increased sweep cause a reduction in shock drag, this reduction in drag is not accurately captured, whilst the increase in drag from the increased wetted surface area is, creating a net increase in drag.

4.4 Conclusions

In this chapter the T.A.C.E program created for the purposes of this research has been calibrated and validated, for varying structural fidelity models. The modularity and flexibility of the analysis process has been highlighted and its compatibility with empirical data has been explored. The aerostructural loop within this tool has been highlighted as the critical link between disciplines, and the importance of this coupling on the behaviour of wing performance characteristics has been explored. From calibration studies it was noted that certain levels of fidelity and certain modifications showed good accuracy and precision, and had a significant impact on the performance. To further validate and investigate the findings of this calibration study, experiments were conducted based on the perturbation of design variables, at given levels of structural model fidelity. The outputs of these studies were grouped as trends for each design variable in question, at each fidelity level.

From the weight trends especially, the sweep ($SWPI$), proved to be the most challenging variable for which to capture performance outputs. The rib sizing, and stiffened panel design, were shown to have an impact on the nature of the trends. Accounting

for the torsion through additional thickness was shown to have significant advantages in reducing the weight for higher fidelity structural models, but lead to oversizing at lower fidelity models. The inclusion of finite element based mass optimisation and the additions of sized ribs, and stringers to the design problem, helped mitigate the need for torsional thickness, and the counteracted any overestimation for most design variables.

It was noted that as the structural model fidelity is lowered the impact of the lack of detail in the analysis creates a quantifiable difference between expected values. This is likely due to a worse starting point and data overhead at the lower structural fidelity levels. It is better therefore to stay closer to the level of structural model and analysis fidelity at a preliminary rather than conceptual level, and to identify modifications which capture the output performance accurately, whilst minimising computational cost. In order to test this, the design space for the design variables in conjunction to each other and the performance outputs, must first be explored in greater detail. The next step includes the creation of sensitivity studies at various levels of structural fidelity to understand top level variable dependencies. This will be done using response surface models to visualise in the design space in three dimensions for Weight, Cost, and Drag.

4.4.1 Contribution to knowledge

As final note we can highlight that the studies in this chapter, whilst seeking to validate and calibrate the T.A.C.E analysis process also offer a contribution to literature. This contribution is the incremental exploration of structural fidelity models within a multidisciplinary analysis process, with respect to calibrated performance trends. A study such as this helps to highlight how incremental development of structural models and analysis methodologies, can help to highlight an optimal point for computational expense and accuracy. These studies can act as a bench mark for subsequent fidelity based developments to the industry based system upon which T.A.C.E is based, and to help other developing programs of similar nature to identify variable structural fidelity capability. In addition the different fidelity models used offer distinct advantages and disadvantages, which when assessed in isolation are limited to local performance metrics such as stress, and deflection. However when analysing such models in a multidisciplinary analysis chain, their performance can be gauged with respect to each other. As all models are represented within the same program and the variance between the fidelity levels is more obvious, and easier to assess.

As an additional contribution, the studies in this chapter add to the body of work in Keane and Nair (2005), chapter 12. The studies conducted there explore the performance trends for Tadpole alone, whereas this work enhances the knowledge captured and demonstrates how these trends change with varying structural fidelity.

Chapter 5

Wing Sensitivity Analysis

5.1 Introduction

The sensitivity analysis presented in this chapter focuses on the assessment of the design space and design variables, at various levels of structural fidelity. This allows the designer to understand the location of optimal designs (to designate a trust region) and to structure the optimisation problem; objective, constraints, and bounds to improve the design space optimisation and exploration. In practice this can be achieved through mathematical discretisation of governing equations for a given analysis method or tool, and through the use of gradient calculation methods for these known functions. However if the design space is unknown or the analysis tool is a black box, visualisation and design space sampling can often be the initial point of call in order to understand the sensitivity of the design variables, for the given design space.

In this chapter the design variables (SG,AR, $SWPI$, t/c_{r}) utilised in chapter 4, for performance trend assessment, were paired to assess the sensitivity of performance outputs (Weight, Cost, D/q), with respect to the change in the design variables. In addition these design variables are paired, to gauge their sensitivity to each other. By visualising the performance outputs with respect to each design variable couple and fidelity level, the overarching hypothesis of this thesis could be evaluated. The nature of this research was to help facilitate the goal of design exploration within multidisciplinary systems at early stages of design.

The sensitivity analysis is a method of analysis, which is readily available, easy to utilise, and can enhance or upgrade knowledge capture, to aid design exploration. The identification of sensitivities and visualisation, can help reduce the data overhead between design stages and between different fidelity structural models. This allows reusability of information and recycling of known data. Furthermore the visualisation of design space can help the designer, chief engineer, and design team to identify trust regions,

and variables which are likely to cause non-linearity in trade studies and optimisation, and mitigate the impact of said variables.

In order to assess the sensitivity it was important to identify a method through which the wing design variables and their associated performance variables could be sampled and visualised. The major limitation being that there is no direct access to the governing equations in this coupled system, due to the commercial nature of tools integrated within the T.A.C.E program. Although there were many methods to extract gradient and derivative information directly, the aim of this thesis was not to address gradient calculation methodologies. Here the focus was on understanding the impact of design variable perturbation and fidelity variation, on the design space for aircraft wings. This space was constrained within a design range, established in chapter 4, and could be used to aid design exploration and multipoint analysis within this known region.

In the course of the experiments in this chapter, the differences in the design space at a given level of fidelity were used to identify the advantages/disadvantages of conducting trade studies and formal optimisation at these levels. This helped to determine the sensitivity of the variables and performance outputs, to increasing structural fidelity. Certain variables ($SWPI$) were already known to show greater sensitivity to the fidelity of the analysis than others, and visualisation of the design space, helped identify which methods of exploration or optimisation may be appropriate at a given level. By identifying the sensitivity in the design and the uncertainty, it is possible to determine if the chosen level of fidelity and design variables will give a conservative or optimistic answer. This can then help determine the level of modifications required to prevent a data overhead, when moving from lower to higher fidelity, and from conceptual to preliminary design. In addition the identification of uncertainty in a rapid and physics based approach can help improve the design exploration capability and risk assessment of designs, without the need for single point analysis.

5.2 Sensitivity Analysis Methodology

Prior to the experiments entailed in this chapter, the methodologies and processes implemented are presented. In addition a definition for what is referred to as sensitivity analysis, within this body of work is presented. In general the invocation of the term sensitivity suggests the utilisation of gradient calculation methodology, for derivatives of governing analysis equations or the inputs and outputs of an analysis tool. Here sensitivity refers to the change in the output performance variables due to a change in coupled design variables. This has essentially been assessed partially through the performance trend studies in chapter 4, however in this chapter the design variables sensitivities are assessed for performance outputs, and relationships between design variables. Here no formal gradient calculation methods are utilised. Instead visualisation of the design

space and mapping though regression is preferred, to offer a visual assessment of design variable sensitivity. The aim of these sensitivity studies is to identify the uncertainty in the design, for top level design parameters.

However, firstly we must briefly cover response surface models, design of experiments, and visualisation methodologies which are used to achieve sensitive assessment. This is followed by a presentation of the experimental methodology, for the sensitivity studies in this chapter.

5.2.1 Design of Experiments, Kriging, and Visualisation

Design of Experiments Different design of experiment methodologies have been covered in 2.3, however here for the purposes of the experiment in this chapter the optimal latin hypercube sampling (OLHS) has be utilised. The OLHS method was initially presented by Park (1994). The method is an evolution of the latin hypercube sampling (LHS) method M. D. McKay (1979), which seeks to use a set number of points allocated by the user and distribute these randomly across the design space, with spacing criteria to reduce clustering. However this can lead to suboptimal point distributions, as the determination of the randomly space points is arbitrary and a simple spacing criteria is not sufficient to create a good distribution across the design space.

OLHS seeks to overcome this obstacle through optimisation of the points distribution and the spacing between points, for the given number of points, so that the maximum amount of design space can be sampled. The LHS and OLHS sampling methods are preferred to random or orthogonal sampling, as they provide more efficient, and accurate sampling, whilst being computationally more efficient if the sampled function is expensive. As the T.A.C.E program must be run for each sample point, the OLHS sampling method was chosen for the studies in section 5.3.

Design Visualisation and Response Surface Creation Having identified a sampling method for the sensitivity assessment it was important to determine how best to visualise the design space. Response surface models offer a means to achieve this, however choosing an appropriate method can be difficult. An interpolation technique can be used, however regression methods generally offer improved modelling capability, when working with non-linear or noisy data (from physics based simulations, similar to the trends in section 4.3.2). Also by Keane and Nair (2005), where optimisation is the goal of the response surface creation, the use of regression can help avoid basins of attraction, introduced by interpolation. Making design exploration and optimisation less prone to artificial (unrealistic or optimistic) designs and local minima respectively. For the experiments in this chapter, where there is a lack of knowledge of the design space; kriging was chosen, for a regression based surface creation. In addition due to

the possibility of analysis failure for a given design, the robustness and accuracy of the kriging methodology was seen as desirable, to offset any missing data.

A further advantage of kriging is the exploitation of probable error data and the screening of design variables through hyperparameter tuning. This capability allows the prediction of infill points (via various infill methodologies highlighted in Parr et al. (2010)), which can improve the accuracy and reduce error in the models, whilst refining data for ranking purposes. This can be important as it helps improve the reliability of exploration results through identification of design drivers (reducing uncertainty). However a limitation of kriging is its relative difficulty to deal with over 10 design variables and 1000 points. This in addition to the expense of tuning parameters and creating the surface, means that kriging its limited to application with a small amount of design variables and points. Regardless for studies in this using up to 4 design variables, kriging is ideally placed to provide reliable and accurate models.

The pyKriging module developed by Paulson (2015), based on the methodology presented in Forrester et al. (2008) and Jones (2001) was used to achieve response surface modelling. This software includes the sampling, kriging, and interface required to implement the sensitivity analysis in section 5.2.2. When the data points are sparse, the tuning of the kriging hyperparameter can also be achieved within this software using inbuilt optimisation. The creation of design of experiments for multiple dimensions and the capability to access black box functions to gather the output data, is an additional advantage of this software. As the function itself can be unknown in many engineering cases, this module is flexible and suited for use in modular multidisciplinary codes. As an additional benefit pyKriging facilitates the visualisation of the outputs response surfaces for up to three dimensions.

5.2.2 Sensitivity Analysis Methodology and Process

The kriging process seen in figure 5.1 works by utilizing the T.A.C.E program as a black box function. Initially the global analysis parameters are configured and the structural fidelity level is chosen. The user can specify which design variable pair, to create a sensitivity study for. Here the wing design variables (SG, AR, $SWPI$, t/c_{r}), create a choice of six pairings. Following the determination of all fixed analysis information, the sampling process is initiated for 2 variables using an optimal latin hypercube, with a budget of 50 points.

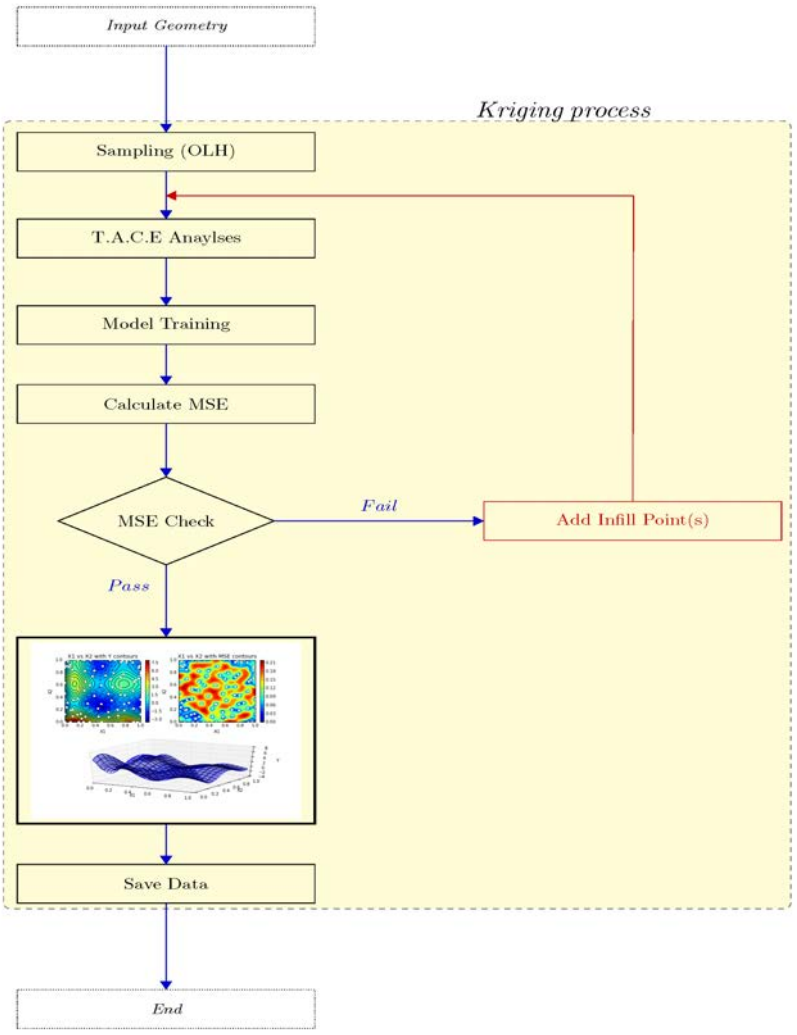

Figure 5.1: Kriging process for wing design variable sensitivity analysis and design space visualisation.

Note for use in T.A.C.E directly, the design of experiments points are scaled within the design variable range, identical to the range the studies in chapter 4. Note if a n analysis run is unsuccessful, it is removed, to avoid failure in model training. The response surface is then trained, as the shape of the objective function for the output variables is unknown, no functional information is provide. In order to increase the speed in training, particle swarm optimisation (PSO) is used for hyperparameter tuning, followed by a local gradient based optimisation, using sequential quadratic programming (SQP). Note that for the kriging hyperapraemter tuning the only constraint is the minimum possible value for the hyperparameter p, which is set to 1.5. Hyperparameters such as Θ and p, act to maximise the likelihood of observed data, this improves the data fitting, as parameters are then chosen so that they model the function behaviour with greater consistency.

Note within this experiment it is possible to add points to the model in order to improve accuracy, via a mean squared error (MSE) convergence loop. The loop adds data points

incrementally using an MSE infill criteria, driving mean squared error to a lower value. However when the models created are relatively mundane, this practise is detrimental to the modelling as often design points are placed in the fringes of the design space, to expand the convex hull. This can lead to numerical noise in the outer reaches of the design space, causing the mean squared error to fluctuate until these edges are over populated.

The models are visualised in the manner seen in figure 5.2, where the top two figure are the two dimensional visualisations of the design variables, against their respective output variable, with the mean squared error plotted across the design space. The bottom figure presents a three dimensional visualisation of the overall design space. This modelling process is applied to each variable pair at each distinct level of structural fidelity, for each primary output. Note for each structural fidelity level the appropriate sub-design problems and optimisation modes are used, which reflect the optimal trend performance in chapter 4. These modification at each level can be seen in table 5.1.

Table 5.1: Checklist of Modification at each Structural Fidelity Level in Sensitivity Analysis Studies

Fidelity	Mass Opt. Mode		TT	Ribs	Stringers
	I	II			
Beam (Level I)	✓	×	×	×	×
3D (Level II)	✓	×	✓	✓	×
3DS (Level III)	✓	✓	×	✓	✓

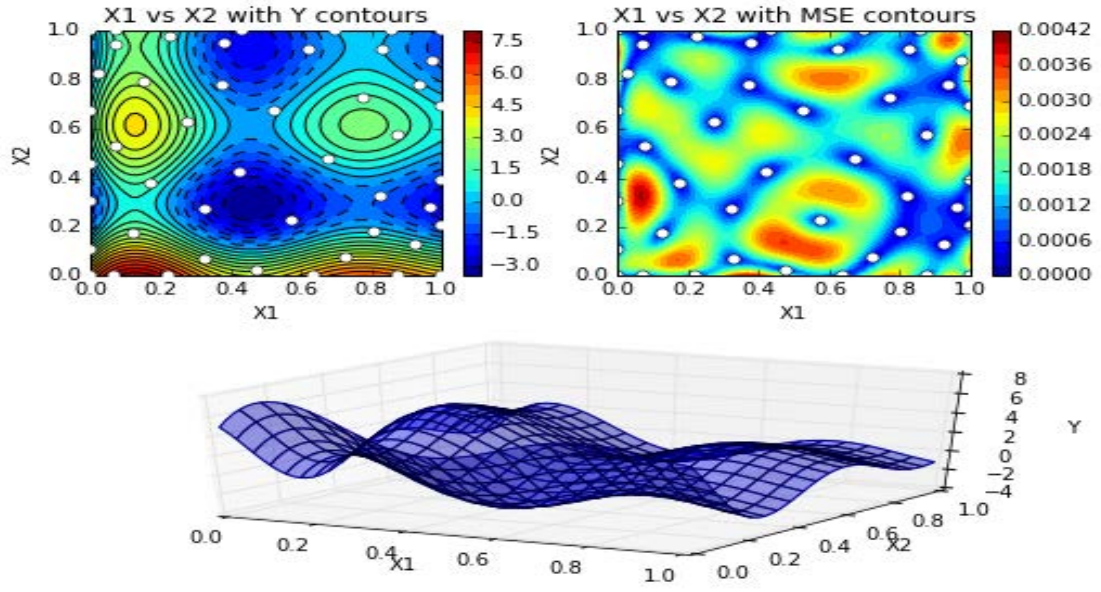

Figure 5.2: Example visualisation from the pyKriging(Paulson (2015)) module using an arbitrary two dimensional test function.

5.3 Wing Performance subject to Design sensitivity

The following sections provide visualisations of two design variable pairs (*AR-SG*, and t/c_r-$SWPI$) at each fidelity level. These visualisations are categorised by the output (weight, cost, D/q) in question and the level of fidelity (I, II , and III). Note in addition to these visualisations, tables of mean squared error results for each response surface model, for each pair, and fidelity level are provided, in tables 5.2 to 5.4. Note for the remaining pairs, the response surface visualisations can be found in appendix B.

5.3.1 Sensitivity Analysis Data and Error

Table 5.2: Mean Squared Error(MSE) of sensitivity RSM at Fidelity level I

Pair	Output		
	Weight	Cost	Drag
AR-SG	0.00677	0.006213	0.00124
AR-t/c	0.00865	0.004267	0.00018
AR-SWPI	0.0054	0.0161841	0.003849
SG-t/c	0.001666	0.00399	0.001729
SG-SWPI	0.004959	0.003019	0.002608
t/c-SWPI	0.011722	0.004314	0.002018

Table 5.3: Mean Squared Error(MSE) of sensitivity RSM at Fidelity level II

Pair	Output		
	Weight	Cost	Drag
AR-SG	0.046581	0.232450	0.221005
AR-t/c	0.01565	0.002555	0.002931
AR-SWPI	0.018837	0.008779	0.002896
SG-t/c	0.001888	0.004795	0.002715
SG-SWPI	0.001975	0.013747	0.00214
t/c-SWPI	0.015233	0.004039	0.003447

Table 5.4: Mean Squared Error(MSE) of sensitivity RSM at Fidelity level III

Pair	Output		
	Weight	Cost	Drag
AR-SG	0.033859	0.030072	0.008213
AR-t/c	0.051357	0.04885	0.005025
AR-SWPI	0.050184	0.048152	0.003471
SG-t/c	0.019563	0.023555	0.013422
SG-SWPI	0.0.041171	0.025792	0.012517
t/c-SWPI	0.504701	0.0.023039	0.00457

5.3.2 Sensitivity Analysis For Aspect Ratio with Area

5.3.2.1 Weight

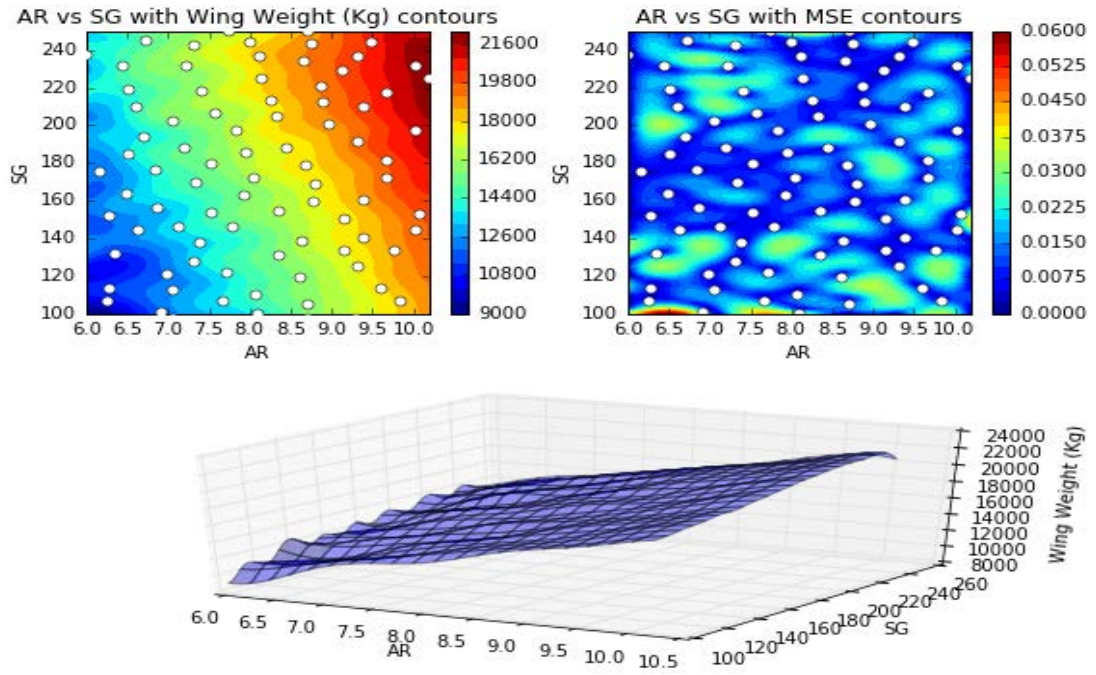

Figure 5.3: Visualisation of Weight (Ton.) for *AR-SG* variable pairing at fildeity level I.

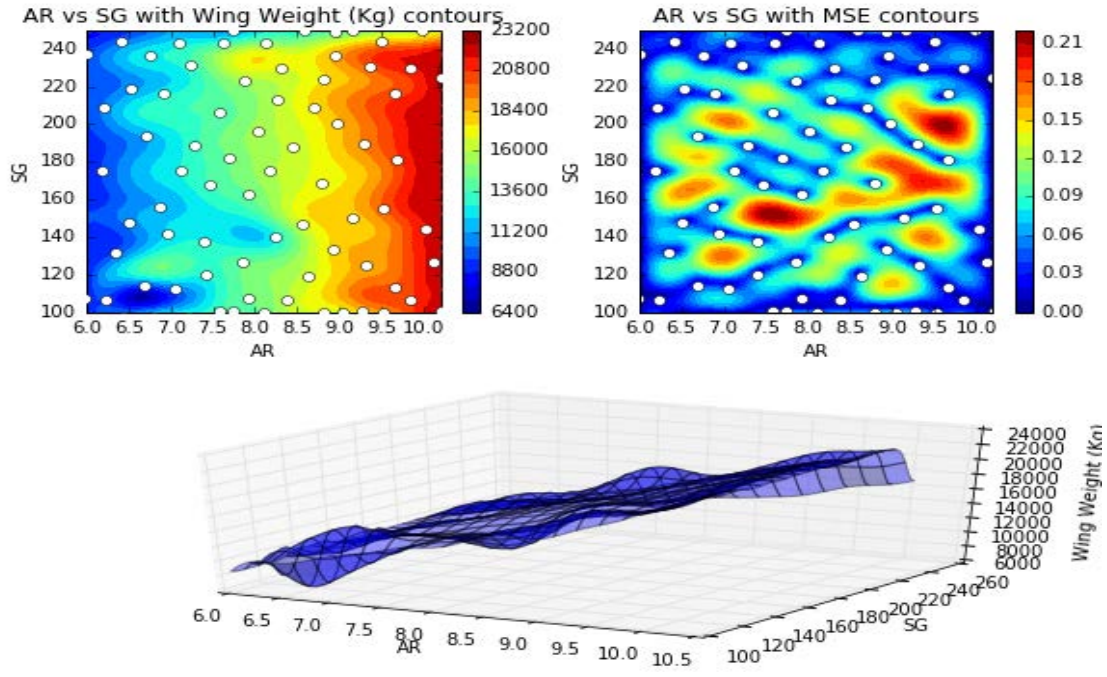

Figure 5.4: Visualisation of Weight (Ton.) for *AR-SG* variable pairing at fildeity level II.

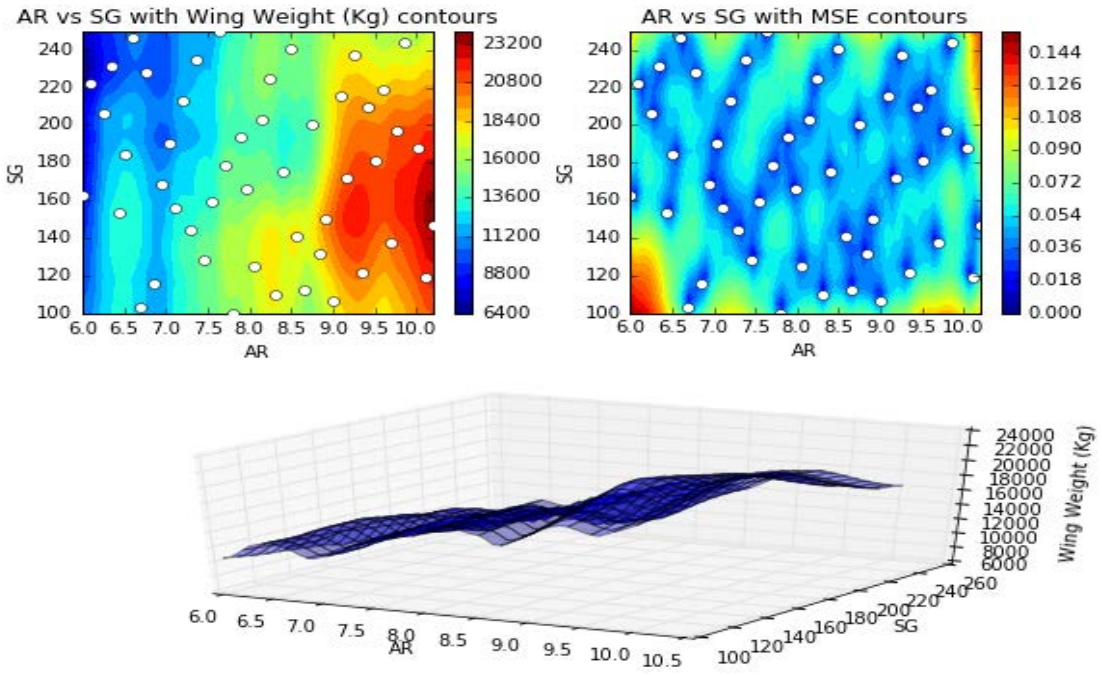

Figure 5.5: Visualisation of Weight (Ton.) for *AR-SG* variable pairing at fildeity level III.

5.3.2.2 Cost

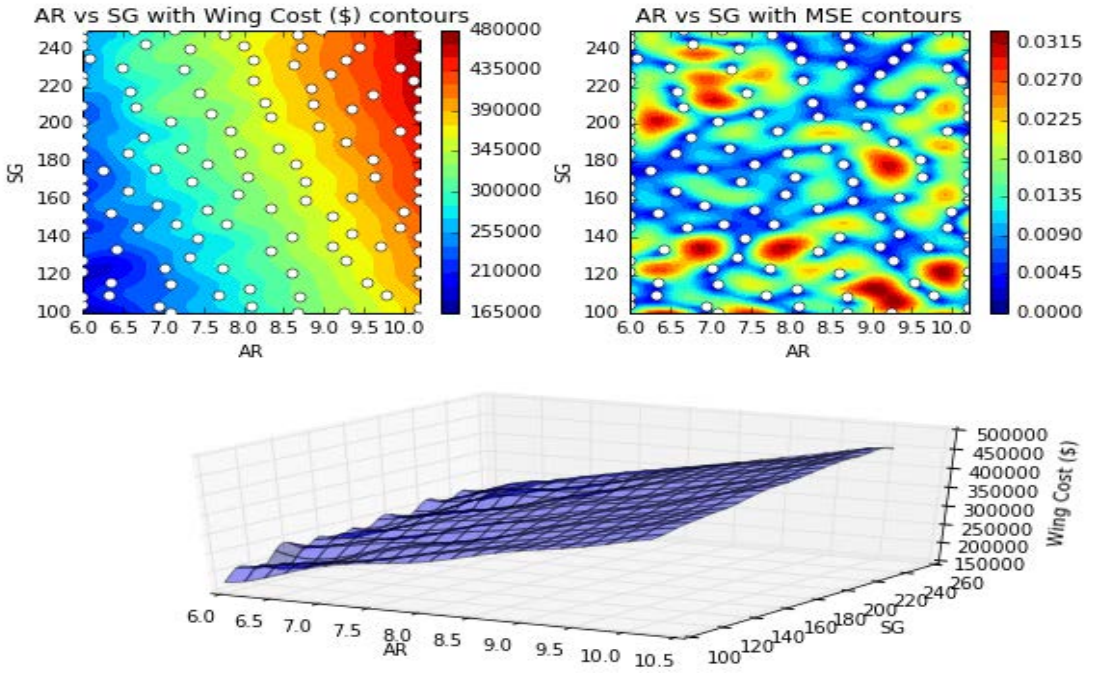

Figure 5.6: Visualisation of Cost ($) for *AR-SG* variable pairing at fildeity level I.

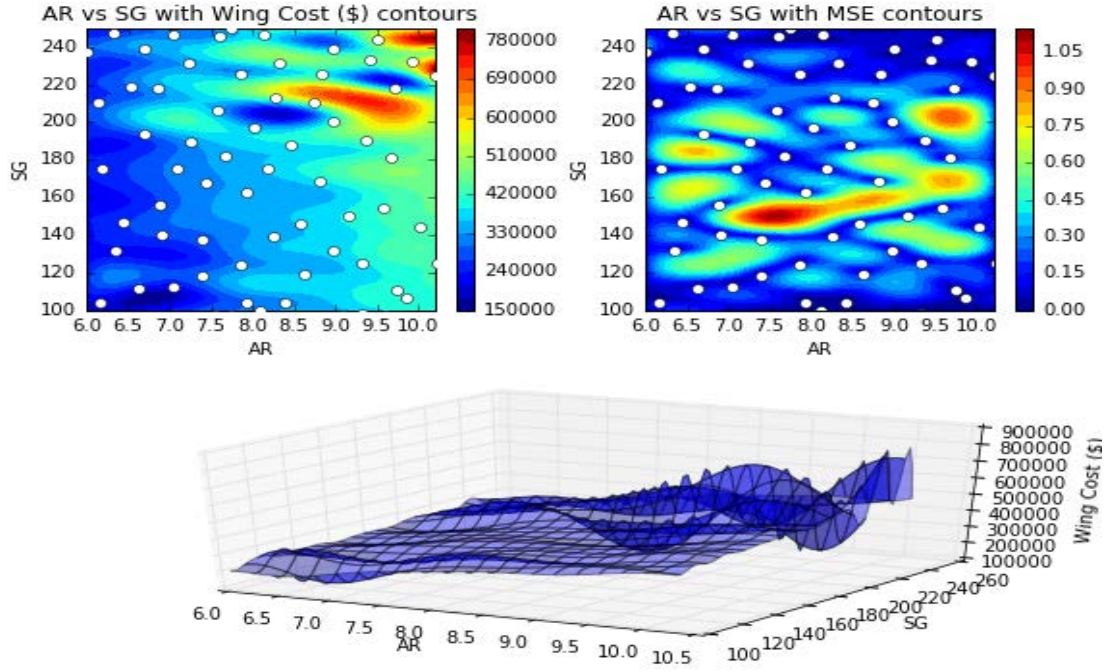

Figure 5.7: Visualisation of Cost ($) for *AR-SG* variable pairing at fildeity level II.

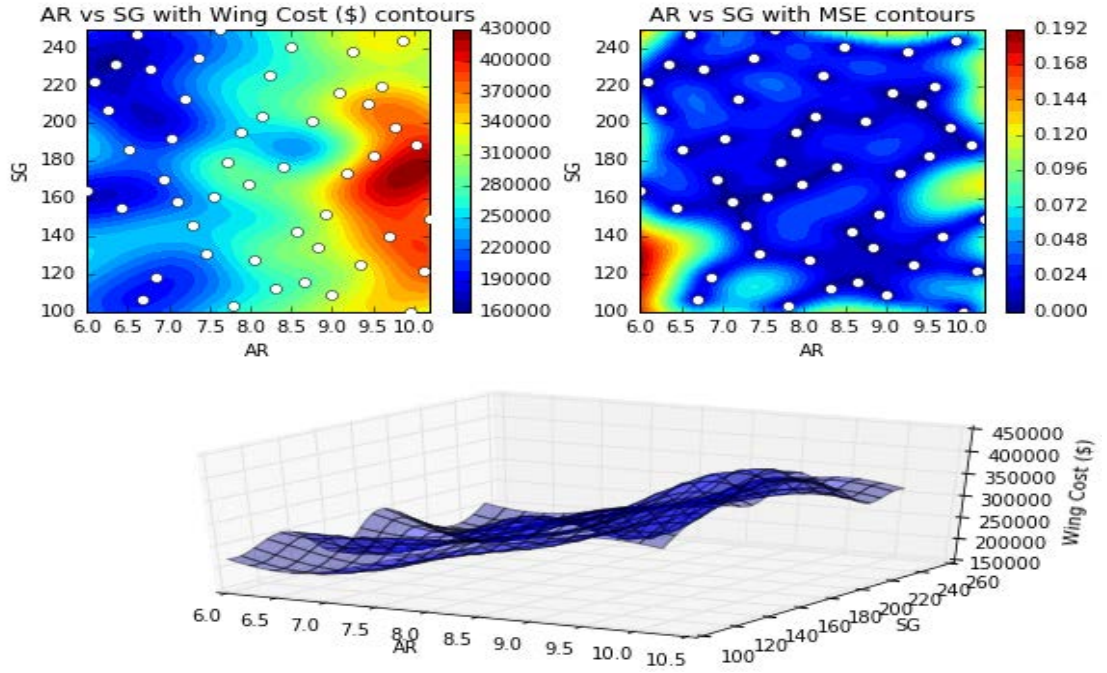

Figure 5.8: Visualisation of Cost ($) for *AR-SG* variable pairing at fildeity level III.

5.3.2.3 Drag

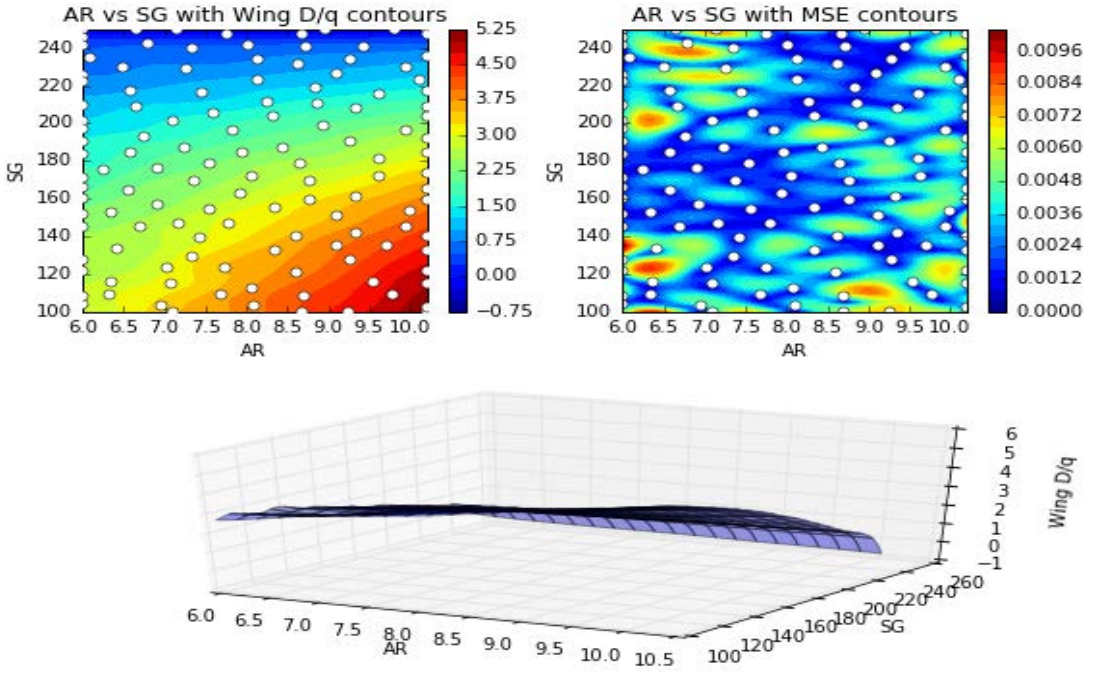

Figure 5.9: Visualisation of D/q for *AR-SG* variable pairing at fildeity level I.

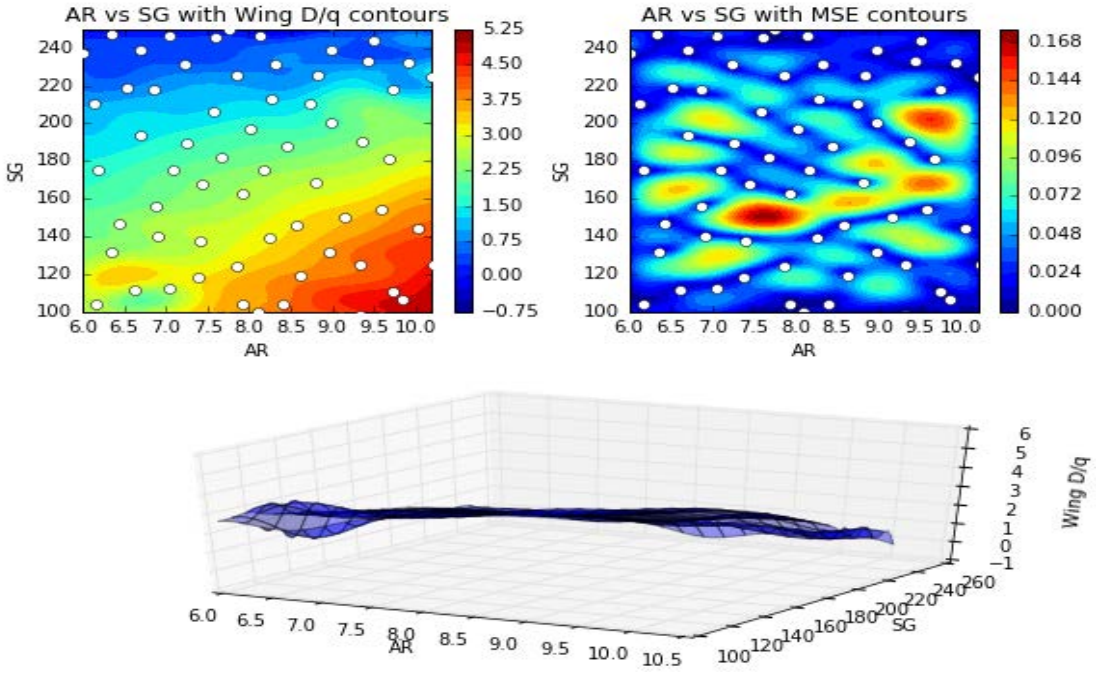

Figure 5.10: Visualisation of D/q for *AR-SG* variable pairing at fildeity level II.

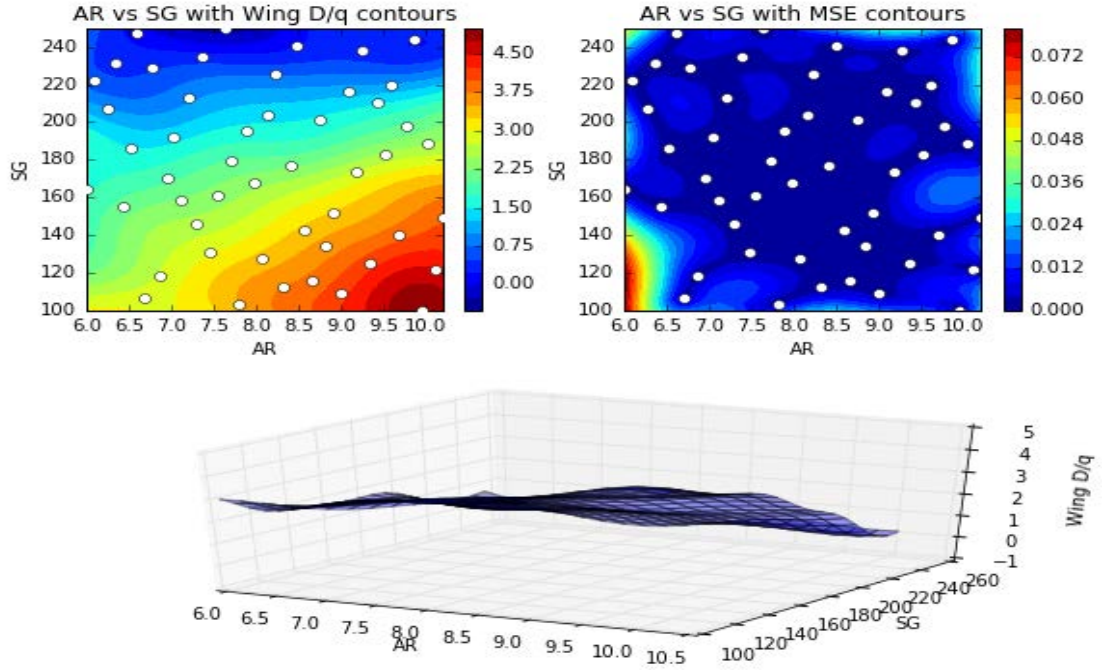

Figure 5.11: Visualisation of D/q for AR-SG variable pairing at fildeity level III.

5.3.2.4 Discussion

The trends in performance suggested at each fidelity level are understandable, as larger values or AR and SG are expected to yield a higher weight and cost. Note in weight (in figures 5.3 to 5.5) and cost (in figures 5.6 to 5.8), for models at structural fidelity level I and II, there is a flat region (shelf) at higher values of AR. At level I, this shelf appears initially at the fringes of the surface, along the edges of the design space, but is more prominent at level II. The key difference between levels I and II is the model fidelity and the addition of rotation information in aerostructural analysis, this leads to the change in the design space, which has greater local variation. At structural fidelity level III for cost and weight, the observed trends are noisier, when compared to previous fidelity levels. For drag (D/q) (in figures 5.9 to 5.11) however there is minimal change between fidelity levels.

The physical implications of the additional structural fidelity is the introduction of noise, and non-linearity to the performance trends. These are real issues in design process and are a direct representation of the so called data overhead. This noise is a reason why higher fidelity optimisation problems become prone to local solutions, when using global design variables. The navigation of this design space is non-trivial and difficult. Understanding the reasons for this non-linearity in reference to the design variables, can help determine which fidelity levels offer the easiest route to optimal designs.

5.3.3 Sensitivity Analysis For Thickness-to-Chord ratio at wing root with Sweep

5.3.3.1 Weight

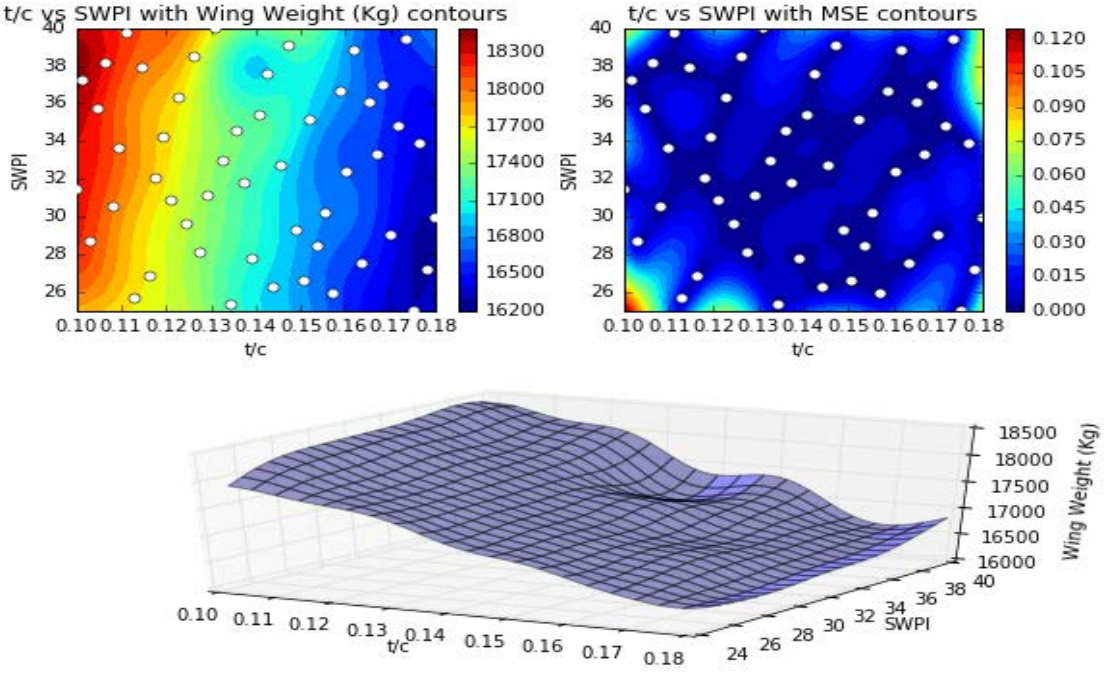

Figure 5.12: Visualisation of Weight (Ton.) for t/c_{r}-$SWPI$ variable pairing at fildeity level Beam I.

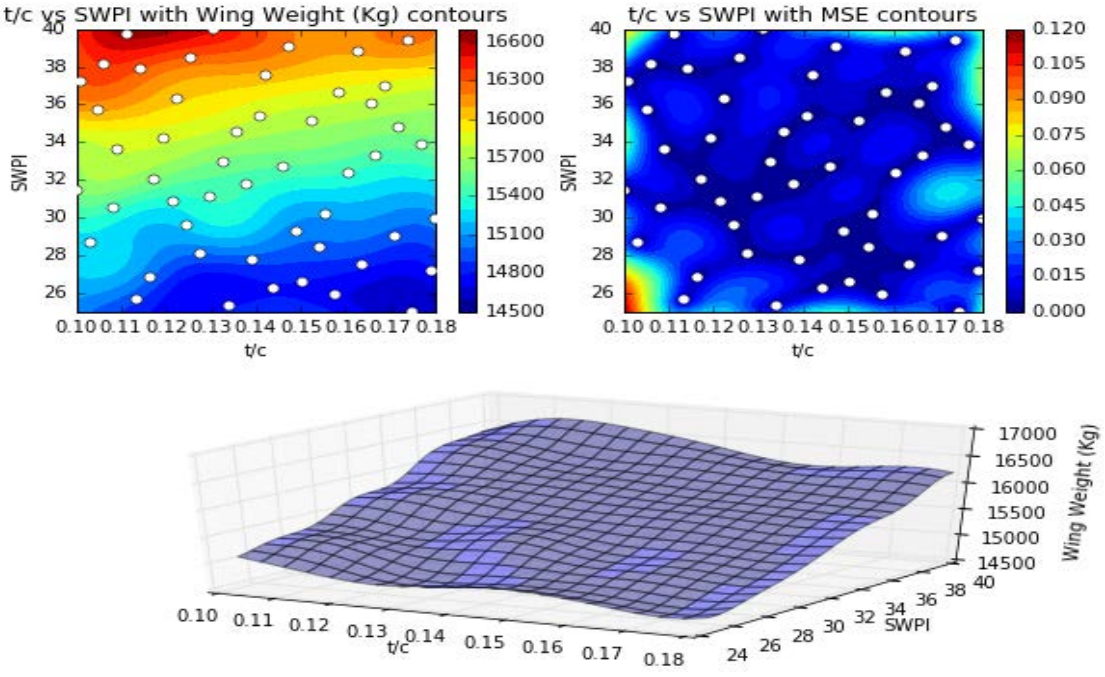

Figure 5.13: Visualisation of Weight (Ton.) for t/c_{r}-$SWPI$ variable pairing at fildeity level II.

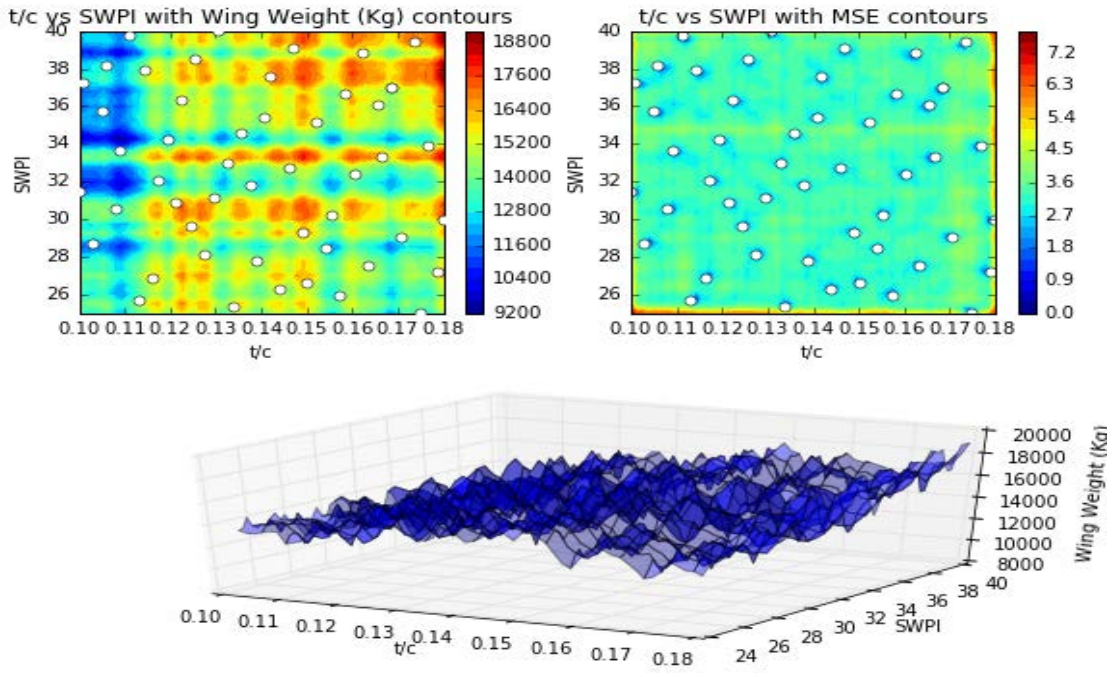

Figure 5.14: Visualisation of Weight (Ton.) for t/c_{r}-$SWPI$ variable pairing at fildeity level III.

5.3.3.2 Cost

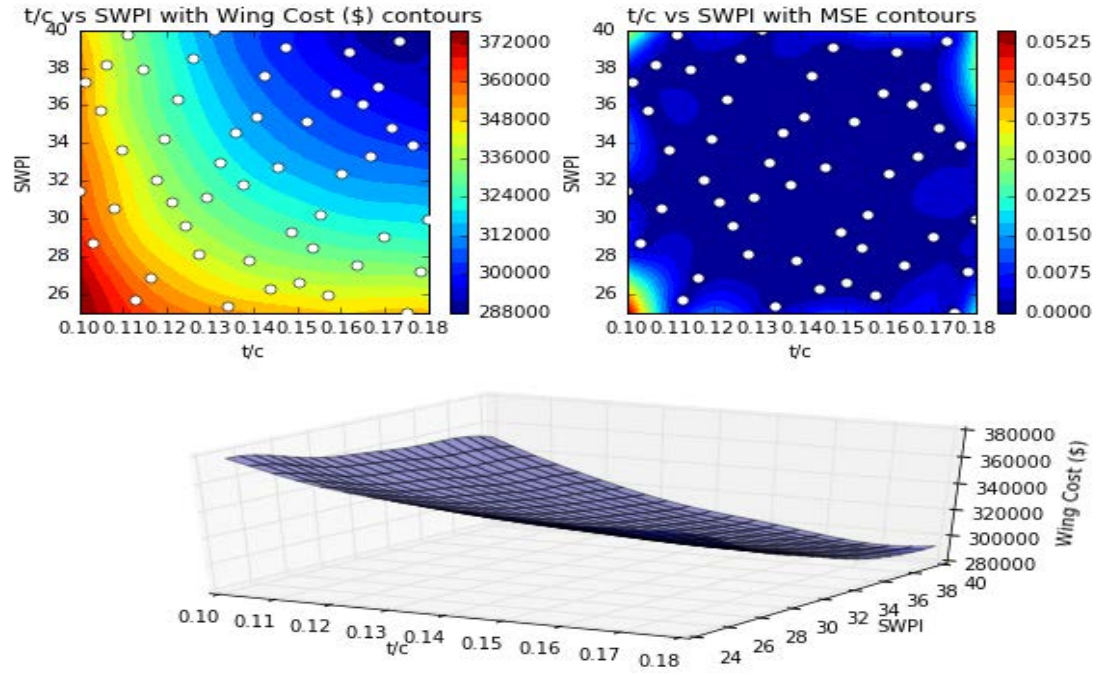

Figure 5.15: Visualisation of Cost ($) for t/c_{r}-$SWPI$ I variable pairing at fildeity level I.

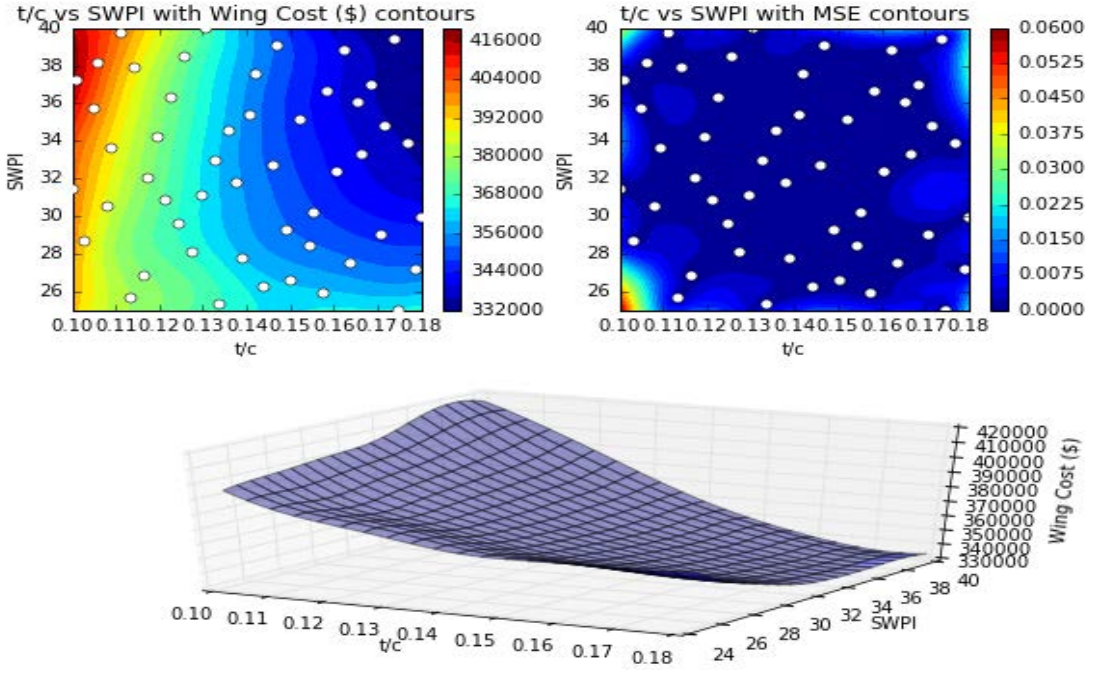

Figure 5.16: Visualisation of Cost ($) for t/c_{r}-$SWPI$ variable pairing at fildeity level II.

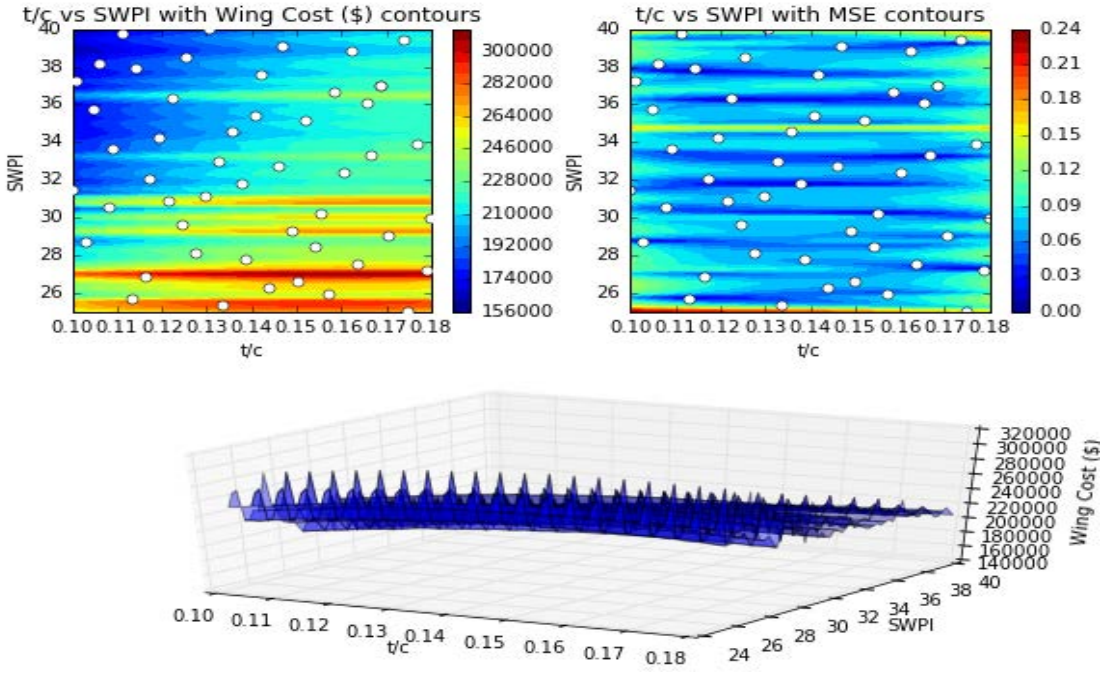

Figure 5.17: Visualisation of Cost ($) for t/c_{r}-$SWPI$ variable pairing at fildeity level III.

5.3.3.3 Drag

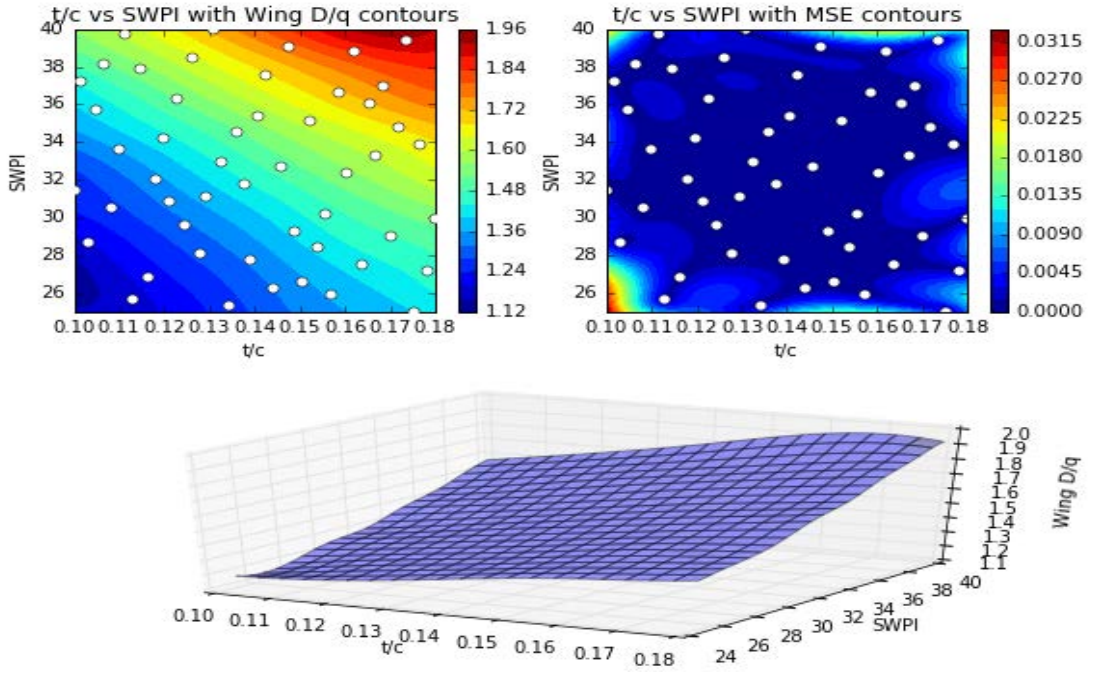

Figure 5.18: Visualisation of D/q for t/c_r-$SWPI$ variable pairing at fildeity level I.

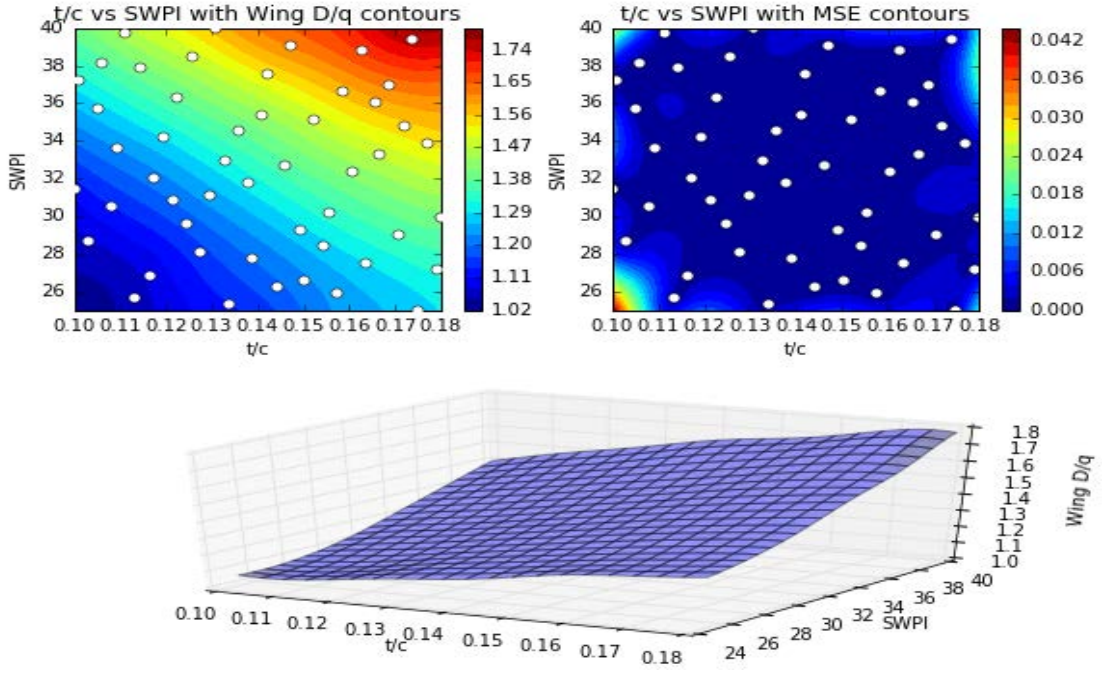

Figure 5.19: Visualisation of D/q for t/c_r-$SWPI$ variable pairing at fildeity level II.

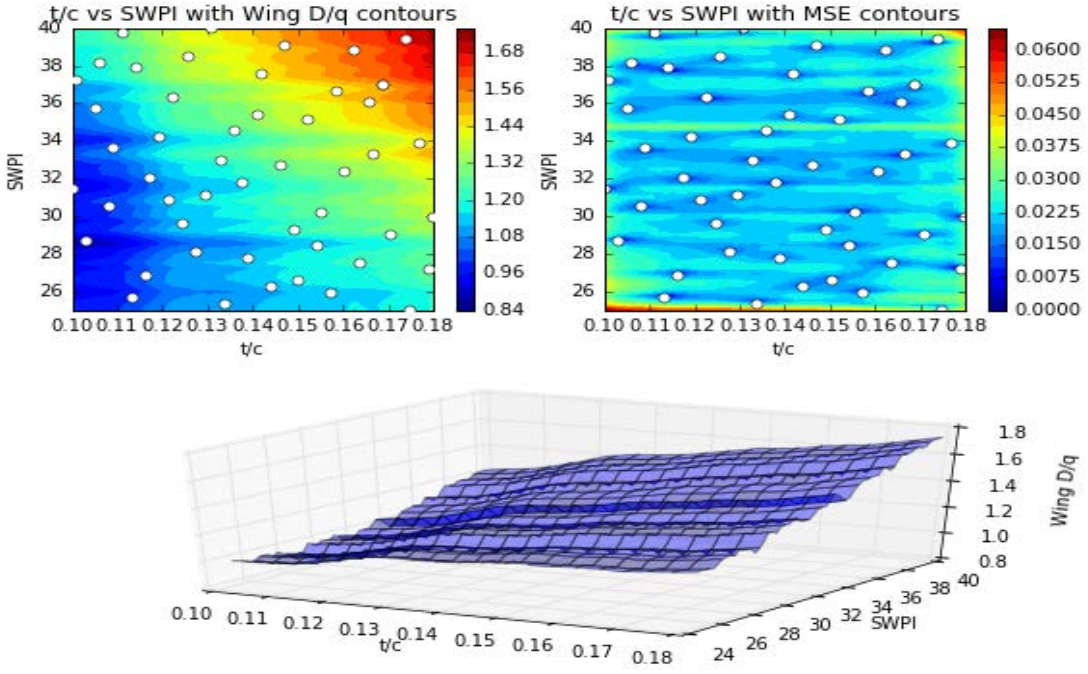

Figure 5.20: Visualisation of D/q for t/c_{r}-$SWPI$ variable pairing at fildeity level III.

5.3.3.4 Discussion

This variable pairing is an example of the importance of modelling sweep with greater fidelity and accuracy, in the finite element analysis and aerodynamic analysis. The comparison of the response surface for weight in particular between fidelity level I and II is difficult, as the surfaces are different. This is likely due to the substantial impact of the improved aerostructural coupling. At level I (figure 5.12), for weight, t/c_{r} becomes the dominant variable as larger value is preferred to reduce weight, with higher sweep causing an increase in weight. This behaviour is still present at fidelity level II (figure 5.13), but there is a skew towards lower sweep values for minimum weight designs. At this fidelity level the sweep is dominant and clearly dictates the behaviour of the response surface. Note now that t/c_{r} has marginal impact on the weight at a given sweep, and the dominance between this variable pair is reversed, at higher fidelity.

At level III, we see drastic noise and trend deviation. In this case the noise is likely due to local minima in the stress optimisation, caused by conflicting physical behaviour, which is a result of changes in the loading. Both $SWPI$ and t/c_{r} have conflicting implication on the load distribution, whilst $SWPI$ seeks to reduce drag, the increase in t/c_{r} increases it. This conflict is not easy to capture using such low fidelity aerodynamics, or simplified aerostructural coupling. In addition to this the non-linear behaviour of the stringers, creates noise inducing factors which influence the rather chaotic trends observed at fidelity level III (figures 5.14, and 5.17).

The weight trend behaviour observed at all levels, is somewhat similar for the cost trend. For levels I and II, it is clear that the minima region remains identical at high $SWPI$ and t/c_{r}. However the maxima region shifts from low t/c_{r} to high $SWPI$ at level II, as once again the $SWPI$ becomes dominant. Note for D/q (figures 5.18 to 5.20), there is relatively little change in the response surface at all levels. This implicates that the inaccuracies at fidelity level III for weight and cost trends, are predominantly linked to the structural and stress optimisation.

5.4 Conclusions

In general SG is a dominant variable at all levels of structural fidelity, however where the fidelity is lower it can skew the design space. In contrast at lower fidelity $SWPI$ has the least impact, however as the fidelity increases sweep introduces non-linearity to the design space. AR similarly to $SWPI$, becomes more influential when there is greater structural fidelity. Finally t/c_{r} does introduce some non-linearity at higher fidelity, when coupled with $SWPI$ especially. Generally it is easy to predict the impact of t/c_{r} on the design space as often it is the non-dominant partner. However at high fidelity, it can lead to noisy data, where stress optimisation is implemented.

For drag performance, the sensitivity studies and subsequent plots suggest that greater structural fidelity will improve exploitation of drag performance. This reinforces that aerodynamic analysis should include structural model details and should avoid using reduced order structural models. More complex structural models with aerostructural coupling are beneficial to exploring optimal design spaces, when conducting top level optimisation, in the aerodynamic domain.

The trends established at fidelity level I are conservative and mask non-linear effects, imposed by AR and $SWPI$, but capture trends from $SG$and t/c_{r}. Capturing accurate AR and $SWPI$ trends requires an increase in structural fidelity. However there are greater challenges related to traversing a non-linear design space, when optimising for global performance. If better trust regions for minima solution can be located for these variables, in incremental steps it is possible to achieve efficient design evolution and exploration. Knowing that for certain design variables it is acceptable to reduce the design space at a lower fidelity, allows the exploration of trust regions at higher fidelity for non-linear variables such as AR and $SWPI$.

5.4.1 Key Observation

We note that overall in the design spaces with feature predominant global changes to the wing such as SG and AR, and to a lesser extent $SWPI$ there is relatively linear behaviour observed at fidelity levels I and II, with non-linearity becoming influential at level

III. For $SWPI$ and t/c_r, which have a more subtle impact on the wing performance, we see that at level III, there is noise due to conflicting and competing physical behaviour. To achieve conformity and accuracy at this level when driving aerodynamic performance globally, and structural performance locally, a significant investment is required to fine tune and calibrate aerodynamics, and finite element analysis. This highlights a tipping point in structural fidelity investment, from models with conservative structural model representation. The design space exploration capability in T.A.C.E, has a clear penalty, where reducing fidelity allows trend exploration, but subject to penalties at higher fidelity.

Therefore to understand the nature of the design space we must observe these performance characteristics, with respect to all variables, and to each other. This can be achieved through numerous visualisation techniques. It also becomes clear that significant investment in response surface models at level III will not be beneficial, as a large expense in computational analysis may results in a complex non-linear, and noisy design spaces. The degradation of the surface quality at level III, is also noatble in the increasing mean square error, for each model and pairing in section 5.3.1. Therefore a methodology must be explored to enhance fidelity level II response surfaces, to capture level III sensitivities, whilst reducing the penalties of data overhead. This is best achieved through the use of data fusion, a technique explored by Keane and Nair (2005), and Piperni et al. (2013).

5.4.2 Contribution

In this chapter there are three clear objectives achieved with respect to the aims and this thesis. The studies in this chapter provide a benchmark for design space exploration for top level design parameters, and help quantify the global coupled behaviour of these variables, for key performance characteristics. This is done within an industrial context, and with industrial goals in mind. In addition the sensitivity plots help bridge the gap between complex response surface models with a greater number of design variables, reducing the stigma towards black box optimisation tools.

By building a data base of known and validated results, there is a metric for data comparison when using more complex response surface model. These results are from a code which has been calibrated and validated against known performance characteristics. The visualisation of the design space helps designers prioritise which design variable to freeze and vary in optimisation studies. Furthermore, they can help establish constraints for optimisation and trade-off studies, allowing greater design space exploration and optimisation.

The trends established are not absolute or precisely reflective of industrial trends, and feature limitations, however they demonstrate the steps required to reduce data overhead, and introduce design search capability. They achieve this through demonstrating the nuances in design variable coupling and perturbation, and how fidelity variation affects the design space, and sensitivity of design variables. This helps to determine which levels of fidelity are suitable for optimisation, and at which levels additional consideration should be given to certain variables.

Finally a clearer answer as to which fidelity level is most suitable for use in design exploration, and industrial multidisciplinary optimisation has been found. The results implicate that fidelity level II is suitable for exploration, with the caveat that there is some conservatism and a penalty for physics based analysis. It is clear that at fidelity level III, significantly greater investment is required in detailed analysis parameters. As the aim is to improve exploration capability, we suggest that level II is ideal, but enhance this level can be enhanced further for exploration and optimisation capability, by including data from level III. This improves accuracy, by including additional physics based data.

5.4.3 Design Space Exploration

A means by which to can assess the overall influence of design variables together on the performance output design space, at each fidelity level, is through further surrogate modelling, and data visualisation. Visualisation techniques such as parallel axis plots, and hierarchical axis plots, can help sift through raw data accurately and visualise multiple design variables in two dimensions. Response surface models can also facilitate data fusion to help map higher fidelity data with lower fidelity data, in order to improve the accuracy of the lower fidelity models. This technique is ideal for mitigating the noise we observe at fidelity level III, whilst enhancing level II data. This is a level where minor investment allows the capture of non-linear complex physics, without noise in the design space. This effectively offers a solution to two industrial design problems, data overhead, and design exploration.

In addition, using all four design variables for response surface creation helps achieve multi-objective multidisciplinary optimisation. This optimisation can create Pareto fronts, which helps to locate ideal trust regions and non-dominated solutions. Such fronts can highlight the competition between performance characteristics at each fidelity level, and show the designer which performance quantity is subject to greater penalisation, or greater exploration capability. From these visualisations it is possible to identify regions where cumulative non-linear effects are minimised, and non-dominated solutions are feasible. The visualisations and multidisciplinary optimisation, aid in the establishment of an exploration methodology to achieve greater exploration of the design space, as seen in Chapter 6.

Chapter 6

Response Surface Creation for Design Exploration

6.1 Introduction

Presented in this chapter is a designs exploration methodology, where the outputs from T.A.C.E are visualised, optimised, and evaluated for sensitivity, for top level design variables of the wing. This is done through the creation of four dimensional design of variables, which are visualised using parallel coordinates and Hierarchical Axes technique (HAT), and trained using Kriging. The surrogates created can be used for multi-objective evolutionary optimisation for Pareto front creation. The visualisation techniques are presented as a means by which global performance trends can be identified for multivariate data, and to visualise multidimensional design spaces in order to improve optimisation. The Pareto front creation using evolutionary multi-objective optimisation is shown to aid design space exploration and improve decision during optimisation between the conceptual and preliminary design stages. The visualisation, optimisation, and front creation is implemented for all fidelity levels so that comparisons can be made between low and high fidelity design spaces. Note for fidelity level III in this chapter, the raw data is replaced by fidelity level II data enhanced through substitution of data from fidelity level III.

6.2 Visualisation & Optimisation Methodology

6.2.1 Introduction

The following section provides information on the creation of new surrogate models for all design variables for each performance output, at each structural fidelity level.

In addition to this a three step visualisation methodology, to implement design space exploration is presented. This methodology has three key visualisation techniques, all centred on the manipulation of raw data from design of experiments and utilisation of surrogate models in optimisation. The three steps refer to the three techniques and the order in which they should be implemented.

Firstly, having raw data allows further assessment of trends, and variable sensitivities. Parallel axis plots to visualise trends in raw data, can confirm the impact of structural fidelity variation, and allows ranking of performance metrics. The ranking of performance outputs to assess best possible designs, helps illustrate trends in design variables. This can help to locate trust regions and to identify which variables are more susceptible to noise. This can be implemented at various levels of fidelity, to further understand the behavioural trends.

Secondly having visualised trends in the raw data, surrogate models can be created using kriging, as seen previously in chapter 5. These models for a larger number of design variables are difficult to visualise if the number of dimensions exceeds three. Hierarchical Axis Plots can help to condense design space variation for multiple variables using two dimensional visualisation. The details of this are discussed in section 6.2.3. Variables with less sensitivity or linearity can be discretised, and the design space can be assessed for variation of the sensitive or non-linear variables. This helps to qualitatively and quantitatively assess patterns in non-linear behaviour over the design space.

The third step in the visualisation is the assessment of performance outputs with respect to each other. Having assessed the sensitivity of design variables to the performance metrics, the relationship of these outputs to each other must be evaluated. Pareto fronts from multi-objective optimisation using a population based methods are a means to achieve this. The data generated from optimisation can be assessed using Pareto optimality criteria, and non-dominated regions of optimal results can be visualised. Pareto front visualisation can help locate trust regions which are not always investigated during the design process.

This three step methodology is key to demonstrating how academically viable solutions can be implemented with trust in other multidisciplinary systems. This is subject to investment in variable fidelity capability and design space assessment using surrogate modelling.

6.2.2 Parallel Axis Plots

Parallel coordinates is a visualisation technique which allows multivariate data of N dimensions to be analysed. This allows behavioural patterns to be established and traced as combinations of parameters. This visualisation is helpful when investigating databases of information, and was initially proposed in Inselberg and Dimsdale (1990).

In order to visualise a data set this technique assigns a series of vertical axis for each design variable, scaled within a design range and intersected by connecting lines. Where the intersection point on each axis marks the value of the variable represented by that axis. Through this visualisation patterns in the data can be identified, where movements between vertical axes dictates positive or negative relationship(s) between variables. In addition pattern recognition can be aided through data sorting where the outputs variables can be ranked and assigned different colour schemes. This allows key design drivers and outliers in the data to be recognised, Goel et al. (1999).

In this chapter the raw data from a design of experiments of 250 points at each fidelity level, was parsed through a parallel coordinate visualiser. This allows the assessments of trends within this raw data. The ranking of each output variables ($Weight$, $Cost$, D/q) through minimum values, allowed the visualisation of the top 5%, next 20%, and worst 75% of the data as block patterns. These patterns were compared to the data trends in chapters 5 and 4, and compared for each fidelity level. Note that in addition to the parallel axis plots, the mean standard deviation (MSD) has been calculated for the raw data. These plots can be seen in appendix C, and are a useful guide to judge the impact of fidelity variation on the average performance trends.

An example of a parallel axis plot for an arbitrary function with four variables

$$Y = x_1 + x_2^2 + x_3^3 + x_4^4 \tag{6.1}$$

Is found in figure 6.1. For this values closer to 1 for output Y are prioritised and the colour red is representative of the best designs (top 5%), blue is representative of the next 20%, and green represents the worst 75%.

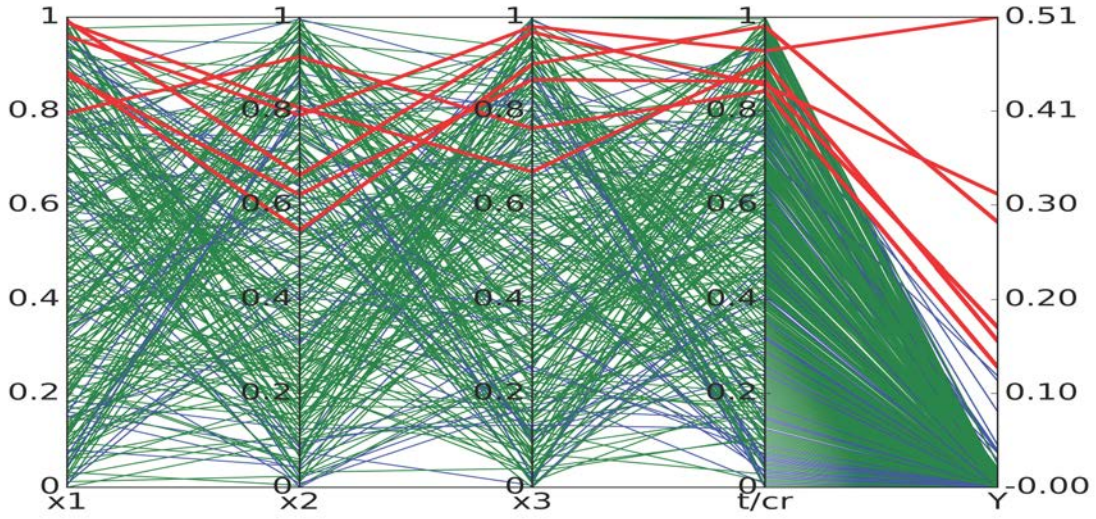

Figure 6.1: Parallel axis plot of 250 point data set in four dimensions for output (Y) of equation 6.2.

6.2.3 Hierarchical Axis Plots

Hierarchical Axis Technique (HAT) for data visualisation was initially suggested by Mihalisin et al. (1991). This technique is designed to aid in the visualisation of data with multiple dimensions, past the limit of human visualisation capability. It is designed to visualise non-grid like and/or non-scalar data, and is ideally suited for design of experiments, or response surface model data, with three or more dimensions. This works by visualising the design space for a given variable, or output for two variables in two dimensions, for fixed values of two other variables. The fixed variable values are changed, and the design space visualisation is conducted for each variation, creating a two dimensional visitation of four design variables, for output variable. This strategy was implemented for engineering problems by Holden and Keane (2004).

An example of HAT plot visualisation can be seen in figure 6.2, where the output Y of function

$$Y = x_1 + x_2^2 + x_3^3 + x_4^4 \tag{6.2}$$

Is visualised for variables x_3 and x_4 at fixed values of x_1 and x_2. This example demonstrates how complex response surfaces or design of experiment data can be visualised, allowing the designer to understand the variation of an output with respect to the design variables of interest.

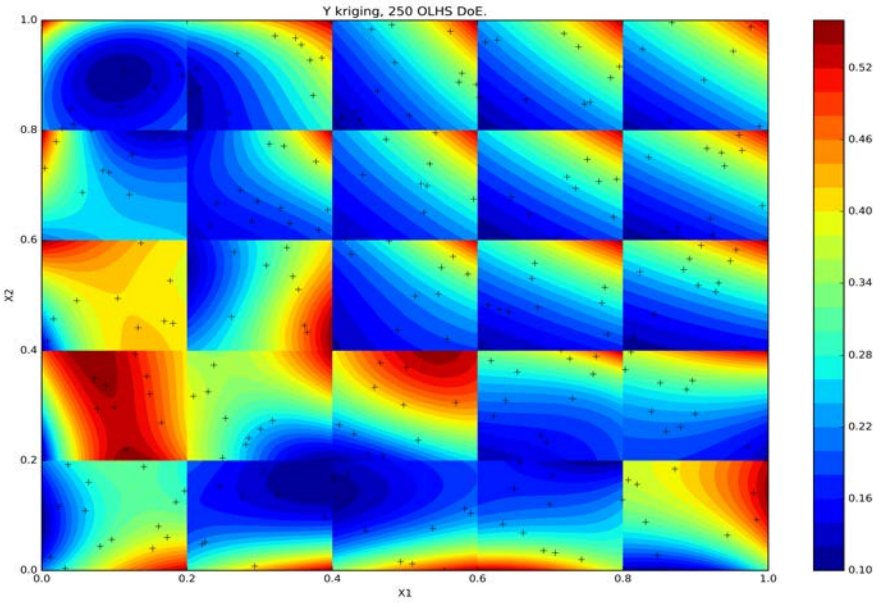

Figure 6.2: Hierarchical Axis Technique (HAT) plot of 250 point data set in four dimensions for output (Y) of equation 6.2.

6.2.4 Pareto Fronts

In this work during the process of design sensitivity assessment and objective visualisation, each performance output has been visualised independently. However with access to surrogate models for all variables, at each fidelity level, the outputs can be compared simultaneously. This is possible through the use multi-objective optimisation and visualisation. The aim is to use each surrogate for multi-objective optimisation allocating an equal weighting for each performance output. As the response surface models allow cheap evaluation of the data, this process can be cheap computationally and offers the designer a three dimensional view of the objective functions at each fidelity level. The process of multi-objective optimisation to determine the visualised data sets is covered in section 6.2.5.2.

Pareto fronts are based on the visualisation of data which satisfies Pareto optimality criteria Pareto (1906), applied to a multi-objective problem Stadler (1979) and Stadler (2013). The Pareto optimality criteria when applied to a multi-objective problem is a method by which to determine which solutions in the feasible range are not dominated by a single optimisation objective. This allows the location of a region of feasible optimums, where the solutions are not skewed in favour of a given objective.

For visualisation the objectives outputs are treated as axes, where up to three objectives can be visualised through scatter plots. Further to this the non-dominated points which fulfil the optimality criteria, can be sorted and highlighted and interpolated to create a curve or surface, aiding the visualisation of the Pareto front. The interpolation between points is achieved using Delaunay triangulation. Three dimensional Pareto fronts from T.A.C.E outputs using the response surface models created in this chapter, can be seen in section 6.3. For visualisations the weight sum method was used to calculate the dominated points, which are then used to create a three dimensional surface.

6.2.5 Optimisation using Response Surfaces

6.2.5.1 RSM Methodology

The exploration for all variables at the three given levels of structural fidelity, can be achieved using surrogate models. At each level of fidelity a budget of 250 points is given for a four dimensional design space, for SG, AR, $SWPI$, and t/c_{r}. These variables are scaled and the T.A.C.E analysis is run for each sample set, following which three kriging models are trained. A model is created for each performance output. Note level I and II are run directly from T.A.C.E for this design of experiments budget. However for level III, as discussed previously, the level II results are instead enhanced through substitution of data from level III. This is done initially for 10% of the data, where level III points are substituted into the level II data set. Substitution is preferred over fusion,

as the design of experiments remains identical at all levels of fidelity. The surrogate models for each fidelity level are stored and are readily accessible for improvement or re-training.

For the process of the process of Pareto front creation, multi-objective optimisation was implemented. The creation process for which is identical to the process in section 5.2.2, figure 5.1, with an increased number of variables, and a larger design of experiments of 250 points.

6.2.5.2 Multi-objective Optimisation

Within the design process, results in a single objective analysis methodology, where a key discipline is prioritised and optimised for performance. It is then up to connected disciplines to ensure that the solution identified by the key discipline, is viable. A method to avoid this complication is to conduct multi-objective optimisation for the performance of several disciplines, with a weighting factor for each disciplinary objective function. However this can lead to skewed results, as the distribution of weighting factors can create solutions dominated by a particular discipline.

The creation of Pareto fronts can allow the identification of non-dominated solutions prior to substantial investment in disciplinary and global preliminary optimisation. In this chapter the T.A.C.E process is used to instantiate response surface models for multi-objective optimisation. Which facilitates design exploration and trust region identification. This expands the knowledge base for design exploration and can be applied to explore novel design spaces. This approach improves the management of optimisation problems and trade studies by creating optimisation work packages, which provide greater flexibility. Examples of different approaches to multi-objective optimisation can be found in Fonseca and Fleming (1995).

Within the T.A.C.E program care has been taken to capture the design process and key disciplinary interactions. Through surrogate modelling it has been shown that design space visualisation is possible, and beneficial to the understanding of performance characteristics, and global design variables. Using response surfaces for performance outputs, multi-objective optimisation at a global level was possible. Following this Pareto fronts for $Weight$, $Cost$, and $Drag$ at each fidelity level were created.

In this chapter the response surface models created were utilised for efficient and cheap analysis of the objective values, allowing large population sizes initially and leading to much shorter lead times. This proves that investment in such models can lead to improved design capabilities. These runs have a substantially low set up cost, and are easy to repeat, as the largest expense is the generation of raw analysis data. This data can also be enhanced and expanded allowing future studies.

Within this chapter the chosen population based method is the academically known NSGAII algorithm, Deb et al. (2002), which has been implemented in a python module known as DEAP, Fortin et al. (2012). The details of parameters utilised in the Evolutionary Algorithm (EA), can be found in section 6.4. Note the multi-objective optimisation is formulated such that all three objectives (Weight, Cost, Drag) are weighted equally, and minimised subject to the conventional range for the design variables already established in previous chapters. In addition the outputs are normalised for use in fitness function creation, to avoid large deviation in the datasets utilised for front creation.

6.3 Results of Visualisations: Step 1 and 2

6.3.1 Step 1: Parallel Axis Plots

6.3.1.1 Weight

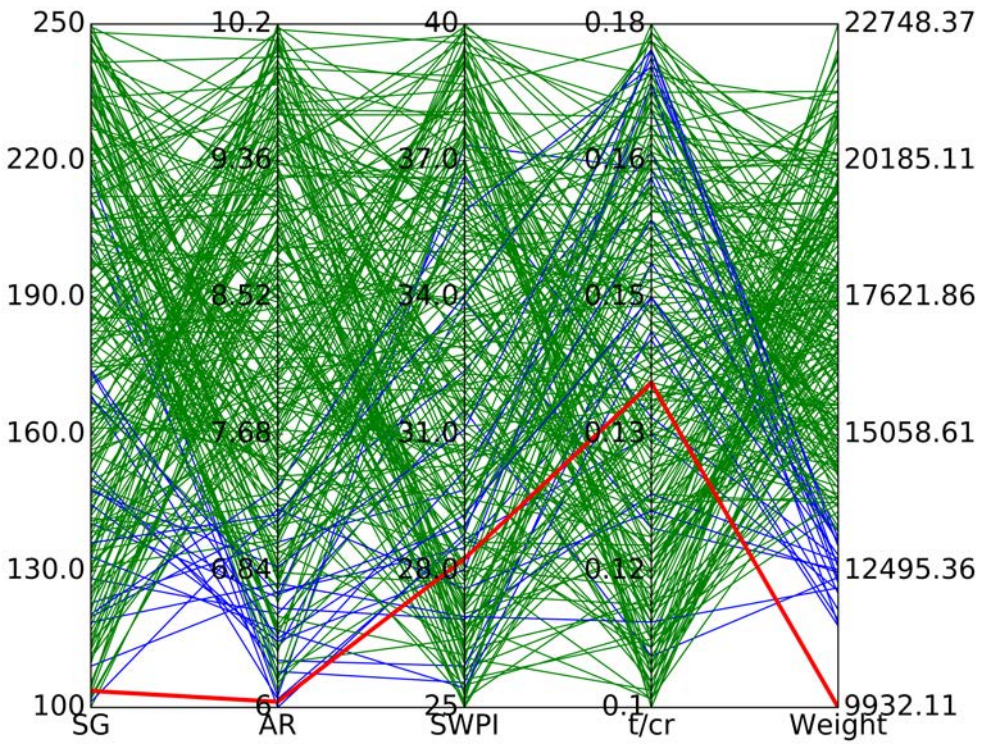

Figure 6.3: Parallel axis plot of 231 point data set in four dimensions for output (Weight) for T.A.C.E fidelity level I.

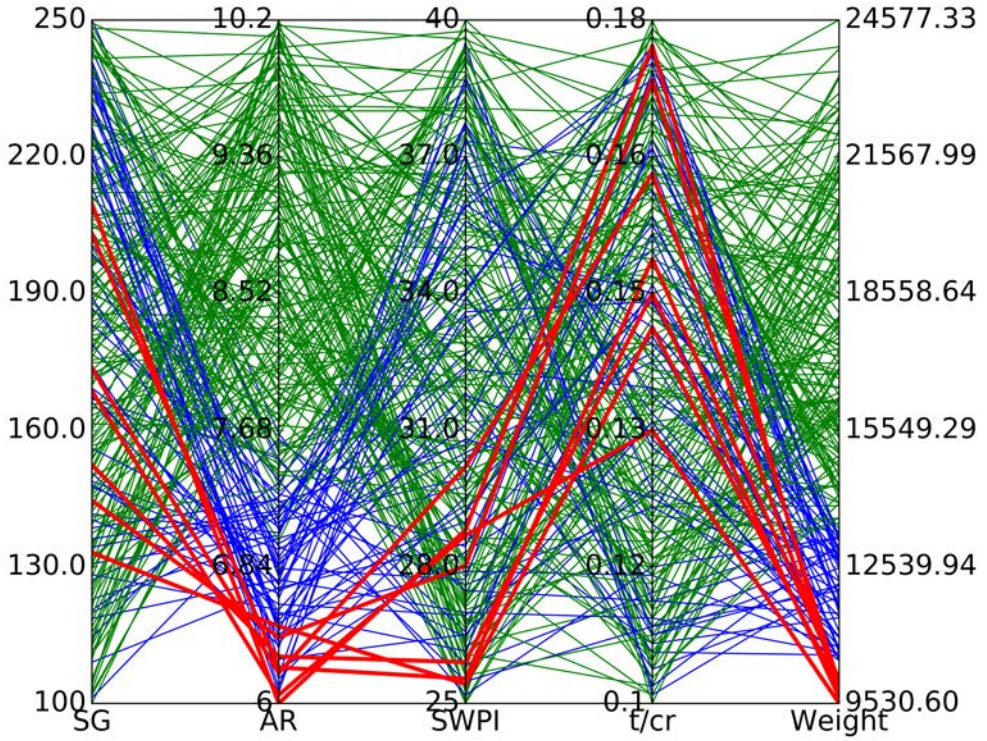

Figure 6.4: Parallel axis plot of 227 point data set in four dimensions for output (Weight) for T.A.C.E fidelity level II.

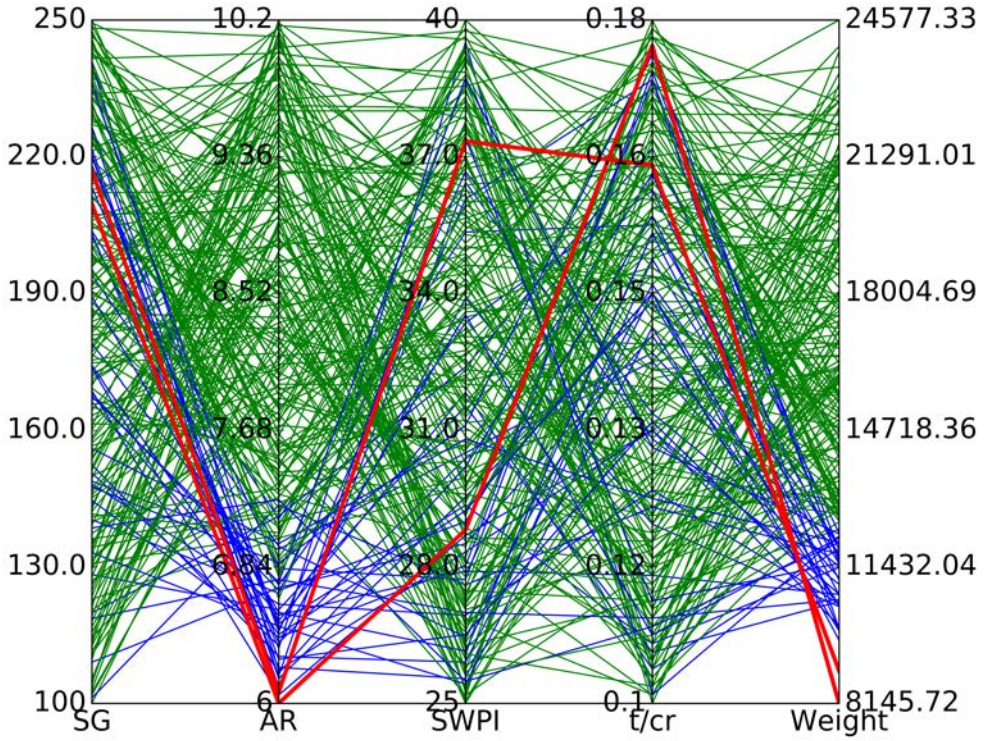

Figure 6.5: Parallel axis plot of 227 point data set in four dimensions for output (Weight) for T.A.C.E fidelity level III.

6.3.2 Discussion: Weight

Parallel axis plots trends show interesting results as we move from fidelity level I to II and then to the enhanced level II results (known as level III). For weight (figures 6.3, 6.4, and 6.5) we note that overall the trends are very similar between levels, however note that at level I and III there are fewer minimum designs. In addition the main difference between the trends is the relative conservatism in AR and $SWPI$ values at level. This can be relatively easily explained due to the lack of complex physics which can be captured at this level for the given variables. However the converse is true at level III, where $SWPI$ is no longer conservative, however the uncertainty caused by the substitution of level II data, leads to a deficit of minimum performance values.

In addition the limitations of the full potential method are detrimental to the exploitation of these variables, this is less apparent at level II where greater detail is available in the aerostructural coupling. However that the range over which the weight can vary is smaller at level I, demonstrating that at this level it is not possible to explore the full design space effectively. At level III the minimum boundary is reduced implying that the possible minimums observed at level II are marginally conservative.

6.3.2.1 Cost

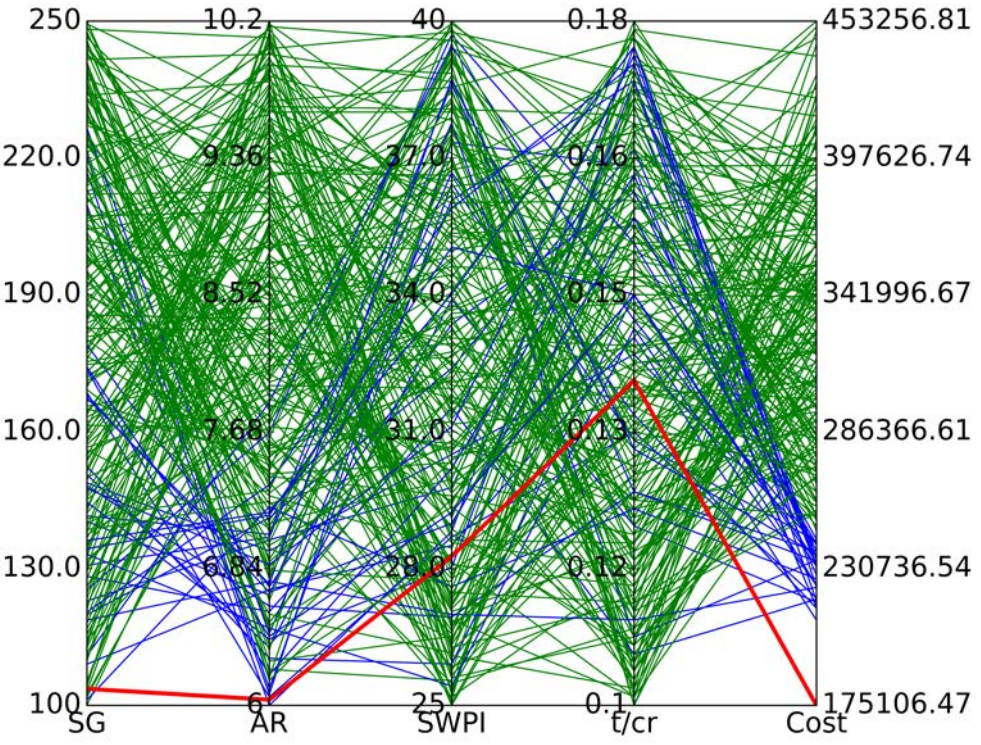

Figure 6.6: Parallel axis plot of 231 point data set in four dimensions for output Cost for T.A.C.E fidelity level I.

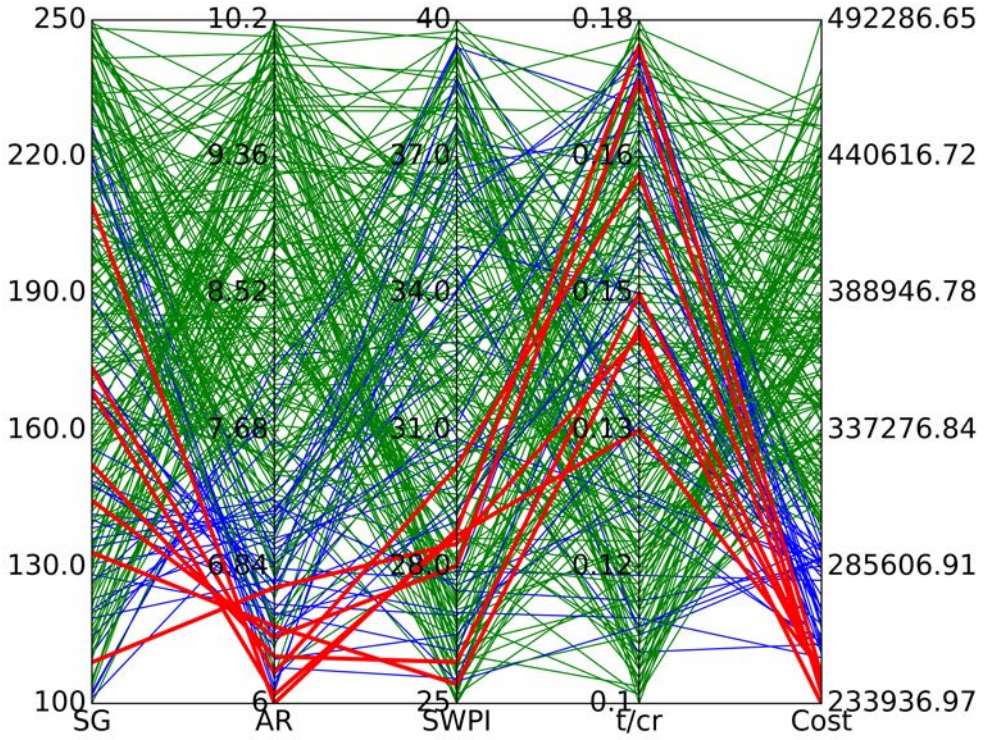

Figure 6.7: Parallel axis plot of 227 point data set in four dimensions for output Cost for T.A.C.E fidelity level II.

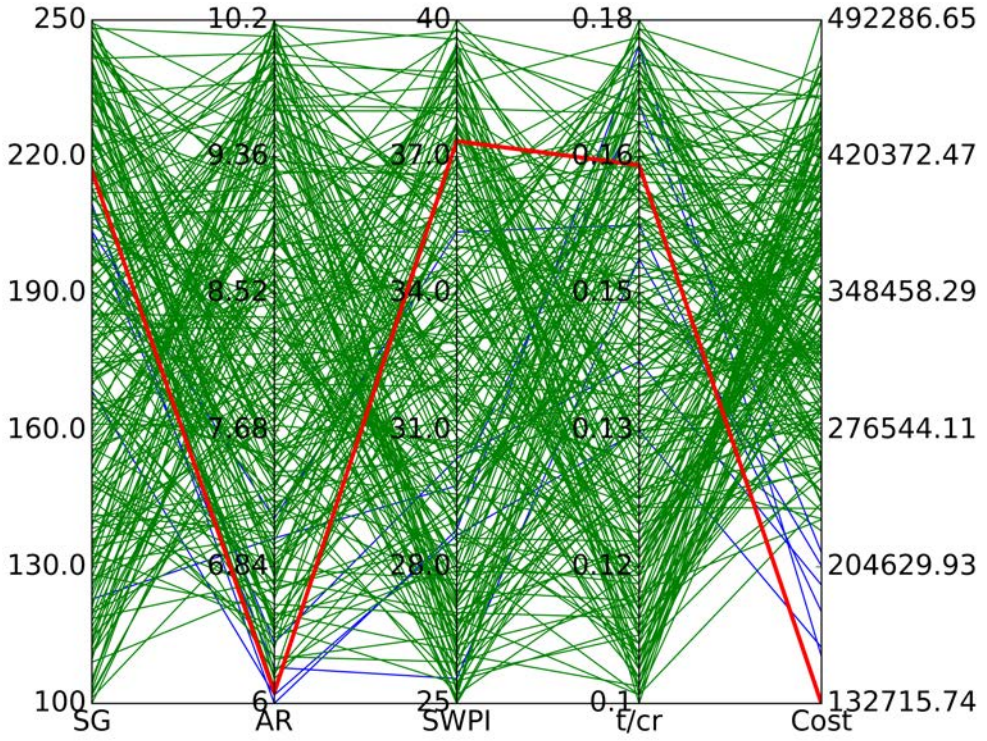

Figure 6.8: Parallel axis plot of 227 point data set in four dimensions for output Cost for T.A.C.E fidelity level III.

6.3.3 Discussion: Cost

For cost (figures 6.6, 6.7, and 6.8), there is a clear disparity between trends at level I and II, and to a lesser extent III. Especially for t/c_r and $SWPI$. The full impact of higher sweep and aspect ratio is not captured at level I and the trends suggest it is not possible to have radically high values for $SWPI$ in particular, to achieve minimum cost. However with the addition of fidelity at level II for $SWPI$ in particular, there is now a concentration of sweep, over a small range. Note at level III once the uncertainly and noise changes the complexions of cost trends, and high sweep is prefer for minimum designs. Though a dearth of trends for the best 25% of designs could mean this trend is an outlier.

As a final note for cost, the range over which the level I cost values vary, is smaller and lower, converse to CADCO software trends in variable perturbation studies, chapter 4. There is some optimistic predication of cost at lower fidelity. At level II and III, the minimum boundary in particular is expanded showing that there is greater scope for exploration.

6.3.3.1 D/q

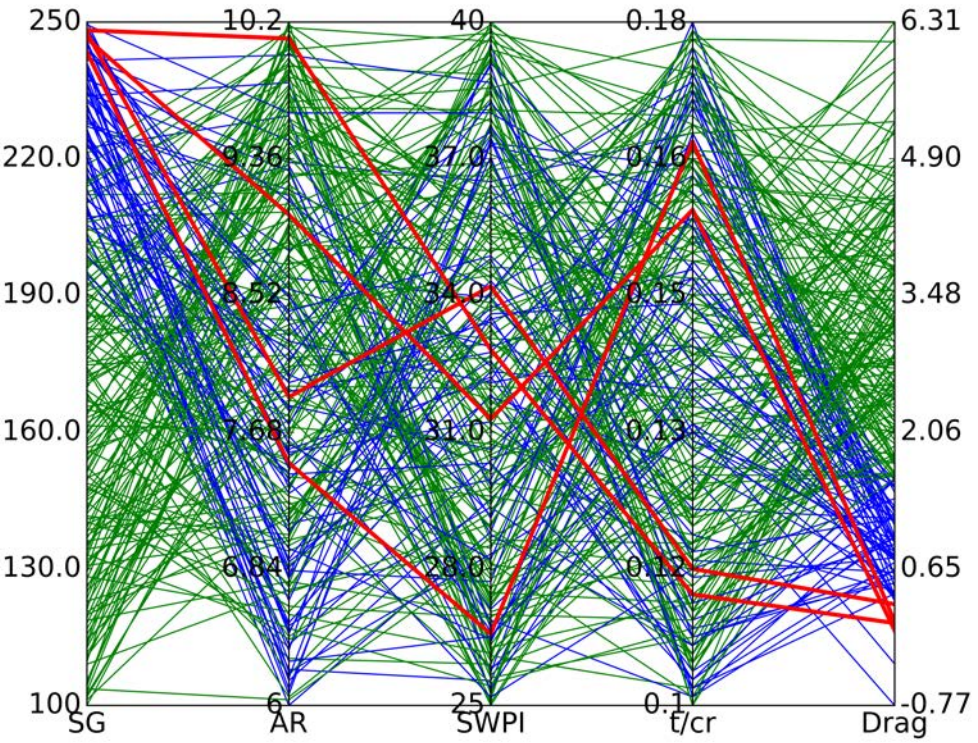

Figure 6.9: Parallel axis plot of 231 point data set in four dimensions for output (Drag) for T.A.C.E fidelity level I.

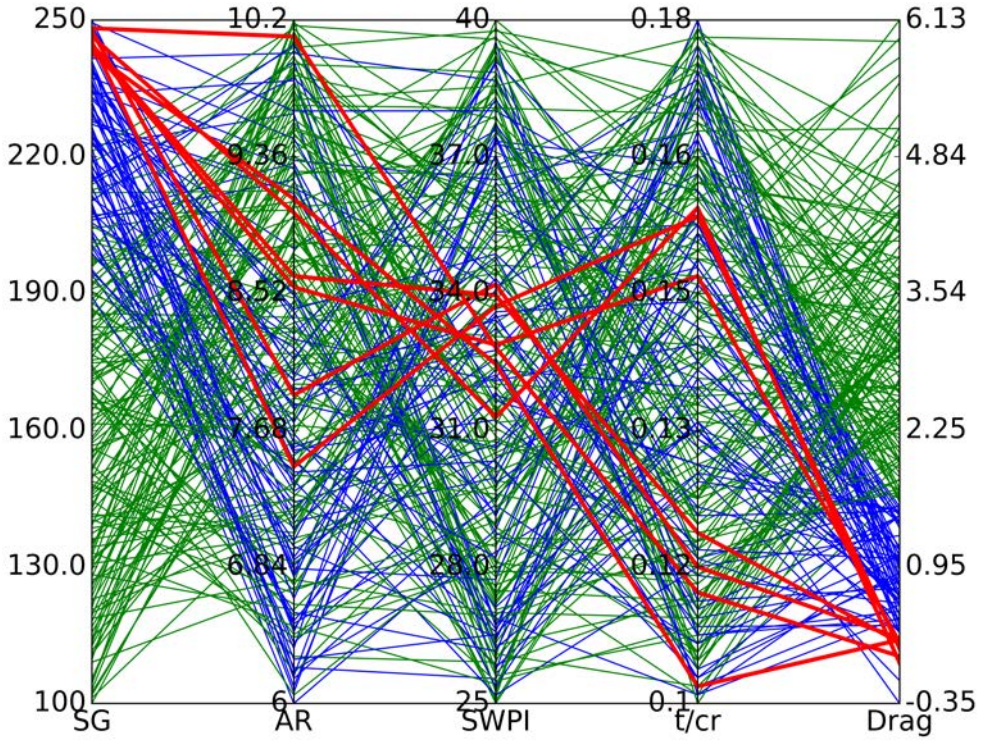

Figure 6.10: Parallel axis plot of 227 point data set in four dimensions for output (Drag) for T.A.C.E fidelity level II.

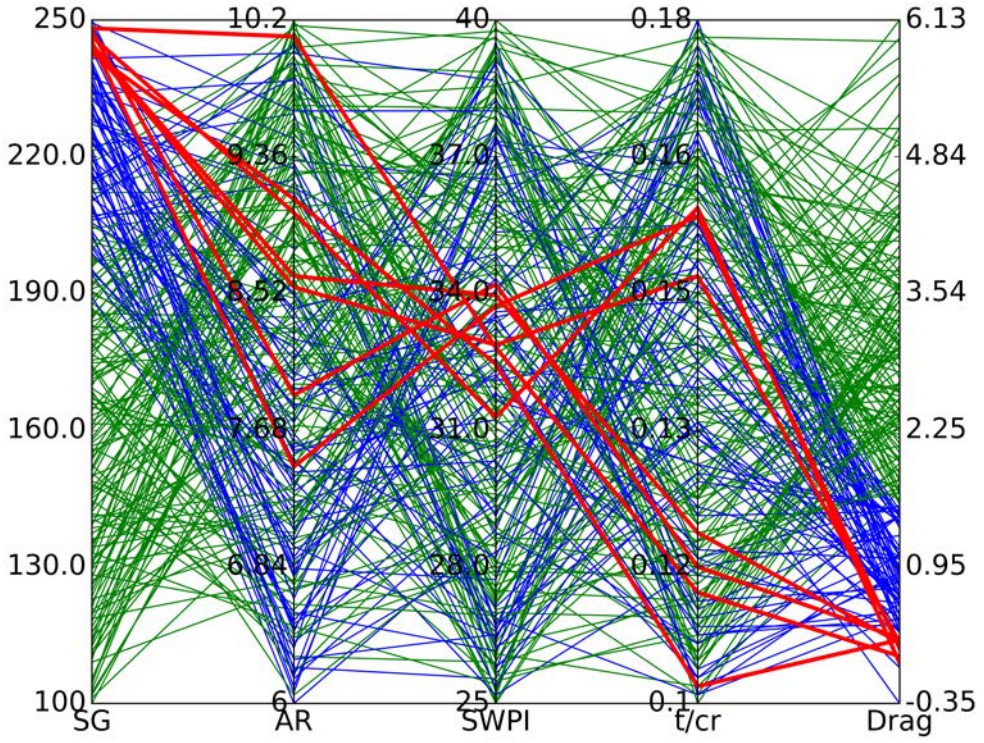

Figure 6.11: Parallel axis plot of 227 point data set in four dimensions for output (Drag) for T.A.C.E fidelity level III.

6.3.4 Discussion: Drag

For parallel axis plots for drag (figures 6.9, 6.10, and 6.11), there are very minimal variations from level I to II. The main difference between the higher and lower fidelity models is the variation of $SWPI$, where at lower fidelity there are some lower sweep values available. At a higher fidelity level there is a concentration of sweep values for minimum drag design. Interestingly there is little change at level III, implying that the substitution methodology for design of esperiments values at level III, has a greater detriment to cost, and weight trends. This is as substituted points from level III feature finite element analysis based mass optimisation, which has a larger impact on linked performance quantities such as weight, and cost. Level II offers the greatest weight, cost, and drag exploration capability as highlighted by the breadth of trends at this level of each of these performance outputs.

6.3.5 Step 2: Hierarchical Axis Plots

6.3.5.1 Weight

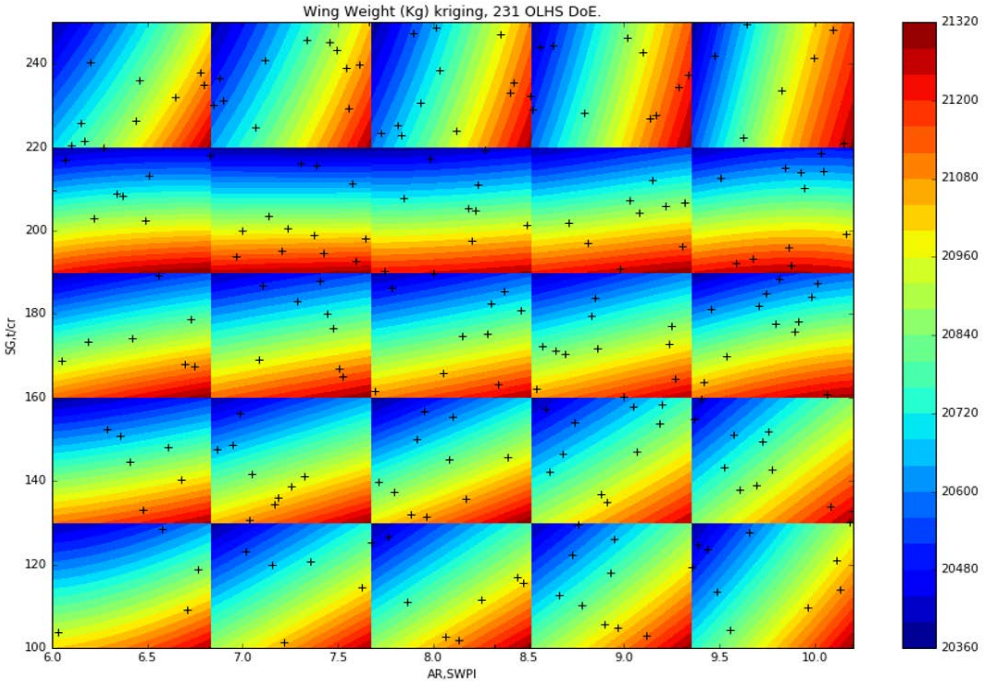

Figure 6.12: Hierarchical Axis Technique (HAT) plot of 231 point data set in four dimensions for output (Weight) for T.A.C.E fidelity level I.

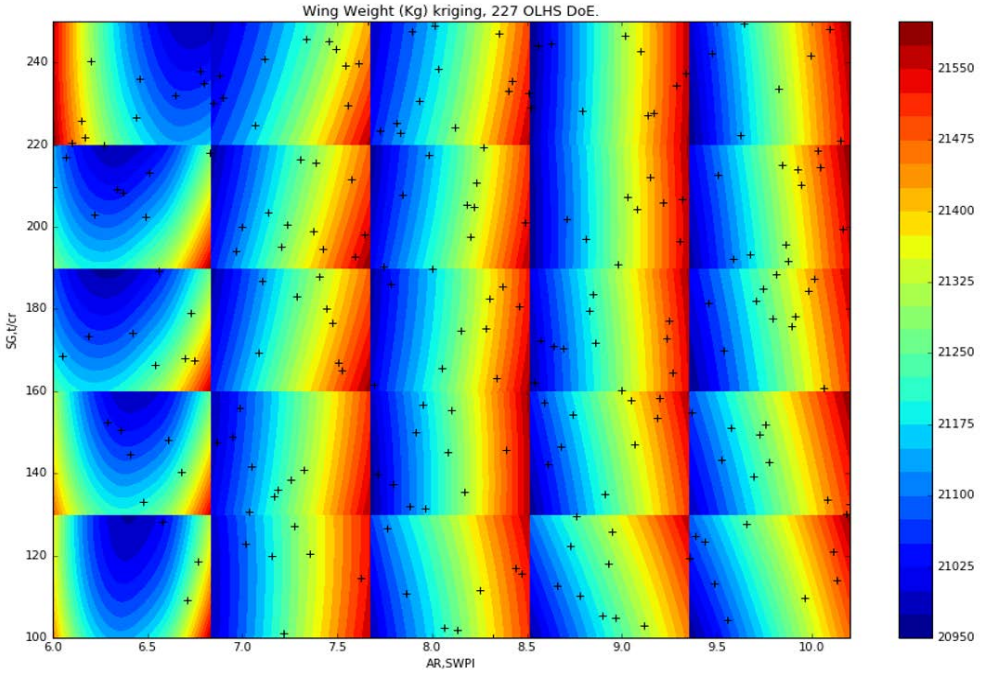

Figure 6.13: Hierarchical Axis Technique (HAT) plot of 227 point data set in four dimensions for output (Weight) for T.A.C.E fidelity level II.

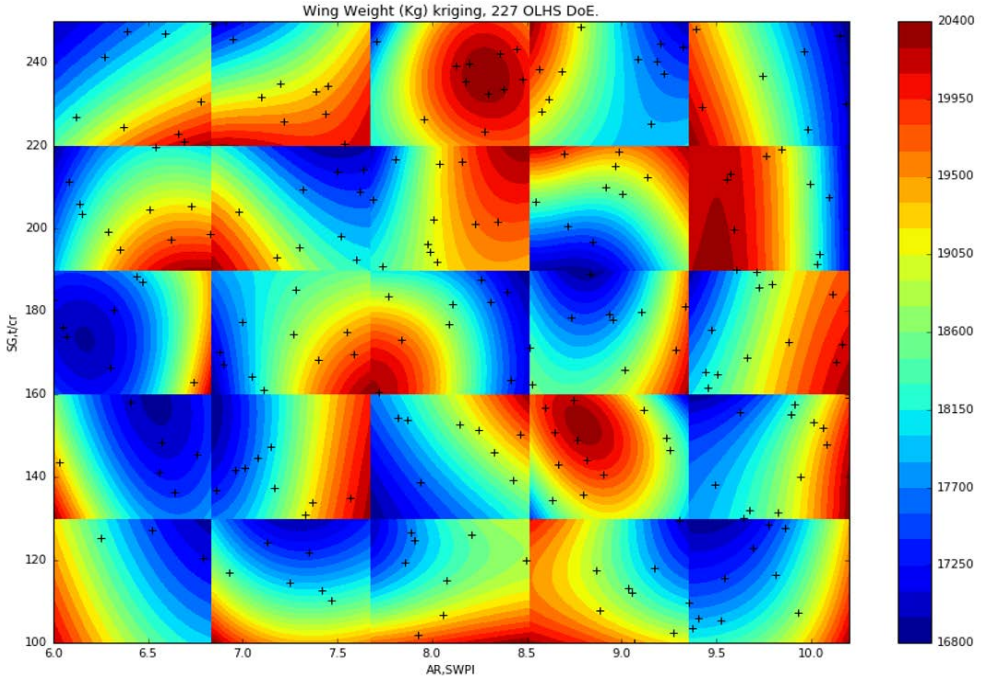

Figure 6.14: Hierarchical Axis Technique (HAT) plot of 227 point data set in four dimensions for output (Weight) for T.A.C.E fidelity level III.

6.3.6 Discussion: Weight

The HAT plot visualisations demonstrate the introduction of complex behaviour with changing structural fidelity, and indicate divergence from the established behaviour in previous studies, trends, and calibrations. When assessing these HAT plots, the mean standard deviation plots in appendix C are an important reference.

For weight what we note is that at level I, SG, and AR are the dominant variables, and the trends observed for variable sensitivity studies (in section 5.3), are reflected in the HAT plot 6.12. The linear trends observed vary at very high values of SG. At level II, there is a shift in the influence of the dominant parameters towards $SWPI$. Due to improved aerostructural coupling, $SWPI$ has a greater influence on the region of minimum weight at low AR. This is reflective of physical behaviour, as for shorter, stubbier wings, the variance of sweep will greatly impact the structural performance, and hence weight. However in general the remaining trends are fairly linear and easy to understand.

Clear divergence from the known behaviour is observed at level III. Here the substitution of 10% of the raw data, has a clear impact on the uniformity, and linearity of the design space. At this level the design space is difficult to navigate and local minima regions are observed. This suggests that using this level for design exploration without significant investment in structural sizing is not feasible. These findings are confirmed by the average mean standard deviation plots for weight (figure C.1, figure C.2, and figure C.3), where the average value starts at over 16,000 Kg at level I, drops to around 14,300 Kg at level II, and then goes up to around 14,750 Kg, at level III. This suggests that although level I is conservative as expected, level III does not improve the overall design exploration, as implied by the parallel axis plot for this level in figure 6.5.

6.3.6.1 Cost

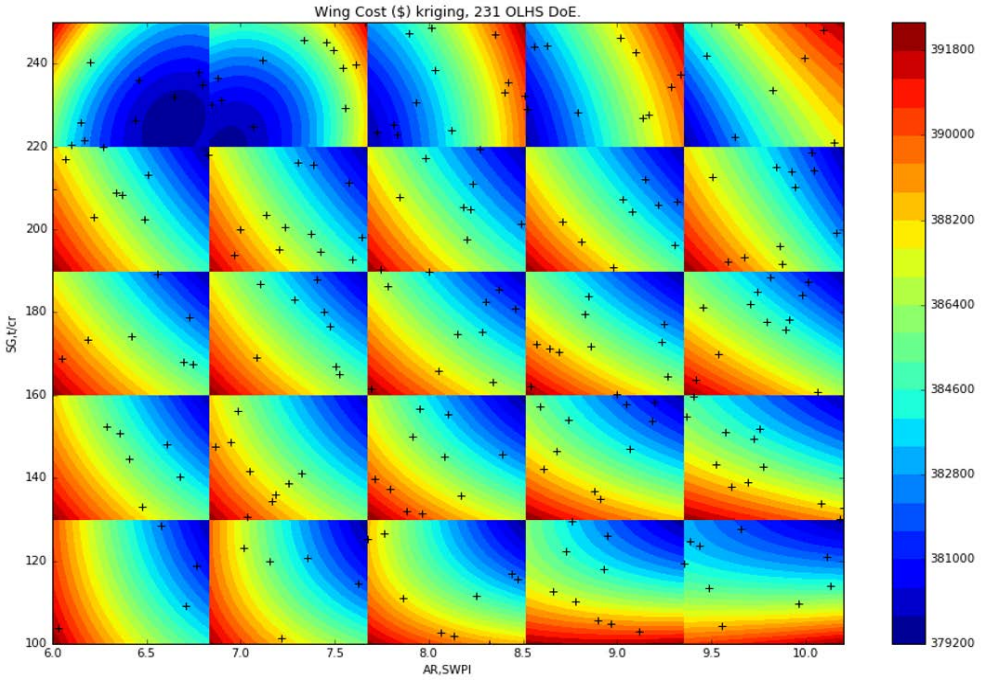

Figure 6.15: Hierarchical Axis Technique (HAT) plot of 231 point data set in four dimensions for output (Cost) for T.A.C.E fidelity level I.

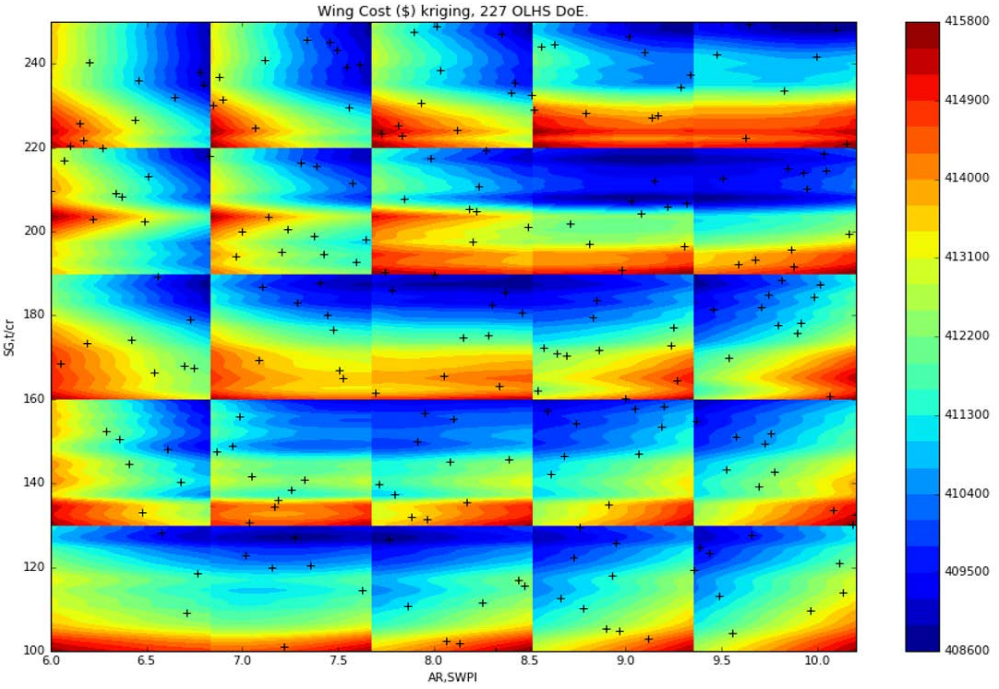

Figure 6.16: Hierarchical Axis Technique (HAT) plot of 227 point data set in four dimensions for output (Cost) for T.A.C.E fidelity level II.

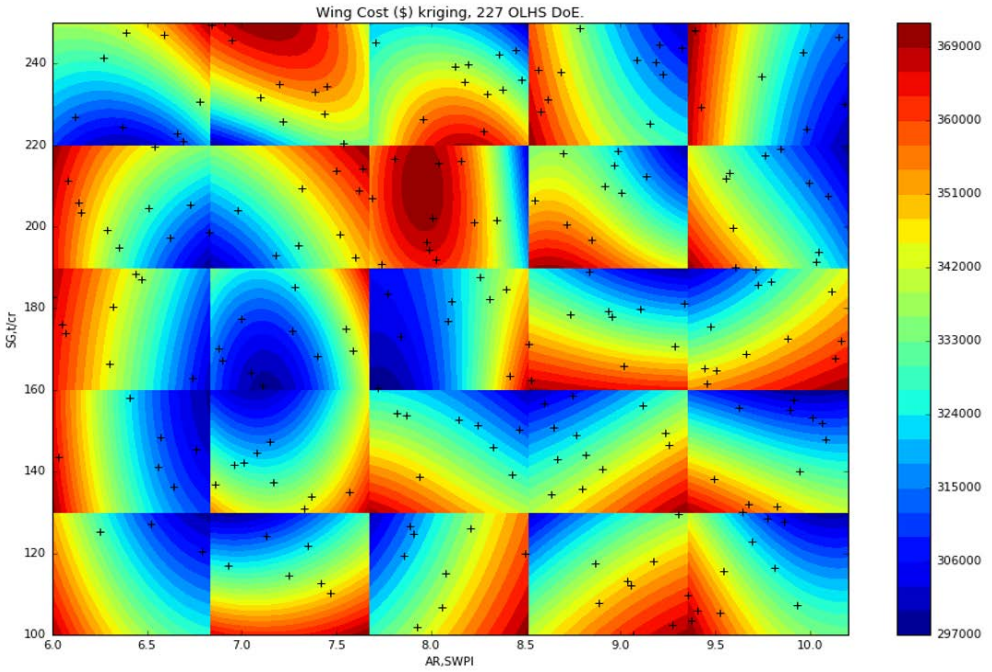

Figure 6.17: Hierarchical Axis Technique (HAT) plot of 227 point data set in four dimensions for output (Cost) for T.A.C.E fidelity level III.

6.3.7 Discussion: Cost

For cost, at level I (figure 6.15) the SG and AR are primary drivers of the design space behaviour. However variance can be seen at higher SG values. At level II, 6.16, this is corrected and we see a clear and concise trend, and a design space is easy to navigate and explore though gradient based optimisation techniques. Note at this level the range over which the cost varies is small. However at level III, figure 6.17, the observed trends disappear, and the range over which the cost varies is substantially larger than at the previous levels.

This behaviour is reflected in the mean standard deviation plots for cost at level I (figure C.4), II (figure C.5), and III (figure C.6), respectively. In these plots there is a shift from level I to II, towards a higher average value. However at level III, there is a substantial drop in the average value, moving further away from established T.A.C.E cost trends.

6.3.7.1 D/q

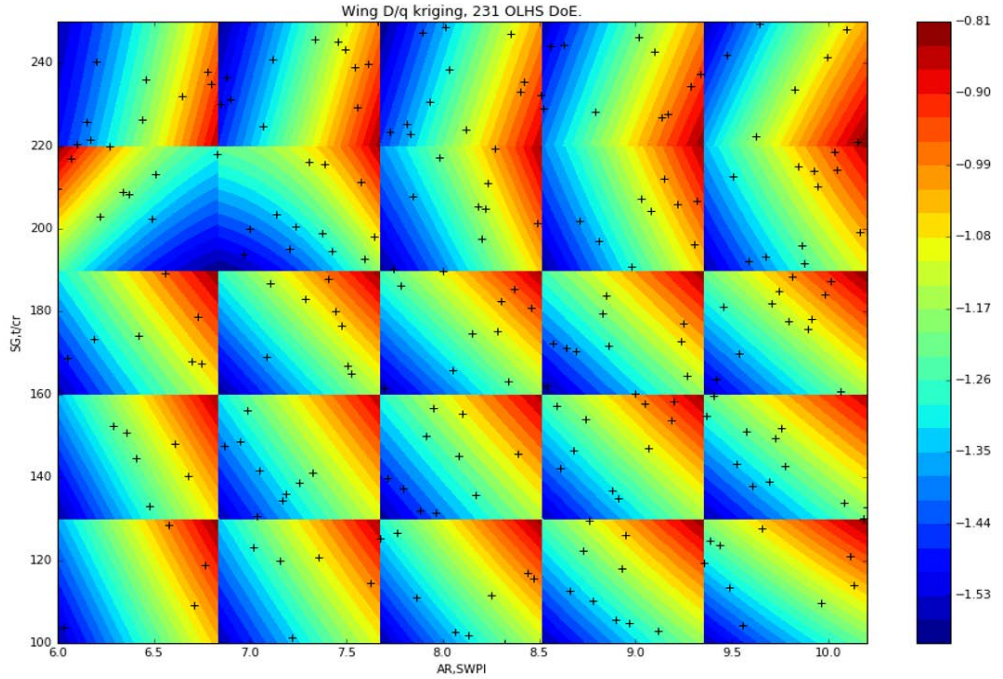

Figure 6.18: Hierarchical Axis Technique (HAT) plot of 231 point data set in four dimensions for output (Drag) for T.A.C.E fidelity level I.

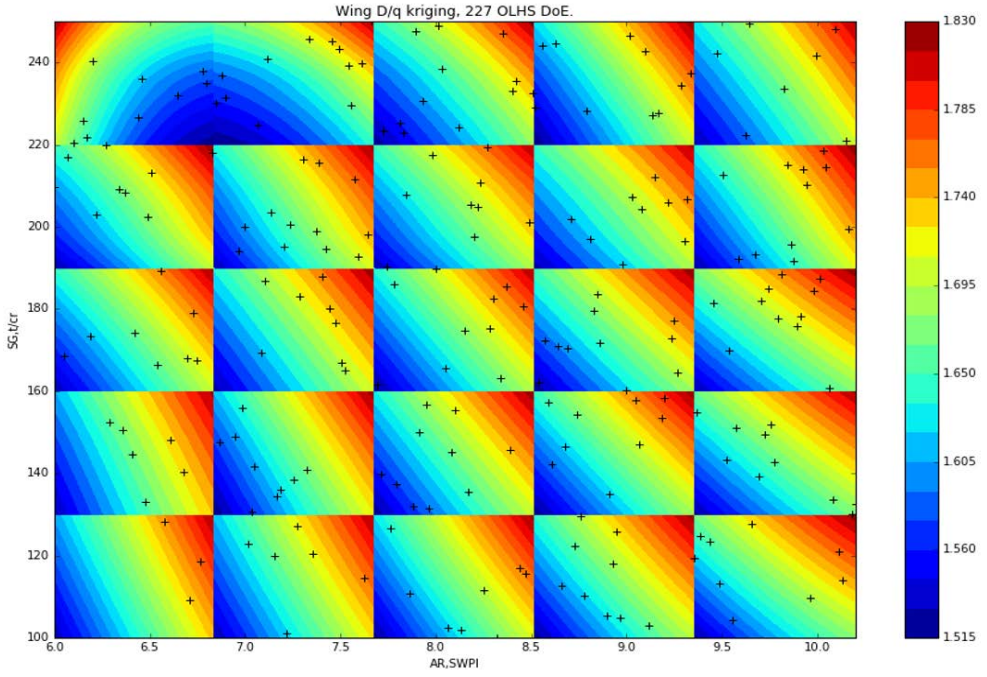

Figure 6.19: Hierarchical Axis Technique (HAT) plot of 227 point data set in four dimensions for output (Drag) for T.A.C.E fidelity level II.

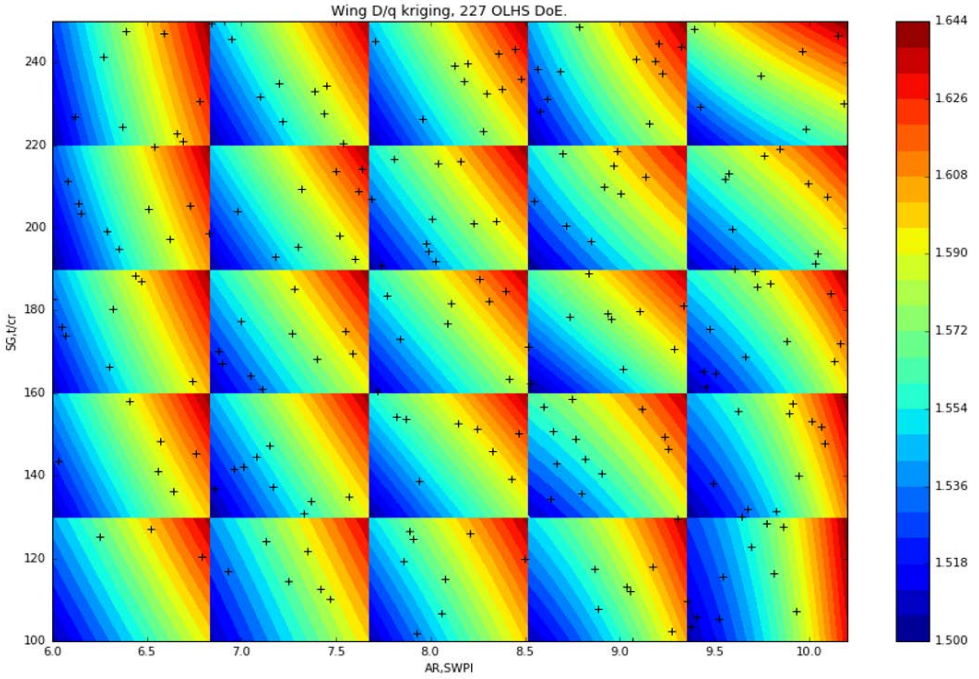

Figure 6.20: Hierarchical Axis Technique (HAT) plot of 227 point data set in four dimensions for output (Drag) for T.A.C.E fidelity level III.

6.3.8 Discussion: Cost

Finally for D/q at level I (figure 6.18), a very clear trend with reversal at high values of SG is noted. Moving to level II (figure 6.19), we see that $SWPI$ is influential in the correction of this reversal. The corrections offered by improved aerostructural coupling, are affected at very high values of AR, where the full potential aerodynamics method is known to fail in the capture of shock behaviour. From level II to III (figure 6.20, there is very little change in the design space. The data substitution has a positive impact on the design space, correcting the behaviour at higher AR to be in line with the global design space trend. This is confirmed by the mean standard deviation plots, where at level II and level III, in figures C.8, and C.9 respectively, no variation in the mean standard deviation is noted.

At level I in particular for all HAT plots, there is a clear region of trend reversal at higher values of SG, there are three likely reasons for this; low quality aerodynamics, low quality regression, or a lack of data. The full potential aerodynamics method has limitations concerning shock behaviour linked to sweep, and it is not infeasible that this is the reason for this reversal. The drag HAT plots with higher fidelity data correct this limitation, at level III. It can be argued that poor regression in this area may be an issue. Considering the mean squared error values from table 6.1 this might be the case.

6.3.9 Mean Squared Error for HAT plot RSMs

Table 6.1: Mean Squared Error(MSE) of HAT RSMs

Level	Output		
	Weight	Cost	Drag
I	0.032935	0.044940	0.058834
II	0.009211	0.009697	0.005487
III	0.023188	0.031894	0.005098

6.3.10 Discussion: Mean Squared Error

At level I, the mean squared error for all fidelity surrogate models is higher than corresponding models at level II, and level III. This is surprising as at level III there is clear non-linearity in the designs space. Note that the process of creating the surrogate models featured manual calibration to improve mean squared error behaviour. To correct this additional data points, or higher fidelity data would be required. Both poor regression and the limitations of the aerodynamics analysis results in this trend reversal. It is important to note that models at level II show exceptionally low mean squared error values, implying that the behaviour captured at this level is accurate and ideal for design exploration and optimisation.

6.4 Multi-objective Optimisation and Pareto Fronts

In this section the Pareto fronts created, using multi-objective optimisation of response surface models, are presented. Note that for levels I and II, the data sets used for surrogate modelling are linked to the fidelity levels established. However at level III, data substitution has been implemented. In addition the parameters used for optimisation using NSGA, can be seen in table 6.2. These parameters are identical for each optimisation and have been manually tuned. Note that the Pareto fronts are visualised using Delaunay triangulation of the dominant points. Where these points have been selected using the weighted sum method. Finally note where possible the range of the axes in these figures have been fixed at the values seen in table 6.3. However where the data set from the genetic algorithm exceeds the ranges identified, they have been expanded to visualise the entire data set, and Pareto front.

Table 6.2: GA parameters for NSGA II

Parameter	Value
Population	1000
Offspring size	500
Number of Generations	500
Crossover Probability	0.75
Mutation Probability	0.25
Objective Fitness	-1.0

Table 6.3: Pareto plot axes ranges

Output	Min.Value	Max. Value
Weight (Kg)	7500	25000
Cost ($)	200,000	600,000
D/q	-1.0	7.5

6.4.1 Pareto Fronts

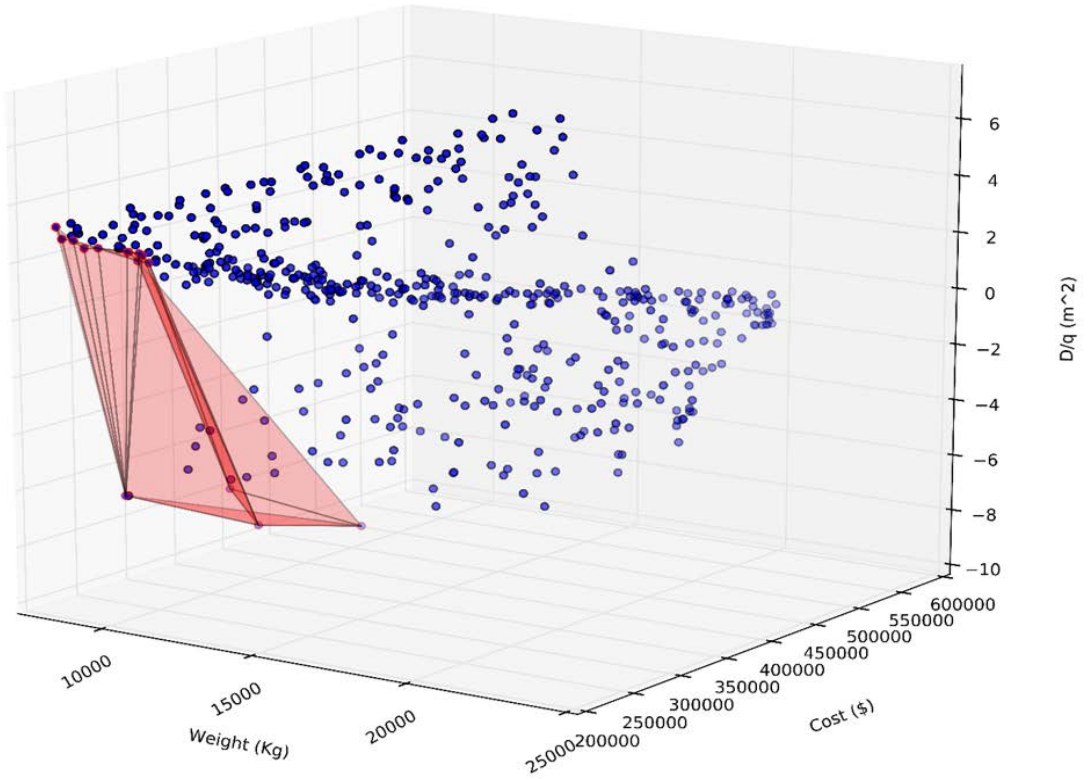

Figure 6.21: Pareto front of 227 point data for multi-objective optimisation at T.A.C.E fidelity level I.

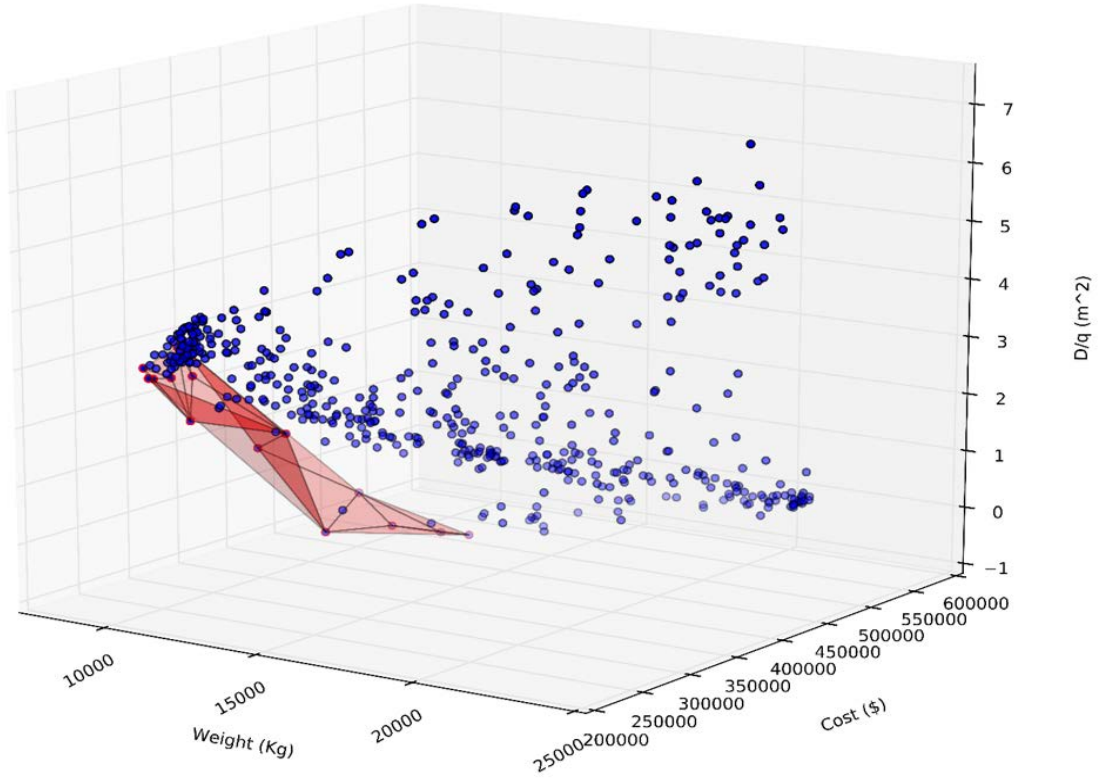

Figure 6.22: Pareto front of 231 point data for multi-objective optimisation at T.A.C.E fidelity level II.

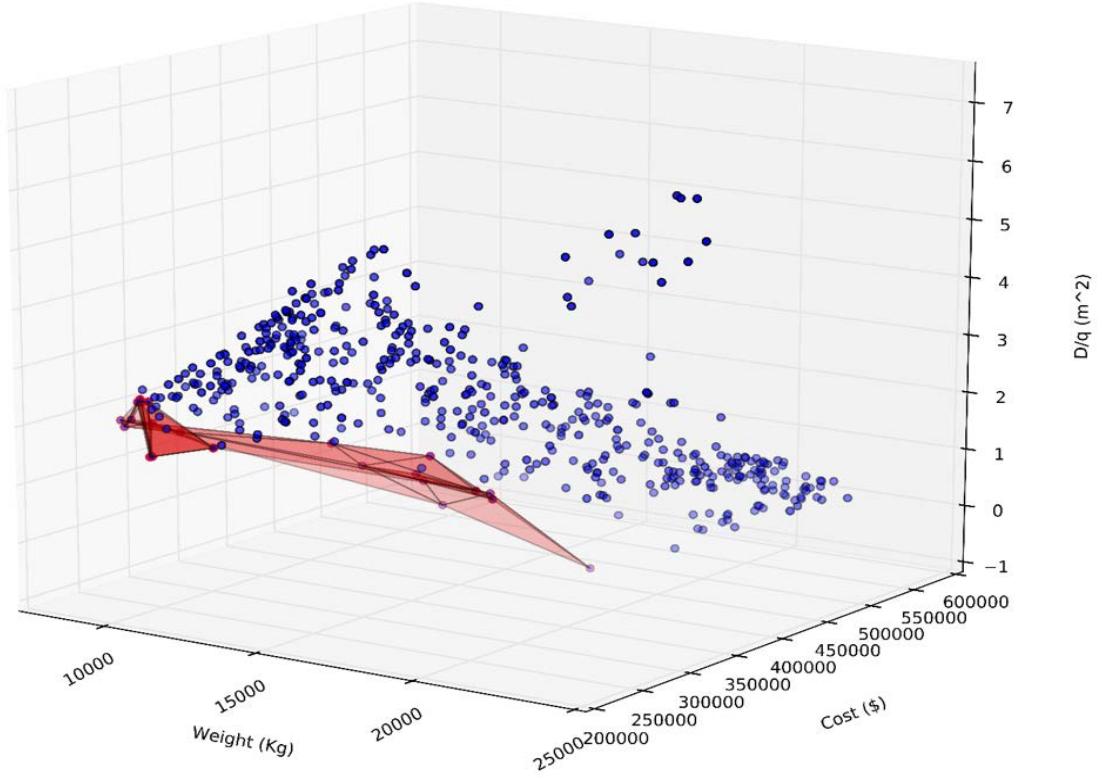

Figure 6.23: Pareto front of 231 point data for multi-objective optimisation at T.A.C.E fidelity level III.

6.4.2 Discussion

Pareto front plots from levels I, II, and III are shown in figures 6.21, 6.22, and 6.23 respectively. Alongside the Pareto fronts the remaining population from the final genetic algorithm iteration are displayed in all plots. When moving from level I, to II, and then III, the design space condenses at each level. At the level II, there is a very large spreads of data, however some of these designs are conservative or outliers, as the bulk of the population is condensed along very narrow bands. This issue is alleviated at level II, where the data is spread over a large range, and there is also a large scope for exploration. At level III the banding is reduced substantially, and there is a large area within which the majority of the population is located.

Moving from level I to II, the region over which data is spread is varied and there are avenues for performance exploration. At level III, it is a clear the addition of higher fidelity data points, resulting in a clustered population. This represents the design space shrinking. However this cluster may be prone to noise from the surrogate model at this level, and may change drastically with another run of the optimiser. The only level where there is significant confidence in the results is level II.

The Pareto fronts are interesting and at level I, the outlying points have a large influence in the shape of the front. The low cost and drag outliers in particular have the greatest influence. At this level the aerostructural coupling has clear limitations, in addition to aerodynamic analysis deficiencies, these outliers are skewing the front. This level I front presents the impact of such outliers in low fidelity optimisation. At level II (6.22), the healthy distribution of point at the population extremities helps to create a refined surface which represents a large scope for exploration in, all three performance quantities. This surface is relatively expansive and reflects minimum trend behaviour. Optimisation along this surface is also likely to lead to a balanced non-dominant design, which is ideal for design exploration in multidisciplinary optimisation. Here the balance of performance quantities can lead to new designs. As opposed to designs which are skewed by the design process, towards aerodynamic performance.

Finally at level III (6.23), the front is reflective of the clustering of the data points. The outliers have little impact, but the nature of the surface is steep in relation to cost, and weight in particular. At this level cost, and weight are affected, and this front illustrates that optimisation for these variables will lead to results which are dominant in one performance output. The steepness of the front confirms this, as gradient based optimisation along this front will lead to high cost, and weight designs, which minimise D/q.

6.5 Conclusions

To conclude, through use of visualisation techniques and analysis data, level II of structural model fidelity was proven to be best suited for design space exploration. This was confirmed through the trends found in parallel axis plots, the low mean square error response surface models, and the Pareto front at this fidelity level. In addition the data substitution methodology highlighted, for use in level III, offers no substantial advantage, without investment in fidelity level III to meet standards in structural sizing.

The data utilised in surrogate model creation, provide databases of knowledge at each fidelity level. These can be accessed via visualisation methodologies to provide, greater understanding of a design space, and trends in data. These databases can also be expanded for use in multiple studies. Each time an optimal or interesting design is located at the given fidelity level, it can be included in the database of knowledge, and its influence can be assessed through the three step visualisation methodology.

It is clear that the three step visualisation is only possible, if previous steps have been taken to create trends, and build response surface models which assess sensitivity. This allows greater confidence in implementing visualisation strategies, as the findings can be validated against known data. The visualisations offer access to raw data, and help reduce stigma towards surrogate modelling methods. This is important as such information is not often readily available. Response surface modelling methods, can be incorporated into multidisciplinary systems and codes and offer direct access to global behavioural characteristics, when can be useful when steering design optimisation.

6.5.1 Contribution

The key contribution of these experiments is in highlighting how visualisation methodologies can aid multidisciplinary optimisation. The three step visualisation methodology is shown to introduce design exploration capability, and alleviate data overhead, whilst helping to confirm the desirability of given structural models for optimisation purposes.

Chapter 7

Discussion, Conclusions, Contributions and Future Work

7.1 Achievements and Contributions

7.1.1 Achievements & Contributions

This thesis outlines the development of a multidisciplinary analysis program based on the design process for manufactured aircraft wings. This T.A.C.E program was created using commercial tools, to model the analysis process. It was calibrated and validated using trusted conceptual designs tools, and performance trends. The program successfully implements variable fidelity structural modelling, driven by parametric modelling and parameterisation of top level wing design variables. Though validation, and calibration, the program was shown to help identify an ideal structural model fidelity to help model performance trends.

Furthermore kriging, and response surface models were used to expand design knowledge at various fidelity levels, though visualisation. The surrogate models were created for top level designs variables and traditional performance metrics. These models demonstrate that there is a tipping point in structural fidelity where the nature of the design space becomes non-linear and noisy. This point was found to be pre investment in structural sizing. These response surfaces were used to validate and expand known performance trends for each wing design variable in question, and provide a bridge in data for more complex response surface models using multiple designs variable. These models and their use was designed to reduce data overhead in multidisciplinary optimisation.

Further to this a three step visualisation methodology was presented and its applicability for design space exploration was demonstrated. This methodology featured surrogate model creation, data manipulation, and multi-objective optimisation. Demonstrating

the ease with which these techniques can be utilised. This was the culmination to this work and demonstrates how the highlighted problems in the design process can be answered, using the identified methodologies.

As noted many of the achievements of this work are based on the creation of the T.A.C.E analysis program, and the demonstration of design exploration capability using the program as an input. However these achievements can be subcategorised into individual contributions, which are as follows:

1. The creation of a commercial-off-the-shelf multidisciplinary analysis program (T.A.C.E), which is reflective of an design methodology and limitations. This program facilitated exploration and optimisation without the transfer of sensitive data, and at lower cost, relative to existing programs. Using T.A.C.E structural fidelity variation experiments were conducted, to identify a structural fidelity level which was appropriate for the given multi-objective optimisation capability. This helped to provide guidelines as to which fidelity level is best suited to bridge the data gap between the conceptual and preliminary design stages.

2. The program was calibrated, validated and used as part of successful sensitivity, design exploration, and optimisation studies. This was done with respect to a trusted conceptual design tool; Tadpole. This program also implemented aerostructural analysis capability at each level of fidelity.

3. T.A.C.E allows the instantiation of multipoint and multi-fidelity analysis with successful design space visualisation and assessment of top level wing design variables. This capability moves away from standard practise of single point analysis.

4. The created analysis program has a plug-and-plug capability, which allows analyses tools of various fidelity to be substituted in to the code. In addition this program can be simply placed within a given local computational environment and run successfully, given that the appropriate software is installed and available to access.

5. Analysis using T.A.C.E can be driven for numerous performance metrics, and disciplinary outputs. Structural analysis and aerodynamic metrics such as lift, drag, rotation, and stress can be used to drive the global analysis. In addition performance outputs such as weight, and cost, can also be utilised. Allowing full flexibility and robust multidisciplinary analysis.

6. The calibration and trend studies in chapter 4, expand the knowledge from chapter 12 of Keane and Nair (2005). This body of work presents performance trends for the given top level designs variable, for Tadpole. Here these results are expanded for varying structural fidelity models. This increase in the knowledge for performance trends can improve future research on this topic.

7. The sensitivity studies in chapter 5, offer validation of the trends established in chapter 4, for each performance output, and design variable. The response surface models created help to reduce data overhead, as they offer information on variable, and output sensitivity, not readily available in an analysis chain.

8. The three step visualisation methodology aggregates numerous design exploration methods, in a step by step implementation, and improves understanding of the design space. The three methods highlighted; parallel axis plots, HAT plots, and Pareto fronts, are all useful optimisation tools which are sometimes met with scepticism. By having numerous response surface models, and trends in behaviour, the overall design exploration capability is enhanced, and reliability is improved.

9. A means by which to implement multidisciplinary optimisation has been presented in chapter 6 where a four dimensional kriging models at different fidelity levels are used to conduct population based multi-objective optimisation, using NSGA II. The results from these optimisation studies were used for Pareto front creation, allowing further gradient based optimisation, if required.

10. The structural fidelity at level II, when utilised in the three step visualisation was shown to aid in the exploration of novel designs. This was apparent in the Pareto front for this fidelity level (figure 6.22), which was well shaped, and not dominated by any single optimisation objective or outlying results.

11. The ranking capability demonstrated in parallel axis plots is very beneficial to multi-objective optimisation formulation. As knowing the sensitivity and ranking of the designs variables helps to constrain the optimisation problem, and improve convergence towards an optimal designs.

12. Overall this work also contributes to the field of multidisciplinary optimisation, and as it offers a method by which incremental trust can be built in multidisciplinary analysis systems and codes. In addition it offers guidelines to locate an appropriate level of structural fidelity for a given analysis program, to successfully achieve optimisation and design exploration.

13. Finally the collection of visualisation techniques in a three step method and the incremental building of trust in response surface models is unique to this work. A succinct guideline on the implementation of multidisciplinary optimisation capability in MDAACE, based on the findings in this thesis can be found in appendix D.

14. The data used for response surface creation in 6, provides databases of information at each fidelity level, which can be expanded, and manipulated in further studies. These databased form the template for further research using T.A.C.E, and in the field multidisciplinary analysis.

7.2 Conclusions

1. From the studies in chapter 4, good accuracy with Tadpole performance trends is demonstrated from the outputs of T.A.C.E analysis for weight in. Note that for trends in drag, the full potential method is the limiting factor in the capture of accurate trends, as it does not allow accurate shock capture for high sweep. The cost analysis, lacks the accounting of non-recurring costs which can be modelled. However the costing tool trends are reasonably matched for most variables. In addition all trends are consistent with other levels of fidelity within T.A.C.E, showing that there is consistency in the outputs.

2. As identified fidelity level II is shown to be ideal for design exploration, and multi-objective optimisation. At this level there is optimism in the trends, and the design space is expansive with many possible trends, which can lead to minimum performance. Optimisation at this level is shown to produce a reasonable Pareto front. This level has a sectional sizing procedure, and features physics based finite element analysis, and improved aerostructural coupling, when compared to level I.

3. Response surface models using a limited number designs variable such as those seen in chapter 5, heled top validate performance trends and offered assessment of the design space. In addition these models allowed the assessment of design variable sensitivity to each other and performance outputs. In further experiments these smaller models were used to validate models for N design variables, and reaffirm trust in the larger models.

4. The three step visualisation methodology is unique to this work and shows the aggregation of three methodologies, to enhance design exploration capability in conjunction with surrogate models. The methods are successful demonstrated at various levels of fidelity, and surrogates are used to implement multi-objective optimisation using NSGA II. These methods in conjunction are shown to provide substantial information on the raw analysis data, validating the underlying physics, and helping to illustrate the global design space for multiple variables, and performance outputs. This was achieved using HAT plots, and Pareto fronts respectively. This three step method was shown to be beneficial to multidisciplinary optimisation capability and can enhance knowledge of the design space.

5. From sensitivity studies for fidelity level III (shown in section 5.3), it becomes apparent that in order to successfully include structural sizing, there must be detailed investment in the mass optimisation methodology to include sizing analysis. This is done in via a rapid sizing tool. The creation, implementation, and validation of such a tool is beyond the scope of this thesis, and would require an additional

period of research. It is accepted that level II results are prone to noise, and must be treated with some minor scepticism, with regards to absolute sizing outputs.

6. The T.A.C.E program is limited by the fidelity of the fixed analysis modules. These modules include the aerodynamics, weight estimation, and cost estimation. The results from this program must be assessed with these limitations in mind. Further work would include the development of these methods to reflect the needs of the design process, and to overcome limitations in the results.

7. The results, whilst being limited must be assessed with regards to how they affect the aims of this thesis; which include the selection of appropriate structural fidelity, reduction of data overhead, and introduction of design exploration and optimisation. In this respect all three aims have been achieved. Structural fidelity variation was shown to be used in conjunction with performance trend assessments, in chapters 4, and 5, to help select a suitable level of fidelity, which balances accuracy and cost. In addition response surface models and the three step visualisation method was shown to provide a route to multi-objective optimisation. Finally the incremental development of trends, surrogate models, and databases of information, were presented as means by which to reduce the data overhead between design stages.

7.3 Future Work

The suggested future work involves implementing enhancements to the T.A.C.E program. These can be categorised under two branches; improvements and additions. Discussed below are both the suggested improvements and additions, their merits, and potential means by which they can be implemented.

- The most immediate means by which to expand the design capability is to upgrade the aerodynamics methodology. This can be done using of Euler or RANS methods using commercial tools. This reduces the difference between the fidelity of the aerodynamics in the T.A.C.E program and those applies in a detailed design process. This overcomes the fundamental weakness of the full potential method and allows complex physical phenomena such as turbulence to be modelled. Note this would however increase the analysis time significantly.

- Modification to the structural sizing would improve the analysis and optimisation capability. This can be achieved by adding further detail in structural sizing for compression. By adding additional modes such as torsional buckling and some combined modes the overall stringer optimisation capability would be improved. In addition a finite element analysis based panel verification could be implemented

to check the Eigen values for each stiffened panel. An important addition is introduction of panel sizing for tension, this could be achieved via methods similar to that of Chintapalli et al. (2010).

- Improvements could also be made to the cost module. The primary limitation of this module is the lack of calibration with current standard tools. In addition the tools lacks the ability to calculate non-recurring costs which can be a significant portion of the cost. These improvements can be achieved by using a numerical calibration factors and some updates to the underlying equations, to reflect up to date manufacturing capabilities.

- A loads module would allow improved understanding of the design at different certification cases, and help to introduce phenomena such as gust, and fatigue, improving the utility of the aerostructural coupling. This would improve the overall design as certification would feature more prominently in the analysis.

- The weight estimation methodology does not reflect standard practise or state of the art methodology. The obvious step would be to adopt predictive weight accounting methods. However as discussed these methods are endemic of the need for detail in the optimisation problem and limit design space exploration. Therefore it would be recommended to introduce the neural network based structural mass estimation methodology, demonstrated by Hannon (2011), and Agyepong (2012).

- A simpler way to enhance the contributions of the T.A.C.E program to multidisciplinary literature in the future would be to implement more optimisation and novel design configuration studies. This could be done through the use of different optimisation algorithms, objective functions, and constraints. In addition a demonstration of methodology for novel design i.e. semi blended could help illustrate how variable fidelity can improve design exploration capabilities.

- Finally it should be noted that the studies in this thesis were limited to metallic wings. The exploration of composite technologies and modification to include the analysis of composite wings would be important in enhancing the analysis capability of the T.A.C.E program.

References

Agyepong, L. (2012). *Application of Neuro-Fuzzy Systems to Aircraft System Weight Estimation*. Ph. D. thesis, The University of Leeds.

Ainsworth, J., C. Collier, P. Yarrington, R. Lucking, and J. Locke (2010). Airframe wingbox preliminary design and weight prediction. In *69th Annual Conference on Mass Properties, Virginia Beach, Virginia*, pp. 41.

Ajal, R., M. Friswell, D. Smith, and A. Iskveren (2013). A conceptual wing-box weight estimation model for transport aircraft. *Aeronautical journal 117*(1191), 533–551.

Alvey, V. and D. Emero (1967). Structures cost effectiveness. *Journal of Aircraft 4*(3), 218–223.

Amadori, K., C. Jouannet, and P. Krus (2008). Aircraft conceptual design optimization. ICAS.

Amadori, K., M. Tarkian, J. Ölvander, and P. Krus (2012). Flexible and robust cad models for design automation. *Advanced Engineering Informatics 26*(2), 180–195.

Ardema, M. (1988). Body weight of hypersonic aircraft: Part. *Technical Report NASA TM-101028*.

Ardema, M., M. Chambers, A. Patron, A. Hahn, H. Miura, and M. Moore (1996a). Fuselage and wing weight of transport aircraft. *SAE Transactions 105*(1), 536–1552.

Ardema, M. D. (1972). Structural weight analysis of hypersonic aircraft.

Ardema, M. D., M. C. Chambers, A. P. Patron, A. S. Hahn, H. Miura, and M. D. Moore (1996b). Fuselage and wing weight of transport aircraft. Technical report, SAE Technical Paper.

Ashby, D. L., M. R. Dudley, S. K. Iguchi, L. Browne, and J. Katz (1991). Potential flow theory and operation guide for the panel code pmarc.

Baker, A. and D. Smith (2003). Evolutionary feature based weight prediction. *SAWE Paper* (3303).

Ballhaus, W. F. (1947). *Aerodynamic and geometric parameters affecting aircraft weight.* Ph. D. thesis, California Institute of Technology.

Bao, H. P. and W. Freeman (2002). Process cost modeling for multi-disciplinary design optimization.

Bao, H. P. and J. Samareh (2000). Affordable design: A methodology to implement process-based manufacturing cost models into the traditional performance-focused multidisciplinary design optimization. In *Proceedings of the Eighth AIAA/-NASA/USAF/ISSMO Symposium on Multidisciplinary analysis and optimization, Long Beach, California, USA*, Volume 4839.

Barkanov, E., O. Ozoliņš, E. Eglītis, F. Almeida, M. Bowering, and G. Watson (2014). Optimal design of composite lateral wing upper covers. part i: Linear buckling analysis. *Aerospace Science and Technology 38*, 1–8.

Belie, R. (2002). Non-technical barriers to multidisciplinary optimization in the aerospace industry. In *9thAIAA/ISSMO Symposium of Multidisciplinary Analysis and Optimisation*, pp. 4–6.

Bes-Torres, J., R. Rudsianto, and E. Kay (2012). An intergrated and rapid fem-based weight derivation approach to weight estimation. *SAWE Paper* (3589).

Bindolino, G., G. Ghiringhelli, S. Ricci, and M. Terraneo (2010). Multilevel structural optimization for preliminary wing-box weight estimation. *Journal of Aircraft 47*(2), 475–489.

Bisagni, C. and R. Vescovini (2009). Fast tool for buckling analysis and optimization of stiffened panels. *journal of aircraft 46*(6), 2041–2053.

Bisplinghoff, R. L., H. Ashley, and R. L. Halfman (2013). *Aeroelasticity.* Courier Corporation.

Böhnke, D., F. Dorbath, B. Nagel, and V. Gollnick (2012). Multi-fidelity wing mass estimations based on a central model approach. *SAWE Paper*.

Brezillon, J., A. Ronzheimer, D. Haar, M. Abu-Zurayk, K. Lummer, W. Kruger, and F. Nattere (2012). Development and application of multi-disciplinary optimization capabilities based on high-fidelity methods. *AIAA Paper 1757*, 2012.

Bristow, D. (1980). Development of panel methods for subsonic analysis and design. *NASA CR-3234*.

Bruhn, E. F. (1965). *Analysis and design of flight vehicle structures.* Tri-State Offset Co.

Bulson, P. (1969). *The stability of flat plates.* American Elsevier Pub. Co.

Cavagna, L., S. Ricci, and L. Riccobene (2011). Structural sizing, aeroelastic analysis, and optimization in aircraft conceptual design. *Journal of Aircraft 48*(6), 1840–1855.

Cavagna, L., S. Ricci, and L. Travaglini (2011). Neocass: an integrated tool for structural sizing, aeroelastic analysis and mdo at conceptual design level. *Progress in Aerospace Sciences 47*(8), 621–635.

Chambers, M. C., M. D. Ardema, A. P. Patron, A. S. Hahn, H. Miura, and M. D. Moore (1996). Analytical fuselage and wing weight estimation of transport aircraft.

Chapman, C. B. and M. Pinfold (2001). The application of a knowledge based engineering approach to the rapid design and analysis of an automotive structure. *Advances in Engineering Software 32*(12), 903–912.

Chedrik, V. (2013). Two-level design optimization of aircraft structures under stress, buckling and aeroelasticity constraints. In *10th World Congress on Structural and Multidisciplinary Optimization*.

Cheeseman, J. (2014). The mysterious art of weight estimation of large civil aircraft. *SAWE Paper* (3629).

Cheesman, J. and D. Smith (2001). Predictive weight accounting within a multidisciplinary engineering organisation. *SAWE Paper* (3146).

Chintapalli, S., M. S. Elsayed, R. Sedaghati, and M. Abdo (2010). The development of a preliminary structural design optimization method of an aircraft wing-box skin-stringer panels. *Aerospace Science and Technology 14*(3), 188–198.

Colson, B., M. Bruyneel, S. Grihon, C. Raick, and A. Remouchamps (2010). Optimization methods for advanced design of aircraft panels: a comparison. *Optimization and Engineering 11*(4), 583–596.

Coroneos, R. M. and S. S. Pai (2012). *Deterministic design optimization of structures in openMDAO framework*. National Aeronautics and Space Administration, Glenn Research Center.

Cousin, J. and M. Metcalfe (1990). The bae ltd transport aircraft synthesis and optimization program. In *AHS, and ASEE, Aircraft Design, Systems and Operations Conference, Dayton, OH*, pp. 17–19.

Dassult (2015). Abaqus cae, research edition. https://www.3ds.com/products-services/simulia/products/abaqus/abaquscae/.

Davendralingam, N. and W. Crossley (2014). Robust approach for concurrent aircraft design and airline network design. *Journal of Aircraft 51*(6), 1773–1783.

Dean, S. (2008). Rh and optimisation, multi-disciplinary design development & application at qinetiq. KATnet II Multi Disciplinary Design & Configuration Optimisation Workshop January.

Deb, K., A. Pratap, S. Agarwal, and T. Meyarivan (2002). A fast and elitist multiobjective genetic algorithm: Nsga-ii. *IEEE transactions on evolutionary computation 6*(2), 182–197.

Deep, R. (2006). *Probability and Statistics, Boston*. Elsevier Publishing Company.

Di Pasquale, D., C. Holden, T. Kipouros, and M. Savill (2014). An automatic aerodynamic design process in an industrial multi-disciplinary context. In *11th World Congress on Computational Mechanics, WCCM 2014, 5th European Conference on Computational Mechanics, ECCM 2014 and 6th European Conference on Computational Fluid Dynamics, ECFD 2014*, pp. 6241–6252.

Dorbath, F. (2014). Application of a flexible wing modelling and physical mass estimation system for early aircraft design stages. In *Society of Allied Weight Engineers Paper*, Number 3615.

Doty, J. H. (2011). Multi-variate designed experiments for development of a wing weight surrogate model. In *49th AIAA Aerospace Sciences Meeting, AIAA*, Volume 893363, pp. 04–07.

Dowell, E. H., R. Clark, D. Cox, et al. (2004). *A modern course in aeroelasticity*, Volume 3. Springer.

Drela, M. (1989). Xfoil: An analysis and design system for low reynolds number airfoils. In *Low Reynolds number aerodynamics*, pp. 1–12. Springer.

Elham, A. (2013). *Weight indexing for multidisciplinary design optimization of lifting surfaces*. TU Delft, Delft University of Technology.

Elham, A., M. J. van Tooren, and J. Sobieszczanski-Sobieski (2014). Bilevel optimization strategy for aircraft wing design using parallel computing. *AIAA Journal 52*(8), 1770–1783.

ESDU (1962). Buckling in compression of sheet between rivets. *Engineering Sciences Data Unit* (72019).

ESDU (1972). Buckling of flat isotropic plates under uniaxial and biaxial loading. *Engineering Sciences Data Unit* (02.01.08).

Fang, K.-T., D. K. Lin, P. Winker, and Y. Zhang (2000). Uniform design: theory and application. *Technometrics 42*(3), 237–248.

Fonseca, C. M. and P. J. Fleming (1995). An overview of evolutionary algorithms in multiobjective optimization. *Evolutionary Computation 3*(1), 1–16.

Forrester, A., A. Sobester, and A. Keane (2008). *Engineering design via surrogate modelling: a practical guide*. John Wiley & Sons.

Fortin, F.-A., F.-M. De Rainville, M.-A. Gardner, M. Parizeau, and C. Gagné (2012, jul). DEAP: Evolutionary algorithms made easy. *Journal of Machine Learning Research 13*, 2171–2175.

Freeman, J. A. and D. M. Skapura (1991). *Algorithms, Applications, and Programming Techniques*. Addison-Wesley Publishing Company, USA.

Freestone, M. (2003). Full-potential (fp) method for three-dimensional wings and wing body combinationsinviscid flow, part 1: Principles and results. *Engineering Sciences Data Unit Rept. 02013*.

Fudge, D., D. Zingg, and R. Haimes (2005). A cad-free and a cad-based geometry control system for aerodynamic shape optimization. *AIAA 51*, 1–15.

Fujino, M. (2005). Design and development of the hondajet. *Journal of aircraft 42*(3), 755–764.

Gantois, K. and A. Morris (2004). The multi-disciplinary design of a large-scale civil aircraft wing taking account of manufacturing costs. *Structural and Multidisciplinary Optimization 28*(1), 31–46.

Gebbie, D. A., M. F. Reeder, C. Tyler, V. Fonov, and J. Crafton (2007). Lift and drag characteristics of a blended-wing body aircraft. *Journal of aircraft 44*(5), 1409–1421.

Gerard, G. and H. Becker (1957). Handbook of structural stability part i: buckling of flat plates.

Gern, F. H., A. H. Naghshineh, E. Sulaeman, R. K. Kapania, and R. T. Haftka (2000). Flexible wing model for structural sizing and multidisciplinary design optimization of a strut-braced wing.

Gersch, A. (1979). Weight integrated sizing evaluation/wise/- a tool for preliminary design. In *Society of Allied Weight Engineers, Annual Conference, 38 th, New York, N. Y*, pp. 1979.

Ghoman, S. S., R. K. Kapania, P. Chen, D. Sarhaddi, and D. Lee (2012). Multifidelity, multistrategy, and multidisciplinary design optimization environment. *Journal of Aircraft 49*(5), 1255–1270.

Giles, G. L. (1986). Equivalent plate analysis of aircraft wing box structures with general planform geometry. *Journal of Aircraft 23*(11), 859–864.

Giles, G. L. (1989). Further generalization of an equivalent plate representation for aircraft structural analysis. *Journal of Aircraft 26*(1), 67–74.

Giles, G. L., C. L. Blackburn, and S. C. Dixon (1972). Automated procedures for sizing aerospace vehicle structures (saves). *Journal of Aircraft 9*(12), 812–819.

Goel, A., C. Baker, C. A. Shaffer, B. Grossman, R. T. Haftka, W. H. Mason, and L. T. Watson (1999). Vizcraft: A multidimensional visualization tool for aircraft configuration design. In *Visualization'99. Proceedings*, pp. 425–555. IEEE.

Greer Jr, W. R. and D. A. Nussbaum (1990). *Cost analysis and estimating*. Springer.

Grihon, S., M. Samuelides, A. Merval, A. Remouchamps, M. Bruyneel, and B. Colson (2010). Fuselage structure optimsation. In E. J Kesseler and M. Guenov (Eds.), *Advances in Collaborative Civil Aeronautical Multidisciplinary Design Optimization*, Chapter 7, pp. 266–290. AIAA.

Hannon, C. (2011). *Development of new methodologies for the weight estimation of aircraft structures*. Ph. D. thesis, University of Leeds.

Heinrich, R., N. Kroll, J. Neumann, and B. Nagel (2008). Fluid-structure coupling for aerodynamic analysis and design–a dlr perspective. *AIAA paper 561*, 2008.

Hodges, D. H. and G. A. Pierce (2011). *Introduction to structural dynamics and aeroelasticity*, Volume 15. cambridge university press.

Holden, C., R. Davies, and A. Keane (2002). Optimization methodologies in conceptual design. In *In 9th AIAA/ISSMO Symposium on Multidisciplinary Analysis and Optimization Online Proceedings*.

Holden, C. and A. Keane (2004). Visualization methodologies in aircraft design. In *10th AIAA/ISSMO Multidisciplinary Analysis and Optimization Conference*, pp. 4449.

Holden, C. and W. Wright (2000). Optimisation methods for wing section design. In *38th Aerospace Sciences Meeting and Exhibit*, pp. 842.

Hürlimann, F., R. Kelm, M. Dugas, K. Oltmann, and G. Kress (2011). Mass estimation of transport aircraft wingbox structures with a cad/cae-based multidisciplinary process. *Aerospace Science and Technology 15*(4), 323–333.

Hwang, J. T. and J. Martins (2012). Geomach: Geometry-centric mdao of aircraft configurations with high fidelity. In *Proceedings of the 14th AIAA/ISSMO Multidisciplinary Analysis Optimization Conference, Indianapolis, IN*.

Inselberg, A. and B. Dimsdale (1990). Parallel coordinates: a tool for visualizing multidimensional geometry. In *Proceedings of the 1st conference on Visualization'90*, pp. 361–378. IEEE Computer Society Press.

James, B. and A. Dovit (1985). Structural optimization by multilevel decomposition.

Jameson, A. and D. A. Caughey (1977). A finite volume method for transonic potential flow calculations. *AIAA paper 635*.

Jones, D. R. (2001). A taxonomy of global optimization methods based on response surfaces. *Journal of global optimization 21*(4), 345–383.

Kaufmann, M., D. Zenkert, and M. Åkermo (2011). Material selection for a curved c-spar based on cost optimization. *Journal of Aircraft 48*(3), 797–804.

Keane, A. (2003). Wing optimization using design of experiment, response surface, and data fusion methods. *Journal of Aircraft 40*(4), 741–750.

Keane, A. and P. Nair (2005). *Computational approaches for aerospace design: the pursuit of excellence*. John Wiley & Sons.

Keane, A. and N. Petruzzelli (2000a). Aircraft wing design using ga-based multi-level strategies.

Keane, A. and N. Petruzzelli (2007). Using cad-tools and aerodynamic codes in a distributed conceptual design framework. In *In 45th Aerospace Sciences Meeting and Exhibit*.

Keane, A. and J. Scanlan (2007). Design search and optimization in aerospace engineering. *Philosophical Transactions of the Royal Society of London A: Mathematical, Physical and Engineering Sciences 365*(1859), 2501–2529.

Keane, A. J. and N. Petruzzelli (2000b). Aircraft wing design using ga-based multi-level strategies. In *8th AIAA/USAF/NASSA/ISSMO Symposium on Multidisciplinary Analysis and Optimization*, pp. A00–40171.

Kelm, R., M. Dugas, R. Voit-Nitschmann, and M. Grabietz (1999). Influence of aeroelastic tailoring in the multidisciplinary design of a new aircraft. In *NASA CONFERENCE PUBLICATION*, pp. 709–718. NASA.

Kelm, R., M. Läpple, and M. Grabietz (1995). Wing primary structure weight estimation of transport aircrafts in the pre-development phase. In *54th Annual Conference of Society of Allied Weight Engineers, Inc., SAWE Paper*, Number 2283.

Kenway, G. and J. Martins (2014). Multipoint high-fidelity aerostructural optimsaiiton of a transport configuration. *Journal of Aircraft 5*(1), 144–160.

Keye, S., O. Brodersen, and M. B. Rivers (2014). Investigation of aeroelastic effects on the nasa common research model. *Journal of Aircraft 51*(4), 1323–1330.

Koeppen, C. (2007). Method for model-based estimations of system mass in aircraft predesign. In *Proceedings of the 66th Annual Conference of the Society of Allied Weight Engineers. SAWE Paper*, Number 3428.

Komarov, V. A. and T. A. Weisshaar (2002). New approach to improving the aircraft structural design process. *Journal of Aircraft 39*(2), 227–233.

Kraft, D. (1988). A software package for sequential quadratic programming. *Forschungsbericht- Deutsche Forschungs- und Versuchsanstalt fur Luft- und Raumfahrt*.

Krige, D. (1951). *A statistical approach to some mine valuation and allied problems on the Witwatersrand: By DG Krige*.

Kroll, N., M. Abu-Zurayk, D. Dimitrov, T. Franz, T. Führer, T. Gerhold, S. Görtz, R. Heinrich, C. Ilic, J. Jepsen, J. Jägersküpper, M. Kruse, A. Krumbein, S. Langer, D. Liu, R. Liepelt, L. Reimer, M. Ritter, A. Schwöppe, J. Scherer, F. Spiering, R. Thormann, V. Togiti, D. Vollmer, and J.-H. Wendisch (2016). Dlr project digital-x: towards virtual aircraft design and flight testing based on high-fidelity methods. *CEAS Aeronautical Journal 7*(1), 3–27.

Kroo, I., K. Willcox, A. March, A. Haas, R. D, and C. Kays (2010). Multifidelity analysis and optimization for supersonic design. *NASA/CR2010216874*.

La Rocca, G., T. Langen, and Y. Brouwers (2012). The design and engineering engine. towards a modular system for collaborative aircraft design. In *28th International Congress of the Aeronautical Sciences*.

Lassila, T. and G. Rozza (2010). Parametric free-form shape design with pde models and reduced basis method. *Computer Methods in Applied Mechanics and Engineering 199*(23), 1583–1592.

Laughlin, T., J. Corman, and D. Mavris (2013). A parametric and physics-based approach to structural weight estimation of the hybrid wing body aircraft. In *51st AIAA Aerospace Sciences Meeting including the New Horizons Forum and Aerospace Exposition*, pp. 1082.

Ledermann, C., P. Ermanni, and R. Kelm (2006). Dynamic cad objects for structural optimization in preliminary aircraft design. *Aerospace Science and Technology 10*(7), 601–610.

Ledermann, C., C. Hanske, J. Wenzel, P. Ermanni, and R. Kelm (2005). Associative parametric cae methods in the aircraft pre-design. *Aerospace Science and Technology 9*(7), 641–651.

Lee, M., J. Ceisel, Z. Liu, and D. Mavris (2012). A parametric, preliminary structural analysis and optimization approach with manufacturing cost considerations. In *53rd Structures, Structural Dynamics, and Materials and Co-located Conferences, Honolulu, HI*.

Liu, B., R. T. Haftka, and L. T. Watson (2004). Global-local structural optimization using response surfaces of local optimization margins. *Structural and Multidisciplinary Optimization 27*(5), 352–359.

Liu, W. and W. A. Anemaat (2013). A refined method for wing weight estimation and a new method for wing center of gravity estimation. In *AIAA Aviation Technology Integration and Operation Conference, AIAA*, Volume 4371.

Livne, E. (2003, November). Future of airplane aeroelasticity. *Journal of Aircraft 40*(6), 1066–1092.

M. D. McKay, R. J. Beckman, W. J. C. (1979). A comparison of three methods for selecting values of input variables in the analysis of output from a computer code. *Technometrics 21*(2), 239–245.

Macci, S. (1996). Method for predicting wing structural mass at preliminary design stage. *IMechE*.

March, A. and K. Willcox (2012). Multifidelity approaches for parallel multidisciplinary optimization. In *12th AIAA Aviation Technology, Integration, and Operations (ATIO) Conference and 14th AIAA/ISSMO Multidisciplinary Analysis and Optimization Conference*, pp. 5688.

Martins, J. R. (2002). A coupled-adjoint method for high-fidelity aero-structural optimization. Technical report, DTIC Document.

Martins, J. R., J. J. Alonso, and J. J. Reuther (2005). A coupled-adjoint sensitivity analysis method for high-fidelity aero-structural design. *Optimization and Engineering 6*(1), 33–62.

Martins, J. R. and A. B. Lambe (2013). Multidisciplinary design optimization: a survey of architectures. *AIAA Journal 51*(9), 2049–2075.

Maskew, B. (1987). Program vsaero theory document: a computer program for calculating nonlinear aerodynamic characteristics of arbitrary configurations.

Masseanalyse, A. (2008). Luftfahrttechnisches handbuch, band masseanalyse.

Mastroddi, F., M. Tozzi, and E. Mastrella (2012). Mdo analyses of wing structures for a complete aeroelastically constrained aircraft. *CEAS Aeronautical Journal 3*(1), 67–77.

Matheron, G. (1973). The intrinsic random functions and their applications. *Advances in Applied Probability*, 439–468.

Matlab. Tri surface plots using delaunay triangulation in matlab. https://plot.ly/matplotlib/trisurf/. Accessed: 2016-09-05.

Matthews, P. C., D. W. Standingford, C. M. Holden, and K. M. Wallace (2006). Learning inexpensive parametric design models using an augmented genetic programming technique. *AIE EDAM: Artificial Intelligence for Engineering Design, Analysis, and Manufacturing 20*(01), 1–18.

McGowan, A.-M. R., P. Y. Papalambros, and W. E. Baker (2014). Mdo and cross-disciplinary practice in r&d: A portrait of principles and current practice. *Arbor 1001*, 48109.

McKay, M. D., R. J. Beckman, and W. J. Conover (2000). A comparison of three methods for selecting values of input variables in the analysis of output from a computer code. *Technometrics 42*(1), 55–61.

Megson, T. H. G. (2012). *Aircraft structures for engineering students*. Elsevier.

Menzel, S., M. Olhofer, and B. Sendhoff (2006). Direct manipulation of free form deformation in evolutionary design optimisation. In *Parallel Problem Solving from Nature-PPSN IX*, pp. 352–361. Springer.

Merval, A., M. Samuelides, and S. Grihon (2006). Application of response surface methodology to stiffened panel optimization. In *47th conference on AIAA/ASME/ASCE/AHS/ASC Structures, Structural Dynamics, and Materials Conference*.

Mihalisin, T., J. Timlin, and J. Schwegler (1991). Visualizing multivariate functions, data, and distributions. *IEEE Computer Graphics and Applications 11*(3), 28–35.

Morris, M. D. and T. J. Mitchell (1995). Exploratory designs for computational experiments. *Journal of Statistical Planning and Inference 43*(3), 381–402.

Murman, E. and J. Cole (1970). Calculation of plane steady transonic flow. In *8th AIAA Aerospace Sciences Meeting*, pp. 70–188.

Nawjin, N., M. van Tooren, J. Berends, and P. Arendsen (2006). Automated finite element analysis in a knowledge based engineering environment. In *In AIAA Technical Conferences paper*.

Neill, D., E. Johnson, and R. Canfield (1990). Astrosa multidisciplinary automated structural design tool. *Journal of Aircraft 27*(12), 1021–1027.

Niu, C. (1988). *Airframe structural design: practical design information and data on aircraft structures*. Conmilit Press.

Niu, M. Y. C. (1999). *Airframe Stress Analysis and Sizing*. Conmilit Press.

Nurdin, A., N. Bressloff, A. Keane, and C. Holden (2012). Shape optimisation using cad linked free-form deformation. *Aeronautical Journal 116*(1183), 915–939.

Padula, S. L. and R. E. Gillian (2006). Multidisciplinary environments: a history of engineering framework development. In *11th AIAA/ISSMO Multidisciplinary Analysis and Optimization Conference*, pp. 7083.

Pareto, V. (1906). *Manuale di economia politica*, Volume 13. Societa Editrice.

Park, J.-S. (1994). Optimal latin-hypercube designs for computer experiments. *Journal of statistical planning and inference 39*(1), 95–111.

Parr, J., C. M. Holden, A. I. Forrester, and A. J. Keane (2010). Review of efficient surrogate infill sampling criteria with constraint handling. In *2nd international conference on engineering optimization*, pp. 1–10.

Paulson, C. (2015). pyKriging python kriging module. http://pykriging.com/. Accessed: 2016-11-24.

Petruzzelli, N. and A. Keane (2001). Wave drag estimation for use with panel codes. *Journal of Aircraft 38*(4), 778–782.

Piperni, P., M. Abdo, F. Kafyeke, and A. T. Isikveren (2007, September). Preliminary aerostructural optimization of a large business jet. *Journal of Aircraft 44*(5), 1422–1438.

Piperni, P., A. DeBlois, and R. Henderson (2013). Development of a multilevel multidisciplinary-optimization capability for an industrial environment. *AIAA journal 51*(10), 2335–2352.

Powell, M. J. (2003). On trust region methods for unconstrained minimization without derivatives. *Mathematical programming 97*(3), 605–623.

Price, A. R., A. J. Keane, and C. M. E. Holden (2011). On the coordination of multidisciplinary design optimization using expert systems. *AIAA Journal 49*(8), 1778–1794.

Queipo, N. V., R. T. Haftka, W. Shyy, T. Goel, R. Vaidyanathan, and P. K. Tucker (2005). Surrogate-based analysis and optimization. *Progress in aerospace sciences 41*(1), 1–28.

Rais-Rohani, M. (1998). A framework for preliminary design of aircraft structures based on process information. *NASA Grant NAG-1-1716*.

Raveh, D. E. (2007). Cfd-based models of aerodynamic gust response. *Journal of aircraft 44*(3), 888–897.

Raveh, D. E. and M. Karpel (1999). Structural optimization of flight vehicles with computational-fluid-dynamics-based maneuver loads. *Journal of aircraft 36*(6), 1007–1015.

Raymer, D. (1989). A conceptual approach', aiaa education series. Technical report, ISBN 0-930403-51-7.

Reeves, J., D. DePasquale, and E. Lim (2010). Affordability engineering: Bridging the gap between design and cost. In *AIAA SPACE 2010 Conference & Exposition*, pp. 8904.

Riks, E. (2000). Buckling and post-buckling analysis of stiffened panels in wing box structures. *International journal of solids and structures 37*(46), 6795–6824.

Robinson, G. and A. Keane (2001). Concise orthogonal representation of supercritical airfoils. *Journal of Aircraft 38*(3), 580–583.

Rocca, G. L. and M. J. van Tooren (2009). Knowledge-based engineering approach to support aircraft multidisciplinary design and optimization. *Journal of a Aircraft 46*(6), 1875–1885.

Ronzheimer, A., F. J. Natterer, and J. Brezillon (2010). Aircraft wing optimization using high fidelity closely coupled cfd and csm methods. In *13th AIAA/ISSMO Multidisciplinary Analysis Optimization Conference*, pp. 9078.

Roskam, J. (1986). *Airplane design*. DARcorporation.

Sacks, J., W. J. Welch, T. J. Mitchell, and H. P. Wynn (1989). Design and analysis of computer experiments. *Statistical science*, 409–423.

Santner, T. J., B. J. Williams, and W. I. Notz (2013). *The design and analysis of computer experiments*. Springer Science & Business Media.

Scanlan, J., A. Rao, C. Bru, P. Hale, and R. Marsh (2006). Datum project: cost estimating environment for support of aerospace design decision making. *Journal of Aircraft 43*(4), 1022–1028.

Schmit, L. and R. Rarnanathznil (1978). Multilevel approach to minimum weight deesign including buckling constraints. *AIAA Journal 16*(2), 97–104.

Schmit, L. A. and B. Farshi (1974). Some approximation concepts for structural synthesis. *AIAA j 12*(5), 692–699.

Schuhmacher, G., I. Murra, L. Wang, O. Laxander, A. OLeary, and M. Herold (2002). The design and engineering engine towards a modular system for collaborative aircraft design. In *In 9th AIAA/ISSMO Symposium on Multidisciplinary Analysis and Optimization*.

Schut, J. and M. van Tooren (2007). Design" feasilization" using knowledge-based engineering and optimization techniques. *Journal of Aircraft 44*(6), 1776–1786.

Schutte, J. F., R. T. Haftka, and L. T. Watson (2004). Decomposition and two-level optimization of structures with discrete sizing variables. In *Proceedings of the 45th AIAA/ASME/ASCEAHS/ASC structures, structural dynamics, and materials conference, AIAA paper*, Volume 1541.

Schweiger, J., M. Bsing, and J. Feger (2012). Multidisciplinary analysis and optimization in the conceptual aircraft design phase to support early mass predictions. *SAWE Paper* (3566).

Sederberg, T. W. and S. R. Parry (1986). Free-form deformation of solid geometric models. *ACM SIGGRAPH computer graphics 20*(4), 151–160.

Semonian, J. W. and J. P. Peterson (1955). An analysis of the stability and ultimate compressive strength of short sheet-stringer panels with special reference to the influence of riveted connection between sheet and stringer.

Sensmeier, M. D., B. T. Stewart, and J. Samareh (2006). Rapid generation and assessment of aircraft structural topologies for multidisciplinary optimization and weight estimation. In *Collection of Technical Papers–AIAA/ASME/ASCE/AHS/ASC Structures, Structural Dynamics and Materials Conference*, Volume 7, pp. 4722–4733.

Shanley, F. R. (1960). *Weight-strength analysis of aircraft structures*. Dover Publications.

Shevell, R. S. (1983). *Fundamentals of Flight*. Prentice-Hall.

Shirk, M. H., T. J. Hertz, and T. A. Weisshaar (1986). Aeroelastic tailoring-theory, practice, and promise. *Journal of Aircraft 23*(1), 6–18.

Shirley, C. M., J. A. Schetz, R. K. Kapania, and R. T. Haftka (2014). Tradeoffs of wing weight and lift/drag in design of medium-range transport aircraft. *Journal of Aircraft 51*(3), 904–912.

Skillen, M. D. and W. A. Crossley (2008). Modeling and optimization for morphing wing concept generation ii. part 1; morphing wing modeling and structural sizing techniques.

Sobester, A. (2014). Four suggestions for better parametric geometries. In *10th AIAA Multidisciplinary Design Optimization Conference*, pp. 1–10. American Institute of Aeronautics and Astronautics.

Sóbester, A. (2015). Self-designing parametric geometries. In *56th AIAA/ASCE/AHS/ASC Structures, Structural Dynamics, and Materials Conference*, pp. 0396.

Sóbester, A. and A. I. Forrester (2014). *Aircraft aerodynamic design: geometry and optimization*. John Wiley & Sons.

Sóbester, A., A. J. Keane, J. Scanlan, and N. W. Bressloff (2005). Conceptual design of uav airframes using a generic geometry service. *AIAA Infotech Aerospace*, 26–29.

Sobieszczanski-Sobieski, J. and R. T. Haftka (1997). Multidisciplinary aerospace design optimization: survey of recent developments. *Structural optimization 14*(1), 1–23.

Stadler, W. (1979). A survey of multicriteria optimization or the vector maximum problem, part i: 1776–1960. *Journal of Optimization Theory and Applications 29*(1), 1–52.

Stadler, W. (2013). *Multicriteria Optimization in Engineering and in the Sciences*, Volume 37. Springer Science & Business Media.

Stanford, B. K. and P. D. Dunning (2014, September). Optimal topology of aircraft rib and spar structures under aeroelastic loads. *Journal of Aircraft 52*(4), 1298–1311.

Stanford, B. K., C. V. Jutte, and C. D. Wieseman (2015, October). Trim and structural optimization of subsonic transport wings using nonconventional aeroelastic tailoring. *AIAA Journal 54*(1), 293–309.

Stodieck, O., J. E. Cooper, P. M. Weaver, and P. Kealy (2015, June). Optimization of tow-steered composite wing laminates for aeroelastic tailoring. *AIAA Journal 53*(8), 2203–2215.

Systemes, D. (2015). Solidworks 2015 x64. https://www.3ds.com/products-services/solidworks.

Thokala, P., J. Scanlan, and A. Chipperfield (2010). Life cycle cost modelling as an aircraft design support tool. *Proceedings of the Institution of Mechanical Engineers, Part G: Journal of Aerospace Engineering 224*(4), 477–488.

Thokala, P., J. Scanlan, and A. Chipperfield (2012). Framework for aircraft cost optimization using multidisciplinary analysis. *Journal of Aircraft 49*(2), 367–374.

Timoshenko, S. and J. Gere (2012). *Theory of Elastic Stability*. Dover Publications.

Toal, D. J. (2009). *Proper orthogonal decomposition & kriging strategies for design*. Ph. D. thesis, University of Southampton.

Tomac, M. and D. Eller (2011). From geometry to cfd gridsan automated approach for conceptual design. *Progress in Aerospace Sciences 47*(8), 589–596.

Torenbeek, E. (1992). Development and application of a comprehensive, design-sensitive weight prediction method for wing structures of transport category aircraft. Technical report, Delft University of Technology.

Torenbeek, E. (2013). *Synthesis of subsonic airplane design: an introduction to the preliminary design of subsonic general aviation and transport aircraft, with emphasis on layout, aerodynamic design, propulsion and performance*. Springer Science & Business Media.

Townsend, J. C., J. Samareh, R. Weston, and W. Zorumski (1998). Integration of a cad system into an mdo framework. *ASA/TM-1998-207672*.

Udin, S. V. and W. J. Anderson (1992). Wing mass formula for subsonic aircraft. *Journal of Aircraft 29*(4), 725–727.

Vanderplaats, G. and D. Kim (1988). Recent developments in multilevel optimisation. In *Proceedings of a symposium cosponsored by NASA Langley Research Center*.

Vepa, R. (2008). Aeroelastic analysis of wing structures using equivalent plate models. *AIAA journal 46*(5), 1216–1225.

Vitali, R., O. Park, R. T. Haftka, B. V. Sankar, and C. A. Rose (2002). Structural optimization of a hat-stiffened panel using response surfaces. *Journal of aircraft 39*(1), 158–166.

Wright, J. R. and J. E. Cooper (2008). *Introduction to aircraft aeroelasticity and loads*, Volume 20. John Wiley & Sons.

Young, W. C. and R. G. Budynas (2002). *Roark's formulas for stress and strain*, Volume 7. McGraw-Hill New York.

Youngren, H., E. Bouchard, R. Coopersmith, and L. Miranda (1983). Comparison of panel method formulations and its influence on the development of quadpan, an advanced low-order method. In *American Institute of Aeronautics and Astronautics, Applied Aerodynamics Conference, Danvers, MA*.

Zhang, K.-S., Z.-H. Han, W.-J. Li, and W.-P. Song (2008). Coupled aerodynamic/structural optimization of a subsonic transport wing using a surrogate model. *Journal of Aircraft 45*(6), 2167–2171.

Zhao, X., R. Curran, and W. J. Verhagen (2014). Aircraft component multidisciplinary design optimization considering cost performance. In *14th AIAA Aviation Technology, Integration, and Operations Conference, American Institute of Aeronautics and Astronautics*.

Appendix A

Kriging Infill Studies

In order to determine the method of infill for the two dimmensional kriging response surface models in the sensitivity studies in chapter 5, a study of infill using three separate twodimensional functions was conducted. These functions are the well-known Branin function seen in equation A.1, The Branin function with noise (introduced via 1 + standard normal vlaue divided by 7, added to each noise free traning value), the simple test function created in pyKriging; known as Paulson A.3, and the exponential function A.2. For these functions the process highlighted in figure 5.1 is adhered to with one change; the method chosen for infill. For each function in question the process is run twice once with improvement in MSE chosen for infill criteria and once with Expected improvement (EI) chosen. The results table A.1 comapres the ouputs for MSE, time, infill points (total number or points capped at 100 including the initial 25 training points), σ^2, and μ are compared. In addition to this the overall variable sensitivity and the response surfaces for each function with each infill method can be seen in figures A.1 to A.6.

$$f(x) = a\big(x_2 - bx_1^2 + cx_1 - r\big)^2 + s(1-t)\cos(x_1) + s \tag{A.1}$$

The Branin function has three global minima and the recommended values of a, b, c, r, s and t are: $a = 1$, $b = 5.1 \quad (4\pi 2)$, $c = 5 \quad pi$, $r = 6$, $s = 10$, and $t = 1 \quad (8\pi)$.

$$f(x) = \big(1 - e^{\frac{-1}{2x_2}}\big)\frac{2300x_1^3 + 1900x_1^2 + 2092x_1 + 60}{100x_1^3 + 500x_1^2 + 4x_1 + 20} \tag{A.2}$$

$$f(x) = 0.5\sin(5x_1) + 0.5\cos(5x_2) \tag{A.3}$$

Table A.1: Kriging for known test functions in 2D Results using alternate infill Methods

Test Function	Infill Type	Points (total)	Time (s)	MSE	σ^2	μ
Branin	MSE	29	39.575	0.000914	9.14177	4.582675
	EI	32	115.135	0.000667	72.274337	13.833716
Branin Noise	MSE	101	1142.778	0.023045	0.136977	0.478631
	EI	101	2008.877	0.243599	0.709401	0.355824
Paulson	MSE	27	27.591	0.000884	0.347653	0.574992
	EI	29	46.698	0.000749	0.364844	0.487719
Curret al.	MSE	44	157.900	0.000859	1.262901	-0.591645
	EI	69	1258.651	0.000952	0.116927	0.153103

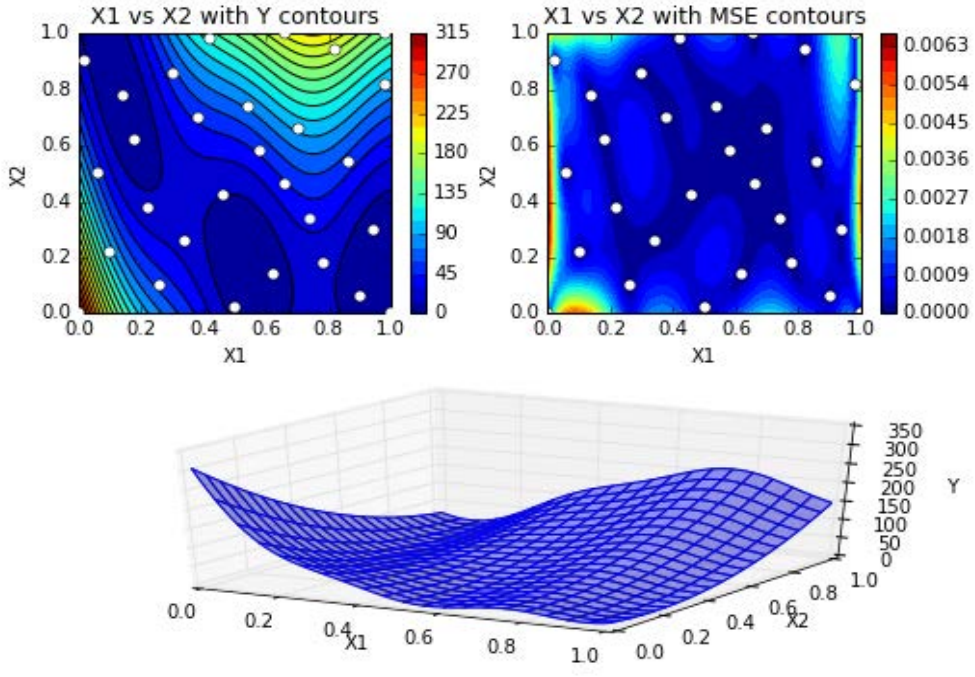

Figure A.1: Branin MSE

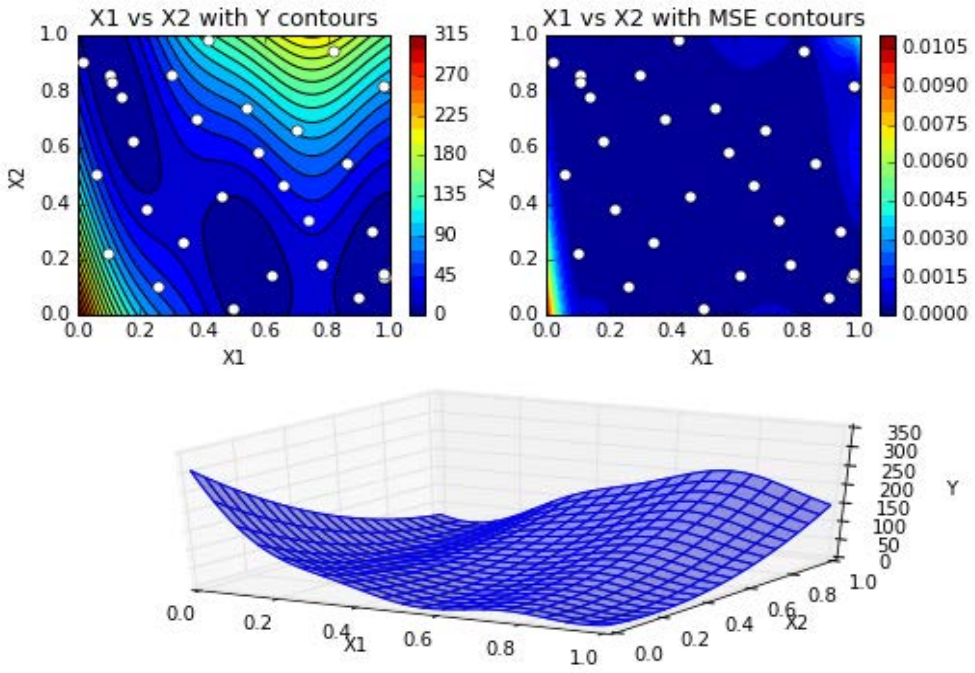

Figure A.2: Branin EI

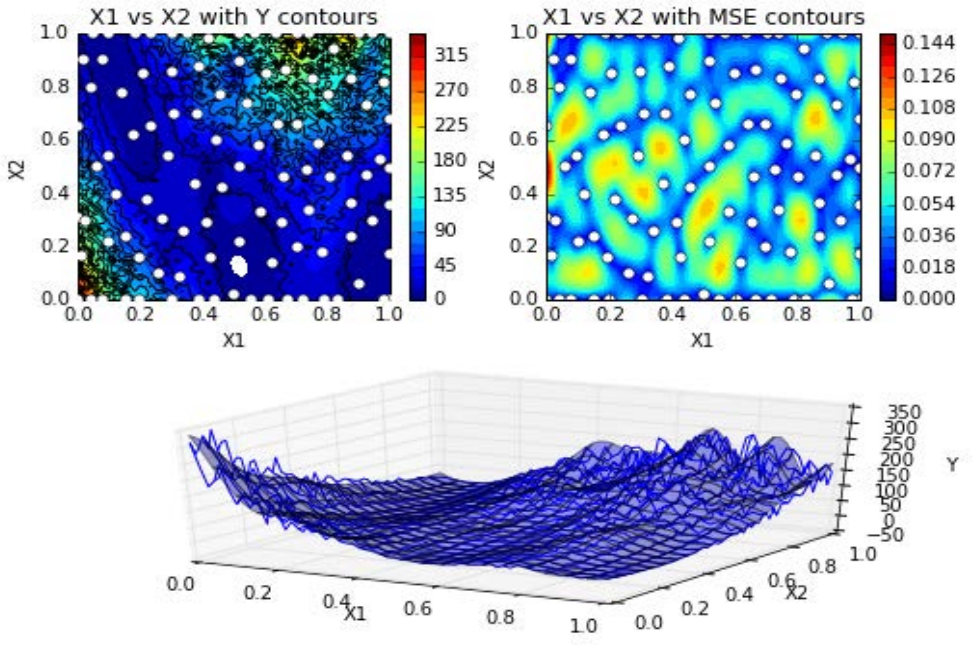

Figure A.3: Branin Noise MSE

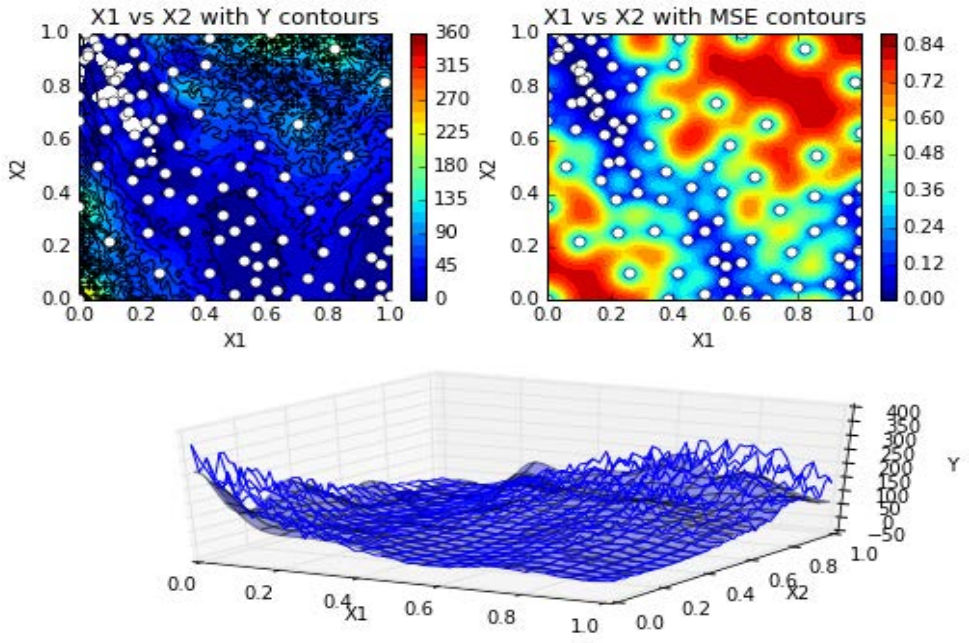

Figure A.4: Branin Noise EI

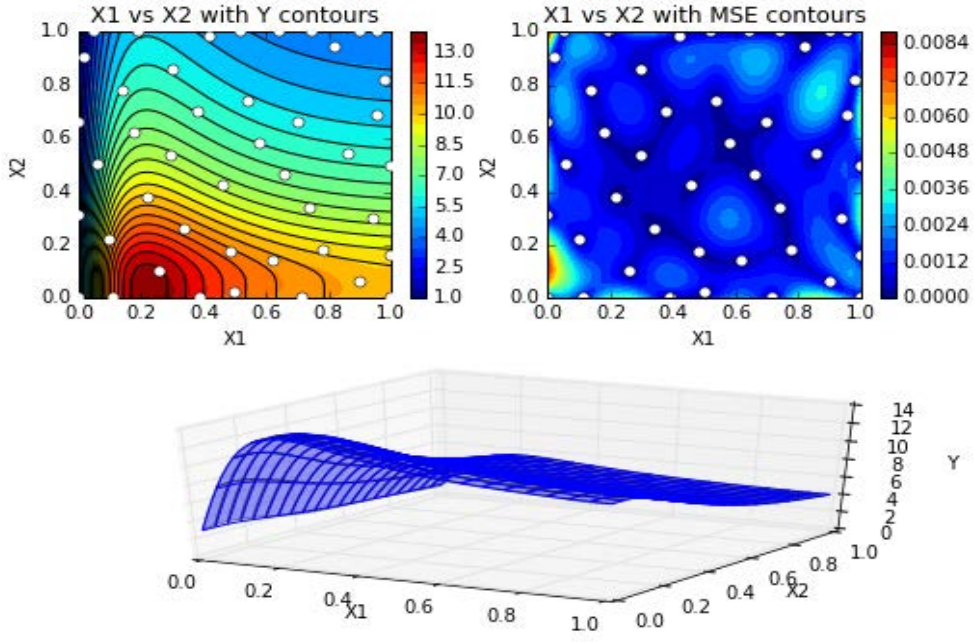

Figure A.5: Curr et al. MSE

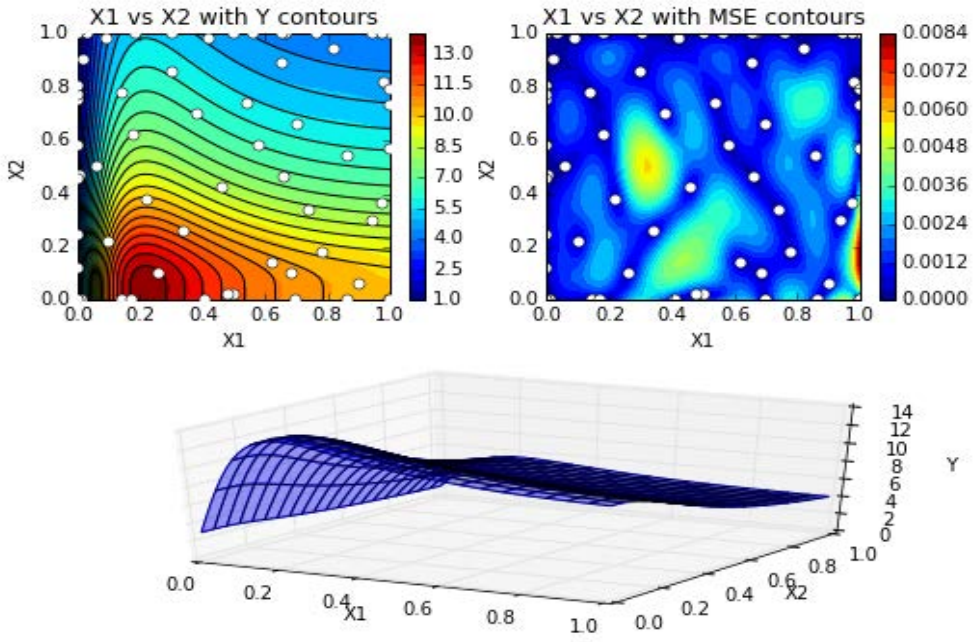

Figure A.6: Curr et al. EI

Appendix B

Sensitivity Studies

Presented in this appendix are results for the sensitivity studies instigated in chapter 5, 5.3. The results here are for the remaining variable pairs, at each level of fidelity, for Weight, Cost, and D/q.

B.1 AR-t/c_r

B.1.0.1 Weight

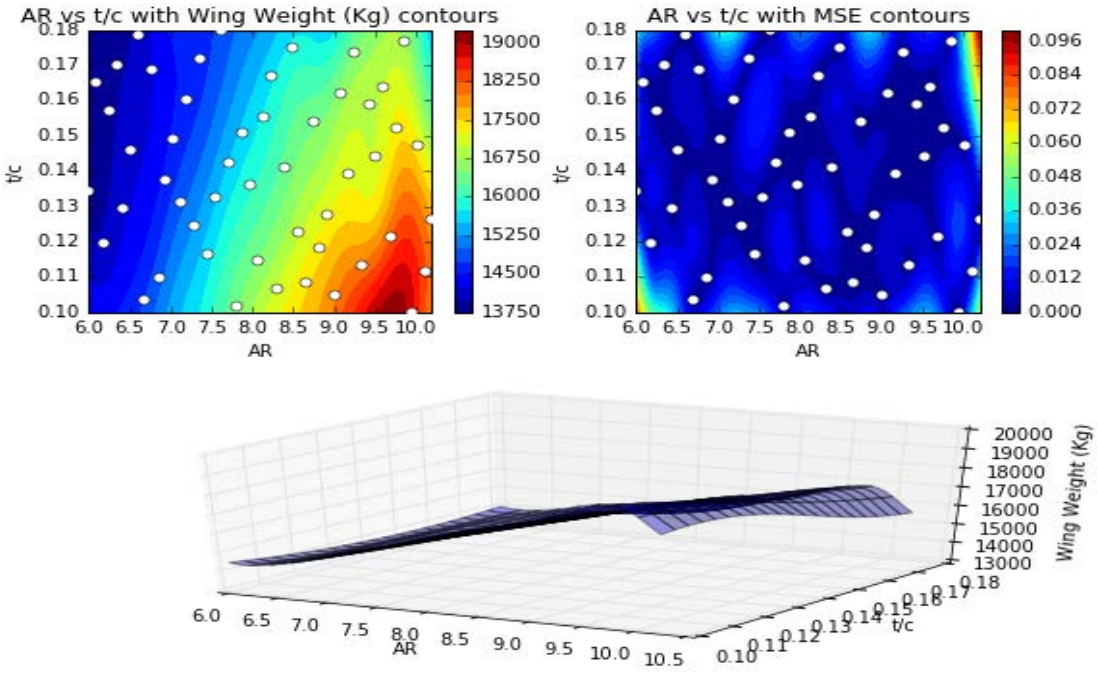

Figure B.1: Visualisation of Weight (Ton) for AR-t/c_{r} variable pairing at fildeity level I.

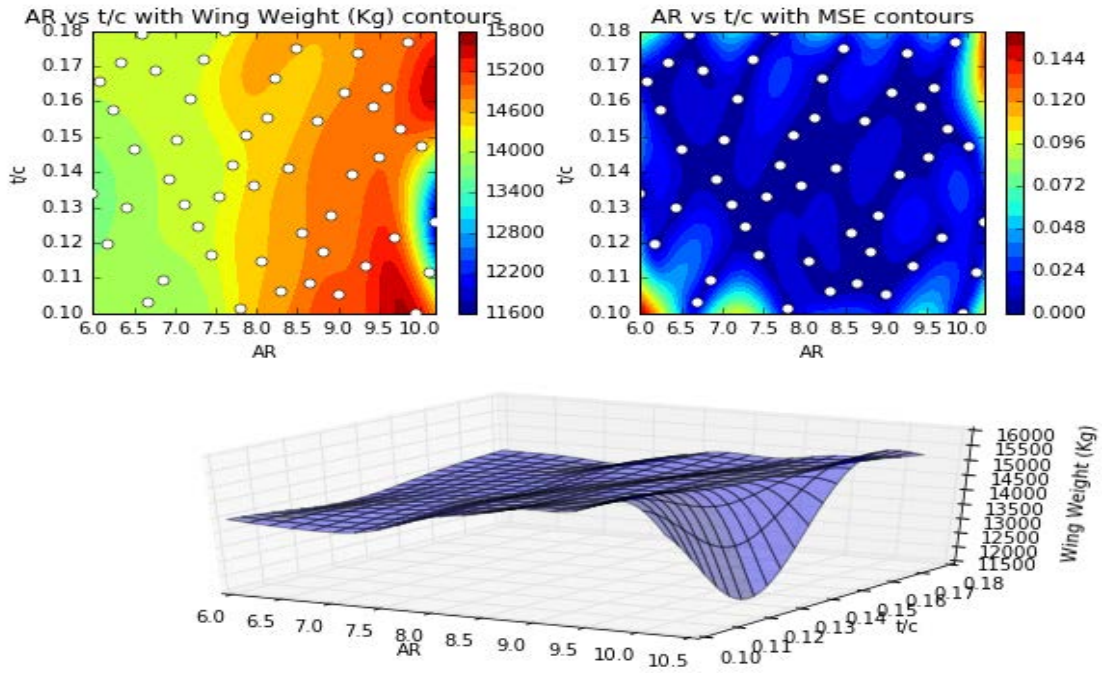

Figure B.2: Visualisation of Weight (Ton) for AR-t/c_{r} variable pairing at fildeity level II.

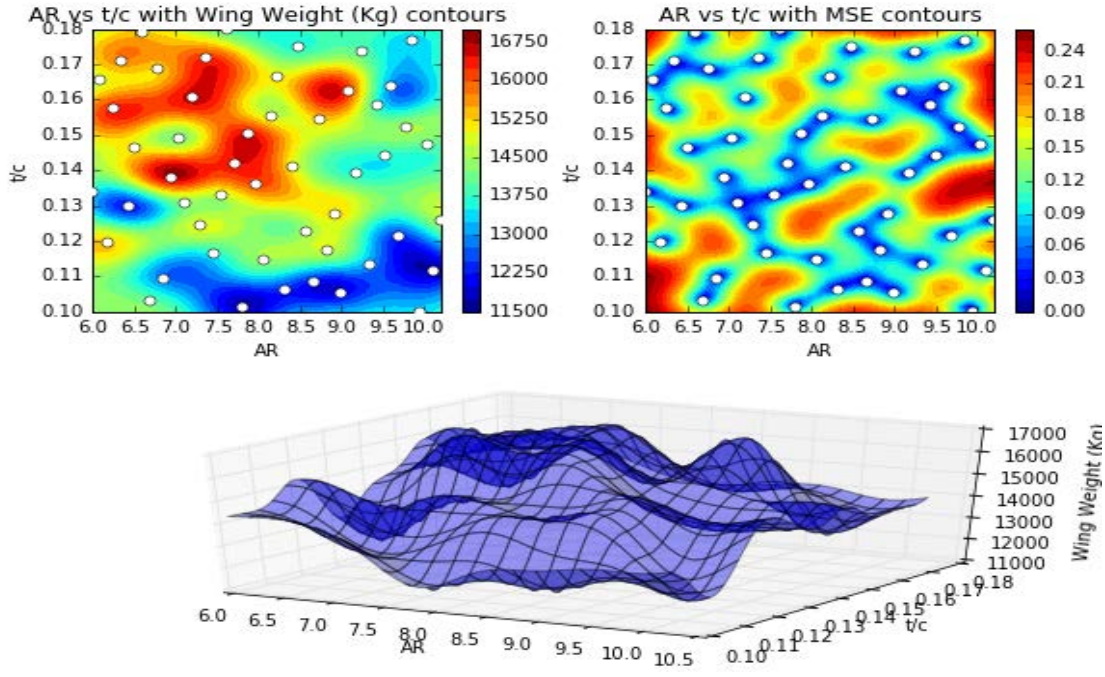

Figure B.3: Visualisation of Weight (Ton) for AR-t/c_{r} variable pairing at fildeity level III.

B.1.0.2 Cost

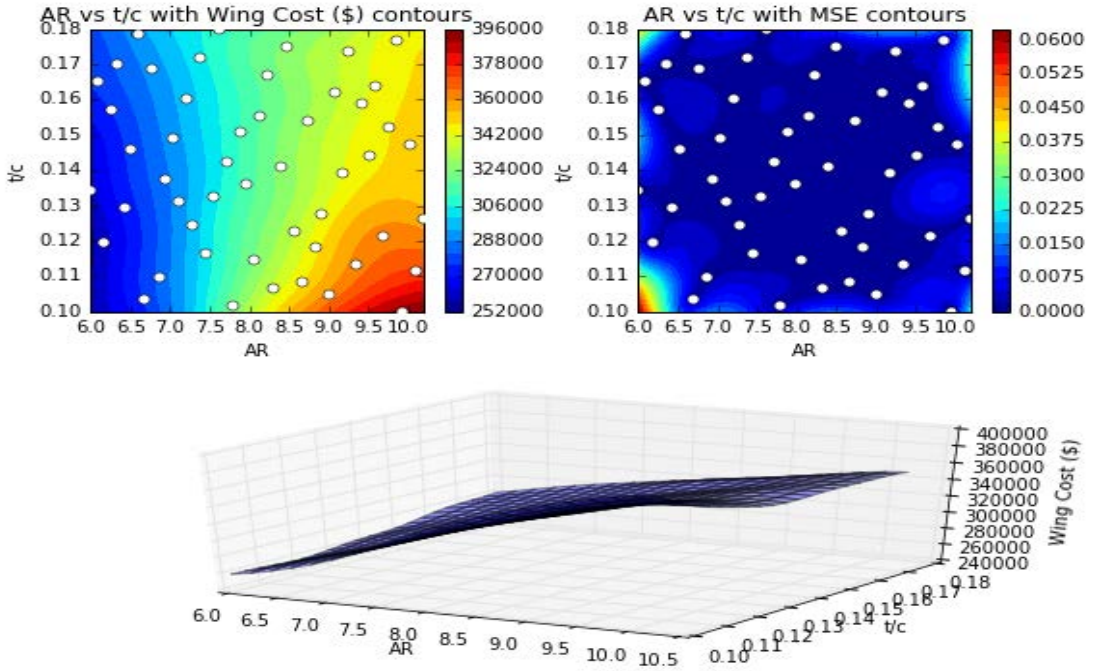

Figure B.4: Visualisation of Cost ($) for AR-$t/c_r$ variable pairing at fildeity level I.

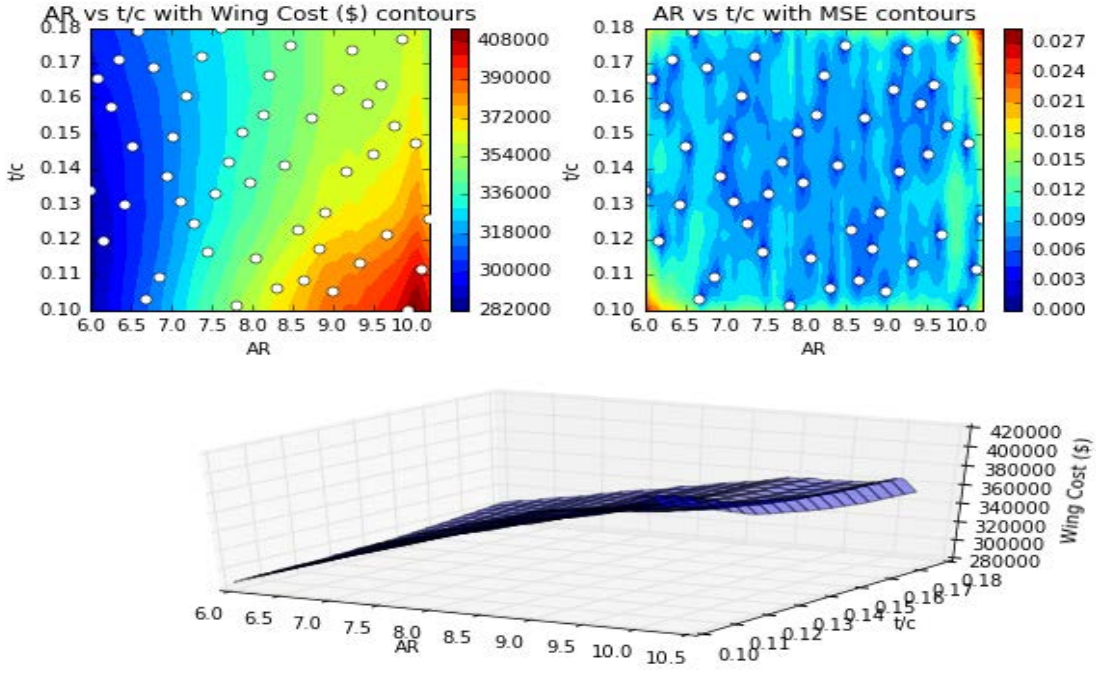

Figure B.5: Visualisation of Cost ($) for *AR*-$t/c_r$ variable pairing at fildeity level II.

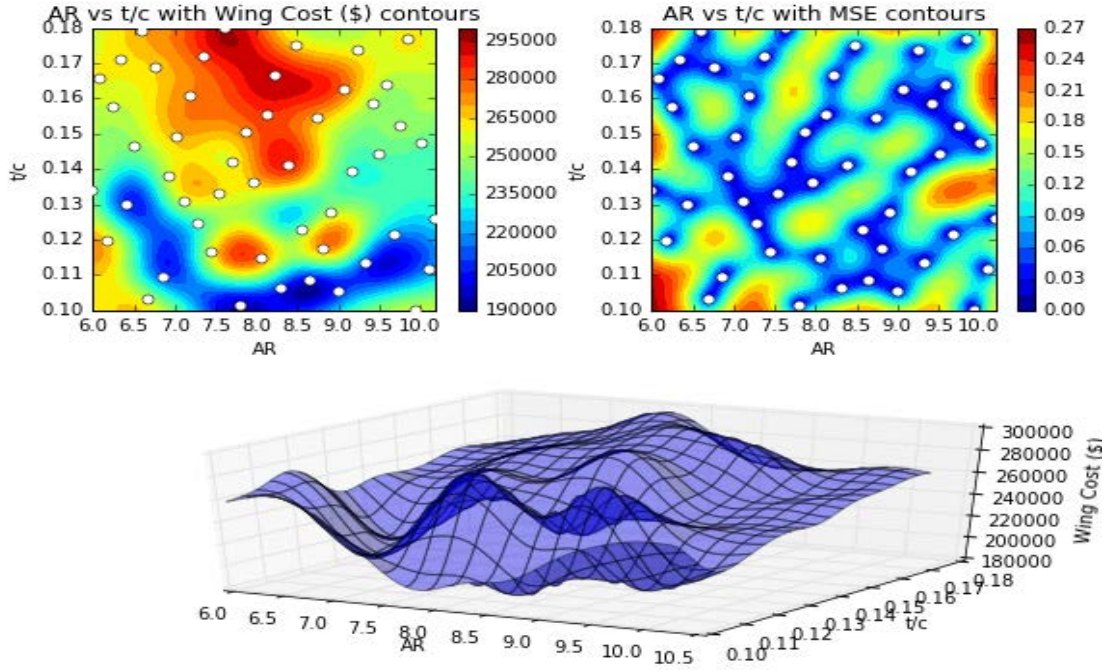

Figure B.6: Visualisation of Cost ($) for AR-t/c_{r} variable pairing at fildeity level III.

B.1.0.3 AR-t/c_r

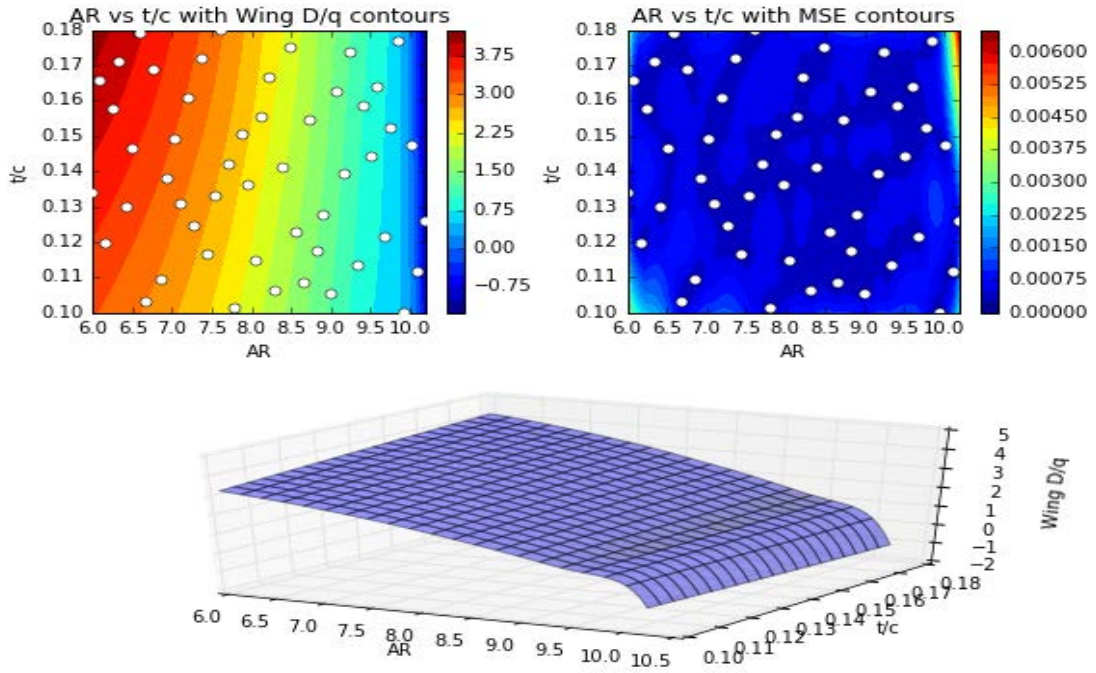

Figure B.7: Visualisation of D/q for AR-t/c_{r} variable pairing at fildeity level I.

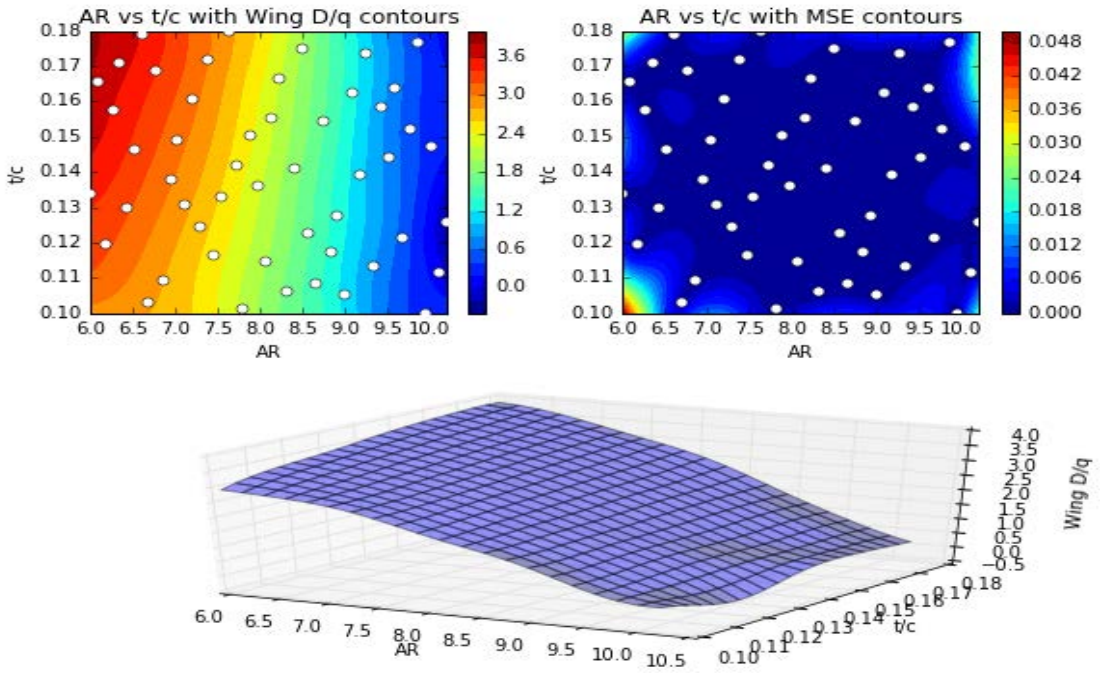

Figure B.8: Visualisation of D/q for AR-t/c_{r} variable pairing at fildeity level II.

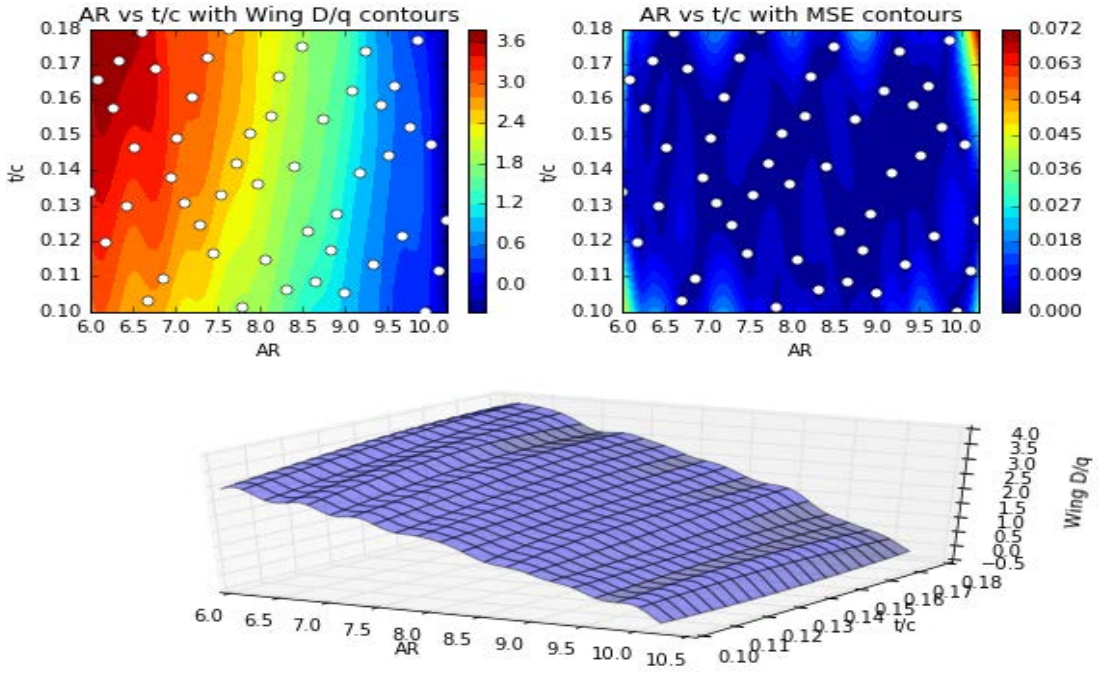

Figure B.9: Visualisation of D/q for AR-t/c_{r} variable pairing at fildeity level III.

B.1.0.4 Discussion

The most notable trends from the three dimensional visualisation of this pair is for the weight (figures B.1, B.2, and B.3), the range over which this changes is significantly

small in comparison to AR-SG, or SG based trends. Here as the wing becomes slender variation of the t/c at the root, has a greater effect than at any where else in the design space. When the wing is at its most slender, the variation in the t/c has an impact on the lift distribution in span and chord wise directions, and the associated moment relief. At the fidelity level I, there is a shelf like effect with a singular peak, suggesting a larger weight is possible at high AR and low t/c, however at level II although this peak is overshadowed by an apparent optimum region, where the t/c leads to a significant improvements in weight at higher AR, for a small region.

For cost (figures B.4 to B.6), what we notice is that as a result of increased fidelity, there is a significant increase in the non-linearly in the RSM surface. The relatively linear trend observed at level I, deteriorates somewhat at level II, with an upward shift and upper and lower cost boundary. This relationship however is not present at level III, where there is now a drastic change in the design space. For D/q (figures B.7 to B.9), we observe minor changes in the trend with the increase in fidelity from level I to II, to III seemingly helping to eliminate the slip or shelf in level I. Note however that at level III, the surface fit deteriorates and the design surface is less smooth, this is echoed in the increase in mean squared error.

B.2 *AR-SWPI*

B.2.0.1 Weight

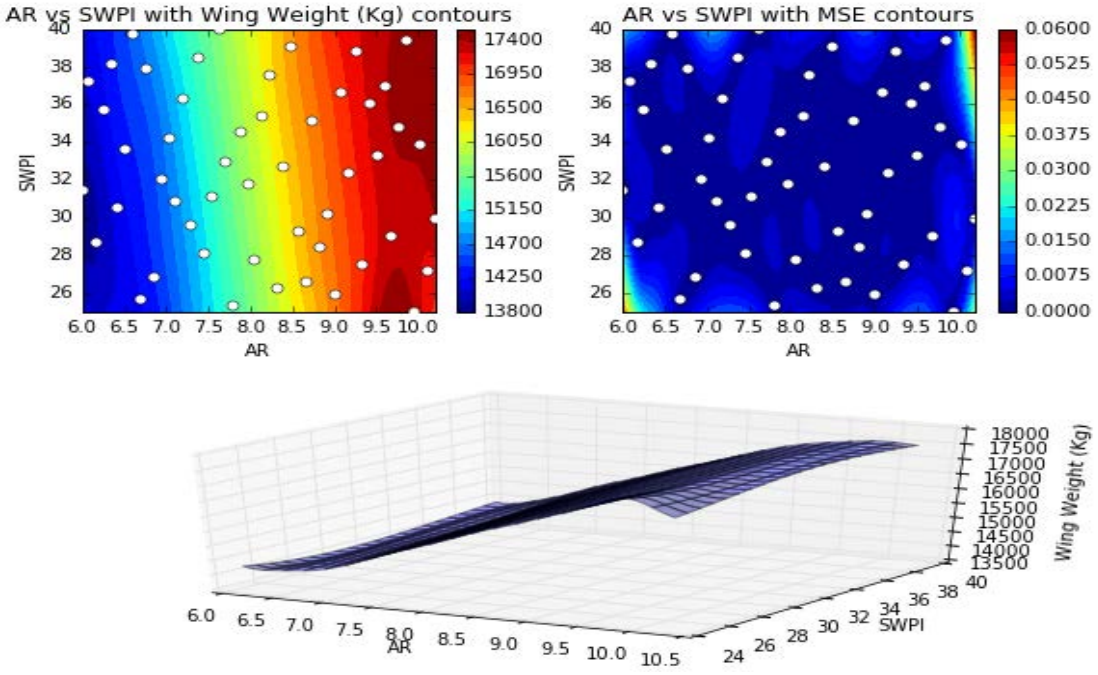

Figure B.10: Visualisation of Weight (Ton.) for *AR-SWPI* variable pairing at fildeity level I.

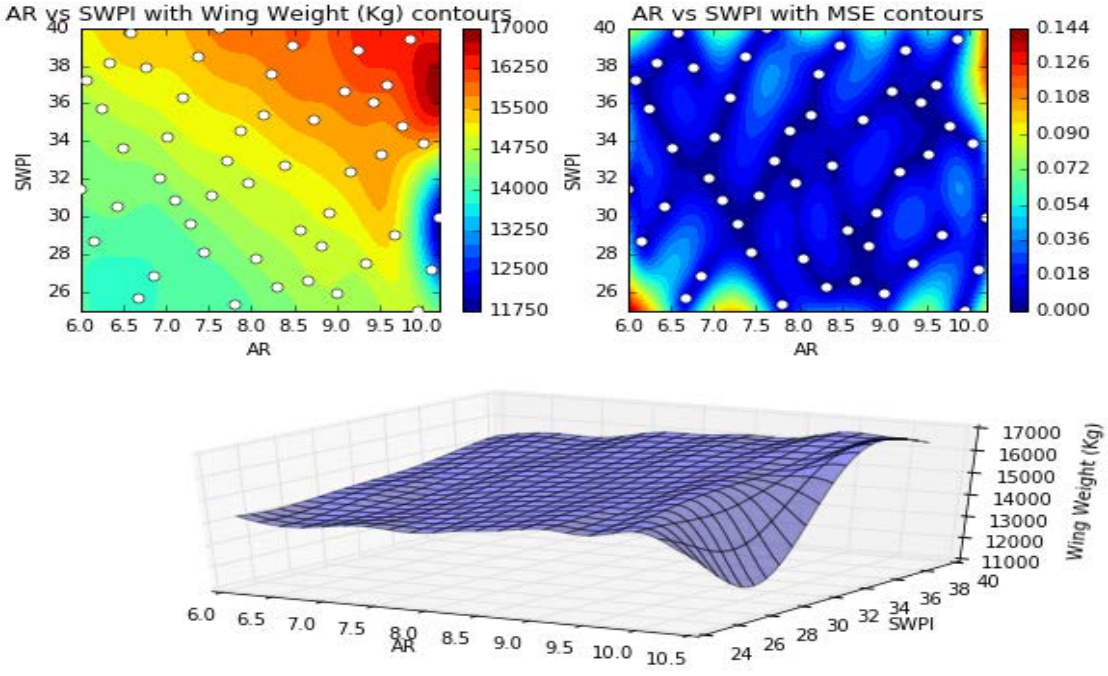

Figure B.11: Visualisation of Weight (Ton.) for *AR-SWPI* variable pairing at fildeity level II.

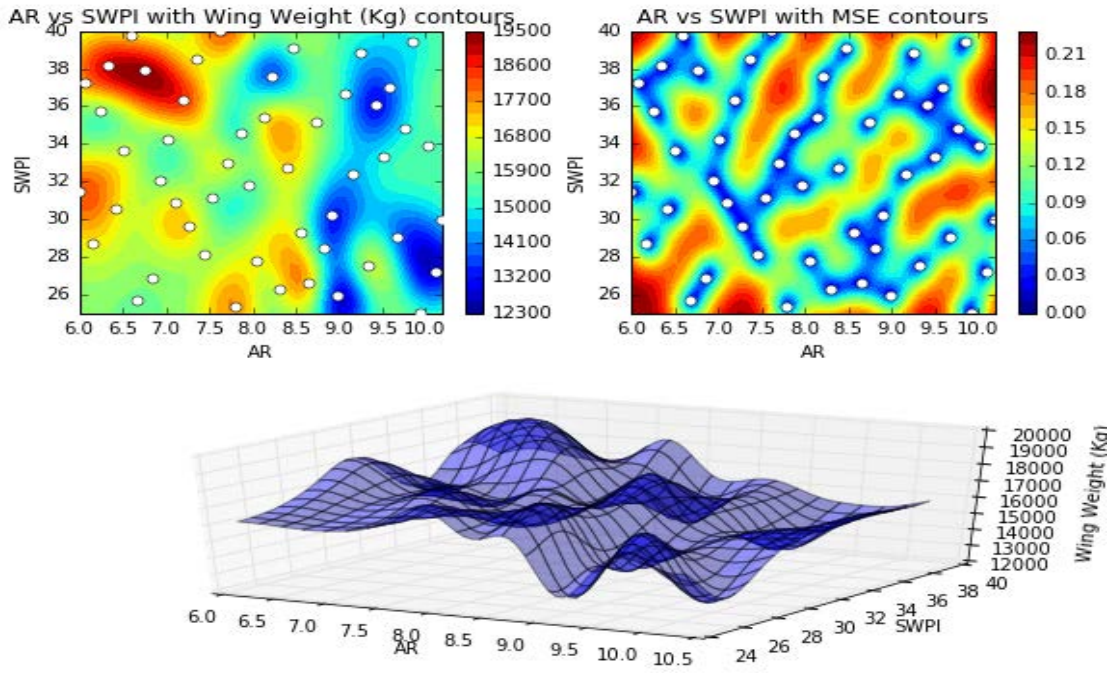

Figure B.12: Visualisation of Weight (Ton.) for *AR-SWPI* variable pairing at fildeity level III.

B.2.0.2 Cost

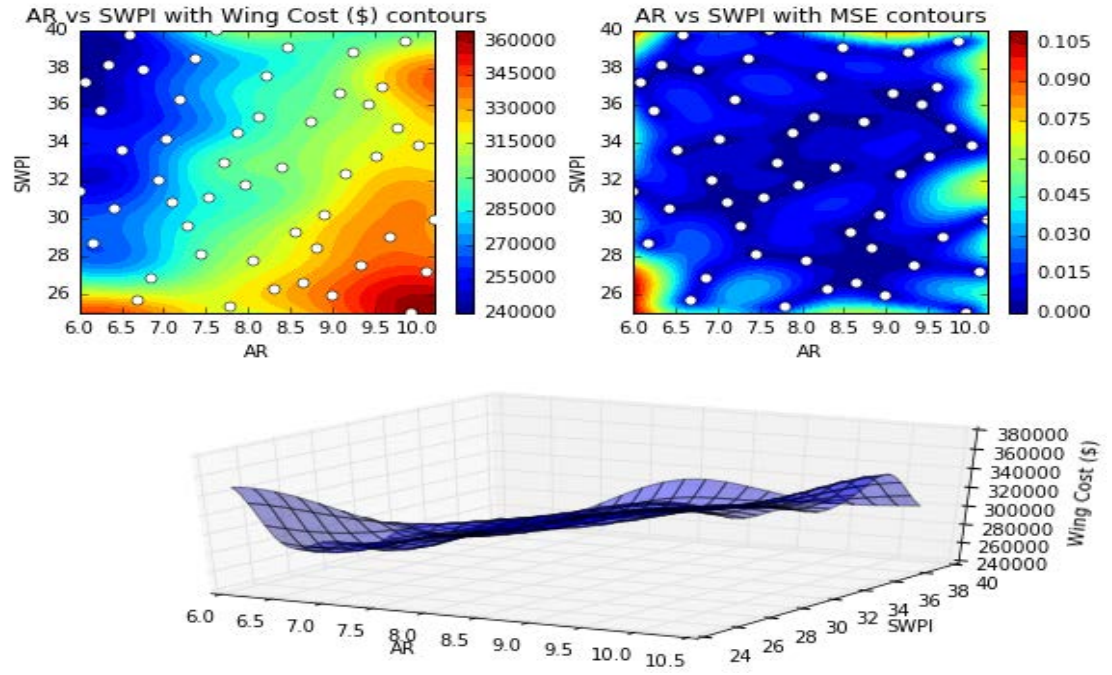

Figure B.13: Visualisation of Cost ($) for *AR-SWPI* variable pairing at fildeity level I.

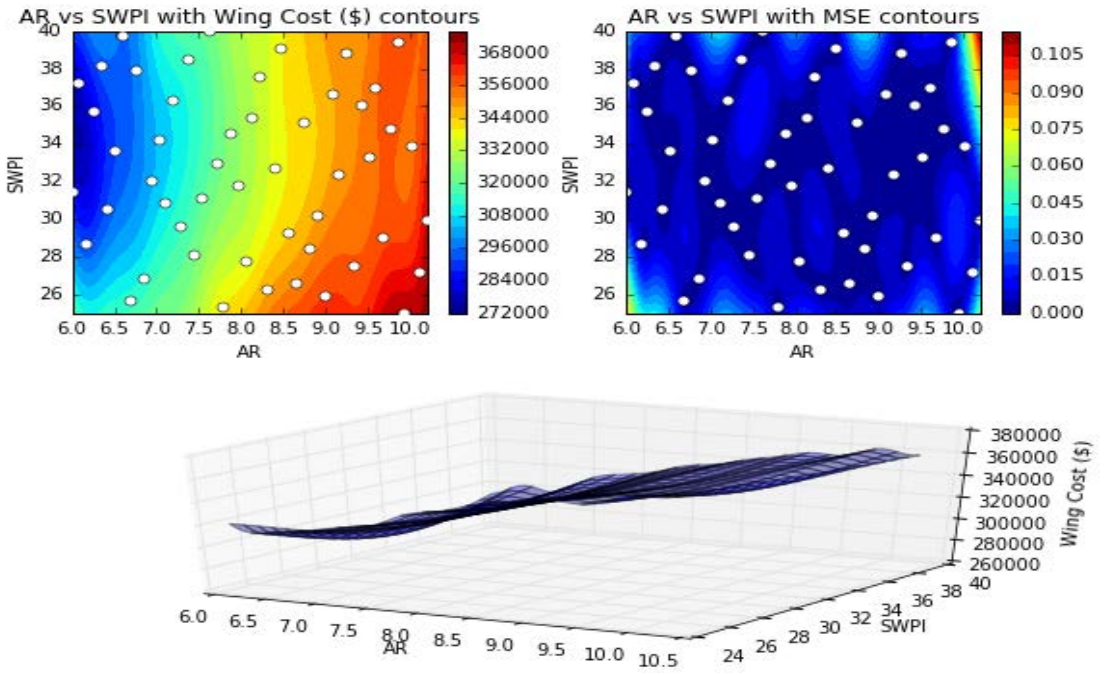

Figure B.14: Visualisation of Cost ($) for *AR-SWPI* variable pairing at fildeity level II.

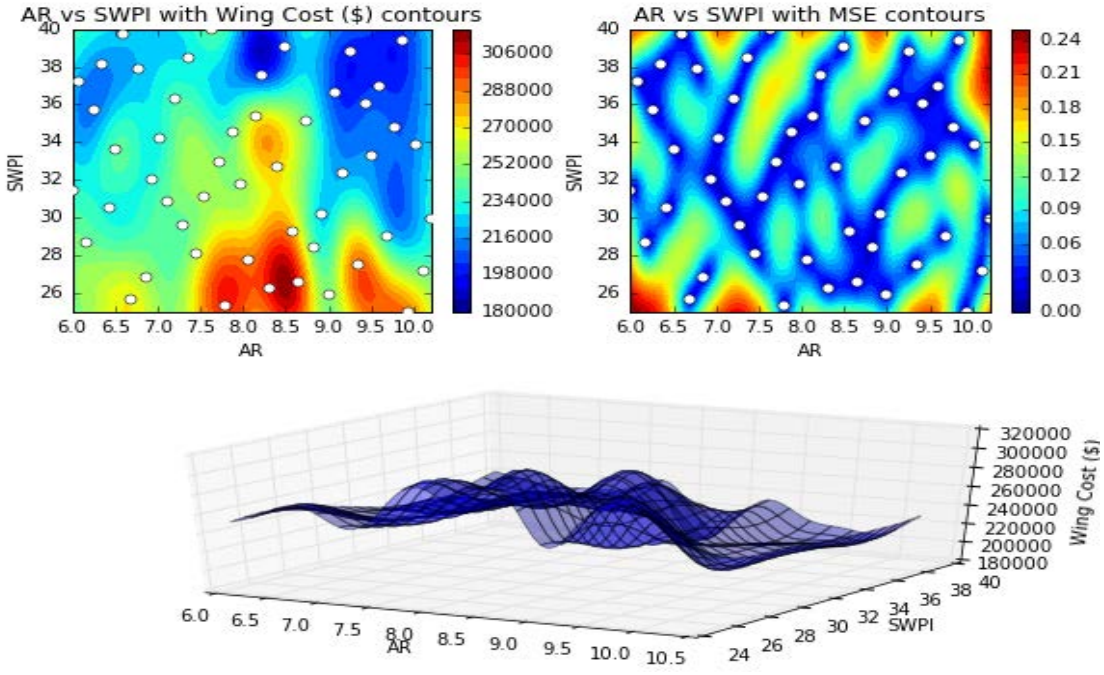

Figure B.15: Visualisation of Cost ($) for *AR-SWPI* variable pairing at fildeity level III.

B.2.0.3 Drag

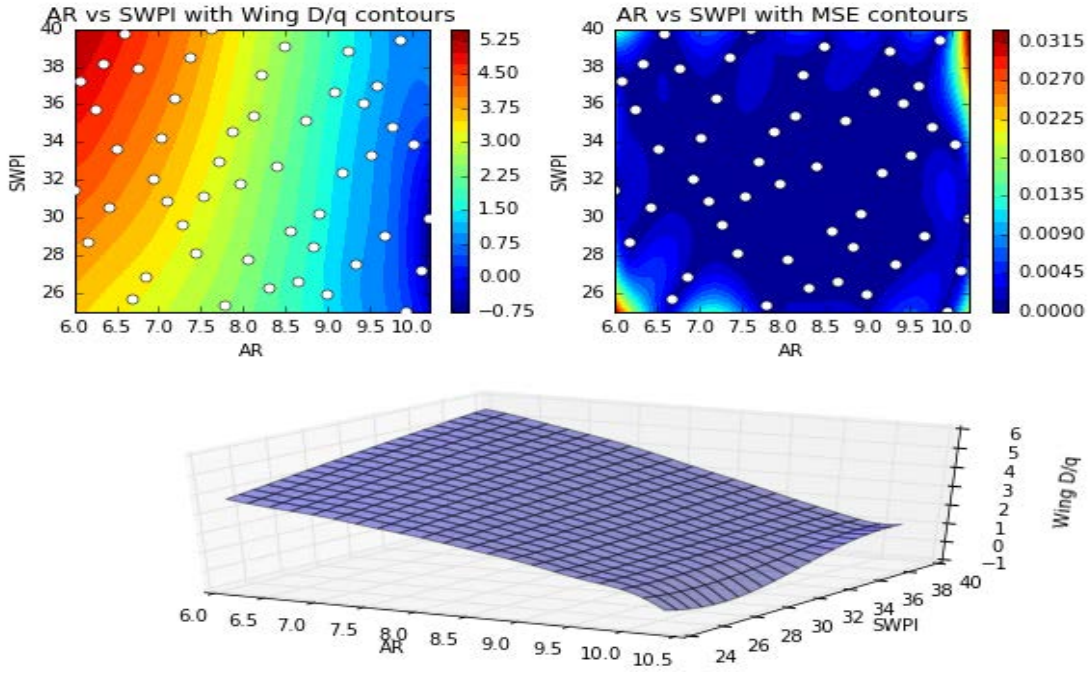

Figure B.16: Visualisation of D/q for AR-$SWPI$ variable pairing at fildeity level I.

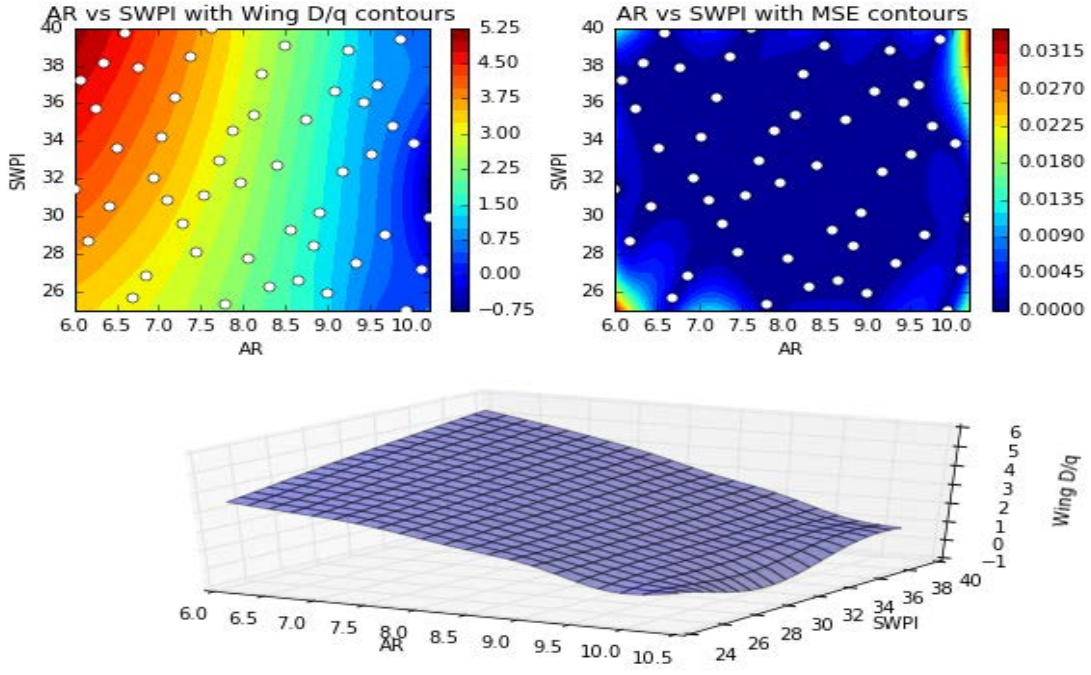

Figure B.17: Visualisation of D/q for AR-$SWPI$ variable pairing at fildeity level II.

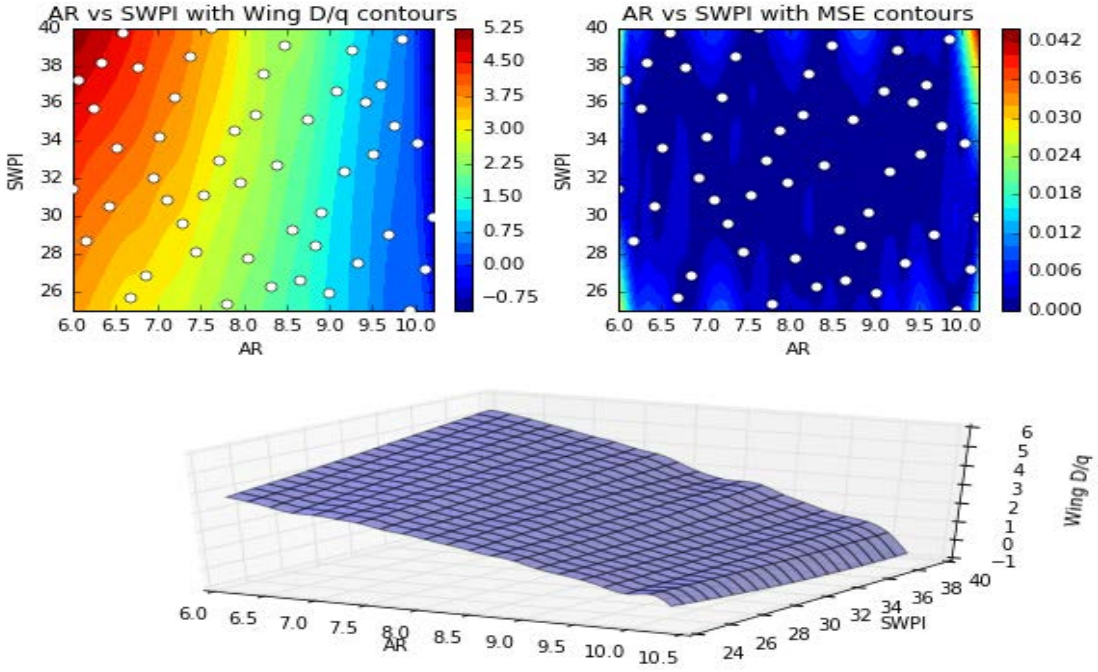

Figure B.18: Visualisation of D/q for *AR-SWPI* variable pairing at fildeity level III.

B.2.0.4 Discussion

Interesting to note for weight that as both variables introduce complex physical phenomena, to the analysis fidelity. In T.A.C.E moving from level to level inherently introduced more complex non-linear physics to the structural model in addition to the complex and sensitive relationship between these variables in aerodynamic analysis. This begins to create greater instability in the design space at level II and then subsequently in level III. For cost even at fidelity level I, there is uncertainty and non-linearity at the designs space fringes, demonstrating that even with lower fidelity structural modelling and simplified aerostructural coupling, both variables are highly sensitive to each other, and cost is sensitive to both.

In both the weight and cost models (figures B.10 to B.12, and B.13 to B.12) it is noticeable that moving from level I to II, *SWPI* becomes the dominant variable. At a higher level of fidelity cost and weight are more sensitive to sweep than aspect ratio, but not by a substantial margin, as the range over for the trends remain similar between fidelity levels. From a structural perspective this variation is viable as increased sweep will lead to greater torsional forces in the wing, this in turn will affect the rotation of the wingbox model FEM, and change the loading and weight. However at level III for both weight and cost, the observed trends are changed and there is now non-linear behaviour in the design space. For drag (figures B.16 to B.18) a slip region reduction effect is observed is observed when moving from level I, to II, III. Where regions of uncertainty

at the fringes of the design space are reduced or removed as a result of increased analysis fidelity.

At this stage a general trend is apparent for AR, which in unison with any variable is sensitive to fidelity change for weight and cost performance, and conservative for drag at lower fidelity.

B.3 SG-t/c_r

B.3.0.1 Weight

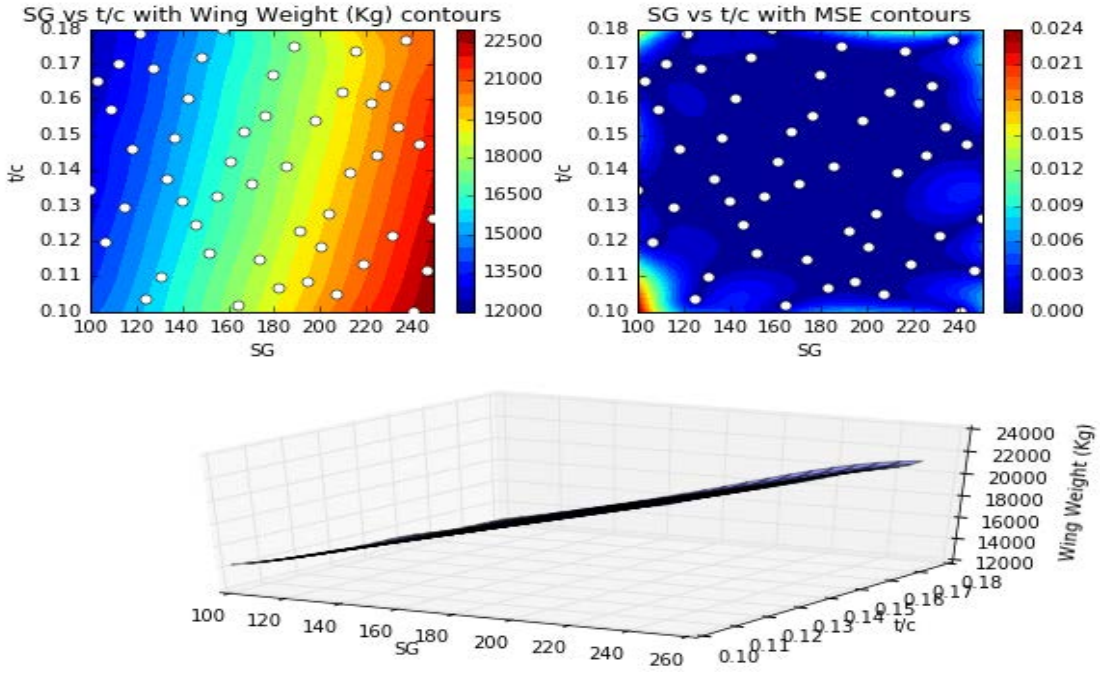

Figure B.19: Visualisation of Weight (Ton) for SG-t/c_r variable pairing at fildeity level I.

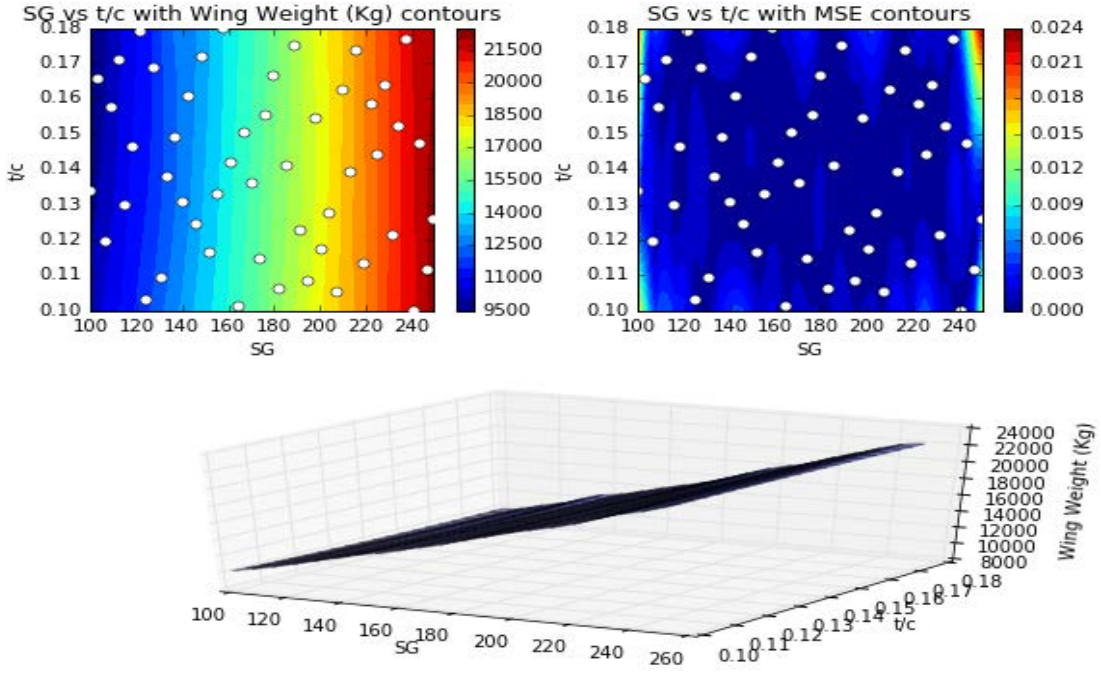

Figure B.20: Visualisation of Weight (Ton) for SG-t/c_r variable pairing at fildeity level II.

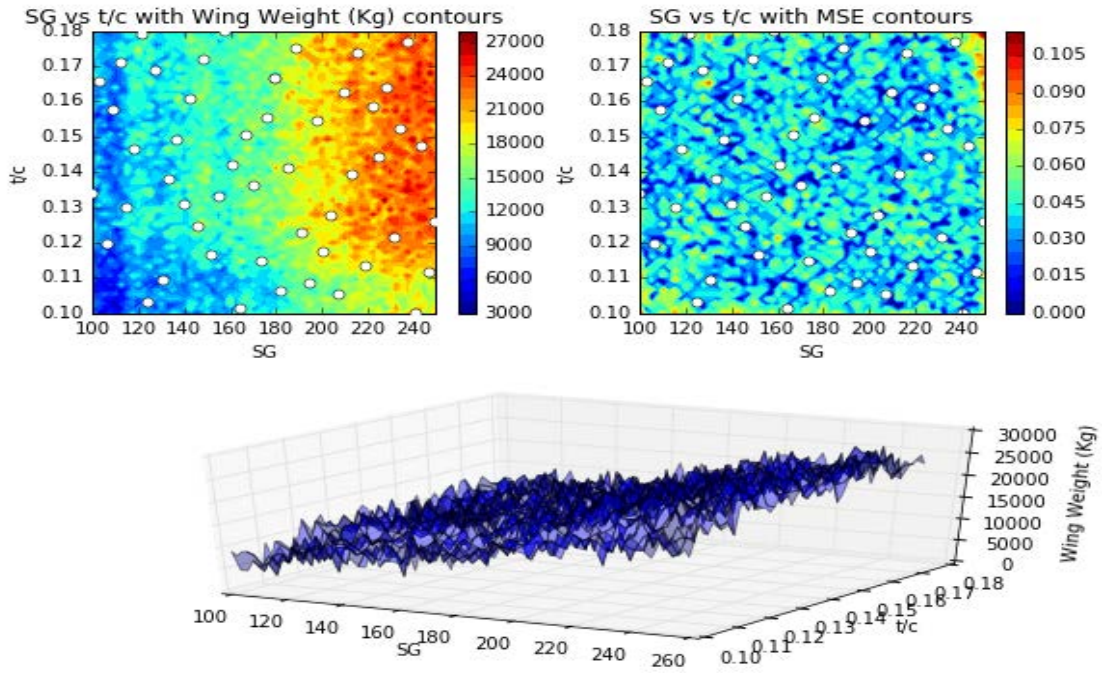

Figure B.21: Visualisation of Weight (Ton) for SG-t/c_{r} variable pairing at fildeity level III.

B.3.0.2 Cost

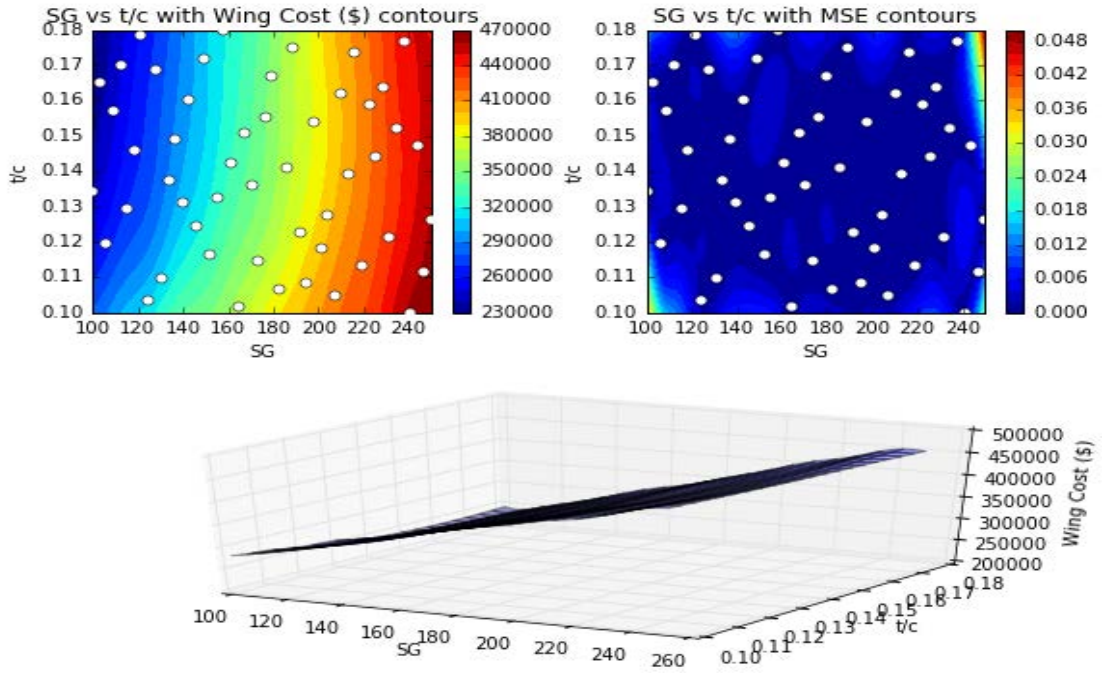

Figure B.22: Visualisation of Cost ($) for SG-t/c_{r} variable pairing at fildeity level I.

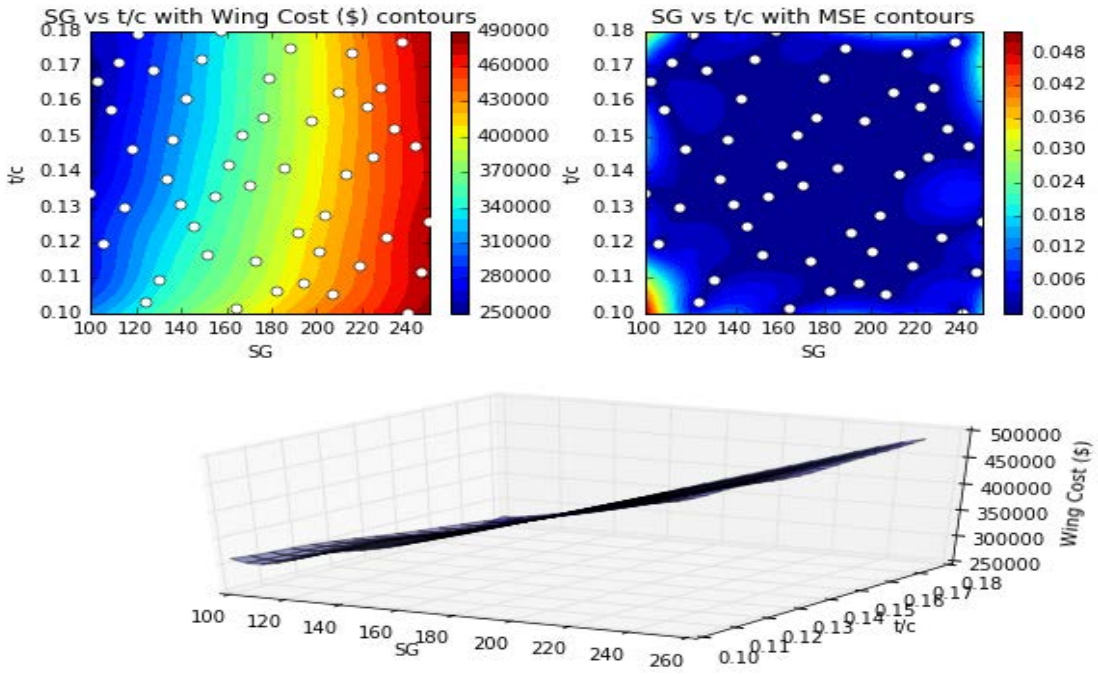

Figure B.23: Visualisation of Cost ($) for SG-t/c_{r} variable pairing at fildeity level II.

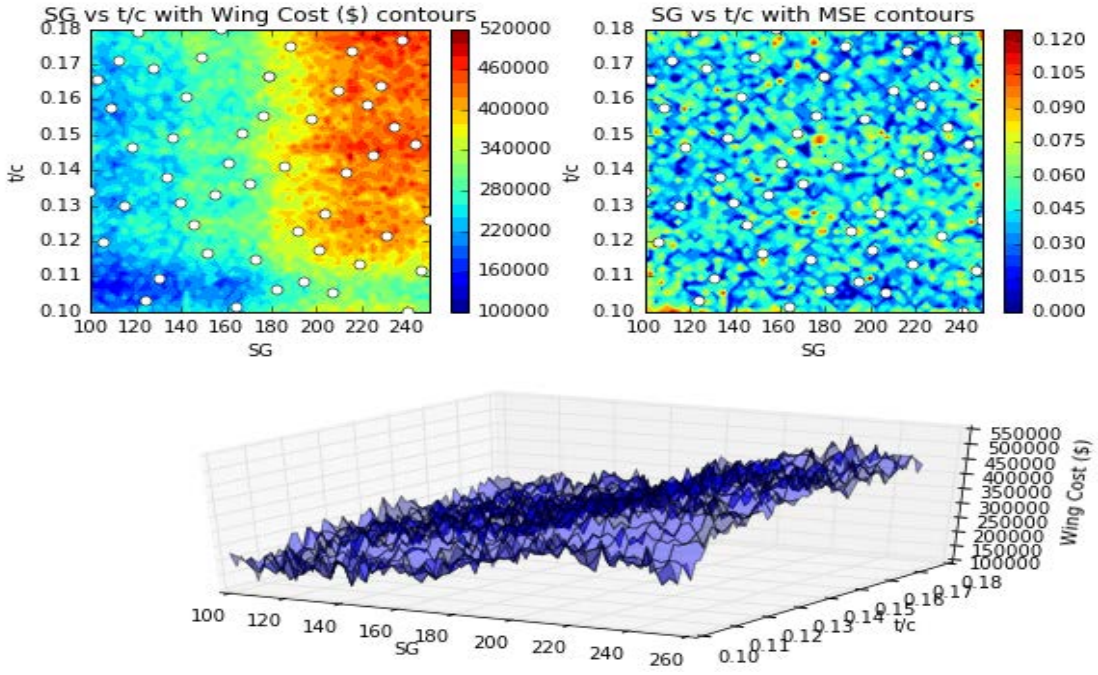

Figure B.24: Visualisation of Cost ($) for SG-t/c_{r} variable pairing at fildeity level III.

B.3.0.3 Drag

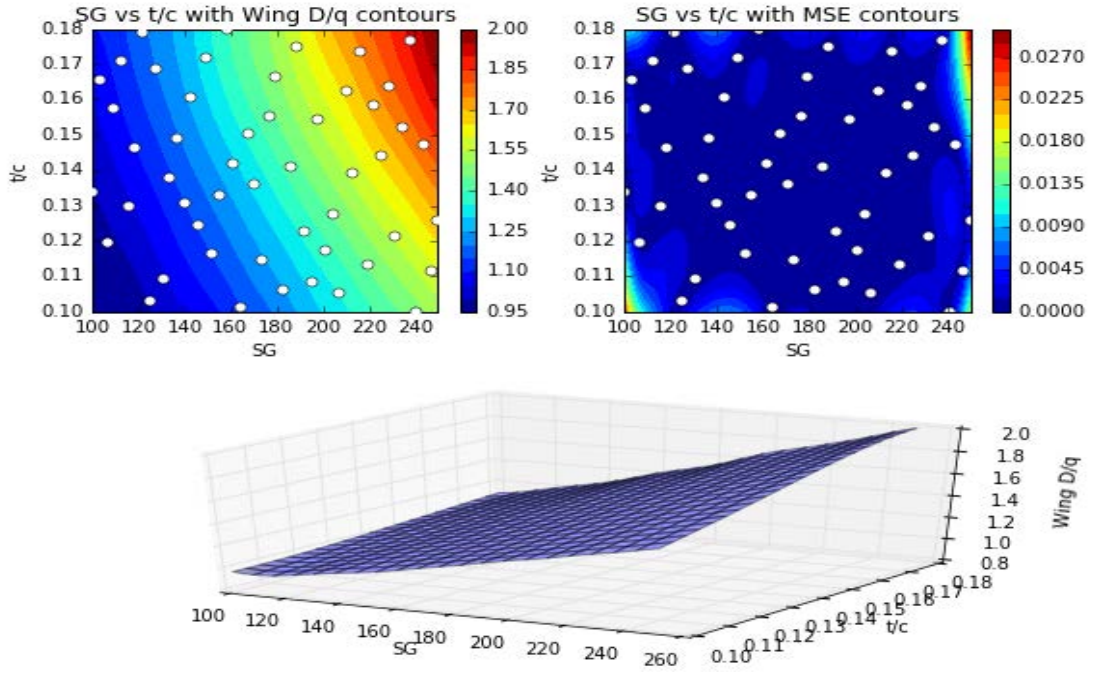

Figure B.25: Visualisation of D/q for SG-t/c_r variable pairing at fildeity level I.

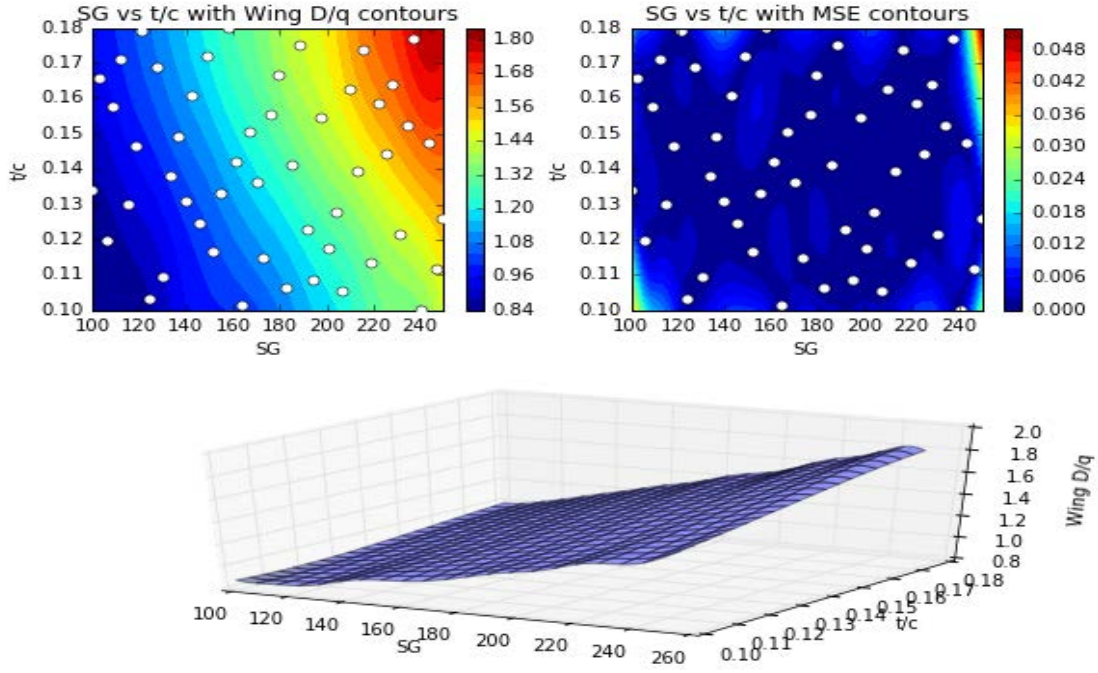

Figure B.26: Visualisation of D/q for SG-t/c_r variable pairing at fildeity level II.

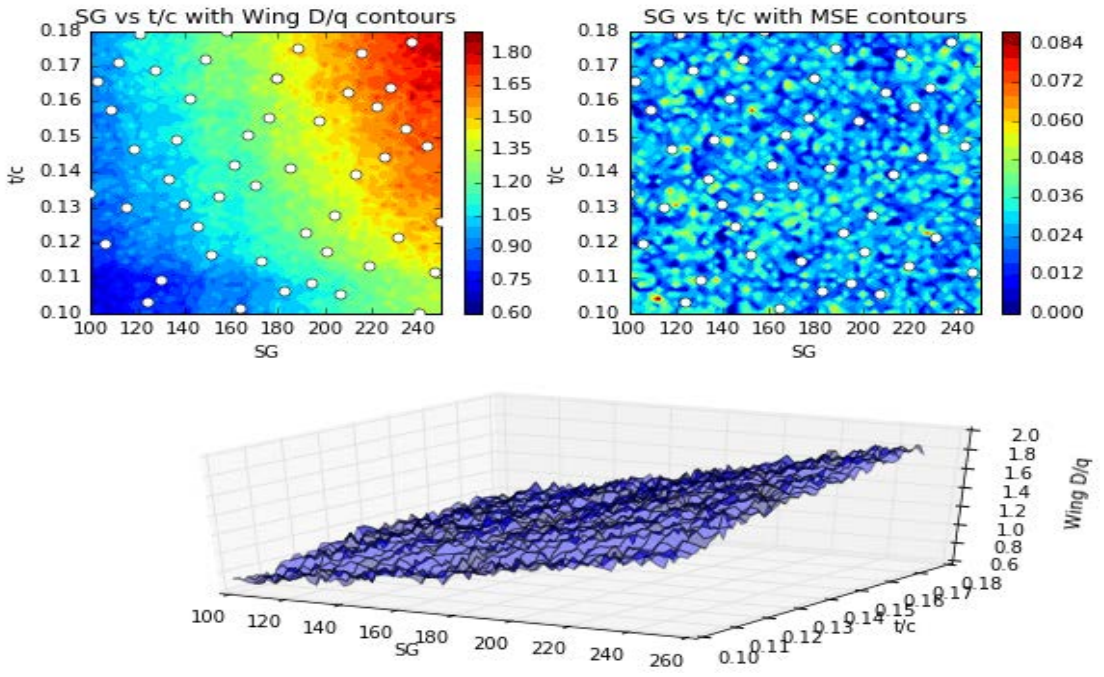

Figure B.27: Visualisation of D/q for SG-t/c_{r} variable pairing at fildeity level III.

B.3.0.4 Discussion

Weight and cost trends at level I, for this pair reflect expected structural behaviour, where larger t/c at each SG band, creates a direction of minimum slope. At level II the weight trend is somewhat altered and a more linear trend is noticed. This linear trends however becomes prone to noise at level III, which is notable in the significantly higher mean squared error values at this level. This presumably is related to the physical impact of stingers, and stress optimisation in conjunction with aerostructural coupling. The perturbation of these variables seems to produce noise in the observed weight, cost and drag. The visualisations of these performance variables can be found in figures B.19 to B.21, and figures B.22 to B.24, for weight and cost respectively.

This is somewhat unique in the trends, as the noise is global, and creates many local peaks and troughs in the design space. This noise is likely generated from the stress optimisation at level III. As noted in the thickness solutions at level III during calibration, the optimisation leads to a stringer dominated design, this in turn affects the load distribution on the wing. As this ratio increases, the stinger is likely to be smaller, however there is greater load alleviation on the inboard wing region, the overall stress in this region is lower, whilst the drag increases. This leads to the stress optimisation being trapped in local stress regions, and failing to reach the maximum allowable stress. Which when spread over many points, can lead to noisy data.

However the overall trends in weight, and cost are as expected. Note for cost there is a very large range of values for the design surface, however the minimum boundary is significantly higher than is pairs featuring more sensitive variables. This demonstrates that although there is a clear penalty for having a large SG, the combination of these variables will not allow the exploration of low cost design. Other variables such as $SWPI$ and AR, allow the exploration of significantly lower cost designs, as demonstrated by the lower boundaries for cost responses in models featuring $SWPI$ or AR.

For D/q (figures B.25 to B.27) we have virtually identical response surfaces when moving up in fidelity levels. However the range over which the D/q varies is slightly larger, in particular at the lower boundary. This implies that the change in fidelity of the structural models, gives access to a greater range of minimal drag values for these variables. Note the D/q values are fairly small even at the maximum boundary, implying that the cumulative effect of these variables on the aerodynamic performance is not only linear, but not critical in terms of design space exploration.

B.4 *SG-SWPI*

B.4.0.1 Weight

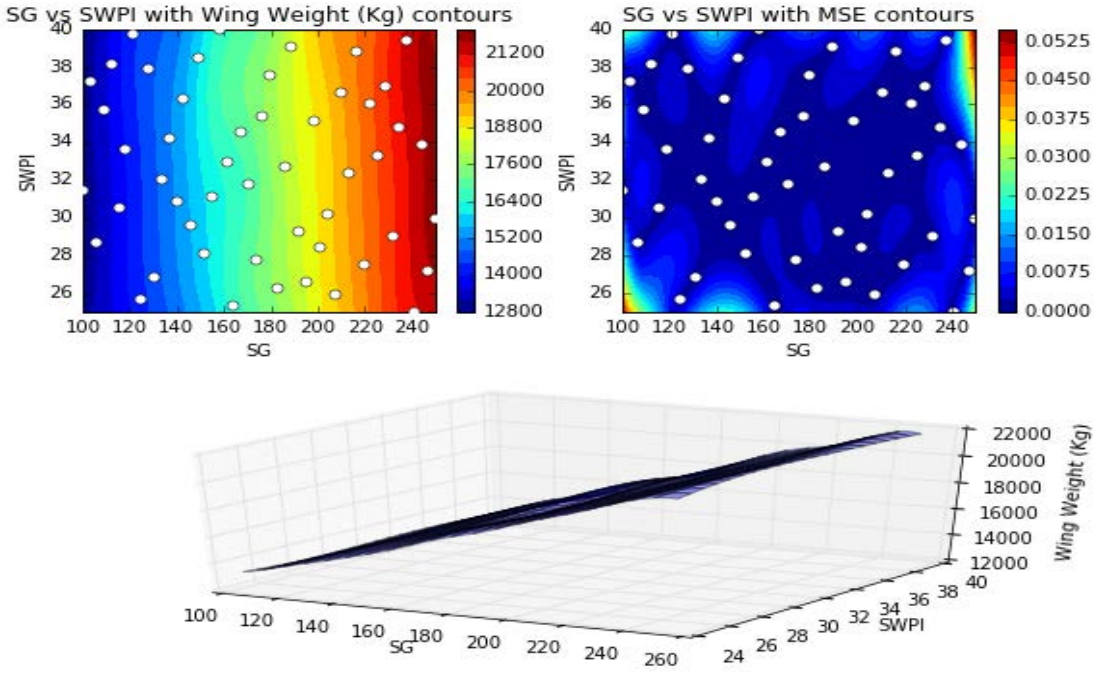

Figure B.28: Visualisation of Weight (Ton.) for *SG-SWPI* variable pairing at fildeity level I.

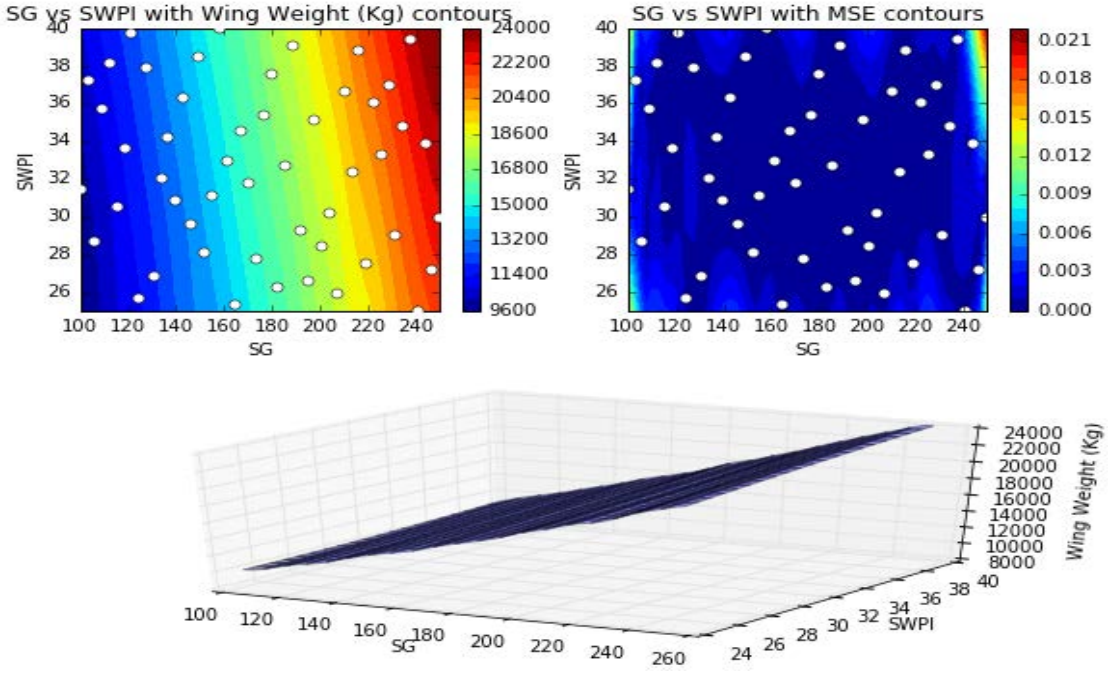

Figure B.29: Visualisation of Weight (Ton.) for *SG-SWPI* variable pairing at fildeity level II.

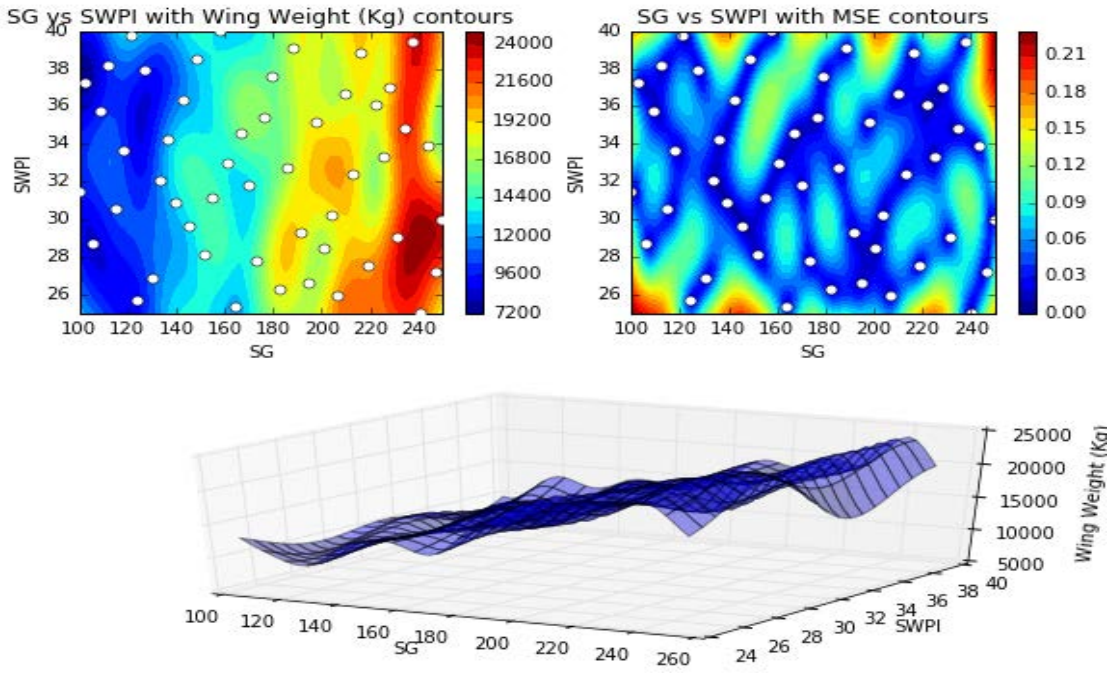

Figure B.30: Visualisation of Weight (Ton.) for *SG-SWPI* variable pairing at fildeity level III.

B.4.0.2 Cost

B.4.0.3 *SG-SWPI*

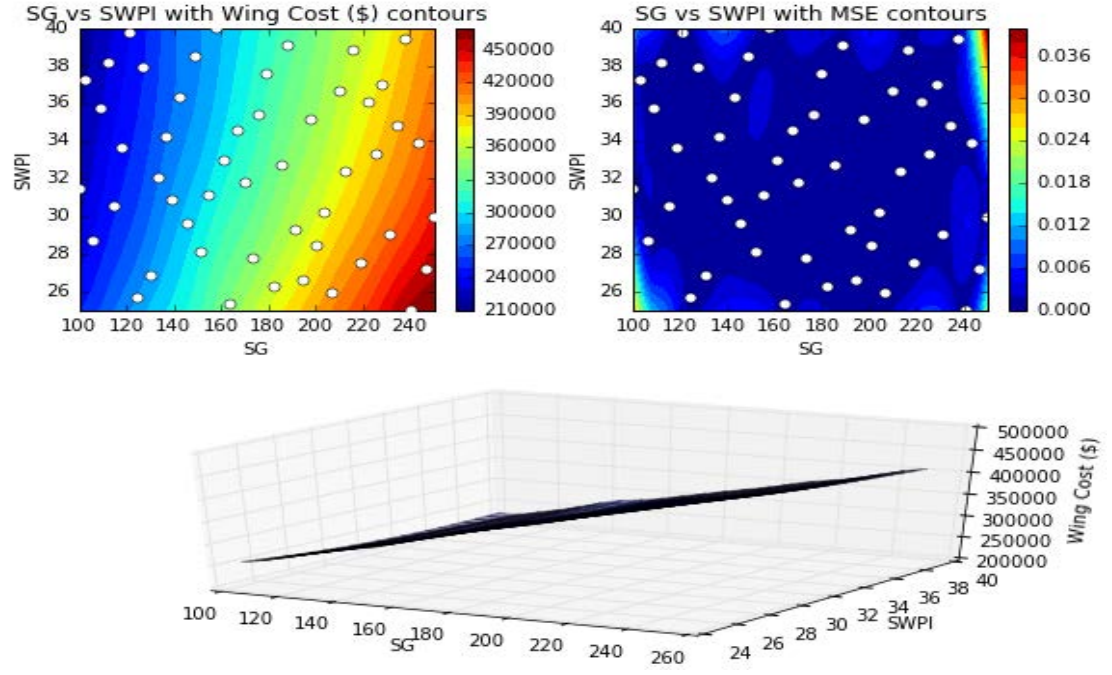

Figure B.31: Visualisation of Cost ($) for *SG-SWPI* variable pairing at fildeity level I.

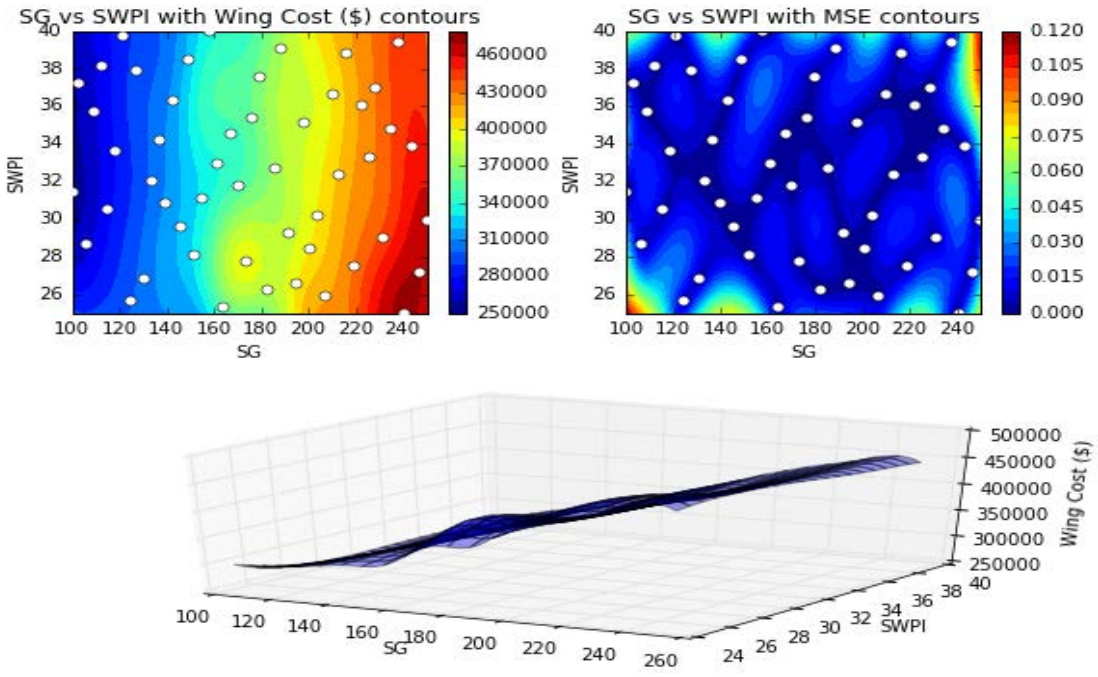

Figure B.32: Visualisation of Cost ($) for *SG-SWPI* variable pairing at fildeity level II.

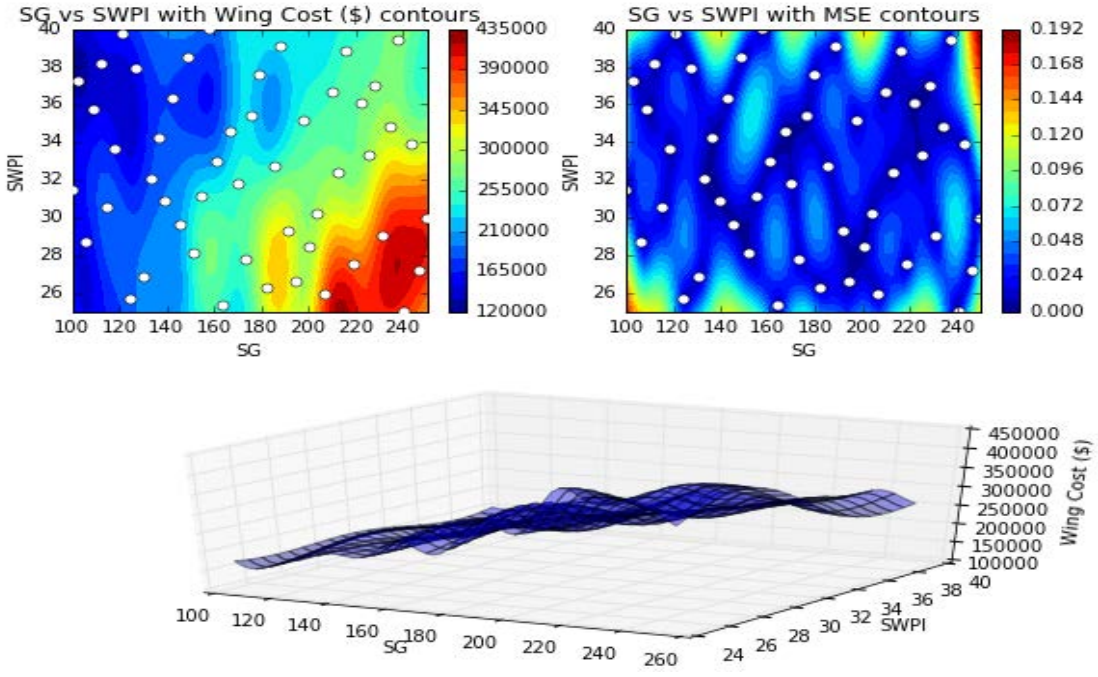

Figure B.33: Visualisation of Cost ($) for *SG-SWPI* variable pairing at fildeity level III.

B.4.0.4 Drag

B.4.0.5 *SG-SWPI*

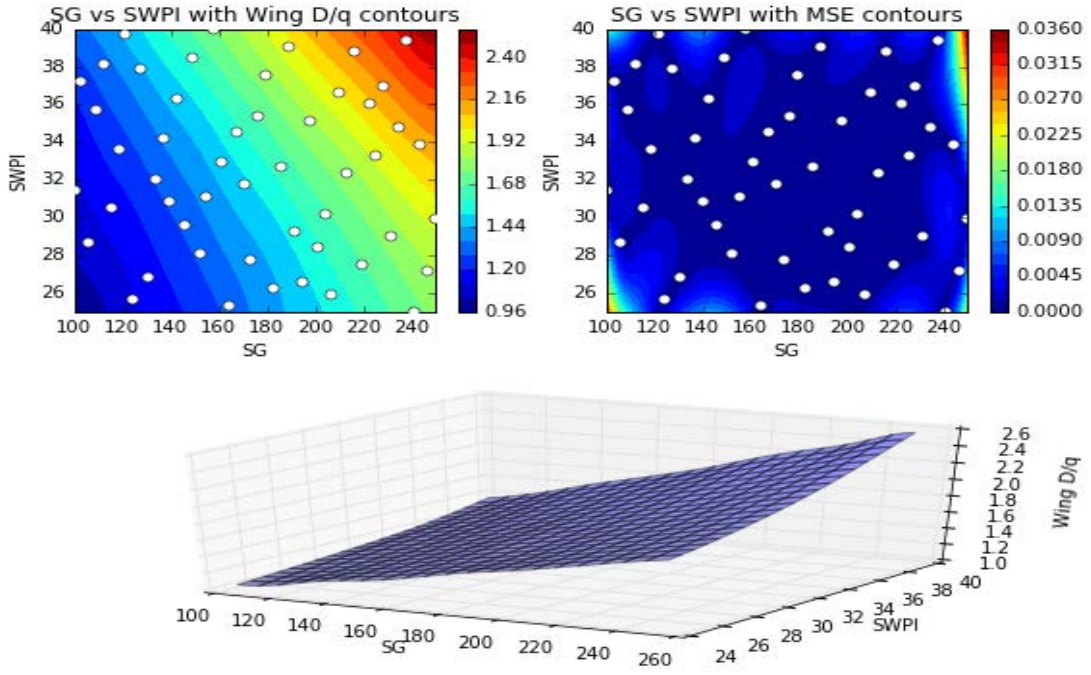

Figure B.34: Visualisation of D/q for *SG-SWPI* variable pairing at fildeity level I.

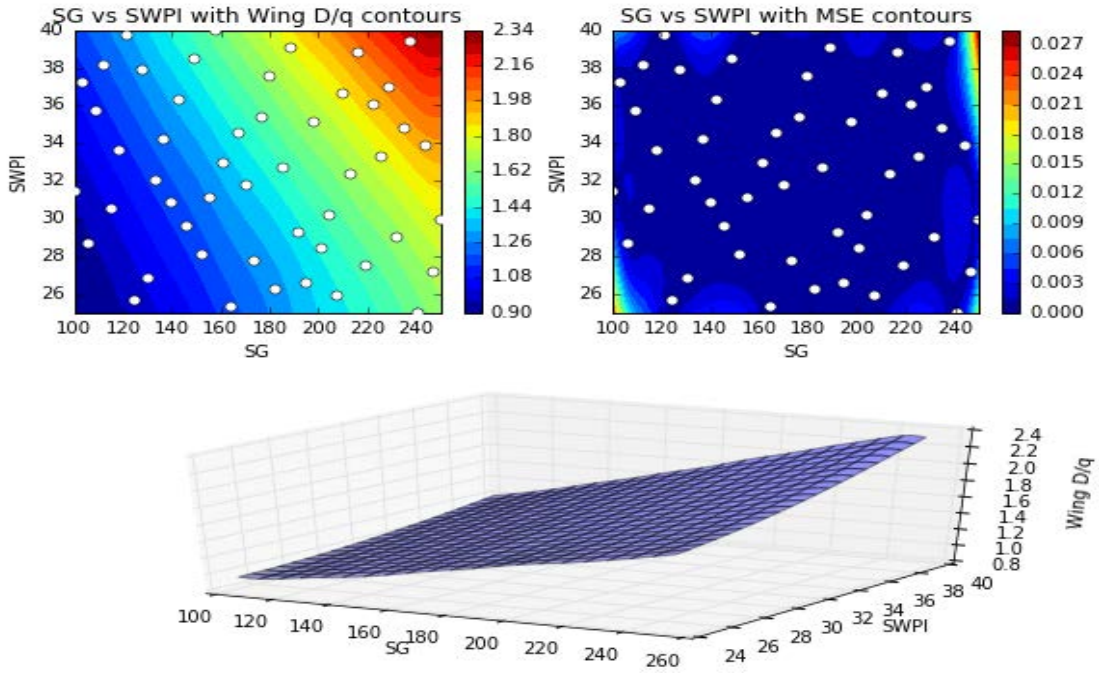

Figure B.35: Visualisation of D/q for *SG-SWPI* variable pairing at fildeity level II.

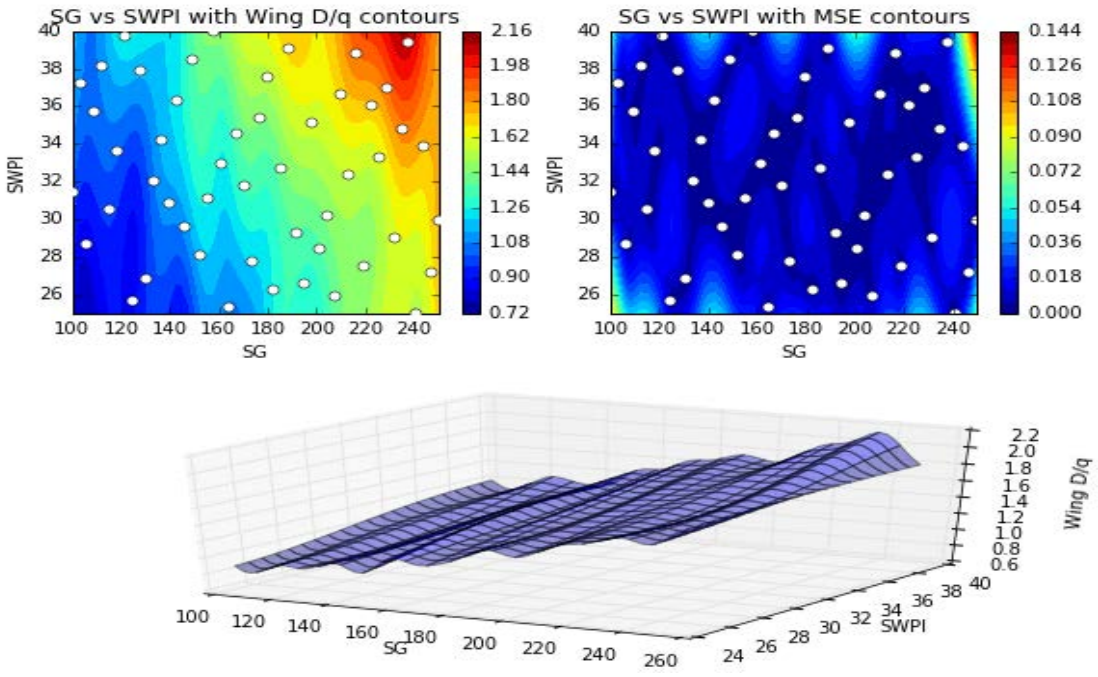

Figure B.36: Visualisation of D/q for SG-$SWPI$ variable pairing at fildeity level III.

B.4.0.6 Discussion

At the level I, for weight and cost, SG is the dominant variable as $SWPI$ effects are more subtle at this level. This changes when the level of fidelity increases. In this pairing for weight (figures B.28 to B.30) , it is clear to see that the introduction of higher fidelity models highlights the non-linearity of the $SWPI$ variable, its sensitivity to SG, and introduces new regions of minimal design, which are in practise hard to explore. At level III the clear effect of stress optimisation on the design space appears to be the exposition of these local optimal regions at the extremities. These regions are close to maximum or minimum operating aircraft $SWPI$ or SG values within the range of conventional aircraft. It would therefore appear that potential high risk design at the edges of this design space may be ideal for exploration and investigation. This confirms the known effects of these design variables on the wing weight, and highlights that these studies are physically accurate.

The cost (figures B.31 to B.33)design space at level I to II for this pair are similar to SG-t/c at this level, however note that both pairs share the SG variable, and there is some consistency in the profile at each fidelity level. Where $SWPI$ and t/c are featured as a pair with SG the range over which the cost varies is practically identical. Implying that when coupled with SG, it is a dominant variable, and dictates the design performance range. With the D/q response surface at level II, we see that there is a clear introduction of non-linearity from the sweep and this has an on the drag surface. Although the overall minimum is still suggested at a smaller SG and $SWPI$ there is now a clear exploratory

minimum region at a mid SG, where there is some trade to had with the sweep of the wing. Note this region is local but none the less is still present in the results from level III.The full set of D/q RSMs can be seen in figures B.34 to B.36.

The dominance of SG is present in all performance outputs with SG as part of the variable, especially at level I. However as you move from level I to II, and II to III $SWPI$ and AR when coupled with SG have more influential. Level I results can therefore be somewhat deceptive to the user, as clearly greater analysis fidelity is required to capture the true impact of certain variables.

Appendix C

Mean standard deviation visualisation for response surface data in chapter 6

In this chapter the Mean Standard Deviation (MSD) for the weight, cost, and D/q of the raw data used for response surface models in chapter 6, are presented for each fidelity level.

C.0.0.1 Weight

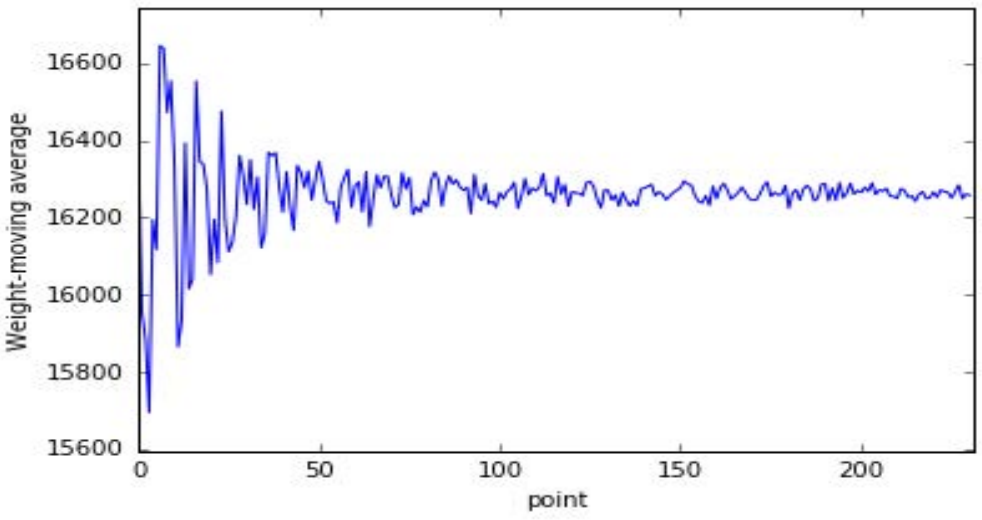

Figure C.1: Mean Standard Deviation for Weight response surface model data for T.A.C.E fidelity level I.

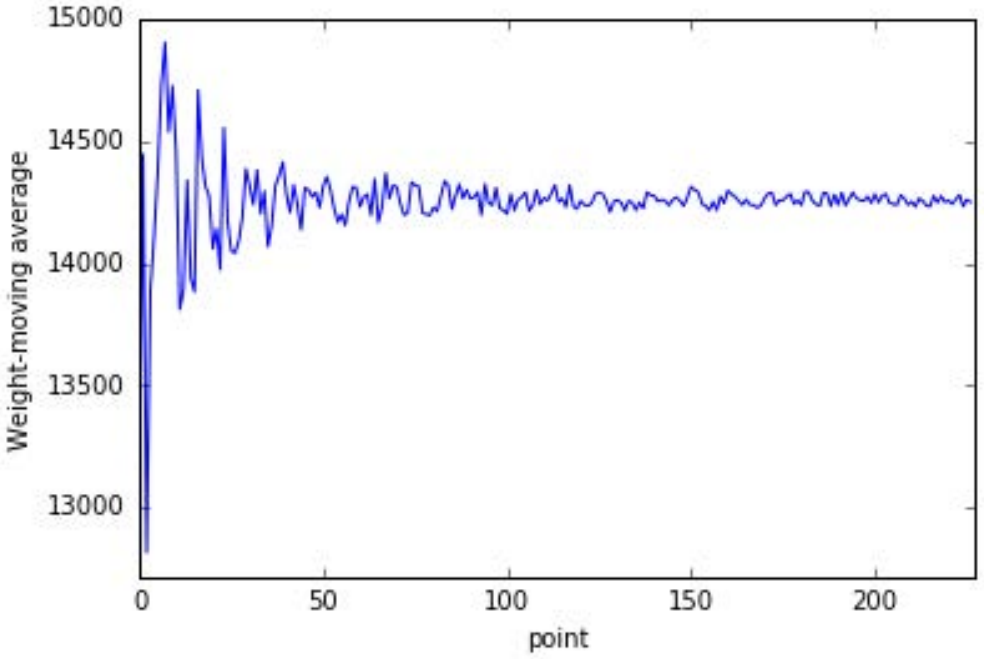

Figure C.2: Mean Standard Deviation for Weight response surface model data for T.A.C.E fidelity level II.

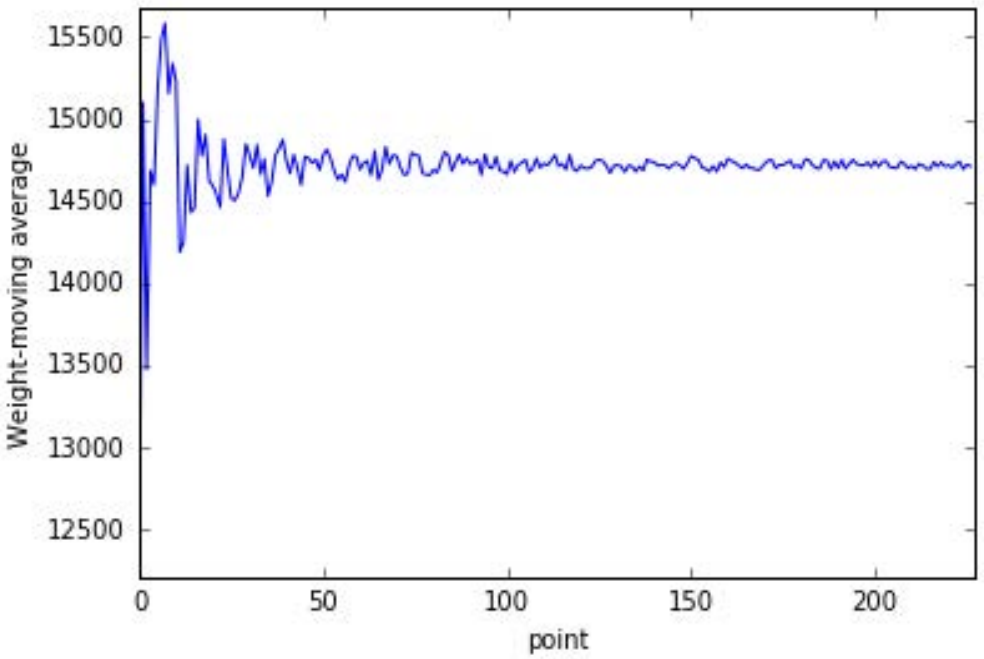

Figure C.3: Mean Standard Deviation for Weight response surface model data for T.A.C.E fidelity level III.

C.0.0.2 Cost

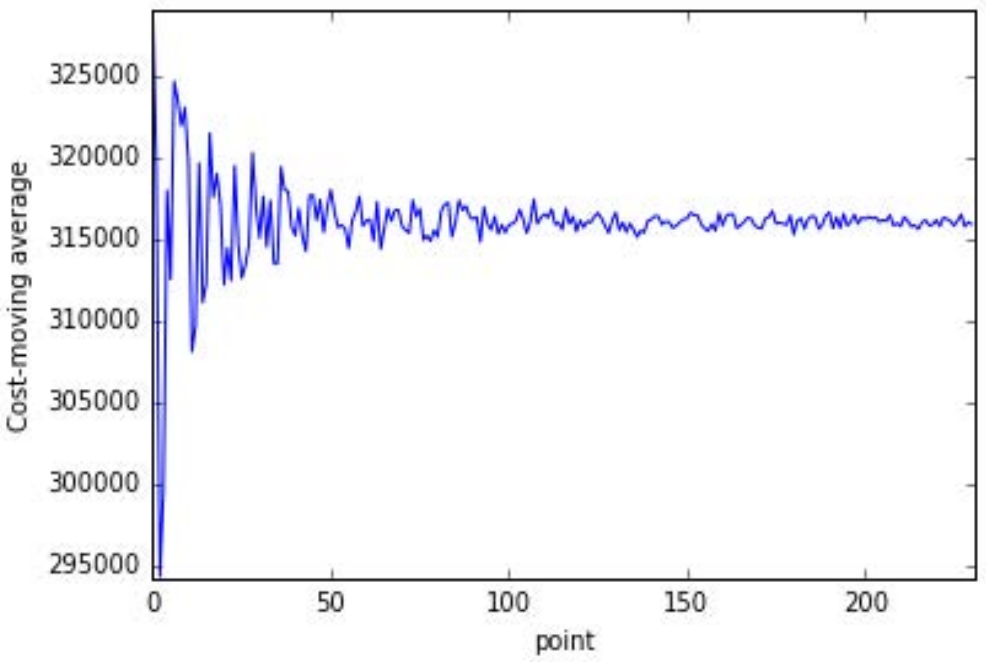

Figure C.4: Mean Standard Deviation for Cost response surface model data for T.A.C.E fidelity level I.

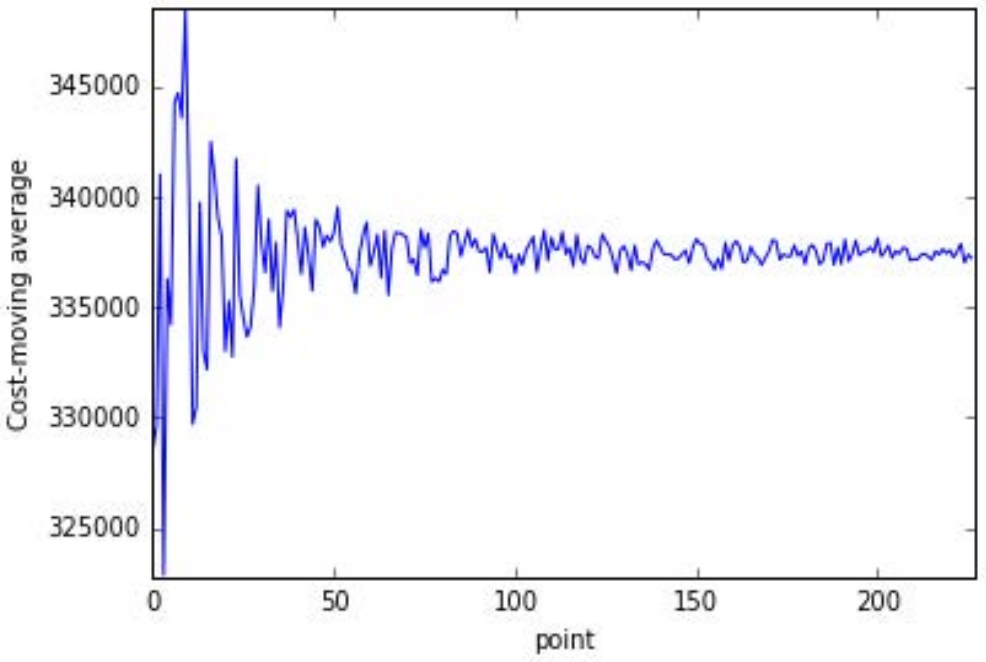

Figure C.5: Mean Standard Deviation for Cost response surface model data for T.A.C.E fidelity level II.

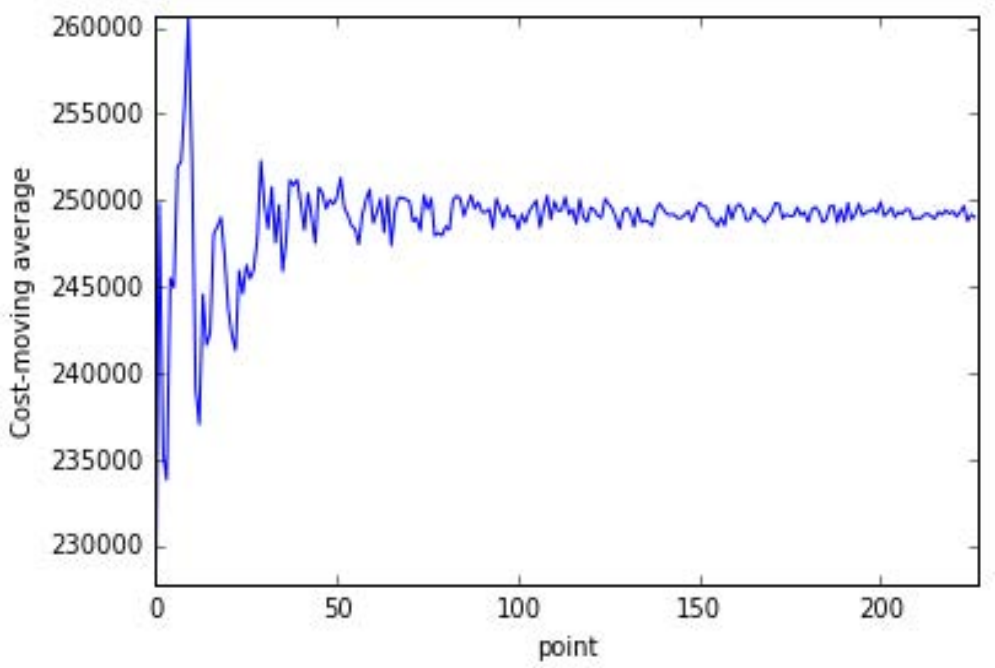

Figure C.6: Mean Standard Deviation for Cost response surface model data for T.A.C.E fidelity level III.

C.0.0.3 D/q

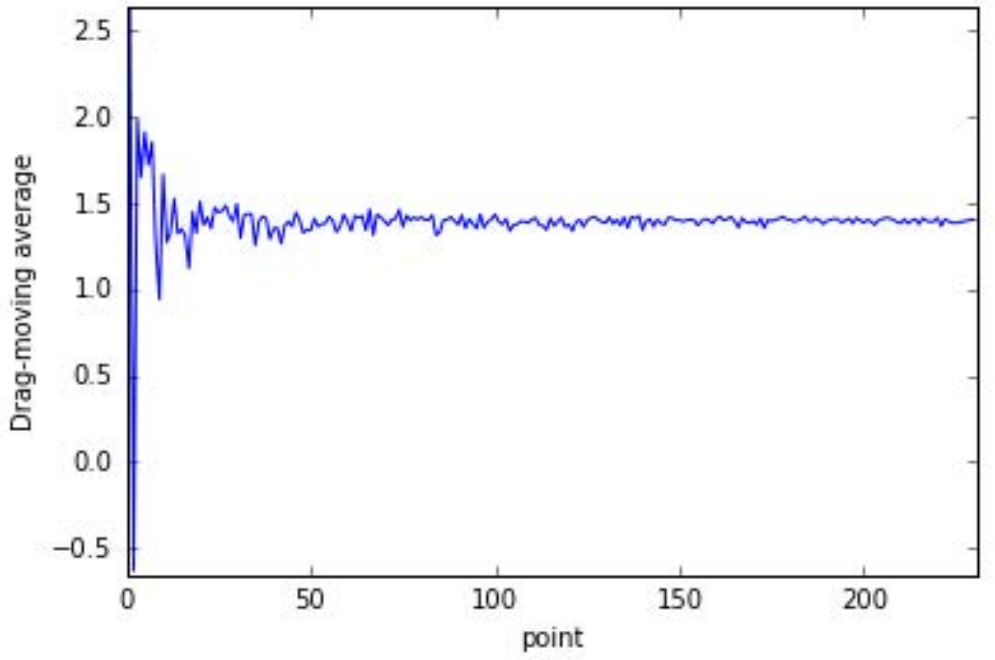

Figure C.7: Mean Standard Deviation for D/q response surface model data for T.A.C.E fidelity level I.

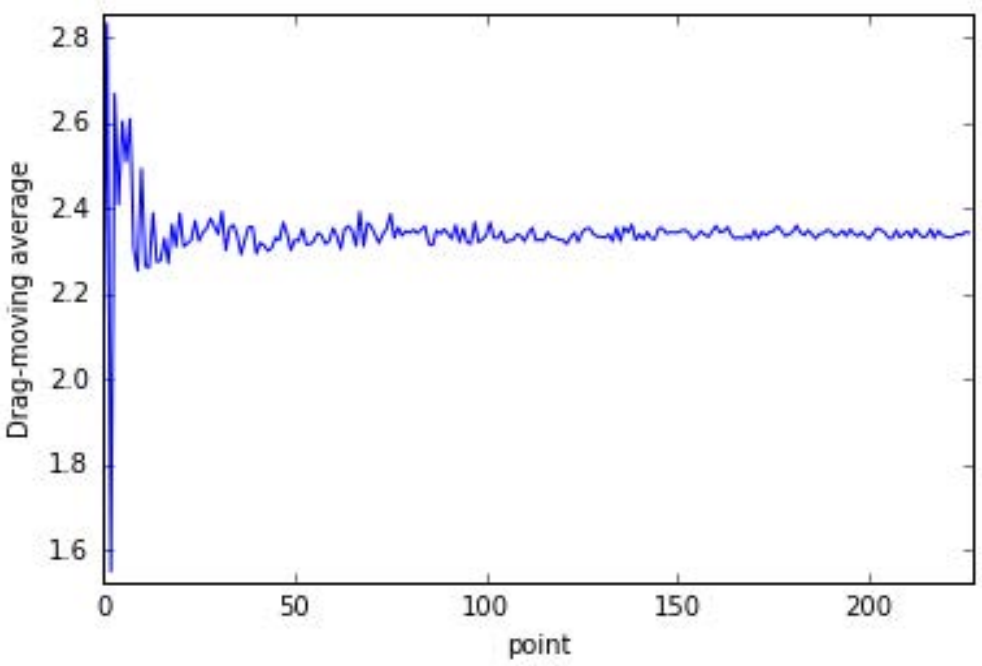

Figure C.8: Mean Standard Deviation for D/q response surface model data for T.A.C.E fidelity level II.

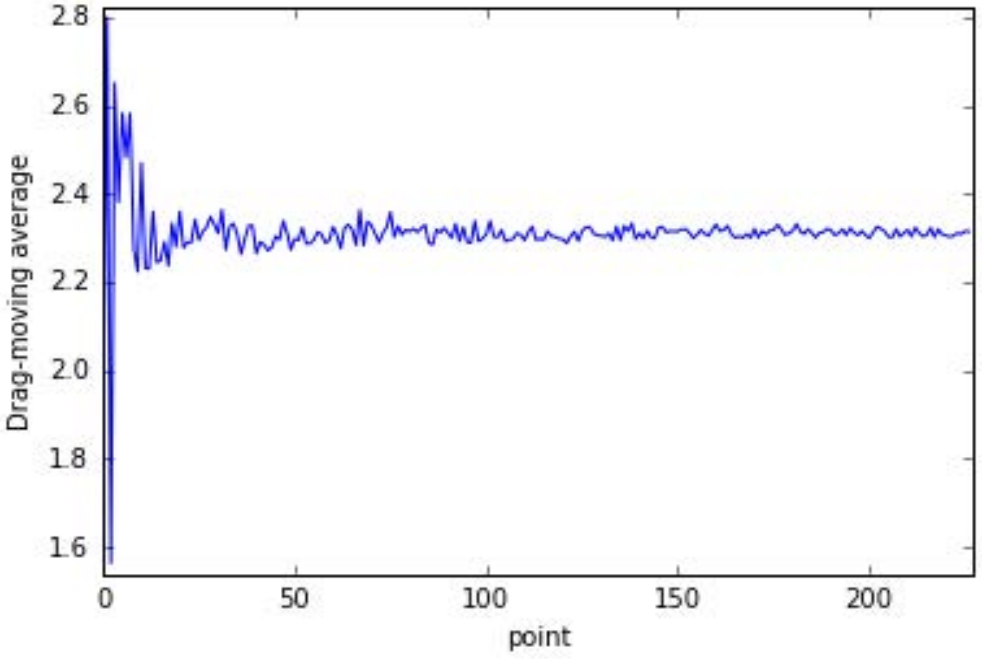

Figure C.9: Mean Standard Deviation for D/q response surface model data for T.A.C.E fidelity level III.

Appendix D

On the Implementation Multidisciplinary Optimisation in Industry

In order to implement the capabilities established in chapters 3 to 6 in industry, several steps would need to be undertaken. As noted in the previous chapters there is clear benefit to having structural fidelity variation, aerostructural coupling, and response surface models based design space visualisation, to achieve multi-objective optimisation. All three of these capabilities implemented in T.A.C.E, demonstrate the applicability of academic methodology within industry to achieve multidisciplinary optimisation. There some key steps which can be undertaken to utilise the finding of this thesis within industry, are presented.

Firstly we must note that the addition of structural fidelity variation has been key to reducing a problem associated with data overhead. This issue as previously stated arises due to lack of key information on the design, when it is transferred from conceptual to preliminary design. This issue is endemic of the need for higher fidelity data at the preliminary design stage and effects the process of analysis within MDAACE, limiting its potential for multidisciplinary optimisation. As demonstrated in this thesis by implementing multi-fidelity structural models, this overhead issue can be minimised, as design information can is aggregated. The question arises as to how to implement this within industry.

As two levels of fidelity exist already between conceptual and preliminary design stages for structural design, the identification a level of fidelity between these models is important. In T.A.C.E studies and chapter 6, it was identified that in order to capture the sufficient level of non-linear performance, and complex physics, the minimum amount of structural information required is does not have to include specific structural sizing.

This level can function as an intermediary stage where further trade studies can be accomplished. The second step is to identify which features in the structural models or modelling process are dependent of high fidelity data. These dependencies must then be minimised and if possible removed. The reason for this is to allow unconstrained exploration of the structural design space, which is very important when exploring novel design spaces. When top level variables are being optimised or traded, there must be a level of flexibility in the model. Note this new level must prioritise flexibility and robustness, where accuracy is captured through physics based analysis.

This leads to the final step, the identification of appropriate physics based analysis. As identified in T.A.C.E to compensate for the need for high fidelity aerodynamics data, aerostructural couplingg was implemented to ensure greater capture of physical phenomena. Often in industry there are reliance on high fidelity data which interacts with the structural analysis, these must be minimised to allow the capture of appropriate physics and computational expense. Else the benefits of this intermediary level are mitigated. The fidelity levels between disciplines can have some mismatch but coupling can overcome the inaccuracies and conservatism of lower fidelity models. The aerostructural coupling is crucial to the implementation of multidisciplinary optimisation capability in MDAACE. This in particular is a difficult concept to implement in industry as the safety culture in aerospace leads to a lack of trust in unknown methods, and as shown in T.A.C.E chapters 4, steps must be taken to validate the lower outputs against legacy data, or an established tool.

Finally interfaces must be built to utilise data, through response surface models and data visualisation techniques. Throughout this thesis visualisation capabilities have been favoured in order to highlight the impact of visualisation, on the practical design and optimisation. Note the response surface models creation, and three step visualisation of the design space is only possible once effort has been made to introduce structural fidelity variation and to capture appropriate physics at the newly identified intermediary fidelity level. Having achieved these, it is possible to then go on and create response surface models. Within this thesis kriging has been identified as ideal for a small number of design variables, however this is not always the case if there are a large number of design variables. T.A.C.E demonstrates that it is possible to conduct global optimisation by utilising top level design variables in addition to lower fidelity structural models, and a multidiscciplinary optimisation which can support optimisation and multi-point analysis. Therefore it is possible in industry to propagate these variables. Note when there are a large number of global designs variable, response surface models must be built and validated incrementally to reach the goal of creating a trustworthy response surface models, for all top level design variables.

Note when building response models using structural fidelity variation capability , the designer has a choice to create relatively cheap models and to enhance these with data from higher fidelity analysis. This process can help to improve design space exploration

and multidisciplinary optimisation capability The raw data from the response surface models can be used to identify trends in performance, through parallel coordinates, and three dimensional response surfaces, and to achieve visualisation of design space through HAT plots, and even global multi-objective visualisations such as Pareto fronts. These visualisation techniques are powerful tools in multidisciplinary optimisation and should be utilised more efficiently within industrial multidisciplinary frameworks. Global process tools in industry, offer an easy and ideal platform to achieve this. They allow multidisciplinary frameworks to be wrapped inside an interactive platform and run with some degree of autonomy, and offer optimisation algorithms and sate of the art visualisation techniques. Which as demonstrates can help determine the validity of optima, the nature of a non-trivial novel design space, and to identify possible limitations of the analysis process. As incorrect trends become easier to identify, and limitations on the analysis are clear to see.

Having a databases of information from response surface model creation at a given level of fidelity, gives access to all appropriate design exploration information. The databases capture appropriate sub-design problems whilst balancing computational resources. Such databases provide all disciplines a joint resources, which can be accessed and utilised, ensuring consistent transfer of data across the multidisciplinary platform. In practise this can improve the consistency of data transfer and multidisciplinary research. The databases can become a focal point of multidisciplinary optimisation and reduce data overhead between fidelities as every trade study (regardless of fidelity), improves the understanding of the design space. Allowing each subsequent study to have improved data assurance and confidence, building trust in multidisciplinary optimisation capabilities.